

Univerzita Karlova v Praze

1. lékařská fakulta

Doktorský studijní program v biomedicíně
Buněčná a molekulární biologie, genetika a virologie



Mgr. Martin Panigaj

Úloha buněčného prionového proteinu v erytroidní diferenciaci

The role of cellular prion protein in erythroid differentiation

Disertační práce

Vedoucí disertační práce: Ing. Karel Holada, Ph.D.

Praha, 2011

Prohlášení:

Prohlašuji, že jsem závěrečnou práci zpracoval samostatně a že jsem řádně uvedl a citoval všechny použité prameny a literaturu. Současně prohlašuji, že práce nebyla využita k získání jiného nebo stejného titulu.

Souhlasím s trvalým uložením elektronické verze mé práce v databázi systému meziuniverzitního projektu Theses.cz za účelem soustavné kontroly podobnosti kvalifikačních prací.

V Praze, 16. 05. 2011

Martin Panigaj

Podpis

Identifikační záznam:

PANIGAJ, Martin. *Úloha buněčného prionového proteinu v erytroidní diferenciaci. [The role of cellular prion protein in erythroid differentiation]*. Praha, 2011. 126 s., 2 příl. Disertační práce. Univerzita Karlova v Praze, 1. lékařská fakulta, Ústav imunologie a mikrobiologie. Vedoucí závěrečné práce: Ing., Holada, Karel. Ph.D.

Abstrakt

Buněčný prionový protein (PrP^C) je evolučně konzervovaný protein, exprimovaný na povrchu buněk různého původu. Přestože PrP^C hraje zásadní roli v patogenezi neurodegenerativních chorob, jeho fyziologická funkce zůstává neznáma. Prionové choroby jsou charakteristické dlouhou dobou latence, během které nejsou diagnostikovatelné žádnou konvenční metodou. Krev by mohla být ideálním materiálem pro vývoj takových testů, bohužel vlastnosti PrP^C na krevních buňkách a jeho funkce není dosud spolehlivě vysvětlena. Naše práce ukázala, že jednotlivé lidské červené krvinky exprimují pouze malé množství PrP^C, ale vzhledem k počtu erytrocytů v krvi představuje tento protein většinu PrP^C vázaného na krevní buňky. Na základě našich dat usuzujeme, že PrP^C na povrchu erytrocytů je unikátně modifikován. Podobná modifikace by v případě patologického PrP mohla znesnadňovat diagnostiku prionových chorob z krve. Je prokázáno, že v průběhu prionových onemocnění dochází k deregulaci transkripce erytroidních genů a že PrP^{-/-} myši mají oslabenou odpověď vůči experimentálně navozené anémii. Pro objasnění úlohy PrP^C v erythropoéze jsme proto sledovali jeho expresi u myších erytroidních prekursorů *in vitro* i *in vivo*. Prokázali jsme, že v průběhu diferenciac buněk dochází k regulaci povrchové exprese PrP^C na erytroidních prekursorech z myší sleziny a kostní dřeně. Závislost exprese PrP^C na průběhu erytroidní diferenciac jsme potvrdili i na modelu myší erytroleukemické buněčné linie (MEL). Pomocí RNA interference (RNAi) jsme vytvořili erytroleukemické buněčné linie se stabilně sníženou expresí PrP^C, u kterých jsme ukázali, že za normálních podmínek je diferenciac MEL buněk nezávislá na expresi PrP^C. Metodu RNAi jsme dále použili pro studium důležitosti exprese PrP^C při propagaci prionů v neuronální buněčné linii CAD5.

Klíčová slova

Buněčný prionový protein, erytroidní diferenciac, RNA interference, fyziologická úloha

Abstract

The cellular prion protein (PrP^C) is evolutionary conserved protein expressed in cells of various origins. Although PrP^C plays a basic role in the pathogenesis of the fatal neurodegenerative prion disorders, its physiological role remains enigmatic. Prion diseases are characteristic by long latency period during which they are not identifiable by any conventional methods. Although the blood is an ideal material for developing of screening tests, little is known about traits of PrP^C and its role in blood cells. We showed that human erythrocytes express low amounts of PrP^C per cell, but due to the high numbers of erythrocytes, they are major contributors to the pool of blood cell-associated PrP^C. Based on our biochemical characterization we propose that PrP^C on human erythrocytes is uniquely modified. Such a modification in abnormal prion protein may complicate screening tests for prion diseases in blood. It was reported that prion diseases deregulate the transcription of erythroid genes, and PrP^{-/-} mice demonstrate a defective response to experimental anemia. To investigate the role of the PrP^C in erythropoiesis, we studied the protein's expression on mouse erythroid precursors *in vivo* and *in vitro*. We showed that surface expression of PrP^C on erythroid precursors in bone marrow and spleen follows similar pattern as the cells mature. We demonstrated that the regulation of PrP^C expression in differentiating murine erythroleukemia cells (MEL) cells resembles its regulation seen *in vivo*. Using RNA interference (RNAi) we created MEL lines with stably silenced expression of PrP^C, which showed that under normal conditions PrP^C seems dispensable for erythroid differentiation of MEL cells. We further used RNAi methodology to study the effect of PrP^C silencing on the propagation of prion infection and its influence on neuronal CAD5 cell culture.

Key words

Cellular prion protein, erythroid differentiation, RNA interference, physiological role

Acknowledgement

*In memory of Jozef Gavlák, *1932 - †2009.*

I would like to thank to my advisor Dr. Karel Holada for his guidance and his effort to explain that if an experiment brings me a lemon I should make lemonade.

I am indebted to Barbora, Martina, “DBF” Peter, Alena, Olga, and Zorka from our institute for sharing their ideas with me and for their direct involvement in my research. My exceptional thanks belongs to Hanka Glierová from our laboratory for her help and work with flow cytometry. There would be hardly any progress in experiments with cell cultures and gene delivery without help by Jana Čmejlová, Ph.D. and Radek Čmejla, Ph.D. (The Institute of Hematology and Blood Transfusion, Prague). Peter Svoboda, Ph.D. from Institute of Molecular Genetics of the ASCR helped me with RNA interference.

It would be a very hard to get through my Ph.D. study without the support of my closest, so I would like to thank to my wife Anastázia for her love and patience when I was sometimes more interested in a cell cultures instead of her. Of course, I owe my deepest gratitude to my parents and close family for their love and trust in me.

Our research was supported by Grants: GAČR 310/08/0878, GAČR 203/07/1517, 310/05/H533, MŠM0021620806, and GAUK 203429. Furthermore, my study was also supported by International Visegrad Fund, and Foundation “Nadání, Josefa, Marie a Zdeňky Hlávkových”.

Content

Author disclosure.....	1
Identification note.....	2
Abstract / Czech and keywords.....	3
Abstract / English and keywords.....	4
Acknowledgement.....	5
Content.....	6
Abbreviations.....	10
1. Introduction.....	15
1.1. Structure of the gene coding PrP ^C	15
1.2. Molecular characteristic of PrP ^C	16
1.3. PrP ^{TSE} pathological isoform of PrP ^C	17
1.4. Physiological function of PrP ^C	18
1.4.1. PrP ^{-/-} mice.....	18
1.4.2. RNA interference of PrP ^C	19
1.4.3. Proposed function of PrP ^C	22
1.4.3.1. Antiapoptotic function.....	22
1.4.3.2. Protection against copper mediated oxidative stress.....	24
1.4.3.3. PrP ^C in signalling cascades.....	25
1.4.3.4. PrP ^C in iron metabolism.....	27
1.4.3.5. PrP ^C in cell adhesion.....	28
1.4.3.6. PrP ^C and endogenous retroviruses.....	28
1.5. Erythropoiesis.....	30
1.5.1. Introduction.....	30
1.5.2. Regulation of erythropoiesis.....	31
1.5.2.1. Erythropoietin is primary erythropoietic growth factor.....	31
1.5.2.2. Epo regulation.....	32
1.5.2.3. Stem cell factor.....	33
1.5.2.4. Iron as a regulator of erythropoiesis.....	33
1.5.2.5. Regulation of erythropoiesis on transcriptional level.....	34
1.5.2.6. Involvement of miRNA in erythropoiesis.....	35
1.5.3. Murine erythroleukemia cells- <i>in vitro</i> model of erythroid differentiation.....	36
1.6. Expression and the role of PrP ^C in blood cells.....	38

1.6.1. PrP ^C expression on blood cells.....	38
1.6.2. The role of PrP ^C in hemathopoiesis.....	39
1.6.3. PrP ^C support self- renewal of Long Term Hematopoietic Stem Cells.....	39
1.6.4. The role of PrP ^C in cells of immune system.....	40
1.6.5. PrP ^C is involved in anemia recovery.....	40
1.6.6. <i>Prnp</i> gene is regulated in growth arrested and differentiated MEL cells.....	42
1.6.7. Erythroid genes are deregulated with prion pathogenesis progression.....	43
1.6.8. Blood as a source of prion infectivity and specimen for diagnosis of prion disease.....	43
2. Aims of the study.....	46
3. Material and methods.....	46
3.1. Human samples.....	46
3.2. Cell cultures.....	46
3.3. Animals/ Mice.....	47
3.4. Chemicals.....	48
3.5. Flow cytometry.....	48
3.6. Preparation of brain homogenates and cell lysates.....	49
3.7. Isolation of erythrocyte ghosts.....	49
3.8. Electrophoresis and western blot.....	50
3.9. Deglycosylation.....	50
3.10. <i>In vitro</i> modification of brain PrP ^C by N-hydroxysulfosuccinimide biotin, hydrogen peroxide and glyoxylic acid.....	51
3.11. Cloning- creation of retroviral vectors expressing shRNAs.....	51
3.12. Transfection of the pSilencer 5.1. retro U6 vector expressing shRNAs to MEL cells....	54
3.13. Confirmation of the pSilencer 5.1. retro U6 vector integration by PCR.....	55
3.14. Retroviral transduction of target cells.....	55
3.15. RNA isolation and Reverse transcription.....	57
3.16. Quantitative real time PCR.....	57
3.17. Spectrophotometric determination of hemoglobin content in MEL cells.....	58
3.18. Uptake of radiolabeled ⁵⁹ Fe-transferrin by MEL cells.....	59
3.19. Infection of MEL cells with RML prion strain.....	59
3.20. Cell blot assay.....	59
3.21. Statistics.....	60
4. Results.....	61

4.1. Characterization of human PrP ^C associated with erythrocytes suggests explanation for quantitative differences in the literature.....	61
4.1.1. Characterization of erythrocyte PrP ^C	61
4.1.2. The influence of <i>in vitro</i> modification of brain PrP ^C on the binding of mAb 3F4.....	63
4.1.3. FACS analysis of 3F4 and 6H4 binding to CD71 ⁺ erythroid cells in cord blood.....	64
4.2. Expression of PrP ^C is regulated during murine erythroid differentiation.....	65
4.2.1. Expression of PrP ^C differs on individual murine erythroblast subpopulations.....	65
4.2.2. Differential regulation of PrP ^C during inducer mediated erythroid differentiation.....	66
4.2.3. PrP ^C is upregulated after treatment with inhibitor of histone deacetylases.....	68
4.2.4. Inhibitor of differentiation does not prevent expression of PrP ^C	69
4.3. Introduction of RNAi methodology and optimization of gene delivery methods for the study of PrP ^C role.....	71
4.3.1. Transfection of pSilencer 5.1. retro U6 vector coding anti- <i>Prnp</i> shRNAs did not led to PrP ^C downregulation.....	71
4.3.2. Optimization of retroviral delivery by „packaging cell lines“.....	75
4.3.3. RNAi by shRNA of second class led to stable and efficient PrP ^C silencing.....	76
4.4. Silencing of <i>Prnp</i> gene by RNAi suggests that PrP ^C is dispensable for erythroid differentiation <i>in vitro</i>	81
4.4.1. Similar proliferative capacity and viability during differentiation was observed in all MEL lines irrespective of <i>Prnp</i> expression.....	81
4.4.2. Silencing of <i>Prnp</i> expression does not interfere with erythroid differentiation <i>in vitro</i>	83
4.4.3. Low expression of PrP ^C does not influence iron uptake in MEL cells.....	85
4.4.4. All differentiating cells respond similarly to lower level of iron.....	85
4.5. Utilization of RNAi in study of infectious prion propagation in cell culture.....	86
4.5.1. Preliminary attempts to infect MEL cells with RML infected brain homogenate suggest that MEL cells do not propagate infectious PrP.....	86
4.5.2. RNAi leads to efficient silencing of <i>Prnp</i> gene in CAD5 cells.....	88
4.5.3. Downregulation of PrP ^C expression significantly reduce PrP ^{TSE} formation.....	90
4.5.4. RNAi of <i>Prnp</i> gene does not cure RML infected cells.....	91
4.5.5. Expression of endogenous retroviruses in CAD5 cells.....	91
5. Discussion.....	93
5.1. Characterization of human erythrocyte-associated PrP ^C	93
5.2. Expression of PrP ^C is regulated during murine erythroid differentiation.....	96

5.2.1. Establishment of cell lines with stable silenced <i>Prnp</i> expression.....	98
5.2.2. Influence of <i>Prnp</i> silencing on erythroid differentiation <i>in vitro</i>	101
5.3. Effect of <i>Prnp</i> downregulation on propagation of infectious prion protein in cell culture and expression of endogenous retroviruses.....	103
6. Conclusion.....	106
7. References.....	107
7.1. Online references.....	125
8. Supplements.....	126

Abbreviations

5-AzaC	5-Aza-2'-deoxycytidine
7-AAD	7-Aminoactinomycin D
AGO2	argonaute 2 protein
AHSP	alpha-hemoglobin stabilizing protein
Bax	BCL2- associated X protein
BCIP/NBT	5-bromo-4-chloro-3-indolyl-phosphate/ nitroblue tetrazolium
BFU-E	Burst forming units- erythroid
BM	bone marrow
BPE	BSA, PBS and EDTA
BSA	bovine serum albumin
cAMP/PKA	cyclic adenosine mono phosphate dependent kinase A
CD34	cluster of differentiation 34, transmembrane sialomucin protein
CD71	cluster of differentiation 71, transferrin receptor
cDNA	complementary deoxyribonucleic acid
CFU-E	colony forming units- erythroid
CML	N ^ε -(carboxymethyl)lysine
CMPs	common myeloid progenitor
CNS	central nervous system
CSF	cerebrospinal fluid
CTRL	control sample
DEX	dexamethasone
DiOC₆	3,3'-dihexyloxacarbocyanine iodide
DMEM	Dulbecco's modified eagle medium
DMSO	dimethylsulfoxide
DNA	deoxyribonucleic acid
Dpl	doppel protein
DSFRL	desferral
dsRNA	double stranded RNA
EDRF	erythroid differentiation related factor
EDTA	ethylenediaminetetraacetic acid
EGFP	enhanced green fluorescent protein

Eif2ak2	eukaryotic translation initiation factor 2-alpha kinase 2
ELISA	enzyme-linked immunosorbent assay
Epo	erythropoietin
EpoR	erythropoietin receptor
Eraf	erythroid associated factor
Erk	extracellular regulated kinase
ERV-L	endogenous retrovirus-like
ERVs	endogenous retroviruses
Ery.A	basophilic erythroblasts
Ery.B	late basophilic and polychromatic erythroblasts
Ery.C	orthochromatic erythroblasts and reticulocytes
FACS	fluorescence- activated cell sorting
FBS	fetal bovine serum
FITC	fluorescein isothiocyanate
FOG1	friend of GATA1
FSC	forward scatter
GA	glyoxylic acid
Gapdh	glyceraldehyde-3-phosphate dehydrogenase
GATA1	GATA-binding factor 1
GFP	green fluorescent protein
GM-CSF	granulocyte-macrophage colony stimulating factor
GPI	glycosylphosphatidylinositol
Hba-a1	hemoglobin alpha adult chain 1
HIF	hypoxia inducible factor
HMBA	hexamethylene bisacetamide
HRE	hypoxia Response Element
HSCs	haematopoietic stem cells
IAP-1	intracisternal A particle 1
IgG	immunoglobulin G
IL-3	interleukine-3
IRE	iron responsive element
ISGs	interferon stimulated genes
KO	knockout

LMP	MSCV/LTRmiR30-PIG
LRP	laminin receptor precursor
LR	laminin receptor
LT-HSC	long-term hematopoietic stem cells
LTR	long terminal repeats
mAb	monoclonal antibody
MEL	murine erythroleukemia cells
MEPs	megakaryocyte-erythroid progenitors
miRNA	micro RNA
MLV	murine leukemia virus
MoMuLV	moloney murine leukemia virus
MPPs	multipotent progenitors
mRNA	messenger RNA
MuRRS	murine retrovirus-related sequences
Myb	myeloblastosis oncogene
MW	molecular weight
N⁶mAdo	N6-methyladenosine
Nt	nucleotides
Oas1a	2'-5' oligoadenylate synthetase 1A
PBS	phosphate buffered saline
PCR	polymerase chain reaction
PE	phycoerythrin
PGK	phosphoglycerate kinase eukaryotic promoter
PK	proteinase K
PLTs	platelets
PMCA	protein misfolding cyclic amplification
PMSF	phenylmethylsulfonyl fluoride
PNGase F	N-glycosidase F
PPS	pentosan polysulphate
pre-miRNA	precursor micro RNA
pri-miRNA	primary micro RNA
Prnd	doppel protein gene
Prnp	cellular prion protein gene

Pro.E	proerythroblasts
PrP^C	cellular prion protein
PrP^{TSE}	pathological prion protein
pVHL	von-Hippel Lindau protein
qRT-PCR	quantitative real time PCR
RBCs	red blood cells
RML	rocky mountain laboratory mouse scrapie strain
RNA	ribonucleic acid
RNA pol III	RNA polymerase III
RNAi	RNA interference
Rnase1	ribonuclease L
RT	room temperature
RTCs	reticulocytes
SCF	stem cell factor
SCF-R	stem cell factor receptor
sCJD	sporadic Creutzfeldt- Jakob disease
SCRL	scrambled
SD	standard deviation
SDS-PAGE	sodium dodecyl sulfate- polyacrylamide gel electrophoresis
SEM	standard error of measurement
SFFV	spleen focus-forming virus
shRNA	short hairpin RNA
shRNAmiR	short hairpin RNA in context of micro RNA
siRNA	short interfering RNA
spi-1	SFFV proviral integration site
ssRNA	single stranded RNA
TBS	tris buffer saline
TBST	tris buffer saline tween
TBSTM	tris buffer saline tween milk
Tf	transferrin
TfR	transferrin receptor
TMB	tetramethylbenzidine
TSA	trichostatin A

TSE	transmissible spongiform encephalopathies
UNT	untreated sample
UTR	untranslate region
vCJD	variant Creutzfeldt- Jakob disease
VSV-G	vesicular stomatitis virus glycoprotein
WB	western blot

1. Introduction

The cellular prion protein is protein of unknown physiological function expressed in various tissues with the highest level of expression in brain. It is conservative through the whole vertebrae class. Together with its pathological isoform (PrP^{TSE}) plays a crucial role in prion diseases. Also known as Transmissible Spongiform Encephalopathies (TSE), they are group of rare fatal neurodegenerative diseases affecting mammals. In humans most of them arise spontaneously (80%) without any detectable cause, 19% are caused by a genetic predisposition and only 1% are of infectious origin. However, all TSEs share common traits: spongiform degeneration of brain, accumulation of resistant form of prion protein in central nervous system (CNS) and lack of systematic immunological response (Prusiner et al., 1998).

1.1. Structure of the gene coding PrP^C

PrP^C is coded by *Prnp* gene whose sequence is already known for many species including humans. Locus for *Prnp* is located on 2nd or 20th chromosome in mice or humans, respectively. In all species, *Prnp* gene contains three exons, although the second exon may not be present in the hamster and human mRNA (Li and Bolton, 1997), (Lee et al., 1998). The open reading frame is encoded only in the third exon. Regulation of the *Prnp* promoter depends on a cell line. Fisher et al. observed that introducing PrP-encoding transgene requires at least one intron for efficient expression of PrP^C (Fischer et al., 1996). In addition to promoter, exon 1 and intron 1 are key regions for *Prnp* promoter activity. The exon 1 inhibits promoter activity when intron 1 was deleted. The intron 1 has intrinsic promoter activity because it can initiate expression in the absence of *Prnp* promoter (Haigh et al., 2007). Furthermore, Haigh et al. who identified a putative TATA box within intron 1 of the bovine *Prnp* gene challenged previous classification of *Prnp* as a housekeeping gene due to its lack of TATA box. However, when the mouse sequence was analyzed by the same methods, a TATA box was not found, but the strong promoter activity was predicted within the same region (Haigh et al., 2007). Several putative binding sites for transcription factors controlling *Prnp* promoter activity have been proposed. The intron 1 is supposed to be essential for full promoter activity and contains putative binding sites for e.g. heat shock factor 2, myocyte enhancer factor 2, E4 promoter-binding protein 4, nuclear matrix protein 4/cas-interacting zinc finger protein, regulatory factor X1, thyrotrophic embryonic factor, and ecotropic viral integration site (Kim et al., 2008). In addition to these factors, p53 and Sp1 may regulate transcription of *Prnp* as well (Qin et al., 2009).

1.2. Molecular characteristic of PrP^C

PrP^C is predominantly membrane GPI-anchored (at position Ser 231) glycoprotein (Stahl et al., 1987), but small portion of PrP^C is also in a soluble form. GPI-anchored form is concentrated in detergent-resistant discrete sphingolipid-sterol rafts (Peters et al., 2003), (Oesch et al., 1985). After the post-translational modifications (adding of GPI-anchor and N-linked oligosaccharides, cleavage of N-terminal 1-23 signal sequence and 231-253 signal peptide for GPI-anchor), which take place in endoplasmic reticulum and Golgi apparatus, it consists from 208 amino-acid residues with the molecular weight (MW) 30-35 kDa (Fig. 1). MW slightly differs due to the heterogeneity of oligosaccharides bound in two positions- N181 and N197. So far, more than 50 different oligosaccharide structures linked to the PrP^C were detected. We can recognize three major forms of PrP^C mono-, di-, and unglycosylated form. Between positions C179 and C214 is disulfide bond (Rudd et al., 2001), (Ermonval et al., 2003). C-terminus forms stable globular structure containing three α -helices, on the other hand N-terminus is flexible formed structure.

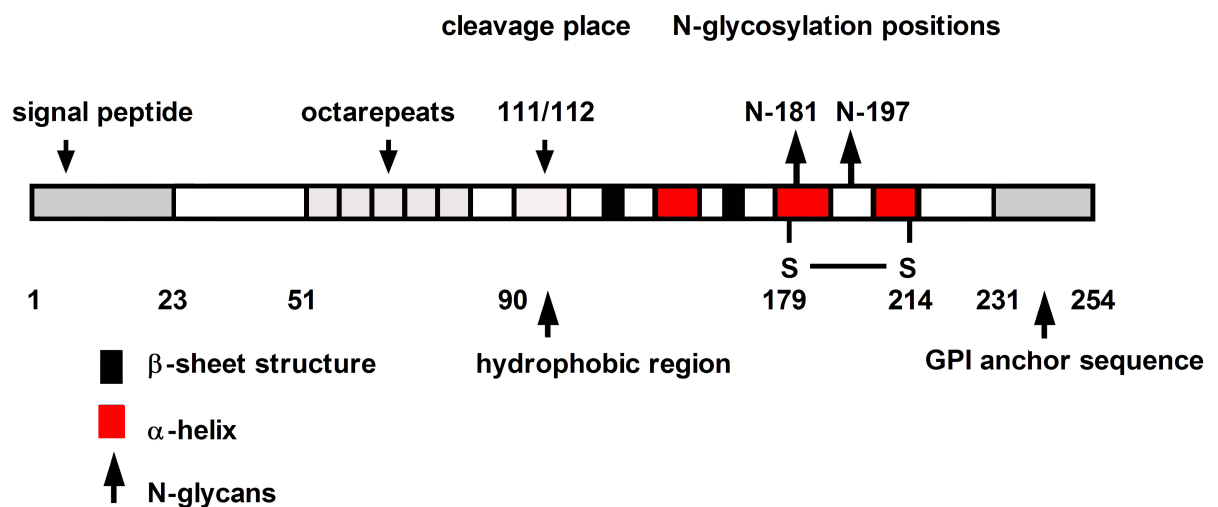


Figure 1: Schematic structure of PrP^C before post-translational modifications (adding of GPI-anchor and N-linked oligosaccharides, cleavage of N terminal 1-23 signal sequence and C terminal 231- 254 signal peptide for GPI-anchor). Final product has MW 30-35 kDa, which slightly differs due to the heterogeneity of oligosaccharides in positions- N181 and N197. Between the positions C179 and C214 is disulfide bond. Stable globular C-terminus contains three α -helices, whereas N-terminus is flexible structure.

1.3. PrP^{TSE} pathological isoform of PrP^C

Major event common to all TSEs is process of structural change from PrP^C to the abnormal isoform- PrP^{TSE}. During this conformational change, proportion of β -structure increases from 3% to 43%, while α -structure slightly decreases from 43% to 34%. The mechanism is poorly understood, but according the prion hypothesis, pathological prion molecules modify conformation of adjacent normal PrP^C molecules to the aberrant form directly by physical contact (Kupfer et al., 2009). Heterogeneity of PrP^C, presence of different glyco- and truncated forms may contribute to existence of the various PrP^{TSE} strains with different organotropism, incubation time, ability to cross the species barrier and so forth (Pan et al., 2002). The cell localization of this transition is unknown, since PrP^C cycles between the cell surface and early endocytic compartment in association with clathrin-coated pits (Shyng et al., 1994) or migrates to late endosomes and lysosomes via caveolae-containing endocytic structures (Vey et al., 1996). Situation is quite complicated since an unknown “third player” so called “protein X” or maybe more factors could be involved in the process of PrP^{TSE} formation (Telling et al., 1995). Some experiments show that nucleic acids may still participate in the prion propagation. Mixing of infected and uninfected brain homogenates led to the propagation of PrP^{TSE}, but after depleting of endogenous single-stranded RNA (ssRNA) Deleault and colleagues did not detect any amplification of PrP^{TSE}. Adding of exogenous RNA extracted from uninfected tissues increased prion amplification 24-fold, but the nature of relevant ssRNA is unknown. Process seems to be the species specific, because the RNA isolated from invertebrates did not support PrP^{TSE} amplification. Involvement of such additional factors in conversion from PrP^C to PrP^{TSE} gives rise a question if these cofactors in different species could be also somehow responsible for TSE strain diversities (Deleault et al., 2003). In addition, an interaction of small highly structured RNA with the human recombinant PrP (hrPrP) in absence of PrP^{TSE} caused resistance of hrPrP to proteinase K (Adler et al., 2003). Since such converted hrPrP was not infectious, it is questionable how tightly it could reflect *in vivo* conditions. Although Deleault did not observe influence of DNA to PrP^{TSE} amplification, Zou et al. using antibodies against DNA or against g5p, a single stranded DNA binding protein, immunoprecipitated from human brain homogenates PrP^{TSE}, but not PrP^C. However, as they wrote it remains unclear if binding of PrP^{TSE} to the DNA occurred after homogenization or such complex may originate also *in vivo* (Zou et al., 2004). If also nucleic acids are involved in PrP^C to PrP^{TSE} conversion then it has to be answered in which cell compartment they could interact together. Presence of nucleic acids in conversion and amplification of PrP^{TSE} does not go against “protein only hypothesis” since it counts with host encoded DNA and/or RNA and

not with RNA/DNA cotransferred with infectious agents. However, Manuelidis isolated novel circular DNAs from highly infectious culture and brain preparations. Both isolates resisted nuclease digestion. Uncovered sequences could have a role in TSE infections despite their apparently harmless, low-level persistence in normal cells (Manuelidis, 2010).

Castilla with coworkers contributed to this discussion showing that the only presence of infectious particle is enough for the conversion of PrP^C to PrP^{TSE}. In their experiment, they were able to mimic PrP^{TSE} propagation by *in vitro* cyclic amplification of PrP^{TSE}. Product of this cyclic amplification shares similar biochemical and structural properties like natural PrP^{TSE} preserving even its pathogenicity (Castilla et al., 2005). Although their work brought strong support for “protein-only hypothesis”, unfortunately answer for question of “protein only hypothesis” does not answer the question of what harms cells in the brain. Misfolded proteins has long half-life and accumulate as amyloid deposits in CNS, but presence and accumulation of nonneuronal PrP^{TSE} is not pathogenic. However, arresting the conversion of PrP^C to PrP^{TSE} within neurons during scrapie infection prevents prion neurotoxicity (Mallucci et al., 2003). Therefore, what directly kills the neuronal cells remains unclear. Could it be some toxic intermediate product during PrP^C to PrP^{TSE} shift or a lack of physiological PrP^C function? Recently it has been suggested that prions themselves are not neurotoxic but catalyse the formation of toxic species from PrP^C. Production of neurotoxic species is triggered when prion propagation is in plateau phase, leading to a switch from autocatalytic production of infectivity (exponential phase) to a toxic (plateau phase) pathway (Sandberg et al., 2011). Nevertheless, neurotoxic PrP properties may be tightly linked to the physiological role of PrP^C in cell.

1.4. Physiological function of PrP^C

1.4.1. PrP^{-/-} mice

The rational approach to an elucidation of the protein role may be to switch off such protein e.g. by creating knockout animal. This approach was also applied in effort to find out a role of PrP^C in mice. However, studies showed that mice lacking PrP^C surprisingly do not suffer from a loss of PrP^C, but are resistant to TSE infection and do not propagate PrP^{TSE} (Büeler et al., 1992), (Büeler et al., 1993). In other words, loss of the protein seemed to be more beneficial instead of malicious, quite unbelievable phenomena for highly conservative protein. Although, these experiments did not solve the mystery of PrP^C function, brought us interesting results.

First two knockout murine lines *Prnp*^{0/0} Zurich I (Büeler et al., 1992) and *Prnp*^{-/-} Edinburgh (Manson et al., 1994) had normal development and their behavior did not show any alteration, except some minor defects in circadian rhythm and sleeping (Tobler et al., 1996). More excitement were from next knockout lines *Prnp*^{-/-} Nagasaki (Sakaguchi et al., 1996), Rcm0 (Moore et al., 1999) and *Prnp*^{0/0} Zurich II (Rossi et al., 2001). These animals succumbed to degeneration of Purkinje cells and loss of myelin coat in peripheral nerves. In addition, symptoms disappeared when such animals were treated by *Prnp* transgene. The results seemed to be clear- symptoms were caused by lacking of normal PrP^C. However, detailed insight into the methods used in creation of these mice strains revealed the reason. By depleting of *Prnp* gene newly discovered gene *Prnd* lying downstream got under the *Prnp* promoter leading to the overexpression of *Prnd* gene in neurons (Moore et al., 1999), (Moore et al., 2001). Product of this gene, named Doppel protein (Dpl), is membrane bound GPI-anchored protein consisting from 179 aminoacid residues with sequence similarities to C-terminus of PrP^C. Dpl is constitutively expressed in high level in testes where it is essential for the sperm development and its lack causes male sterility (Behrens et al., 2002). Its expression in brain is tiny, but in above-mentioned knockout model, Dpl overexpression and absence of PrP^C resulted in onset of ataxia and death of cerebellar neurons. Neurodegeneration can be rescued by PrP^C expression. Considering Dpl homology with PrP^C, several models for Dpl-PrP^C interactions were described in which both proteins could bind to the same ligand with opposite effects or they have antagonistic functions in apoptotic pathway where PrP^C could be involved in neuroprotective way and Dpl in pro-apoptotic way. Nevertheless, the physiological role of PrP^C remains obscure.

1.4.2. RNA interference of PrP^C

RNA interference (RNAi) is considered as a one of the promising approaches to examine gene function. It provides advantage to avoid generating of knockout animals. The field of RNAi biology is relatively young and was introduced to wider scientific community only in last decade. However, the RNAi has been soon recognized to play crucial role in nearly all physiological or pathological processes. RNAi is an evolutionary conserved sequence specific gene knockdown that is induced by double-stranded RNA (dsRNA). The RNAi machinery can be triggered by experimentally designed and delivered, or endogenous sources of dsRNA. The natural endogenous pathway is initiated by micro RNA (miRNA) genes. Mature miRNAs are 19-24 nucleotide (nt) non-coding ssRNA molecules that regulate the expression of target genes through perfect or imperfect binding mostly to the 3'-UTR (untranslated region) of mRNA. Disproportion between the relatively small number of miRNA genes and number of

their target genes (in human 10%- 30% of all genes) can be interpreted that a one miRNA can potentially target several hundred genes and furthermore a single mRNA can be a target of multiple miRNAs. Endogenous RNAi pathway begins with transcription of primary miRNAs (pri-miRNAs) by RNA polymerase II into long RNA hairpin molecule. Subsequently, a complex that contains the RNase III enzyme Droscha processes primary transcripts resulting in ~70-90 nt stem-loop structures with 2-nt 3' overhangs known as precursor miRNAs (pre-miRNAs). The dsRNA-binding protein Exportin-5 then transports the pre-miRNA from nucleus into the cytoplasm. In cytoplasm, the pre-miRNA is recognized probably based on 2-nt 3' overhangs by complex of proteins containing Dicer. Dicer subsequently cleaves the pre-miRNA at single site ~22 nt from the end of the hairpin. Mature miRNA are symmetrical with 2-nt 3' overhangs at each end. However, only single strand is loaded to RNA-induced silencing complex (RISC). The mature miRNA binds to its target mRNA 3'-UTR while Argonaute protein 2 directs RISC to translational repression and subsequent mRNA degradation. This is true in case of imperfect miRNA binding, however, target mRNA is cleaved in case of perfect binding (Fig. 2) (Kim et al., 2009), (Winter et al., 2009).

First attempts to downregulate PrP^C expression dates back to 2003 where two reports occurred. They showed that transfection of anti-*Prnp* siRNAs to neuroblastoma N2a cells efficiently silenced PrP^C expression in dose response manner. Silencing led also to abrogation of PrP^{TSE} propagation in chronically scrapie infected N2aS12sc⁺ cells (Daude et al., 2003). The second group used rabbit kidney cells (RK13) cotransfected by the inducible plasmid expressing ovine PrP^C with the one of two vectors expressing shRNA. They showed that silencing effect depends on the degree of complementarity to target species specific mRNA (Tilly et al., 2003). Golding et al. reported that RNAi could be utilized to suppress PrP^C for production of prion disease resistant livestock and thus preventing transmission of prion diseases to humans via prion-contaminated meat. They described a strategy for using RNAi-based technique to create a cloned transgenic fetus with efficiently reduced expression of PrP^C (Golding et al., 2006). Pfeiffer et al. examined the potential of RNAi in therapy of prion disease *in vivo*. Since previous methodological approach using transfection of siRNAs or plasmid carrying anti-*Prnp* shRNAs by Daude and Tilly groups led only to transient downregulation of PrP^C, Pfeiffer's group used lentiviral vector which upon delivery to target cells is able to integrate to host cell genomic DNA. By injecting of lentiviral vector coding shRNA to the brain of prion-infected mice, they achieved reduced PrP^C expression and therefore less PrP^{TSE} formation in vicinity of delivery site. Nevertheless, prion diseases are typical by disseminated degeneration of neurons

over the brain. Therefore, beside the efficient, specific, and safe vector design, improved mode of lentiviral vector delivery should be found to target larger areas of tissue (Pfeifer et al., 2006). Although, initial experiments showed the potential power of RNAi method in possible therapy of prion diseases, RNAi based experiments focused on function of PrP^C have not brought us deeper insight as was expected.

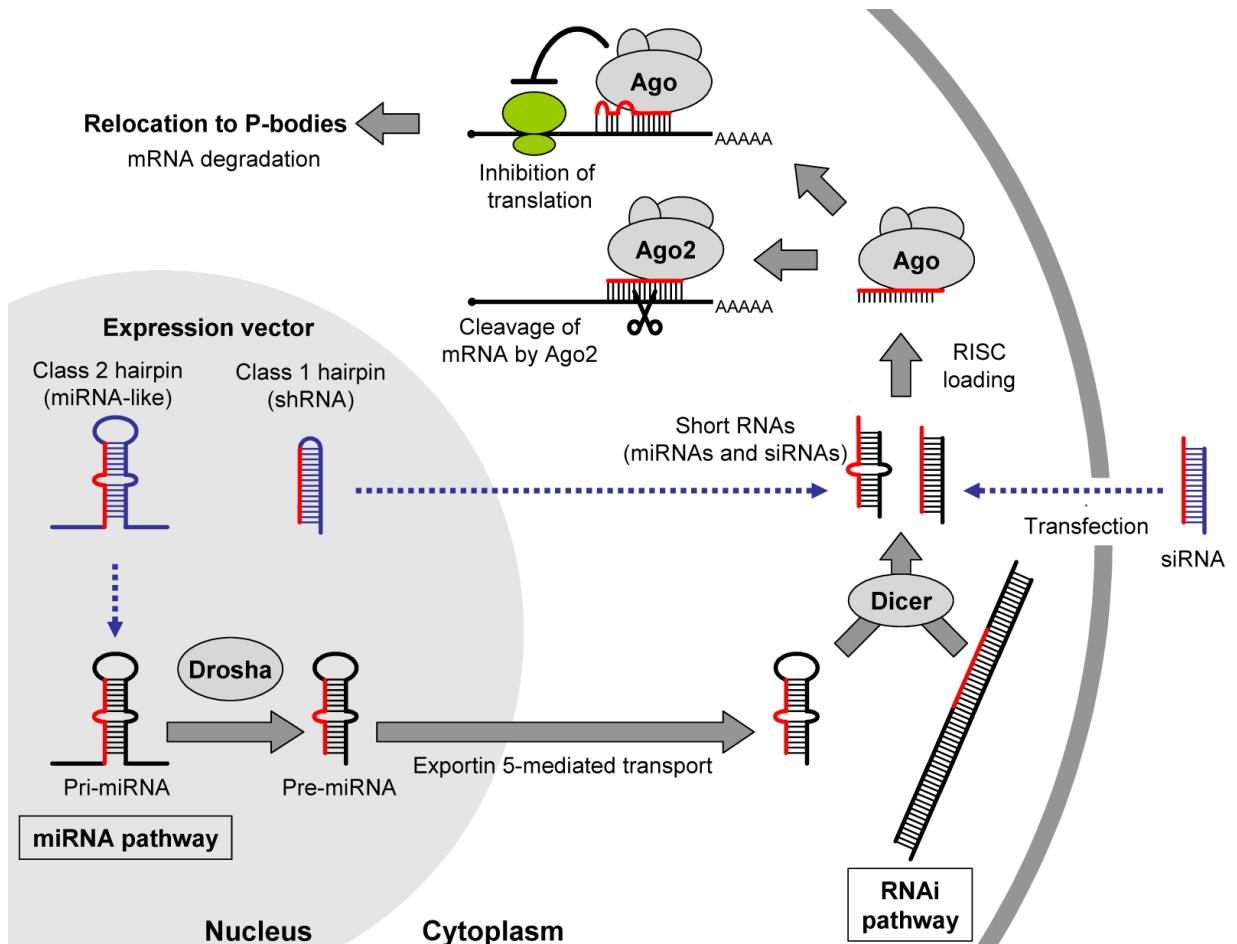


Figure 2: The schematic overview of the RNAi pathway triggered by endogenous micro RNA (miRNA) and exogenous short interfering RNA (siRNA) pathway. RNAi may lead to two mechanisms of post-transcriptional silencing, which share a common pathway. If the mRNA is directly cleaved or translation is inhibited depends on the degree of homology with a target mRNA, and the type of Argonaute protein (Ago). Pri-miRNA= primary miRNA; pre-miRNA= precursor miRNA; shRNA= short hairpin RNA. Published with kind permission from Dr. Svoboda (Svoboda, 2007).

1.4.3. Proposed function of PrP^C

Subcellular localization of any protein and its role in cell is tightly connected. PrP^C undergoes endosomal cell cycle internalized via clathrin-coated pits or caveolae-like domains. However, its primary localization where it exerts its role seems to be membrane rafts. Many receptors can be found in rafts, suggesting a high concentration of signaling complexes. These membrane domains then could act as multi-signaling ports (Horejsí et al., 1999), (Hoessli et al., 2000). Presence of PrP^C in such signaling gates suggests its role in some signal transduction pathways. As discussed below many roles in different tissues have been assigned for PrP^C. However, the amount of possible interactors may be misleading. Are these pathways equal as for their importance? Do these interactions act also *in vivo*? Therefore, relevance of all these interactions seems to be questionable.

The most highly abundant expression of PrP^C was found in developing and mature neuronal tissue. In addition, PrP^C was found in many other cells/ tissues e.g. Sertoli cells, spermatocytes, spermatids (testes), epididymis, follicular dendritic cells, megakaryocytes, haemopoietic progenitors, monocytes, red blood cells, endothelial cells etc. (Ford et al., 2002). From the below discussed physiological roles in various tissues can be inferred common or overlapping theme or proposal for its function differs but are not mutually exclusive. Nevertheless, PrP^C function in many tissues was not examined at all. So far, there is no consensus about PrP^C role in organism but several cellular processes are favored. One of the most frequently discussed cellular roles of PrP^C is a survival-promoting effect on neuronal and nonneuronal cells, which has been observed *in vitro* as well as in *in vivo*.

1.4.3.1. Antiapoptotic function

Some proteins are expressed only during the special conditions e.g. stress. Some of them are expressed continually in the absence of stress stimuli and may wait for their turn. Thus introducing the stress conditions to an experiment may help to elucidate role of such proteins. Since as shown below, neuronal cell cultures derived from Zurich I and Nagasaki murine strains were sensitive to external apoptotic stimuli we can speculate that PrP^C could be one of the proteins for „special-events“. This is suggested by its dispensability in normal circumstances, but its loss has impact on cell fitness during the stress conditions. Such alternative was observed in PrP^{-/-} mice after comparison with wild-type mice that were subjected to restraint stress, electric foot shock, or swimming. Among non-stressed knockout and wild-type animals, there was no significant difference in performance of tests measuring the anxiety levels and locomotion. However, PrP^{-/-} mice, after acute stress provoked by a foot

shock or a swimming trial, showed a significant decrease in anxiety levels and decreased locomotion when compared with control animals (Nico et al., 2005). Simple stress condition in cell culture could be facilitated by incubation of cells in serum-free medium as was shown in cells derived from PrP^{-/-} mice, which were more sensitive to serum withdrawal than cells derived from PrP^{+/+} mice (Kuwahara et al., 1999). Although details are not still known, several authors described association with apoptosis under stress conditions. Occurrence of cleaved Caspase-3 and PARP, increase of Bax and decrease of Bcl-2 expression as well as morphological changes and DNA fragmentation were described in neuronal cell line Hpl 3-4 derived from hippocampus of PrP^{-/-} mice. On the other side, transfection with *Prnp* transgene did not alter levels of Bax, Bcl-2 and p53 expression (Kim et al., 2004). Exact position of PrP^C in biology of apoptosis remains unanswered. Some reports demonstrated that intensity of cell protection mediated by PrP^C depends on the type of apoptotic trigger. There was reported only 30% success against oxidative stress with comparison to 100% against Bax mediated pathway (Bounhar et al., 2001).

Bcl-2 is one of the most important anti-apoptotic proteins in cell death regulation. It interacts through its BH2 domain with cytosolic pro-apoptotic Bax protein. Octarepeat domains of PrP^C present limited similarity to Bcl-2 BH2 domain, which suggest possible acting of PrP^C in Bcl-2 like manner (Bounhar et al., 2001). Deleting of these N-terminal octarepeats, which are required for copper binding and may play some role in oxidative stress, has prevented its neuroprotective function. In contrast to PrP^{-/-} mice, animals expressing recombinant PrP^C with truncated N-terminus postnatally underwent neuronal degeneration. How PrP^C interacts with Bax is unclear because Bounhar and coworkers discovered that GPI-anchoring is not necessary for the anti-apoptotic function of PrP^C since the free PrP^C can also maintain neuroprotective signal. A role in cell protection was observed also in wild-type neuroblastic cells from retinal explants. Apoptosis in cell culture was triggered by anisomycin, which inhibits protein synthesis. The effect of PrP^C in this system was investigated by PrP^C binding peptide (residues 113-128 of mouse PrP^C). Binding of peptide to PrP^C in wild-type neuroblastoma cells led to reduction of anisomycin-induced cell death about 50%. No reduction of cell death was observed in cells isolated from PrP^{-/-} mice. Incubation of explants was followed by activation of cAMP dependent kinase A (PKA) and extracellularly regulated kinases (Erk) pathways.

PrP^{-/-} retinal cells did not show such kind of activation. Treatment of PKA with its inhibitor blocked neuroprotection mediated by PrP binding peptide, whereas inhibitor of the Erk-activating protein potentiated the protective effect (Chiarini et al., 2002). It seems also that PrP^C is involved in protection of carcinoma cells. Overexpression of PrP^C rendered MCF-7

breast tumor cells resistant to apoptosis induced by TNF- α , TRAIL, and Bax (Diarra-Mehrpour et al., 2004). Involvement of PrP^C was suggested to cause higher resistance of gastric carcinoma cell lines to chemotherapeutic agents (Du et al., 2005).

However, Christensen and Harris revalued former assays reporting protective activity of PrP^C (Kuwahara and Diarra-Mehrpour) and suggested that presence of PrP^C has only modest effect in cytoprotection *in vitro* (Christensen and Harris, 2008).

1.4.3.2. Protection against copper mediated oxidative stress

First data about possible connection between PrP^C and copper metabolism comes from early 70s when prion-like disease was observed in histological samples from patients treated with Cu²⁺ chelator cuprizone (Pattison et al., 1971). Later it was described that histidine residues in the mammalian most conserved region of PrP^C, octameric (PHGGGWGQ) in N-terminus bind Cu²⁺ with high affinity (Brown et al., 1997), (Stöckel et al., 1998). Binding of other divalent metals are due to lower affinity less probable. Concentration of copper in brain was estimated to be ~ 80-100 μ M but it seems to be higher in specific brain region. This concentration lays in interval 100-500 μ M of copper concentration, which was demonstrated to enhance the internalization of PrP^C in cultured neuroblastoma cells (Pauly and Harris, 1998). Free copper is able to change superoxid to other toxic substances (Fenton reaction). Thus binding of free copper to proteins can reduce toxic risk of free Cu. Presence of PrP octarepeat peptide in neuronal cell culture had protective effect against copper toxicity. The protective effect of this peptide was strongest in cell culture derived from *Prnp*^{-/-} mice (Brown et al., 1998). In neurons, large amount of copper was found in synapses together with PrP^C. In addition, mice expressing higher levels of PrP^C had upon the exposure to radioactive Cu⁶⁷ increased radioactivity in immunoprecipitated Cu,Zn superoxid dismutase (SOD), which is an enzyme important in antioxidant defense. Furthermore, increased levels of PrP^C were linked to increased levels of Cu,Zn SOD activity. However, mice either lacking or overexpressing PrP^C had levels of Cu,Zn SOD mRNA equivalent to those expressed in wild-type mice (Brown and Besinger, 1998). Nonetheless, later *in vivo* study did not confirm contribution of PrP^C to SOD activity (Hutter et al., 2003). Protective role of PrP^C against Cu-mediated oxidative stress was exhibited also in astrocytes (Brown, 2004). Astrocytes are non-neuronal cells that perform many functions, including biochemical support to the nervous tissue, maintenance of extracellular ion balance, and a role in the repair of brain and spinal cord after injuries (Kimelberg, 2010). Astrocytes expressing PrP^C can uptake Cu²⁺ released from neurons. This transfer could be inhibited by an anti-PrP antibody. Furthermore, astrocytes can uptake PrP^C

with bound copper released from neurons. Copper is subsequently bound to ubiquitously expressed metallothionein proteins, which bind both physiological and xenobiotic heavy metals. Metallothioneins thus serve in regulation of metal metabolism and in protection from a variety of stress conditions after exposure to toxic elements such as cadmium and mercury. Copper can be subsequently exported from the brain bound to ceruloplasmin, a major Cu-carrying protein in the blood (Kim et al., 2008). These processes propose that astrocytes play an important role in regulating of Cu^{2+} levels in brain, and PrP^{C} is suggested to participate in this process. Nevertheless, Cu^{2+} uptake is independent on presence of PrP^{C} (Brown, 1999), (Nishihara et al., 1998).

1.4.3.3. PrP^{C} in signaling cascades

Anchoring of PrP^{C} in lipid rafts confers its prospective function in cell signaling. There are known potential interactors but still it is unclear in how manner they are connected together and how the signal is conducted, since PrP^{C} has no direct contact with cytosolic compartment. However, the family of PrP^{C} counter players is still growing. According Aguzzi's recent review several experimental approaches- yeast- two hybrids, co-immunoprecipitations and cross-linking methods identified ~45 distinct proteins interacting with PrP^{C} . They reside in almost all cellular compartments- membrane proteins (N-CAM, Laminin Receptor precursor), soluble/ extracellular (ApoE, Laminin, Plasminogen), cytoplasmic (Stress Inducible protein 1, α -tubulin), mitochondrial (Hsp60) or nuclear (CBP70). However, it is probable that many of the proposed interacting proteins may be false positive results caused by protocol design e.g. artificial exposure of PrP^{C} to unusual proteins in yeast two-hybrid system, detergent in immunoprecipitation allowing unspecific PrP^{C} -protein interactions (Aguzzi et al., 2008).

Mouillet-Richard et al. used *in vitro* neuroectodermal progenitor cells 1C11 with an epithelial morphology lacking neuron-specific functions, which upon induction developed neuron-like morphology and finally differentiated to the two cell lines- serotonergic and noradrenergic. Both lines expressed PrP^{C} continually during the entire differentiation. After the cross-linking of PrP^{C} with antibodies 1A8 and SAF61, they observed time- and lineage-dependent activation of Fyn a member of Src- phosphotyrosine kinases. Although PrP^{C} level was similar in both lineages through the time, activation of Fyn was detectable on 4th day for serotonergic and 12th day in noradrenergic line. Spatial variability was also observed. In both lines neurite fraction of PrP^{C} transduced signal to Fyn in higher level than PrP^{C} localized in cell body. Since the PrP^{C} is located at the outer side of membrane and Fyn in inner side without possibility of direct physical contact, there is a question what transduces signal between them. Authors identified

caveolin 1 α and caveolin 1 β as the most possible transducers. Although results are inspiring, authors were unable to notice any downstream changes (Mouillet-Richard et al., 2000). Moreover, their result was not so far repeated and some authors showed that in their model (rat cerebellar granule cells) PrP^C does not colocalize with Fyn (Botto et al., 2004).

Connection with the Src kinase was also described in human Caco-2/TC7 enterocytes (Morel et al., 2004). In these cells, PrP^C is targeted to the junctional complexes of the lateral membranes of adjacent polarized cells. Co-immunoprecipitation revealed that PrP^C interacts with Src kinase, but not with E-cadherin, which interacts with Src and is the major component of junctional complexes. Connection between PrP^C and Src-family kinases was supported also by Nixon (Nixon, 2005). He hypothesized that if the aggregation of GPI-linked proteins activates Src-family kinases then the aggregation of PrP^{TSE} could promote unregulated activation of kinases. Indeed, in his study he presented supporting findings that the increase of expression in Src-family kinases is due to the presence of PrP^{TSE}. He did not find elevation of Src-family kinases in healthy mice with increased expression of PrP^C. Increase of expression in Src-family kinases occurred concurrently and preceded symptom onset. Similar results were obtained in scrapie propagating ScN2a cell culture and two discrete animal models of prion disease- RML-inoculated mice and in Tg2866(MoPrP-P101L)PrP^{-/-} mice, a mouse equivalent of the PrP mutation causing the familial human prion disease Gerstmann-Strausler-Scheinker disease. However, direct connection between PrP^{TSE} and Src-family kinases still was not demonstrated. The involvement of PrP^C in signaling pathway of presynaptic nerve terminals was suggested also by PrP^C co-immunoprecipitation with Grb2 and Synapsin I. Synapsin I is associated with synaptic vesicles and together with another highly conserved synapsins is required for a regulation of neurotransmitters release. Expression of Synapsin I is not restricted only to neuronal tissue, but it was found also in cells with intensive exocytosis. Grb2 is an intracellularly localized adaptor protein involved in intracellular signal transduction where it links extracellular signals coming to intracellular signaling molecules. Therefore, interaction of Grb2 protein with PrP^C may provide signal from extracellular receptors to intracellular molecules (Spielhaupter and Schätzl, 2001). However, how and where PrP^C interacts with Grb2 and Synapsin I is not known. Solfrosi et al. who found out huge neuronal loss in hippocampal area after cross-linking of PrP^C by antibodies targeting 95-105 region proposed different involvement of PrP^C in neuronal cell signaling *in vivo*. Authors offered speculative explanation that antibodies mediated disruption of survival signal between or among PrP^C and unknown molecules. Interestingly, another antibody used in this work IgG D18 binding to region 133-

157 did not alter the proposed signal. The answer on this discrepancy may lie in the involvement of different region in signal maintenance (Solforosi et al., 2004).

1.4.3.4. PrP^C in iron metabolism

Role of PrP^C in iron uptake and transport, both *in vitro* and *in vivo*, was recently evaluated by Singh with collaborators. They found that overexpression of PrP^C in human neuroblastoma M17 cells correlated with increased level of transitory iron, which serves as a crossroad of cell iron metabolism between labile iron pool and ferritin bound Fe. Concomitant with the iron sufficiency, level of Transferrin (Tf) and Transferrin receptor (TfR) decreased. On the other side, mutated PrP molecules expressed in similar level as PrP^C showed altered levels of labile iron pool and Fe deposits in ferritin. Diverse iron levels specific to mutated PrP were maintained even in the presence of extracellular Fe excess, pointing out to the relevance of PrP^C in the Fe uptake and subsequent transport. Authors suggest that PrP^C function predominantly in uptake of Fe rather than release, since no cell line had altered iron transport to growth medium (Singh et al., 2009a). In their next study, Singh et al. demonstrated systemic iron deficiency in PrP^{-/-} mice, which was rescued after PrP^C introduction. In comparison with wild-type mice, PrP^{-/-} mice exhibited lower levels of iron in the plasma, brain, liver, and spleen. In response to iron insufficiency Tf and TfR compensated the state by increasing their levels and decreasing the levels of the iron storage protein- ferritin. Authors hypothesize that iron deficiency in PrP^{-/-} mice have two reasons- inefficient transport from gut to the blood and impaired uptake by recipient cells. PrP^C in enterocytes mediates iron export from the basolateral membrane of enterocytes to the blood stream rather than uptake from the intestinal lumen. This was supported by the accumulation of radioactive iron in duodenal enterocytes of PrP^{-/-} mice instead of its transport out to the blood like in wild-type mice. Contrary to enterocytes, hematopoietic PrP^{-/-} cells have impaired uptake of Fe despite the compensating effect of Tf/TfR pathway and even despite the sufficient iron level in the spleen and bone marrow. Since most of the iron (~ 80%) is used in erythrocytes, it is not therefore surprising that erythropoiesis in PrP^{-/-} mice is ineffective. Authors did not notice pronounced anemia in PrP^{-/-} mice, however they detected e.g., a mild reduction in hemoglobin levels, a significant reduction in serum iron, and an increased number of circulating reticulocytes (Singh et al., 2009b).

1.4.3.5. PrP^C in cell adhesion

Several studies suggest that PrP^C may function in adhesion or like a recognition molecule. PrP^C was described to bind like a ligand to Laminin receptor precursor (LRP)/Laminin receptor (LR) (Rieger et al., 1997), (Gauczynski et al., 2001). The binding to LRP/LR mediates internalization of PrP^C into clathrin-coated pits. Sense of this interaction is generally unclear, but the role of LR like a receptor for extra cellular-matrix proteins laminin and elastin could propose the possible involvement of PrP^C in this interaction. Laminin is required for cell growth, differentiation, and migration. Upon the blockade of PrP^C by antibodies, Graner et al. observed abolishment of adherence in pheochromocytoma PC-12 cells to laminin leading to inhibition of laminin-mediated differentiation (Graner et al., 2000). It is probable that adhesion is not the sole function of PrP^C, but through the interacting adhesion partners may transduce signal to the cell. For example, PrP^C could interact with intracellular signaling pathway through the transmembrane neural cell adhesion molecules (NCAM) (Santuccione et al., 2005). Authors suggested model in which interaction between PrP^C and NCAM at the neuronal surface promotes recruitment of NCAM to lipid rafts. Translocation of NCAM to lipid rafts subsequently lead to the association of NCAM with the receptor type protein phosphatase α (RPTP α), a Fyn activator. The final result of the activation is enhanced neurite outgrowth.

1.4.3.6. PrP^C and endogenous retroviruses

Endogenous retroviruses (ERVs) are stably integrated in the genome of vertebrates, their origin is derived either from ancient germ-cell infections by exogenous retroviruses or from ancestral retroelements by transposition and recombination. In mice or humans, they compose approximately 10% of the genome sequences. According their sequences they are divided to several groups as reviewed for example by Stocking and Kozak (Stocking and Kozak, 2008). ERVs contribute to diverse pathological and physiological cellular processes, in particular to autoimmunity and reproduction (retrovirally derived proteins Syncytin A and B are crucial for a formation of multinucleated tissue in placenta- syncytiotrophoblast). They confer to genomic plasticity and they may regulate adjacent genes. ERVs are highly susceptible to endogenous and exogenous stimuli- cytokines, steroids (dexamethasone), and some chemicals (5-azacytidine) (Taruscio and Mantovani, 2004). Connection of ERVs with prions dates back to 90s of last century when Akowitz et al. identified Syrian hamster sequences of Intracisternal A Particles (IAP) present in both CJD and uninfected samples. Although they may represent normal endogenous viral contaminants that cosediment with infectivity, their long terminal repeats (LTRs) can drive the expression of many diverse sequences, and it remains to be

elucidated if CJD specific sequences are either transduced, or copackaged with protected IAP complexes (Akowitz et al., 1993). Later Stengel et al. questioned whether scrapie infection might influence the expression pattern of murine ERVs. For this purpose, they compared hypothalamic neuronal GT1 cells and neuroblastoma N2a cells to their counterparts ScGT1 and ScN2a chronically infected by mouse prion adapted RML strain. First, they identified by qualitative microarray analysis six ERVs common for both tested cell lines (*ERV-L*, *MuRRS*, *IAP-1*, *MLV*, *VL30* and *VL30-2*). Quantitative real-time PCR (qRT-PCR) analysis confirmed that prion infection has an influence on *IAP-1* and *MLV* expression in both ScN2a and ScGT1 cell lines. Analysis revealed that there is no common reaction to prion infection shared by all ERVs. Nevertheless, there is a general trend in ERVs regulation depending by the cell lines. Treatment of prion infected ScN2a cells by pentosan polysulphate (PPS) led to the similar level of ERVs expression to uninfected N2a cells. These effects were specific to treatment since the PPS alone did not induce changes in ERVs expression in PrP^{TSE} free cells. The overall result of this study proposes that murine ERVs such as *MLV* and *IAP-1* are responsive to prion infection and are potentially involved in prion pathogenesis (Stengel et al., 2006). Jeong and colleagues described correlation of ERVs expression in humans with sporadic CJD (sCJD) (Jeong et al., 2009). They revealed significant increase in the frequencies of several ERVs in cerebrospinal fluid (CSF) of individuals with sCJD compared to normal controls. Furthermore, occurrence of *HERVW* and *HERV-L* were significantly increased in CSFs of sCJD compared to incidences in individuals with other neurological diseases. Their observation is in agreement with previous studies showing an effect of prion infection on mouse ERVs (Carp et al., 1999), (Lee et al., 2006). Leblanc et al. observed that infection of NIH3T3 cells by Moloney Murine Leukemia Virus (MoMuLV) together with 22L prion strain strongly enhances the release of PrP^C and PrP^{TSE} from coinfecting cells. Furthermore, they observed that prion proteins are released in the supernatant in association with MoMuLV particles confirming thus their association with exosomes. They hypothesize that retroviruses are involved in the spreading of the PrP^{TSE} (Leblanc et al., 2006). Some murine neurovirulent retroviruses, although does not require the prion protein, induce spongiform encephalopathies, which share some features with prion diseases e.g. ataxia, spongiform degeneration, astrogliosis, and lack of infiltrated inflammation (Szurek et al., 1988), (Jolicoeur et al., 1996). However, Leblanc with coworkers observed negative impact of PrP^C on the retroviral infection. They saw that increased expression of PrP^C resulted in a specific decrease of HIV-1 envelope and viral protein R expression. Furthermore, they spotted that HIV infectivity in the presence of PrP^C was reduced up to 4-fold (Leblanc et al., 2004). Nucleocapsid protein as the major nucleic acid-binding protein of the retroviral

particle is tightly associated with the genomic RNA in the virion nucleocapsid, where it chaperones RNA dimerization, packaging, and proviral DNA synthesis by reverse transcriptase. Human PrP^C functionally resembles nucleocapsid protein of HIV-1 and it appears that N-terminal fragment (23-144) of PrP^C possesses the DNA-binding properties, whereas the C-terminal domain is inactive (Gabus et al., 2001a), (Gabus et al., 2001b)

Taken together, it remains to be elucidated if the changes in the expression of ERVs are direct consequence of prion infection or just side effect. Similarly, possible functional link between PrP^C and retroviral infection waits for explanation.

1.5. Erythropoiesis

1.5.1. Introduction

Erythropoiesis is a complex multistep process comprising differentiation of hematopoietic stem cells (HSCs) to mature erythrocytes to maintain steady state level of red cells. In adult humans, almost whole process occurs in the bone marrow. However, in mice erythropoiesis takes place also in the spleen. Erythropoiesis begins from HSCs, which are self-renewing and multipotent, which means that they are ancestors of all blood cell lineages. The erythroid development from HSCs to enucleated red blood cells involves pathway through several cells stages. HSCs give rise to multipotent progenitor (MPPs) cells, which lose self-renewal capacity. The next stage is common myeloid progenitor (CMPs) following by differentiating stage of megakaryocyte-erythroid progenitors (MEPs). After MEPs, we can observe first erythroid lineage-committed cells- early erythroid progenitors BFU-E (Burst-Forming Units- Erythroid) and subsequently late erythroid progenitors CFU-E (Colony-Forming Units- Erythroid). This is the first stage characteristic for erythroid differentiation (Fig. 3). The second phase involves developmental sequence of morphologically identifiable erythroid precursors- proerythroblasts, basophilic erythroblasts, polychromatophilic and orthochromatic erythroblasts. This period of differentiation is characterized by four distinct steps- accumulation of hemoglobin, expansion of erythroblasts, cell size decrease, and irreversible condensation of chromatin leading to loss of nucleus. Whole process advances in association with macrophages within the bone marrow cavity. The cell-cell interaction between macrophage and erythroblasts creates “erythroblast island”, which serves as a stromal microenvironment for erythroid maturation. During this association, macrophage supplies the erythroblasts with iron, brings individual erythroblasts to physical proximity so they can interact each other, and finally macrophage engulfs extruded nucleus from erythroblasts (Fig. 3)

(Chasis and Mohandas, 2008). The final third differentiation part is represented by reticulocyte maturation and erythrocyte circulation. During reticulocyte maturation, translation is interrupted and internal organelles are degraded by autophagy. Rebuilding of cytoskeleton leads to classic biconcave and discoid shape of red blood cell. In humans, 24-48 hours after entering the circulation reticulocytes lose remaining ribosomes and mature to erythrocytes. Red blood cells then circulate approximately 120 days, after which they are recognized and engulfed by spleen macrophages (Ingley et al., 2004), (Wickrema and Kee, 2009).

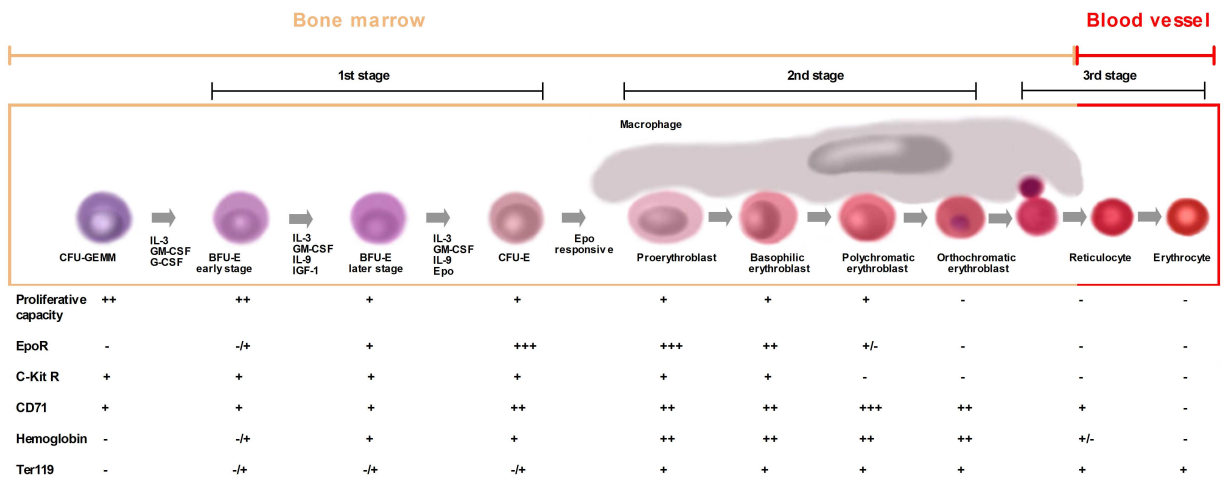


Figure 3: Lineage specific stages of erythropoiesis. Phases of erythrocyte differentiation are divided according the tissue origin (bone marrow and circulation in blood vessels) and erythroid lineage maturation characterized by three progressive steps: 1st stage (Committed progenitors- BFU-E, CFU-E), 2nd stage (erythroblast precursors) and 3rd stage (late reticulocytes and enucleated erythrocytes). Cellular characteristics are based on relative proliferation, cytokine responsiveness, cell surface markers, and/or presence of RNA. CFU-GEMM= colony forming unit-granulocyte, erythroid, macrophage, megakaryocyte; BFU-E= burst forming unit-erythroid; EpoR= erythropoietin receptor; CFU-E= colony forming unit-erythroid; C-Kit R= stem cell factor receptor, CD71= transferrin receptor. Image is modified version of figures by Torbees and Friedman in Erythropoietins, Erythropoietic Factors, and Erythropoiesis: Molecular, Cellular, Preclinical, and Clinical Biology (Elliott et al., 2009) and Palis in Molecular Basis of Hematopoiesis (Wickrema and Kee, 2009).

1.5.2. Regulation of erythropoiesis

1.5.2.1. Erythropoietin is primary erythropoietic growth factor

Erythropoietin (Epo), 30-34 kDa glycoprotein is the main erythroid growth factor. The crucial role of Epo and its receptor (EpoR) is confirmed by knockout studies that showed that Epo^{-/-} or EpoR^{-/-} mice die in embryonic stage. Primary site of Epo production in adult mammals is localized in kidney peritubular interstitial fibroblasts. However, expression of Epo has been

found also in extrarenal tissues (e.g. brain, liver), yet its physiological role in these tissues is not clear. Furthermore, knockout mice for extrarenal Epo are viable with no observable pathological signs. Epo concentrations are inversely related to hemoglobin concentration. In response to Epo stimulation, its concentration in blood can increase several fold depending on hemolytic insult. It is noteworthy that Epo production depends on circadian rhythms. Interestingly, Epo is not required for development of BFU-E *in vivo*. It suggests that Epo does not recruit multipotent cells to erythroid differentiation. Rather, Epo support the growth, survival and differentiation of already committed cells to erythroid differentiation. This is confirmed by the presence of EpoR, which is expressed during normal physiological conditions primarily on CFU-E and immature erythroid precursors. EpoR has not been found upstream of first erythroid committed cells until later BFU-E with the highest expression on CFU-E and proerythroblasts. Epo^{-/-} and EpoR^{-/-} embryos have normal BFU-E and CFU-E counts. Although *in vitro* forming of colonies by BFU-E and CFU-E requires Epo, only CFU-E responses to Epo *in vivo*. Activation of EpoR transduces the signal through the EpoR/Jak2/Stat5 signaling (Jelkmann, 2004), (Torbees and Friedman in Elliott et al., 2009).

1.5.2.2. Epo regulation

Erythrocytes production and Epo concentration in serum is directly correlated. However, the rate of erythropoiesis change is smaller than the rate of Epo expression, which suggests that red blood cell's abundance is mainly controlled by exposure of erythroid-committed cells to Epo and not by Epo concentration itself. The primary trigger for stimulation of Epo expression is oxygen tension. A hypoxia activates Hypoxia inducible factor 1 (HIF1) which binds to enhancer (Hypoxia Response Element, HRE) of *Epo* gene stimulating thus its transcription. HIF are dimeric proteins composed from α - and β -subunit. There are three α - subtypes, but only subtype 1 α - is together with β -subunit considered as primary mediator of hypoxia induced gene expression. Both HIF-1 α and HIF-1 β are continuously produced; their transcription is not elevated by hypoxia induction. However, level of HIF-1 α is barely detectable during normal oxygen level. HIF-1 β is constantly localized in nucleus. During normoxic conditions, HIF-1 α is hydroxylated at the proline residues (402 and 564). Such labeled HIF-1 α is tagged by von-Hippel Lindau protein (pVHL) which forms complex with E3 ubiquitin ligase. Subsequently polyubiquitinated HIF-1 α is immediately degraded by proteasome. During hypoxic conditions, HIF-1 α is not hydroxylated and can enter to the nucleus and dimerize with HIF-1 β . Dimers then bind to HRE and stimulate transcription of target gene (Jelkmann, 2004), (Tsiftoglou et al., 2009).

1.5.2.3. Stem cell factor

In addition to Epo, other growth factors play important role in hemathopoiesis. Notably, Stem cell factor (SCF) and its tyrosine kinase receptor SCF-R (known also as c-kit) perform important role in early hematopoietic cells. Majority of hematopoietic progenitor cells express c-Kit. Its expression is maintained at high level until BFU-E and CFU-E phase, after this stage its level declines and disappears in polychromatophilic and orthochromatic erythroblasts (Fig. 3). Overall signaling pathways downstream the c-Kit are complex and essential for regulating proliferation, survival and promoting immature state. During erythroid differentiation, expression of c-Kit decreases along with decreased proliferation of erythroid progenitor cells (Tamir et al., 2000), (Rönstrand, 2004), (Zhang and Lodish, 2008).

1.5.2.4. Iron as a regulator of erythropoiesis

Iron metabolism, cellular heme and erythropoiesis are inseparably connected. The major source of iron for erythrocyte precursors is iron bound to transferrin (Fe-Tf) in plasma. The low iron supply in the bone marrow results in iron-restricted erythropoiesis or anemia. The level of cellular heme (derived in part from plasma and partially from *de novo* biosynthesis in mitochondria) is very critical in the regulation of erythropoiesis. Heme biosynthesis is dramatically increased under hypoxic conditions or stress erythropoiesis. Moreover, heme regulates the action of transcription factors for globin and nonglobin genes. HIF promotes iron transport by upregulating Tf and the TfR. Furthermore, HIF increases intestinal iron absorption and mobilization of recycled iron from macrophages. Thus, it appears that HIF simultaneously stimulates the erythropoiesis to encounter hypoxia and enhance the availability of iron to fulfill higher demand in erythropoietic precursors. Coupling of erythropoiesis mediated by EpoR signaling and iron metabolism was shown in mice lacking Stat5, which suffered a reduction in the levels of transferrin receptor-1 (TfR-1) on erythroid cells (Nemeth, 2008), (Haase, 2010). Recently, a new mechanism through which hemoglobin may be modulated according to iron status has been proposed. The mRNA of α -hemoglobin stabilizing protein (AHSP) contains a sequence at the 3'-UTR mRNA that resembles the iron responsive element (IRE) (dos Santos et al., 2008). Through this sequence, iron regulates the expression of AHSP, which acts like a molecular chaperone that binds and stabilizes free α -globin during hemoglobin synthesis.

1.5.2.5. Regulation of erythropoiesis on transcriptional level

Central role in erythroid differentiation is facilitated by GATA1, which interacts with other proteins to increase expression of erythroid-specific genes by binding to GATA-binding motif presented in promoters/ enhancer of all erythroid genes. GATA1 is predominantly known as a transcriptional activator of erythroid-specific genes, but it also downregulates several genes (*c-kit* and *c-myc*). GATA1 is expressed in erythroid, megakaryocytic, eosinophils, and Sertoli cells in testis. In erythroid progenitors, its expression is hardly detectable but began rapidly expressed after Epo induction with highest levels in CFU-E and erythroblasts. GATA^{-/-} mice are not viable and die *in utero*. In addition to DNA binding activity, other transcription factors like e.g. Friend of GATA1 (FOG1) enforce their activity through protein-protein interactions. FOG1 is abundantly expressed in erythroid and megakaryocytic lineages alongside GATA1. Its lack shows similar pattern like loss of GATA1 suggesting that FOG1 helps GATA1 in arranging hemathopoiesis. PU.1 is essential for the development of granulocytic, monocytic and lymphoid cells. Its overexpression in murine model results in erythroleukemia, because it blocks erythroid maturation. On the other side, forced expression of GATA1 in myelomonocytic lineage directs cells into erythroid, megakaryocytic and eosinophilic cells. Thus, it seems that GATA1 and PU.1 antagonize each other. GATA1 interferes with PU.1 function by competing with its co-activator c-Jun, whereas PU.1 blocks DNA binding activity of GATA1. C-Myb is a transcription factor activating transcription via interactions with coactivator proteins, mainly CBP/p300. Both coactivators are related proteins, which bind also to others transcription factors. Complex CBP/p300 provides bridging the c-myb with transcription machinery and influence the chromatin context by their acetyltransferase activity. Beside the modification of histones, they acetylate the c-Myb increasing thus its affinity to DNA. Expression of c-Myb is predominantly limited to proliferating progenitor cells and is repressed in differentiating cells. Overexpression of c-Myb leads to inhibition of erythroid and myeloid cell differentiation. C-Myb is required for expansion of erythroid progenitors, but have to be downregulated to permit differentiation to mature erythrocytes. Proliferating proerythroblasts express c-Myb, but downregulate it upon addition of Epo, which stimulate erythroid differentiation. The repression of c-Myb is mediated by GATA-1. Erythroid proliferation depends on the combined action of Epo and SCF, erythroid differentiation requires only Epo. Phenotype of mice with mutated SCF or its receptor (c-Kit) resembles the phenotype of c-Myb deficient mice- prenatal lethality due to the impaired definitive erythropoiesis, but not primitive. It suggests that at least partially c-Kit may mediate function of c-Myb in erythroid cells. Moreover, c-Myb was found to bind to the c-Kit promoter

and inducible inhibition of c-Myb expression in erythroblasts leads to decrease of c-Kit expression. C-Myb was proposed to direct the progenitor cells toward the erythroid commitment. This was shown in mice with reduced c-Myb expression, which led to accumulation of immature cells expressing GATA-2, PU.1 and Fli1, which are normally downregulated to promote erythroid commitment (Perry and Soreq, 2002), (Greig et al., 2008).

1.5.2.6. Involvement of miRNA in erythropoiesis

Unlike in other areas of hemathopoiesis, the role of miRNA in erythropoiesis has not been extensively studied so far (Lawrie, 2010). In the first study where erythroid associated miRNAs was mentioned, authors observed a general increase in miRNA levels during the erythroid differentiation (Lu et al, 2005). Interestingly, miRNA expressed early in erythroid maturation can be found even in erythrocytes. The comparison between reticulocytes and erythrocytes revealed that 83 miRNAs were downregulated in reticulocytes but 8 miRNAs were surprisingly upregulated in erythrocytes (Chen et al., 2008). The role of miRNAs in circulating erythrocytes remains mysterious. Several speculative functions are predicted waiting for the proof. The miRNAs in red blood cells may be part of the defense mechanism against malaria parasite (erythrocyte miR-451 was reported to be transferred to malaria parasite), miRNAs may be released into bloodstream from broken erythrocytes and may be taken up by other cells, or erythrocyte miRNAs can function in macrophages after their engulfment by spleen macrophages (Zhao et al., 2010). It seems that from several regulated miRNAs the locus miR-451/144 plays central role in erythropoiesis. Both miRNAs are regulated by the GATA1 and are highly abundant in reticulocytes and erythrocytes. Mice deficient for the miR-451/144 cluster display an impairment of late erythroblast maturation, resulting in erythroid hyperplasia, splenomegaly, and a mild anemia. Both miRNAs are completely different and probably they target distinct sets of mRNA, thus inhibit erythropoiesis additively. Although miR-451/144 are most highly expressed in erythroid cells, several reports found their involvement also in other tissues, e.g. regulating epithelial polarity or protecting cardiomyocytes against ischemic and oxidative stress (Dore et al., 2008), (Papapetrou et al., 2010). The overall role of miRNA in erythropoiesis was shown in AGO2 deficient mice, which had severe abnormalities in erythropoiesis characterized by accumulation of immature Ter119⁺ cells (O'Carroll et al., 2007).

1.5.4. Murine erythroleukemia cells- *in vitro* model for erythroid differentiation

Infection of susceptible mice strain by Friend spleen focus-forming virus (SFFV) lead to acute erythroleukemia. SFFV encodes unique envelope glycoprotein gp55, which covalently interacts with EpoR. Binding of gp55 to EpoR causes its constitutive activation leading to cell proliferation in absence of Epo signal (Nishigaki et al., 2001). For the efficient infection mice must possess at least one copy of Fv-2^S gene. Gene Fv-2^S encodes truncated short form of the receptor tyrosine kinase Stk (sf-Stk). Mice expressing only full length Stk are resistant to SFFV infection in comparison with mice carrying short form allele. Expression of sf-Stk is limited only on erythroid cells but interestingly have no apparent role in normal erythropoiesis. The early phase of infection is distinguished by rapid increase in number of proerythroblastic cells, which cause hepatosplenomegaly that may lead to death by spleen rupture. Infected proerythroblasts differentiate in absence of Epo or they are hypersensitive to Epo. Although numbers of Friend virus-infected cells increase markedly they are not tumorigenic *in vivo*, instead they still have limited proliferative capacity. However, after two-three weeks post infection, proerythroblast subpopulation blocked in erythroid differentiation emerges and invade organism. This leukemic population is extremely proliferative, may be serially transplanted *in vivo* and is able to establish cell lines *in vitro*- murine erythroleukemia cells (MEL). Malignant transformation of erythroid cells are caused by insertional mutagenesis of Friend virus to the host genomic DNA. Characterization of integrational site showed that in 95% cases SFFV is integrated to locus- *spi-1* (SFFV proviral integration site). Integration of SFFV in *spi-1* locus leads to subsequent overexpression of its mRNA, which is activated by transcriptional enhancers encoded by SFFV LTR sequence. Increased production of Spi-1 protein cooperates with the constitutive signaling from gp55/EpoR/sf-Stk in malignant transformation of proerythroblasts. Furthermore, loss or mutations in p53 tumor suppressor gene boost the growth and survival of leukemic proerythroblast cells. Ectopic p53 expression in such cells reverses apoptosis and hemoglobin production. It was shown that Spi-1 is identical to the transcription factor PU.1, which downregulation is necessary for normal erythroid differentiation. Spi-1/PU.1 abrogates erythroid differentiation by physical interacting with GATA1, however overexpression of exogenously delivered GATA1 can limit tumorigenic potential and restore differentiation program (Ruscetti, 1999), (Moreau-Gachelin, 2008). Interestingly, in 1971 Friend et al. described that incubation of MEL cells (known also as Friend cells) with dimethylsulfoxide (DMSO) return cells to their determination and mimic erythroid differentiation (Friend et al., 1971). Later, hexamethylene bisacetamide (HMBA), the next widely used inducer was described (Reuben et al, 1976). This unique characteristic made MEL cells an extensively used model for

the study of murine erythroid differentiation *in vitro*. Upon induction, proliferative capacity is limited to four-five cell divisions followed by cell cycle arrest. Process is characterized by structural/ morphological (decrease in cell volume and nucleus condensation) and biochemical changes (activation of erythroid genes, hemoglobin accumulation etc.) which resemble natural erythroid differentiation (Sato et al., 1971), (Hyman et al., 2001). The stochastic kinetics of inducer-mediated differentiation consists from two phases. Addition of inducer (HMBA or DMSO) triggers a latent period, which lasts approximately 12-14 hours post induction. This early phase is associated with a number of reversible metabolic changes (Fibach et al., 1977). Upon withdrawal of cells during latent phase from growth medium containing inducer, cells continue in their indefinite proliferation. There is no commitment to terminal erythroid differentiation, which is defined as the capacity of cells to express characteristics of terminally differentiated cells beyond their removal from inducer. After latent period, the proportion of committed cells arises and after 48 hours, most of the cells are irreversibly determined to erythroid differentiation (Chen et al., 1982), (Murate et al., 1984). Induction of MEL cells to erythroid differentiation is connected with the regulation of proto-oncogene expression e.g. *c-myb*, *c-myc*, *c-fos* and *p53*. Particularly regulation of *c-myb* expression may be critical for commitment to terminal erythroid differentiation. HMBA induction leads to the commitment of more than 95% of the cells by 48 hours. This is accompanied by a persistent suppression of *c-myb* transcription and an increase in the *c-fos* and *c-myc* mRNA, which return to levels found in uninduced cells by 12 hours. Dexamethasone, an inhibitor of induced commitment, does not prevent regulation of *c-myb*, *c-myc* and *c-fos* genes in early period but it prevents the persistent suppression of *c-myb* mRNA, which appears to be critical for cell transition to committed phase (Ramsay et al., 1986). Furthermore, Clarke with colleagues observed that continuous *c-myb* expression from exogenously introduced human *c-myb*, driven by an SV40 viral promoter led from a partial to complete inhibition of erythroid differentiation of MEL cells despite a decline of endogenous *c-myb* transcripts (Clarke et al., 1988). Supporting information that *c-myb* expression maintains MEL cells in immature and proliferative state was shown also in MEL cells transfected with construct coding dominant interfering *myb* allele under the transcriptional control of the inducible mouse metallothionein I promoter. Its expression stimulated by ZnCl₂ led to interference with endogenous *c-myb*, hemoglobin production and inhibition of proliferation (Chen et al., 2002).

1.6. Expression and the role of PrP^C in blood cells

1.6.1. PrP^C expression on blood cells

Although the highest expression of PrP^C is in brain, many peripheral tissues including blood cells express PrP^C as well. Its expression is regulated during differentiation to various lineages. In humans, PrP^C was found as early as on bone marrow CD34⁺ multipotential hematopoietic stem cells. During stem cells differentiation to the granulocyte lineage, its expression is downregulated, but is maintained in lymphoid and monocyte lineages (Dodelet and Cashman, 1998). PrP^C was found in T (CD4⁺ and CD8⁺) and B lymphocytes, natural killer cells, monocytes, dendritic cells and follicular dendritic cells (FDCs) (Li et al., 2001), (Barclay et al., 1999), (Isaacs et al., 2008). Expression of PrP^C in human erythroid precursors is also decreasing along maturation towards erythrocytes. Cultivation of CD34⁺ cells in the presence of SCF, IL-3, and Epo led to accumulation of cells in the proerythroblast stage expressing a large amount of intracellular PrP^C with weak cell surface PrP^C. After 11 days, *ex vivo* culture consisted from a heterogeneous population of basophilic erythroblasts and pronormoblasts with lower PrP^C expression and its minimal presence on outer membrane. PrP^C was found mostly in the perinuclear region of pronormoblasts rapidly cycling from the plasma membrane to internal membranes. Subsequently, colocalization experiments suggested that most of the PrP^C is in the endosomal compartment. PrP^C colocalized with the TfR, which is known to be endocytosed in clathrin-coated vesicles. Furthermore, significant proportion of PrP^C on the plasma membrane of erythroblasts is not located in lipid rafts (Griffiths et al., 2007).

A substantial amount of cell-associated PrP^C in blood resides in platelets. Platelet activation leads to upregulation of PrP^C on their surface and release of PrP^C on exosomes and microparticles. Contrary to erythroblasts, majority of PrP^C in platelets is localized within platelet lipid rafts linked to the platelet cytoskeleton (Brouckova and Holada, 2009). Presence of PrP^C on circulating erythrocytes has been already reported (Holada and Vostal, 2000), (Barclay et al., 2002), but so far the proportion of erythrocyte-associated PrP^C on the pool of blood cell-associated PrP^C was largely underestimated (Panigaj et al., 2010).

Comparative analysis of PrP^C expression with different animal species revealed unique patterns of PrP^C expression on blood cell types, with none equivalent to the human pattern (Holada and Vostal, 2000), (MacGregor and Drummond, 2001), (Barclay et al., 2002). Significant differences in PrP^C expression on platelets, erythrocytes and leukocytes isolated from human and nonhuman primates observed Holada with colleagues (Holada et al., 2007). Chimpanzees, rhesus macaques, squirrel monkeys displayed a much higher quantity of total blood cell

membrane PrP^C than humans. In contrast, cynomolgus macaques and lemurs demonstrated substantially lower levels of membrane PrP^C. The expression of PrP^C on erythrocytes seems to be a critical, due to the high proportion of erythrocytes on blood cell count. All species displayed PrP^C on white blood cells, with the highest levels found on human cells. Only humans, chimpanzees, and rhesus macaques expressed PrP^C on platelets. Differential expression of PrP^C in various species including laboratory animals highlights that we should be cautious in extrapolation of observations of prion infectivity associated with blood to humans.

1.6.2. The role of PrP^C in hemathopoiesis

1.6.3. PrP^C supports self-renewal of Long term hematopoietic stem cells

Although bone marrow from PrP^{-/-} mice has normal level of progenitor and differentiated cells, there is an evidence that in some circumstances PrP^C plays role in hemathopoiesis. Flow cytometry analysis showed that PrP^C is already present on the surface of all Long term hematopoietic stem cells (LT-HSC). This was proved by reconstitution of hematopoietic system in lethally irradiated mice, since such repopulation ability is hallmark of LT-HSC. PrP⁺ donor cells isolated from wild type (WT) mice repopulated both lymphoid and myeloid compartments in comparison with PrP⁻ fraction. This suggests that PrP^C is marker for LT-HSCs. Insight to the possible role of PrP^C in activity of HSCs was gain by competitive reconstitution assay. BM cells from PrP^{+/+} or PrP^{-/-} mice were cotransplanted in equal amount together with competitor WT cells to lethally irradiated mice. First recipient mice showed equal donor cells engraftment irrespective of PrP expression. Second irradiated group received BM cells from first group of transplanted mice and interestingly after the engraftment, cells of PrP^{-/-} origin comprised only 30% of blood cells in comparison with PrP^{+/+} cells (60%). The similar trend was observed also in third group of irradiated mice receiving BM cells from the second group. This steady decrease of PrP^{-/-} cells contribution to repopulated blood cells suggests that lack of PrP^C impairs self-renewal of HSCs. To rule out unforeseen effects of competitor BM cells to investigated BM PrP^{+/+} and PrP^{-/-} cells, they were transplanted to lethally irradiated mice without competitor cells. Again, in first group of recipients all mice survived. Second and third group of mice received BM transplants according previous scheme. Interestingly, in second group 86% mice with PrP^{+/+} BM cells survived but only 57% with PrP^{-/-} BM cells. Difference in survival of third group was more profound, 67% PrP^{+/+} BM mice survived but no PrP^{-/-} BM mouse. PrP involvement in the survival of BM cells was confirmed by rescue experiment where PrP^C was retrovirally delivered to PrP^{-/-} BM cells. Half of the mice with exogenously expressed PrP survived but no mice in

control group expressing retrovirally introduced green fluorescent protein (GFP). The same situation was observed when irradiated mice obtained BM cells expressing mutant PrP (deletion 23-72). These supplementing experiments confirmed that full length PrP^C supports engraftment during serial transplantations (Zhang et al., 2006). Interesting regulation of PrP^C expression was found in *ex vivo* culture system for expansion of repopulating HSCs. Only 6% of freshly isolated BM lineage negative cells expressed PrP^C, but after 10 days of cultivation, proportion of PrP^C positive cells increased up to 60%. Surprisingly, all LT-HSCs activity in these cultured cells resided in PrP^C negative cells and not in PrP^C fraction. It shows that expression pattern of PrP^C in fresh HSCs is different from cultured. Identical regulation was described also for receptor tyrosine kinase Tie-2 which is involved in maintenance of quiescent state of BM HSCs. Authors of the study suggest that PrP^C like Tie-2 can act as a sensor for signals generated by the BM microenvironment and play a role in regulation of HSC quiescence (Zhang and Lodish, 2005).

1.6.4. The role of PrP^C in cells of immune system

Several authors recently discussed possible role of PrP^C in immune system (Isaacs et al., 2006), (Hu et al., 2007), (Aguzzi et al., 2008). PrP^C is upregulated shortly after T cells exposure to mitogenic activation with concanavalin A or phytohaemagglutinin (Mabbott et al., 1997). In contrast to the relative ease of PrP^C upregulation in activated T cells, treatment with lipopolysaccharide does not increase PrP^C expression on B cells (Kubosaki et al., 2003). Role in macrophages was shown by de Almeida et al. who observed that *in vitro* macrophages from PrP^{-/-} mice had higher rates of phagocytosis than P^{+/+} macrophages. Their *in vitro* finding was confirmed also *in vivo*, where knockout mice showed more efficient phagocytosis of zymosan particles than wild-type mice (de Almeida et al., 2005). Generally, the role of PrP^C in the immune system is more complex and is out of the scope of this work.

1.6.5. PrP^C is involved in anemia recovery

In mice, 40% of adult BM cells harbor PrP^C, from these more than 80% is erythroid cells (Zhang et al., 2006). Link between PrP^C expression and maturation of erythrocyte precursors was shown in KO mice after experimental induction of hemolytic anemia (Zivny et al., 2008). Three days after treatment with phenylhydrazine, hematocrit decreased similarly in KO and WT mice from ~ 40 to 30%. Recovery of KO mice in day five and seven was behind the recovery of WT mice. Similarly, number of reticulocytes was lower in KO animals for days three and five. On day seven level of reticulocytes was the same for both groups however in WT mice the number decreased on tenth day but in KO stays almost on the same level. In

addition, the response of spleen to anemia was more profound in WT animals than in KO. The weight of WT mice spleens was higher (~ 0.6 g) on fifth day and rapidly decreased on day seven in comparison with KO mice where spleen weight was lower (~ 0.4 g) and remained the same on day seven. After next three days, there was not difference in spleen size irrespective the PrP^C presence. Interestingly, based on the presence of Ter119⁺ cells, no evidence was observed in the number of erythroid precursors in BM cells in neither KO nor WT mice. The same “starting point” before the anemia suggests that impaired onset of recovery in KO mice lies downstream of erythroid differentiation. Authors suggest two possible answers. Although the level of apoptosis before onset of hemolytic anemia is similar, five days after induction the signal- mean fluorescence intensity of apoptotic cells in KO animals was ~ 2-fold higher. The second difference possibly responsible for slow recovery of KO mice was lower Epo production. Both, on the protein level in plasma and on mRNA level in kidneys, significantly higher (3-fold) expression was found in WT mice on day three. Moreover WT mice downregulated Epo in plasma to basal level on day five whereas KO mice on day seven. Similar rapid decrease in corresponding days was observed on the *Epo* mRNA level of WT mice while KO mice decreased *Epo* expression on day five and seven only weakly and both groups achieved basal expression on day ten. In addition, the authors showed that erythroid precursor cells of both origins have the similar potential to produce red blood cells. This was observed after treatment of mice with single dose of darbepoietin. All animals responded by equal production of reticulocytes, which gradually peaked at day three. Higher apoptosis rate in challenged KO mice suggests involvement of intrinsic factors affecting activated erythroid precursors to sustain higher demand for erythrocyte production. However, normal response in all animals to darbepoietin points out that inadequate reaction to anemia of KO mice is not caused by intrinsic factor rather it is caused by lower Epo production. Since Epo production is activated by hypoxia, there may be the problem between hypoxia sensing and/ or induction of target genes (Zivny et al., 2008).

1.6.6. *Prnp* gene is regulated in growth arrested and differentiated MEL cells

The first work describing regulation of PrP^C in erythropoietic model system *in vitro* was done by Gougomas and colleagues. They found out that transcription of PrP^C differed markedly during exponential growth and growth arrested phase. Northern blot showed that *Prnp* mRNA is barely detectable in exponentially dividing MEL cells and becomes gradually upregulated when cell density in culture arises (up to 144 hours). Upon dilution of growth-arrested cells, PrP^C is downregulated again. Similar pattern was observed also in MEL cells induced to erythroid differentiation by DMSO. Upregulation of *Prnp* expression was noted only in committed cells. The highest level of *Prnp* mRNA was at 48 hours, which correlated to >50% of hemoglobin positive cells, then slightly decreased, and again was upregulated at 120 hours after induction of differentiation. During the course at 96 hours, 36% of cells accumulated in G1 phase and 50% in S phase, which was attributed to asynchronous cell population. The *Prnp* gene activation in G1 phase of differentiating cells is not due to the growth arrest mediated by nutrition depletion rather G1 is caused by differentiation. Supporting notion that *Prnp* mRNA accumulation in G1 phase resulted from growth arrest was seen after exposition of differentiating cells to an inhibitor of commitment N⁶-methyladenosine (N⁶mAdo). MEL cells induced to differentiation in presence of N⁶mAdo activated *Prnp* gene in similar manner like untreated cells reaching cell confluence. Furthermore, DMSO resistant cells similarly accumulated *Prnp* mRNA when became confluent. These data indicate that *Prnp* gene is transcriptionally activated in DMSO treated or confluent cells arrested in G1 phase of the cell cycle (Gougomas et al., 2001). These observations led Gougomas et al. to investigate if the growth arrest by serum deprivation will change transcription of *Prnp* gene. Their initial experiments showed that *Prnp* was activated after 60 hours in cells growing under normal serum level, but in culture with 0.1% (v/v) serum *Prnp* was upregulated after 36 hours. On the other side, transcription of gene coding for proapoptotic protein *Bax* was simultaneously suppressed in corresponding time of *Prnp* activation. Activation of *Prnp* and suppression of *Bax* occurred along with detectable DNA fragmentation. Also in terminally differentiated cells, *Bax* was suppressed at time of *Prnp* activation and DNA fragmentation. To find out if there is a correlation between *Prnp* upregulation and apoptosis presented by DNA fragmentation, authors increased *Prnp* level by transfection of MEL cells with vector coding for *Prnp* cDNA. However, DNA fragmentation in differentiated cells with higher *Prnp* transcription was comparable to cells with normal *Prnp* transcription. Similarly, no protective effect was observed in uninduced MEL cells challenged to apoptosis by incubation in 0.25% (v/v) serum (Gougomas et al., 2007).

1.6.7. Erythroid genes are deregulated with prion pathogenesis progression

CNS is the only organ in body functionally affected by TSEs. From that point, it is obvious that most of the research is aimed at PrP^C biology in neurons. However, presence of PrP^C in lymphoid tissue and blood cells plays important role in prion neuroinvasion. During prion infection, prior to brain invasion and occurrence of clinical signs, prions are propagated in peripheral cells of lymphoreticular system and peripheral nerves. This period spans several years and is one of common attributes of TSEs. First connection between prion pathogenesis and erythropoiesis was suggested in mice by downregulation of unknown erythroid specific mRNA during prion disease, at that time named Erythroid differentiation related factor (*EDRF*) (Miele et al., 2001), presently known as Erythroid associated factor (*Eraf*). Subsequent studies showed that mRNA of the unknown gene codes for abundant protein that binds to free α -globin and prevents its precipitation, therefore was named α -hemoglobin stabilizing protein (AHSP) (Kihm et al., 2002), (Feng et al., 2004). Following study revealed that disease progression also affected transcription of several other murine erythroid genes e.g. *Kell*, *GPA*, *band 3* and *ankyrin* (Brown et al., 2007).

1.6.8. Blood as a source of prion infectivity and specimen for diagnosis of prion disease

Natural infection by prion disease is acquired orally or through skin wounds. However, we do not know how exactly the infectious prion protein reaches its peripheral targets. Presence of infectivity in blood may occur before or after invading the CNS. Especially the immune system plays important role in prion diseases. This is based on the observation that immunodeficient mice lacking B and T lymphocytes are resistant to peripheral prion inoculation. This could be reversed by BM transplantation (Lasmézas et al., 1996). FDCs are the principal sites for amplification of PrP^{TSE} in lymphoid tissues during the early phase of infection, before the disease spreads to the nervous system (Brown et al., 1999). However, recently Loeuillet et al. showed that the level of PrP^C expression in the hematopoietic compartment does not influence the time course of the induced disease (Loeuillet et al., 2010). They compared infectivity of two different mouse inoculates ME-7 and RML strains, which neuroinvasion is in both strains dependent upon the presence of FDCs, but have different affinity for BM derived cells. Mice reconstituted with BM expressing different levels of PrP^C (KO, WT and overexpressing) have the same incubation time (Loeuillet et al., 2010). Until recently, in modern societies, the only documented mode of transmission from human to human was iatrogenic cases in which disease was spread via contaminated neurosurgical instruments, tissue grafts or hormones (Brown et al., 2000b). However, since the year 2003,

four cases of probable transmission of vCJD by blood transfusion were described in United Kingdom (UK) (Llewelyn et al., 2004), (Gillies et al., 2009). So far such possibility was documented only in laboratory animals (Hewitt et al., 2006), (Brown, 2005), (Mathiason et al., 2010). It seems that number of vCJD cases in UK decreases (3 vCJD cases in 2010 in comparison to 28 cases in 2000¹). However, due to the long and asymptomatic subclinical phase, number of infected individuals may be higher irrespective to manifestation of disease. These cases may constitute threat of iatrogenic transmission due to the broader organotropism of vCJD. The situation requires development of sensitive and non-invasive detection method for prion diseases. Yet, the effort for a development of such method is complicated by absence of the molecular marker other than PrP^{TSE} itself, although Miele et al. recently found that α_1 -antichymotrypsin (α_1 -ACT) was highly upregulated in brains of scrapie-infected mice and as well in urine of patients suffering from sCJD (Miele et al., 2008).

Blood is an ideal source for diagnostic screening tests, but detection of PrP^{TSE} in blood is problematic. Properties of blood PrP^{TSE} are unknown. Moreover, its detection is complicated by significant amount of poorly characterized PrP^C, which could interfere with PrP^{TSE} detection on blood cells. According current knowledge, most of cell-associated PrP^C resides on platelets and leukocytes. Presence of PrP^C on erythrocytes was proven by flow cytometry, but opinions about its expression on erythrocytes are considerably various (0-50 % of total cell membrane bound PrP^C in blood) (Barclay et al., 1999), (MacGregor et al., 1999), (Holada and Vostal, 2000), (Barclay et al., 2002). Analysis of results suggested that the difference could be caused by the use of different antibodies. To clarify this issue is one of the goals of this study.

The only known difference between PrP^C and PrP^{TSE} is their conformation that enhances difficulties with PrP^{TSE} detection not only in blood. Although several antibodies discriminating PrP^{TSE} were described, none of the PrP^{TSE}-specific antibodies are currently used in commercial diagnostic tests, which usually depend on proteinase K treatment to distinguish partially resistant PrP^{TSE} from sensitive PrP^C (Korth et al., 1997), (Curin Serbec et al., 2004). Interesting approach was adopted by Safar et al., who developed „conformation dependent immunoassay“. Method is based on different affinity of 3F4 anti-PrP antibody to native and denatured PrP^{TSE}. Its epitope is hidden in central part of PrP^{TSE} molecule, but is exposed after its denaturation. Comparison of signals from native and denatured part of sample allows PrP^{TSE} detection (Safar et al., 1998). An et al. established method for the detection of infectious PrP from the blood utilizing the multimeric feature of PrP instead of using protease digestion. They hypothesized that some epitopes that are unique in the monomer protein are present in greater numbers on the multimeric forms. They devised a multimer specific ELISA system which resembles a

traditional sandwich ELISA, except that the capturing antibody, that is attached to a solid surface, and the detecting antibody are directed against the same or overlapping epitopes. This means that capturing antibody blocks epitope on monomer, therefore, it is not found with the detecting antibody. Thus, only protein multimers are detected (An et al., 2010). Soto and coworkers developed technique termed protein misfolding cyclic amplification (PMCA) which enables PrP^{TSE} amplification in the test tube. This method is based on the conversion of large amounts of PrP^C triggered by undetectable quantities of PrP^{TSE}. PrP^{TSE} aggregates are sonicated to generate multiple smaller units, which serve as a seeds for formation of new PrP^{TSE}. The cyclic conditions are analogical to PCR cycling (Saborio et al., 2001). PMCA has been first used to detect PrP^{TSE} in hamster blood showing 6,600-fold increase in sensitivity over standard detection methods. Authors reported a capability to detect as little as 8,000 PrP^{TSE} molecules (Castilla et al., 2005). Recently Tattum with colleagues succeeded to amplify infectious PrP from blood of presymptomatic RML-infected mice (Tattum et al., 2010). They used whole blood reasoning that this is the most practical material to use for blood screening, moreover containing the infectivity associated with all fractions. They did not observe proteinase K resistant PrP in control normal whole blood after several rounds of sonicating by PMCA, suggesting that this represents the amplification of real PrP^{TSE} present in the animals' blood rather than *de novo* generation of PrP^{TSE} that has been already reported (Deleault et al., 2007). Different organotropisms of prion strains represent another challenge for a detection of infectious prion proteins in blood. Recently Edgeworth et al. developed a solid-state binding matrix to capture and concentrate disease-associated prion proteins and coupled this method to direct immunodetection of surface-bound material (Edgeworth et al., 2011). They analyzed a masked panel of 190 whole blood samples from 21 patients with vCJD, 27 with sporadic CJD, 42 with other neurological diseases, and 100 normal controls. From this panel, they positively identified 15 samples all from patients with vCJD showing 71% effectivity of detection (Edgeworth et al., 2011). If infectious prion proteins in patients with sCJD are also present in blood remains unclear, although it should be investigated since sCJD patients comprise 85% of all cases. Importance of vCJD detection in blood is obvious since all so far described cases of PrP^{TSE} transmission by blood transfusion were vCJD. Moreover, vCJD prion strain shows broader organotropism with substantial presence in lymphoreticular tissues (Wadsworth et al., 2001). Occurrence of PrP^{TSE} in peripheral tissues of vCJD patients together with their relatively young age (~30 years) make vCJD patients the most probable source for iatrogenic transmission.

2. Aims of the study

The objective of our studies was to contribute to the understanding of the importance of PrP^C in physiology of blood cells, and its possible involvement in TSE pathogenesis in blood system. The knowledge of the PrP^C biology of blood origin can be subsequently applied in a development of non-invasive detection methods that are not still introduced in general use.

Particular goals of my study:

1. To characterize the biochemical properties of the PrP^C on human red blood cells and to reveal the reason for disproportions in published data concerning quantity of erythrocyte-associated PrP^C.
2. To study the importance of PrP^C expression for erythroid differentiation utilizing murine models.
 - To describe regulation of PrP^C on erythroid precursors during their differentiation *in vivo* and *in vitro*.
 - To introduce and optimize methodology of RNAi into our laboratory.
 - To describe the effect of PrP^C silencing on erythroid differentiation using the model system of MEL cells.
3. To study the effect of prion infection on erythroleukemic MEL and neuronal CAD5 cell cultures with silenced transcription of *Prnp*.

3. Material and Methods

3.1. Human samples

Citrate-anticoagulated blood of healthy volunteers was provided by the Transfusion department of Institute of Hematology and Blood Transfusion in Prague. Samples of cord blood were provided by the Institute for the Care of Mother and Child in Prague. Normal brain samples (lobus frontalis) were provided by the Institute of Pathological Medicine (First Faculty of Medicine, Charles University, Prague, Czech Republic). The collection of samples was conducted in accordance with the Helsinki Declaration.

3.2. Cell cultures

MEL cell line- clone 707 was purchased from European Collection of Cell Cultures (ECACC, Salisbury, UK). MEL and murine fibroblast derived NIH3T3 cells were maintained in DMEM growth medium with high glucose (4.5 g/L), L-glutamine, sodium pyruvate, 10 % fetal bovine serum (FBS), 100 U/mL penicilin and 100 µg/mL streptomycin (all reagencies PAA, Pasching, Austria). Packaging human HEK293 GP2 (Clontech, Mountain View, CA, USA) and Phoenix line (Allele Biotechnology, San Diego, CA, USA) both derived from human embryonal kidney cells were cultivated in the same conditions like MEL and NIH3T3 cells. Catecholaminergic neuronal tumor CAD5 cells (provided by Charles Weissmann Department of Infectology, Scripps, Florida) were cultivated in Opti-mem (Invitrogen, Carlsbad, CA, USA), 10 % FBS, penicilin and streptomycin. All lines were kept in 37 °C, humidified atmosphere with 5% CO₂. For all experiments, MEL cells between 2nd -4th passage were seeded at density 10⁵ cells/mL 24 hours before induction to differentiation by 5 mM HMBA, final concentration (Sigma Aldrich, St. Louis, MO, USA). Cell densities for other cells were adjusted according the purpose of experiment. Viability and cell numbers were determined by Trypan Blue exclusion assay by counting in Bürker chamber or in cell counter- Countess (Invitrogen).

3.3. Animals/ Mice

In the present work we used PrP^{+/+} mice of mixed background (C57BL/6x129/SvxCD1). The study was approved by the Committee on the Ethics of Animal Experiments of the First Faculty of Medicine, Charles University in Prague (Permit Number: 217/07).

3.4. Chemicals

During the study, MEL cells were treated with various chemical compounds to modify their physiology. One day prior to each treatment, MEL cells were diluted in growth medium to cell density 10^5 cells/mL. At point 0 hours, HMBA and/ or appropriate compound were added to growth medium. If not stated otherwise, all chemicals were purchased from Sigma. Azacitidine (5-Aza-2'-deoxycytidine; 5-AzaC) was used to regulate gene transcription by inhibition of methyltransferases- causing demethylation in particular sequence. Similarly, Trichostatin A (TSA) was used to alter gene transcription by inhibition of the class I and II mammalian histone deacetylases. Dexamethasone (DEX) was used to inhibit erythroid differentiation. To chelate iron from growth medium we used Desferral (DSFRL) (Invitrogen). Their respective concentrations are noted later in part "Results".

3.5. Flow cytometry

Quantitative fluorescence-activated cell sorting (FACS) analysis was performed on FACS Canto II flow cytometer (Becton Dickinson, San Diego, CA, USA) equipped with BD FACSDiva Software v6.0 (Becton Dickinson). For detection of PrP^C of human and murine origin we used following monoclonal antibodies (mAbs) at saturating concentrations: FH11, AG4, AH6 (TSE Resource Centre, Compton, UK), 3F4 (MAB1562, Chemicon Inc., Temecula, CA, USA), and 6H4 (Prionics AG, Zürich, Switzerland) labeled either with fluorescein isothiocyanate (FITC) or phycoerythrin (PE). Antibodies bind to different PrP^C epitopes as depicted in the figure 4. Standard beads (Bangs Laboratories, Inc., Fishers, IN, USA) were used for construction of calibration regression line, and the number of immunoglobulin (Ig)G molecules bound per cell was calculated as described previously (Holada et al., 2007).

MEL cells were washed with 1% BSA-PBS and labeled for 20 min, room temperature (RT) in a final volume of 50 μ L with AH6-PE (10 μ L) and 1 μ L of CD71-PE (eBioscience, San Diego, CA, USA). After incubation with mAbs, cells were washed and resuspended in 1% BSA-PBS and analyzed. Viable cells were identified as 7-AAD (Molecular Probes, Eugene, OR, USA) negative population. Mouse BM cells were isolated from femurus by washing with 1% BSA-PBS/ 2 mM EDTA (BPE). Sliced spleen and BM cells were passed through a 40 μ m cell strainer (Becton Dickinson) to eliminate stroma and debris. Approximately one million cells in final 50 μ L volume were labeled 30 min, at 4°C in dark with following mAbs: 4 μ L anti-mouse Ter-119 eFluor 450 (eBioscience), 0.5 μ L anti-mouse CD71-FITC (eBioscience) and 10 μ L of AH6-PE. Labeled cells were then three times washed and resuspended in BPE. Only live cells were acquired. Erythroblast subpopulations from BM and spleen were resolved according

Ter119, CD71 and forward-scatter (FSC) signals. Proerythroblasts (pro.E) were identified like Ter119^{medium} CD71^{high} and FSC^{high} cells. Ter119^{high} cells were divided using both the CD71 and FSC parameters into three populations, labeled Ery.A, Ery.B and Ery.C, as described previously (Liu et al., 2006).

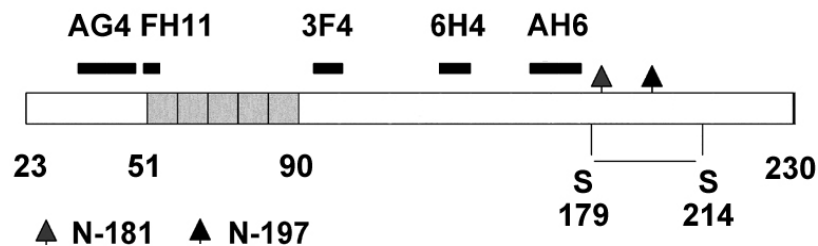


Figure 4: Schematic structure of posttranslationally modified human PrP^C. Locations of the octarepeats region (51-90), two N-glycosylation sites (181, 197) and the disulfide bridge (179- 214) together with anti-PrP^C mAbs epitopes used in the study are shown. In this work we used following mAbs- AG4, FH11, 3F4, 6H4, and AH6.

3.6. Preparation of brain homogenates and cell lysates

Human or murine brain tissue was homogenized (10% w/v) in ice-cold Tris buffered saline (TBS; 20 mmol/L Tris and 145 mmol/L NaCl, pH 7.4) with 1 mmol/L EDTA and 1 mmol/L phenylmethylsulfonyl fluoride (PMSF). Coarse fragments were removed (4000 x g, 10 min, 4°C) and the supernatant was stored frozen in aliquots at -80° C. Prior to lysis, cell cultures were washed 3 times in ice-cold PBS. Pellets devoided of serum proteins were lysed in 150 mM NaCl, 1% TX-100, 0.5% Sodium deoxycholate, 0.1% sodium dodecyl sulfate (SDS), 2 mM MgCl₂, 12 units/μL Benzonase (Sigma) and 50 mM Tris, pH 8.0 including EDTA free protease inhibitor Complete (Roche Diagnostics GmbH, Penzberg, Germany).

3.7. Isolation of erythrocyte ghosts

Blood was diluted 1:1 with platelet wash buffer (PWB; 12.9 mmol/L citrate, 30 mmol/L glucose, 120 mmol/L NaCl and 5 mmol/L EDTA, pH 6.5) and centrifuged (300 x g, 15 min, RT). The numbers of blood cells in individual stages of separation were monitored using a cell counter (ADVIA 60, Bayer, Leverkusen, Germany) and served as a base for estimation of numbers of contaminating cells in separated blood fractions. Erythrocytes were resuspended in cold PBS (pH 7.4) and centrifuged (1500 x g, 10 min, and 4°C). The supernatant and the buffy coat containing leukocytes were discarded together with the upper quarter of the erythrocyte phase. The middle half of the red blood cell phase was diluted with the same volume of PBS

and erythrocytes were lysed with 14 volumes of ice-cold lysis buffer (5 mmol/L sodium phosphate and 1 mmol/L EDTA, pH 7.4). The remaining contaminating platelets and leukocytes were removed using centrifugation (2000 x g, 5 min, and 4°C). Erythrocyte ghosts were sedimented at 20,000 x g (40 min, 4°C), washed three times with lysis buffer, finally resuspended in TBS and stored frozen at -80 °C.

3.8. Electrophoresis and western blot

Proteins were separated on a 10 or 12.5 % sodium dodecyl sulfate- polyacrylamide gel electrophoresis (SDS-PAGE) and transferred to a 0.2 µm nitrocellulose membrane (Bio-Rad, Hercules, CA, USA). Protein concentration in cell culture lysates was adjusted using BCA assay (Thermo Fisher Scientific, Rockford, IL, USA) to 20 µg proteins/lane in SDS-PAGE. Membrane was blocked with TBS with 0.05 % Tween 20, pH 7.4 (TBST), followed by TBST with 5% dry nonfat milk (TBSTM) (Bio-Rad) and incubated with appropriate mAb diluted in TBSTM. Human PrP^C was immunostained with 0.5 µg/mL 6H4 and 1 µg/mL AG4 or 0.5 µg/mL 3F4. Murine PrP^C was detected with 1 µg/mL of both AH6 and AG4 and 0.05 µg/mL 6H4. Anti-actin polyclonal antibody Ab I-19 (0.5 µg/mL) (Santa Cruz, Santa Cruz, CA, USA) was used as a loading control. After washing, the membrane was incubated with antimouse IgG goat F(ab)₂ linked to alkaline phosphatase (Biosource International, Camarillo, CA, USA) or goat anti rabbit (Ig)G alkaline phosphatase (Caltag, Buckingham, UK), both at dilution 1: 4000. Bands were visualized with a 5-bromo-4-chloro-3-indolyl-phosphate/ nitroblue tetrazolium phosphatase substrate (BCIP/NBT). Densitometric analysis was carried out with MiniLumi densitometer software (DNR Bio-Imaging Systems Ltd, Jerusalem, Israel).

3.9. Deglycosylation

Erythrocyte ghosts and brain samples were deglycosylated using PNGase F (New England Biolabs, Ipswich, MA, USA) according to the manufacturer's protocol. The samples were denatured, supplemented with Complete protease inhibitor (Roche Diagnostics), Triton X-100 and incubated overnight at 37°C with 100 U/mL PNGase F. Finally, samples were analyzed using immunoblotting. Fresh untreated erythrocyte ghosts, brain samples and their aliquots incubated overnight without PNGase F served as controls.

3.10. *In vitro* modification of brain PrP^C by *N*-hydroxysulfosuccinimide biotin, hydrogen peroxide and glyoxylic acid

Samples of normal brain homogenate were separated using SDS-PAGE and blotted. Subsequently, the membrane was cut into strips. Individual strips were treated with increasing concentrations of hydrogen peroxide (H₂O₂) (0, 1, 5, 25, 130, and 640 mmol/L) in PBS for 30 minutes at RT or with increasing concentrations of *N*-hydroxysulfosuccinimide biotin (sulfo-NHS-biotin, Thermo Fisher Scientific, Rockford, IL, USA; 0, 0.01, 0.05, 0.1, 0.5, 1, and 10 mmol/L) in PBS (1 hr, 37°C). Incubation with increasing concentrations (0, 6.75, 12.5, 25, 50, and 100 mmol/L) of glyoxylic acid (GA) was performed in 0.2 mol/L phosphate buffer (pH 7.4) containing 150 mmol/L sodium cyanoborohydride for 24 hours at 37 °C (Ando et al, 1999). After incubation, the strips were washed three times with PBS and then developed with mAb 3F4 or 6H4 as described in part “Electrophoresis and western blot”.

3.11. Cloning- creation of retroviral vectors expressing shRNAs

In first approach, we selected two target sequences (1071 and 1830) using the Ambion “siRNA Target Finder”² (Austin, TX, USA), third target site was adopted from the work of Tilly et al. (Tilly et al., 2003). Selected sequences seemed to have no significant homology to other genes except *Prnp* as shown by comparison with database for murine genome³. Subsequently, we used Ambion on-line “Insert Design Tool for the pSilencer™ Vectors”⁴ to design shRNAs (Table 1) matching to pSilencer 5.1. retro U6 vector (Ambion) (Fig. 5).

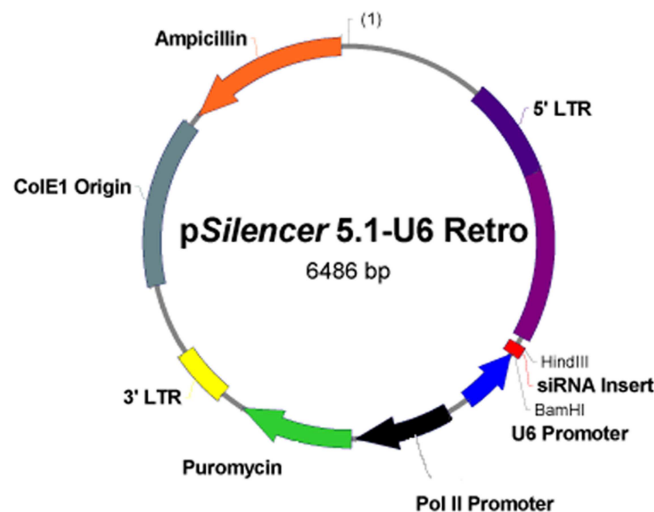


Figure 5: Schematic map of the pSilencer 5.1. retro U6 vector. Ψ= retroviral packaging signal sequence; *Hind*III and *Bam*HI= cloning site for siRNA insert; ColE1 Origin= bacterial origin of replication; Pol II Promoter= promoter for puromycin mammalian resistance marker; 3' and 5' LTR= long terminal repeats; Ampicillin= bacterial resistance marker. Picture from Ambion⁵.

Scrambled (SCRL), control shRNA was part of the kit. Individual complementary single stranded oligonucleotides (EastPort, Prague, Czech Republic) were annealed and cloned with T4 DNA ligase (Fermentas, Burlington, Ontario, Canada) to pSilencer 5.1. retro U6 vector according manufacturer's protocol. Ligated vectors were amplified in transformed *E. coli* DH5 α strain during overnight selection with 100 μ g/mL ampicillin (Sigma). Amplified vectors were isolated with QIAprep Spin Miniprep Kit (Qiagen, Hilden, Germany). Presence of inserts was verified by analysis with restriction endonucleases *Bam*HI and *Hind*III (Fermentas) and sequence accuracy was confirmed by sequencing primed from 5'- TTGTACACCCTAAGCCTC- 3' primer (EastPort).

To achieve more effective silencing of *Prnp* gene we used second generation of shRNAs expressed in context of miRNA (Silva et al., 2005), (Chang et al., 2006) (Fig. 3 and 6).

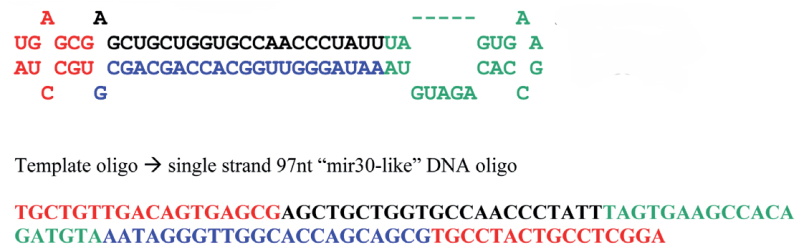


Figure 6: Design of second generation shRNA- shRNAmiR. Upper part of image shows the secondary structure of the mir- designed shRNA. Below is the corresponding oligonucleotide DNA sequence derived from the oligonucleotide RNA. The sequence in red represents the common flanking miR-30 sequences and nucleotides in green denote the miR-30 loop structure. The sense and antisense target sequences shown in black and blue, respectively, are optional by the researcher. The red flanking sequences are used as universal targets to prime a PCR reaction, whereby the entire miR-30- styled shRNA is amplified to produce a PCR product that can be cloned into a recipient vector (Paddison et al., 2004). Adapted with permission from Open Biosystems. Source [Open Biosystems product literature](#)⁶.

Both anti-*Prnp* sequences HP_285770 (LP1) and HP_288208 (LP2) are available in [RNAi codex database](#)⁷ (Table 1) and were purchased cloned in pSM2 (Fig. 7) V2MM_66187 and V2MM_63696 vectors (Open Biosystems, Huntsville, AL, USA). Control nonsilencing shRNAmiR (LN) was ordered in pSM2 retro vector RHS1707 (Open Biosystems). Next two anti-*Prnp* mRNA shRNAs sequences were adopted from literature, LP5 from Pfeifer et al. and LP6 from Tilly et al. (Pfeifer et al., 2006), (Tilly et al., 2003). Both LP5 and LP6 sequences (Table 1) were purchased as oligonucleotides (EastPort) and were processed to meet the criteria for cloning to Murine stem cell virus (MSCV) based retrovector expressing shRNA from LTR promoter (LMP) (Open Biosystems) (Fig. 8).

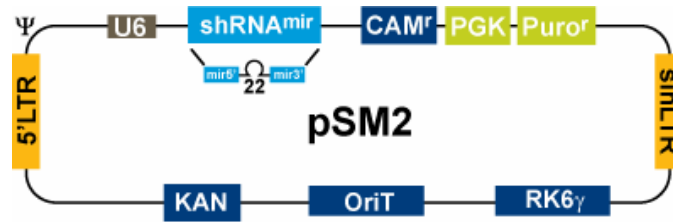


Figure 7: Schematic map of pSM2 retrovector. U6= shRNAmiR promoter, shRNAmiR= shRNA with the flanking miR-30 sequences at each end; PGK= phosphoglycerate kinase eukaryotic promoter; Puro^R= puromycin resistance for mammalian selection; 5'LTR= 5' long terminal repeat; sinLTR= 3' self-inactivating long terminal repeat; RK6 γ = conditional origin of replication (required for the expression of pir1 gene to propagate within the bacterial cell); Kan^r/CAM^r= bacterial resistance marker. Adapted with permission from Open Biosystems. Source Open Biosystems www site⁸.

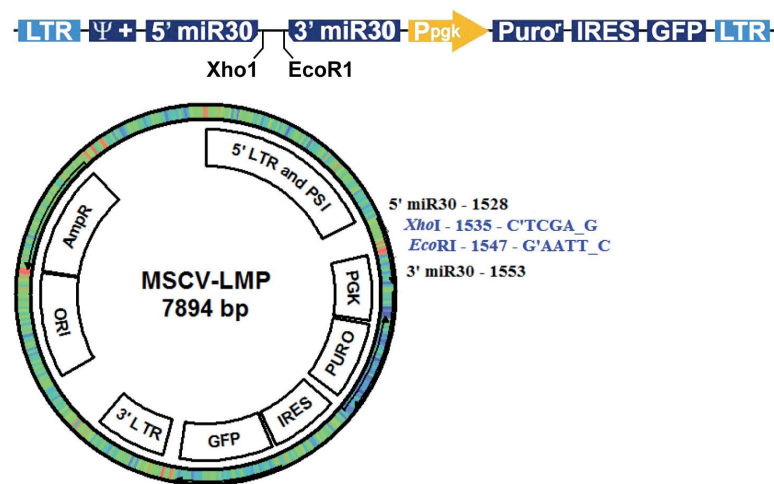


Figure 8: Schematic map of the LMP- Murine stem cell virus (MSCV)-based retroviral vector expressing shRNAmiR from the LTR promoter. Ψ = retroviral packaging signal sequence; *XhoI*/*EcoRI* cloning site; 5' and 3' miR30= common flanking sequence; Puro^R= Puromycin resistance for mammalian selection; PGK= phosphoglycerate kinase eukaryotic promoter; IRES= internal ribosome entry site; GFP= green fluorescence protein; LTR= long terminal repeats; AmpR= ampiciline resistance; ORI= origin of bacterial replication. Adapted with permission from Open Biosystems. Source Open Biosystems www site⁹ and [product literature](#)⁶.

Both oligonucleotides LP5 and LP6 were amplified by PCR using following common pSM2 primers: forward- *XhoI* primer 5`-AAGCCCTTTGTACACCCTAAGCCT-3` and reverse- *EcoRI* primer 5`- ACTGGTGAAACTCACCCAGGGATT- 3` (EastPort). Reaction conditions of PCR were as follows: 0.5 μ L *Pfu* Polymerase (Promega, Madison, WI, USA), 5 μ L of 10X reaction buffer containing MgSO₄ (Promega), 0.5 μ L *XhoI* primer, 0.5 μ L *EcoRI* primer, 1 μ L dNTPs, 41.5 μ L H₂O and 1 μ L DNA template (LP5/LP6), 94° 1', 20 cycles (94° 30", 54° 30", 72° 45"), 72° 10', 4° hold. Amplified product was purified according "Gel Extraction" protocol (Qiagen). Purified PCR amplicons were digested with *EcoRI* and *XhoI* and subsequently purified again to

get rid of digested fragments by running on a 2.5% agarose gel. Desired amplicons were cut from the gel and purified again based on “Gel Extraction” protocol (Qiagen). To prepare LMP retroviral vector for insertion, we first digested it with *EcoRI*/*XhoI* and purified the linearized plasmid by running on a 1% gel. Similarly, we digested pSM2 vectors coding LP1, LP2 and LN sequences and purified them in same manner as LP5/ LP6 inserts. Ligation reaction was performed in 20 μ L reaction with equimolar amounts of insert and vector DNA at RT for 2 hours. Ligated vectors were then transformed to *E. coli* DH5 α strain and selected with ampicillin. Sequences were verified using 5'- CCCTTGAACCTCCTCGTTCGACC-3' sequencing primer in clones that were positive by restriction digest analysis.

<p>389-shRNA * GATCCGCCTTGGTGGCTACATGCTCTCAAGAGAAGCATGTAGCCACCAAGGCCCTTTTTGGAAAAGCT</p> <p>1071-shRNA * GATCCGTACCCCTGGCACTGATGGGTTC AAGAGACCATCAGTGCCAGGGTATTTTGGAAAATGCT</p> <p>1830-shRNA * GATCCACTGCGATAGCTTCAGCTTCTCAAGAGAAGCTGAAGCTATCGCAGTTT TTTGGAAAAGCT</p> <p>LP1-shRNAmiR TGCTGTTGACAGTGAGCGACCTATGTTTCTGTACTTCTATAGTGAAGCCACAGATGTAATAGAAGTACAGAAACATAGGGTGCCTACTGCCTCGGA</p> <p>LP2-shRNAmiR TGCTGTTGACAGTGAGCGAGCAAAGGGTCTACAACCAAAAGTGAAGCCACAGATGTAATTGGTTGTAGAACCCTTTGCGTGCCTACTGCCTCGGA</p> <p>LP5-shRNAmiR TGCTGTTGACAGTGAGCGAAGAACAACCTTTGTGCACGACTAGTGAAGCCACAGATGTAAGTCGTGCACAAAGTTGTTCTGTGCCTACTGCCTCGGA</p> <p>LP6-shRNAmiR TGCTGTTGACAGTGAGCGAGGGCCTTGGCGGCTACATGCTTAGTGAAGCCACAGATGTAAGCATGTAGCCGCCAAGGCCCTGCCTACTGCCTCGGA</p>
<p>Table 1: shRNA and shRNAmiR sequences used in the present study shown as DNA oligo. * number denotes starting position of target site on <i>Prnp</i> mRNA. Sequences 389, 1071 and 1830 were designed for use in pSilencer 5.1. retro U6 retrovector. LP1, LP2, LP5, and LP6 were used in LMP retrovector. Red= stem of shRNA, complementary sequence to <i>Prnp</i> mRNA. Green= loop of shRNA. Direction 5'→3'.</p>

3.12. Transfection of the pSilencer 5.1. retro U6 expressing shRNAs to MEL cells

MEL cells were seeded 24 hours before transfection in 24-well plate in two concentrations- 50 and 150 x 10³ cells per well at final volume of 0.5 mL. For transfection, we used siPORT XP-1 (Ambion) transfection agent with ratio to DNA (retrovectors coding shRNAs- 389, 512, 1071, 1830, and SCRL) as advised by manufacturer. Efficiency of transfection was determined indirectly during selection of cells, where population with the highest viability was considered as transfected with the most optimal ratio of siPORT XP-1 to DNA. Transfected and mock transfected control cells were selected with puromycin. Prior to selection, we found out by “Puromycin killing curve assay” as an optimal effective concentration 0.5 μ g/mL of puromycin. Since pSilencer 5.1. retro U6 vector does not code for any easily observable marker like GFP, we transfected plasmid expressing EGFP (Clontech)

under similar conditions like for pSilencer 5.1. retro U6 vectors to assess transfection efficiency.

3.13. Confirmation of the pSilencer 5.1. retro U6 vector integration by PCR

Inserts in pSilencer 5.1. retro U6 vector stably integrated into the genomic DNA were detected by PCR. Using the Primer ExpressTM software (Applied Biosystems) we designed primers targeting two regions: Insert-300 bp (detecting presence of cloned insert shRNA) and U6-1000 bp (detecting inserted shRNA together with U6 promoter). Primers for PCR were as follows: forward 5'- AGACCAGGTCCCCTACATCGT- 3', reverse 5'- AGGACGCGGGATCCAGTACT- 3' for Insert-300 bp and forward 5'- CCTTTAACGTCGGATGGCC- 3', reverse 5'- TCCATTGTGTCACGTCCTGCA- 3' for U6-1000 bp. DNA was isolated using "genomic DNA purification kit" (Fermentas). Samples were adjusted to 10 µg/mL upon measuring of concentration by absorbance at 260 nm. Two µL of diluted DNA was amplified using PCR master mix (Fermentas) with following thermal profile- 94° 3', 40 cycles (94° 30'', 53° 1', 72° 30''), 72° 10' and hold 4°. Presence of amplicons was visualized by gel electrophoresis.

3.14. Retroviral transduction of target cells

Schematic overview of procedure is shown on Fig. 9. Packaging HEK293 GP2 cells were seeded 24 hours before transfection at density ~ 1.5 x 10⁴ cells/ well (24-well plate). After 24 hours, VSV-G plasmid coding envelope protein of vesicular stomatitis virus (Clontech) was cotransfected to HEK293 GP2 cells in ratio 1:2 with appropriate retrovector (LN, LP1, LP2 and LP5). Plasmids were delivered to cells in ratio 9:1 with Arrest-in transfection agent (Open Biosystems). Three days post transfection of HEK293 GP2 cells, media containing retroviral particles were spun down to pellet eventual contamination by packaging cells (400 x g, 5 min, and 4°C). In parallel, target MEL cells were centrifuged (400 x g, 5 min, and RT), resuspended with fresh medium and 0.25 mL of cell suspension per well was aliquoted in 24-well plate. Growth medium from adherent target CAD5 cells growing in 24-well plate was replaced with 0.25 mL of fresh medium. Supernatant containing viral particles and 1,5-dimethyl-1,5-diazaundecamethylene (Polybrene, Sigma) at final concentration of 4 µg/mL was added to recipient cells in 1:1 ratio. Subsequently, target cells with retroviral inoculum were centrifuged for 90 min at 500 x g, RT.

To ensure successful infection of MEL cells we also employed co-cultivation as another approach for transfer of viral particles from packaging cell line to MEL cells. In this method, 24 hours post transfection, medium in HEK293 GP2 cells was aspirated and ~ 2 x 10⁴ MEL

cells/well were added inside the 0.4 μm pores translucent polyphthalat insert (Beckton Dickinson) in total 0.7 mL volume of fresh media containing 4 $\mu\text{g/mL}$ Polybrene.

After 48 (co-cultivation) or 72 (spinfection) hours of incubation cells were diluted with fresh medium for recovery. Selection started next day by adding puromycin (Sigma) at final concentration of 0.5 $\mu\text{g/mL}$ for MEL cells and 1.5 $\mu\text{g/mL}$ for CAD5 lines. We monitored progress of selection (as a percentage of cells with integrated retrovector) by FACS utilizing expression of retrovirally delivered GFP. MEL cell lines prepared by both methods were mixed when reached >95% of GFP positivity. Overall, during the study, we used MEL and CAD5 cell lines named after appropriate retroviral vector shRNAmiR table 2.

Table 2: Names of transduced MEL 707 and CAD5 cell lines.

Retrovector	Transduced lines		Function of shRNAmiR
LMP	MEL LMP	CAD LMP	Empty vector
LN	MEL LN	CAD LN	Nonsilencing shRNAmiR
LP1	MEL LP1	CAD LP1	Anti- <i>Prnp</i> shRNAmiR
LP2	MEL LP2	CAD LP2	Anti- <i>Prnp</i> shRNAmiR

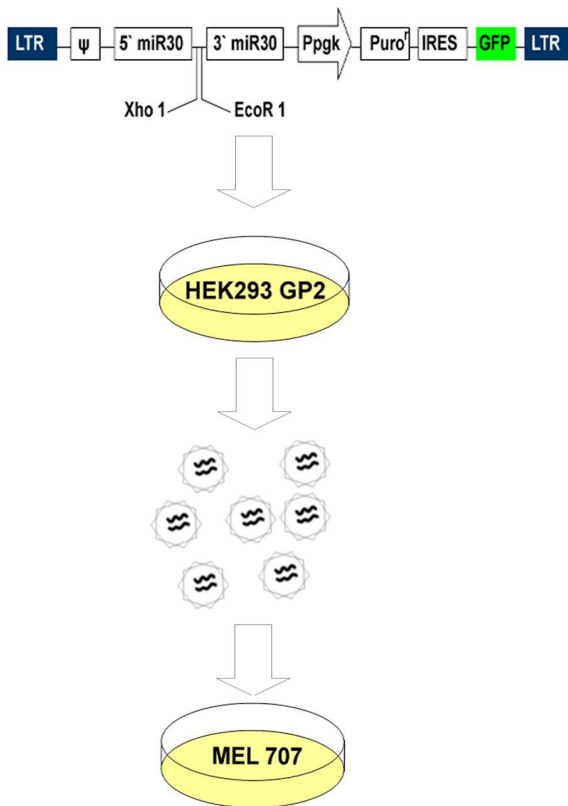


Figure 9: Brief description of retrovirus production by HEK293 GP2 line and its delivery to target cells. HEK 293 GP2 cells express retroviral genes *gag* and *pol*, but *env* gene for envelope protein production must be co-transfected with retrovector. We used VSV-G plasmid expressing the G glycoprotein of the vesicular stomatitis virus. VSV-G protein interacts with phospholipid components of the target cell membrane and promotes the fusion of viral and cellular membranes. VSV-G protein does not require a cell surface receptor and can serve as a substitute viral envelope protein. Assembled retroviral particles are released to growth medium where can be collected and delivered to target cell line. Upon integration to host genomic DNA, MSCV-based retroviral vector expresses shRNAmiR from the retroviral LTR promoter. Stable integrants are selected using puromycin resistance. GFP serves as a marker for retroviral integration.

3.15. RNA isolation and reverse transcription

To preserve RNA integrity, samples intended for future RNA isolation were stored in RNA later solution (Ambion) or processed immediately. MEL and CAD5 cells were collected by centrifugation (400 x g, 5 min, RT) and cell pellet was immediately lysed in RNA Blue solution (Top-Bio s r.o., Prague, Czech Republic). RNA was isolated according manufacturer's manual. RNA pellet was diluted in RNase/ DNase free water and stored at -80°C. Approximate integrity of RNA, based on the visualizing of 28S rRNA and 18S rRNA, was evaluated after 1.5% agarose gel electrophoresis (30 min, 100 V). Concentration of RNA was measured by absorbance at 260 nm. The RNA purity largely varied between 1.9 and 2.2 as was estimated by the ratio of absorbances between 260 and 280 nm. Contaminating genomic DNA was degraded by treatment with the TURBO DNase (Ambion). The RNA integrity, concentration, and purity were revalued like previously. For reverse transcription we used 0.5 µg of DNase treated RNA. Afterwards, RNA was transcribed using RevertAid™ first strand cDNA synthesis kit (Fermentas) in line with the producer protocol. Reverse transcription was primed by the reverse transcriptase using random hexamer primers.

3.16. Quantitative real time PCR

Complementary DNA (cDNA) was tenfold diluted and 2 µL was used for quantitative real time PCR (qRT-PCR) performed in ABI 7300 PCR System (Applied Biosystems, Carlsbad, CA, USA) using TaqMan Universal PCR Master Mix (Applied Biosystems), thermal profile- 95° 10", 40 cycles (94° 15", 60° 1"), and primers/probes detecting genes listed in table 3:

Abbreviation	Applied Biosystem identification mark & gene name:
<i>Bax</i>	Mm00432051_m1; Bcl2-associated X protein,
<i>c-myb</i>	Mm00501741_m1; myeloblastosis oncogene
<i>Eif2ak2</i>	Mm00440966_m1; eukaryotic translation initiation factor 2-alpha kinase 2
<i>Eraf</i>	Order Number- 2217982, Assay ID - EDRF-70; erythroid associated factor, (EDRF)
<i>Gapdh</i>	Mm99999915_g1; glyceraldehyde-3-phosphate dehydrogenase
<i>GATA1</i>	Mm00484678_m1; GATA binding protein 1
<i>Hba</i>	Mm00845395_s1; alpha hemoglobin chain
<i>Oas1</i>	Mm00712008_m1; ribonuclease L (2',5'-oligoadenylate synthetase- dependent)
<i>Prnp</i>	Mm00448389_m1; prion protein
<i>Rnase1</i>	Mm00836412_m1; 2'-5' oligoadenylate synthetase 1A

Relative fold expression levels were calculated using the $2^{-\Delta\Delta Ct}$ method (Livak and Schmittgen, 2001) normalized to the reference *Gapdh* gene- equation 1. Relative fold expression quantities were calibrated specifically for each experiment as stated later in results.

Equation 1: step 1- $\Delta Ct = Ct_{(\text{target gene})} - Ct_{(\text{reference gene})}$
 step 2- relative fold expression $2^{-\Delta\Delta Ct} = 2^{-(\Delta Ct(\text{examined sample}) - \Delta Ct(\text{calibrator sample}))}$

Endogenous retroviruses (Table 4) were quantified with SYBR[®] Green PCR Master Mix (Applied Biosystems) using primers (EastPort) adopted from Stengel et al. (Stengel et al., 2006). Quantitative RT-PCR was performed on ABI 7300 PCR System using default thermal profile. Melting curve analysis of dissociated dsDNA during heating allowed us to assess the specificity of PCR. To exclude the possible contamination of reaction components, negative controls (water) were performed for each experiment with no signal detected.

Table 4: Primers used for the PCR amplification of selected endogenous retroviruses (ERVs).

ERV name	Primers in 5' -> 3' direction	
	Forward	Reverse
<i>IAP-1</i>	GGAGAAGTCCTACCTCAGGGG	GGAGAACAAAATGTCATCCATATA
<i>MLV</i>	CCAGACTTGATCCTGCTACA	CTCAGTCAGCCATCTCTGAC
<i>ERV- L</i>	GTTTTGCCTCAAGTATATAT	CAGCATAATGTCATCAATATA
<i>MuRRS</i>	TTAGCCTCCTCCGAGCTGA	GCCTCTGTCAGCCACCGTTT
<i>VL30</i>	ACCTGGACTAGACTACCACA	GGCTGCGATTAAGATCATC
<i>VL30-2</i>	CTCGCACCTTTTCGCGCTCG	GCGAGGGGATCATCATAACA

3.17. Spectrophotometric determination of hemoglobin content in MEL cells

Hemoglobin concentrations in MEL cell lysates were measured by the tetramethylbenzidine (TMB) assay as described previously (Petрак et al., 2007) with adaptation to 96-well plate. MEL cells were harvested in 24 hour intervals during whole course of erythroid differentiation. Upon washing with ice-cold PBS cell pellets were lysed in 0.14 M NaCl, 0.01 M HEPES, and 1.5% w/w Triton X100, pH 7.4. Cell lysates were centrifuged at 14,000 x g, 20 min, and 4°C. Supernatant was transferred to a new tube and total protein concentration was determined by the BCA assay (Thermo Fisher Scientific). Samples were adjusted to 100 µg/mL and TMB assay was performed in duplicate by adding the reagents in the following order: 10 µL supernatant (or pure lysis buffer for the blank sample), 80 µL deionized water, 20 µL freshly prepared TMB solution in 90% acetic acid. The reaction was started by the addition of 4 µL of 30% H₂O₂. Absorbance was measured after 20 min of

incubation at RT on VICTOR² D fluorometer (PerkinElmer, Waltham, MA, USA) using 660 nm wavelength. Amount of hemoglobin was subtracted from the calibration curve composed of serial dilutions of purified hemoglobin (Sigma).

3.18. Uptake of radiolabeled ⁵⁹Fe-transferrin by MEL cells

Two passages before experiment, MEL cells were adjusted and kept in density 10⁶ cells/mL. In time of analysis, cells were washed with pre-warmed PBS and resuspended in fresh medium. Subsequently, 3 μM transferrin saturated with ⁵⁹Fe was added to cell suspension. At defined time points (1, 2 min 30 sec, 5, 10, 30, and 60 min) aliquotes in triplicates each containing 12x 10⁶ cells were diluted in 10 mL of ice-cold PBS to stop the iron uptake. Finally, cells were three times washed with ice-cold PBS. Cell pellet was finally analyzed by Tesla NA 3601 gamma counter.

3.19. Infection of MEL cells with RML prion strain

MEL cells (MEL 707, LMP, LN, LP1, and LP2) were left 96 hours to reach the confluence. After 4 days, at the time of inoculation, we split the cells into triplicate to fresh growth medium. Subsequently, 10 μL of 10% brain homogenate infected with RML prion strain (prepared as described above in section- “Preparation of brain homogenates and cell lysates”) was diluted in 1 mL of MEL cell suspension reaching final concentration 0.1% of RML brain homogenate. The cells were incubated 24 hours then 0.1 mL of cell suspension was diluted tenfold for the next passage and the rest of the suspension was divided into halves. Both halves were used for cell blot assay, one was washed three times with PBS and the other was used without washing. Passaged cells grew for next 4 days when were processed in the same manner (here described as a first passage). After next 4 days (9 days post infection), passaging was discontinued and all cells were harvested (here described as a second passage).

3.20. Cell blot assay

Cell blot assay was used to examine propagation of RML prions in MEL and CAD5 cell cultures (Bosque and Prusiner, 2000). MEL cells were pelleted by spinning, adjusted to equal volume and pipetted on 0.45 μm nitrocellulose membrane (Biorad) pre-wet in lysis buffer (0.5% natrium deoxycholate, 0.5% Triton X-100, 150 mM NaCl, and Tris-HCl, pH 7.5). After 1 hour drying at RT, the membrane with adhered cell lysates was incubated 90 min at 37°C with 7 μg/mL of proteinase K (PK) in lysis buffer. PK was inhibited by 10 min incubation with 2 mM PMSF. Subsequently, membrane was 10 min treated with 3 M

guanidium thiocyanate in 10 mM Tris-HCl, pH 8.0. After extensive washing in water, cell blot was processed as a normal western blot. PrP^C was visualized using mAbs as described earlier. Presence of infectious PrP in CAD5 cells was examined like in MEL cells except that CAD5 cells were grown on glass slides and at the defined time were transferred by pressing on the pre-wet membrane.

3.21. Statistics

Statistical significance was determined by two-tailed *t*-test (paired or unpaired test) using GraphPad Prism software version 5.00 for Windows (GraphPad Software, San Diego, CA, USA). A *p* value of < 0.05 was considered statistically significant. Error bars are represented by mean ± standard deviation (SD), if not stated otherwise.

4. Results

4.1. Characterization of human PrP^C associated with erythrocytes suggests explanation for quantitative differences in the literature

4.1.1. Characterization of erythrocyte PrP^C

In our initial quantitative analysis of PrP^C on human erythrocytes isolated from eight healthy donors, we observed notable differences in the binding of used antibodies to human red blood cells. The highest number of PrP^C molecules (in assumption that one IgG molecule binds one PrP^C molecule) per one erythrocyte (290 ± 140 PrP^C, median \pm SD) was found by mAb 6H4. Monoclonal antibodies 3F4 and FH11 bound much lower number of PrP^C molecules per cell: 80 ± 35 and 35 ± 20 (median \pm SD), respectively (Fig. 10). In contrast, both mAbs 3F4 and 6H4 bound to platelet PrP^C from identical samples roughly equivalent: 630 ± 150 and 635 ± 280 (median \pm SD) (not shown).

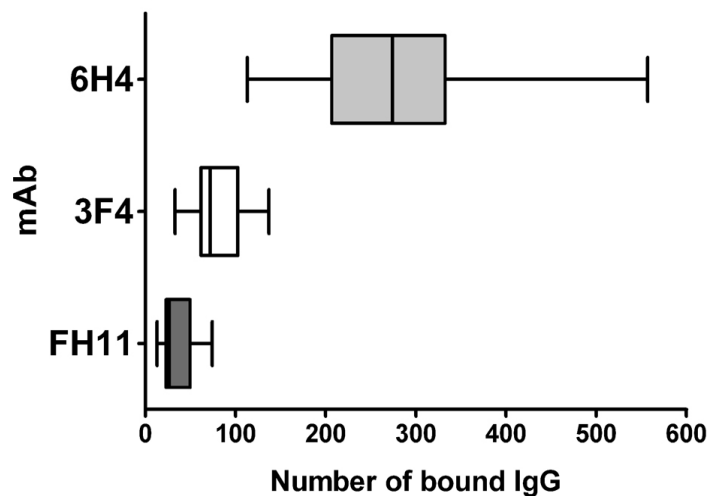


Figure 10: Quantification of PrP^C expression on human erythrocytes using FACS. Binding of mAbs to erythrocytes of healthy human donors was measured using quantitative flow cytometry (n= 8). The range of the data, 50% percentile (box) and median are shown.

We found that 3F4 bound minimally or not at all to PrP^C on western blots of serially diluted erythrocyte ghost samples. Contrary, we detected 3F4 binding to brain PrP^C (Fig. 11B). At the same time, 6H4 detected erythrocyte PrP^C on blots with similar sensitivity to brain PrP^C (Fig. 11A). WB analysis revealed that erythrocyte PrP^C was present mainly in its diglycosylated form, detected as a diffuse band with a molecular weight (MW) slightly higher (35-38 kDa)

than brain PrP^C (Fig. 12A). Deglycosylation of PrP^C with PNGase F led to the detection of a single band with a MW similar to deglycosylated brain PrP^C. No major fragments suggesting a significant presence of truncated forms of PrP^C in human red blood cells were detected. Denaturation of the sample by boiling with SDS or its deglycosylation did not improve the binding of mAb 3F4 to erythrocyte PrP^C (Fig. 12B).

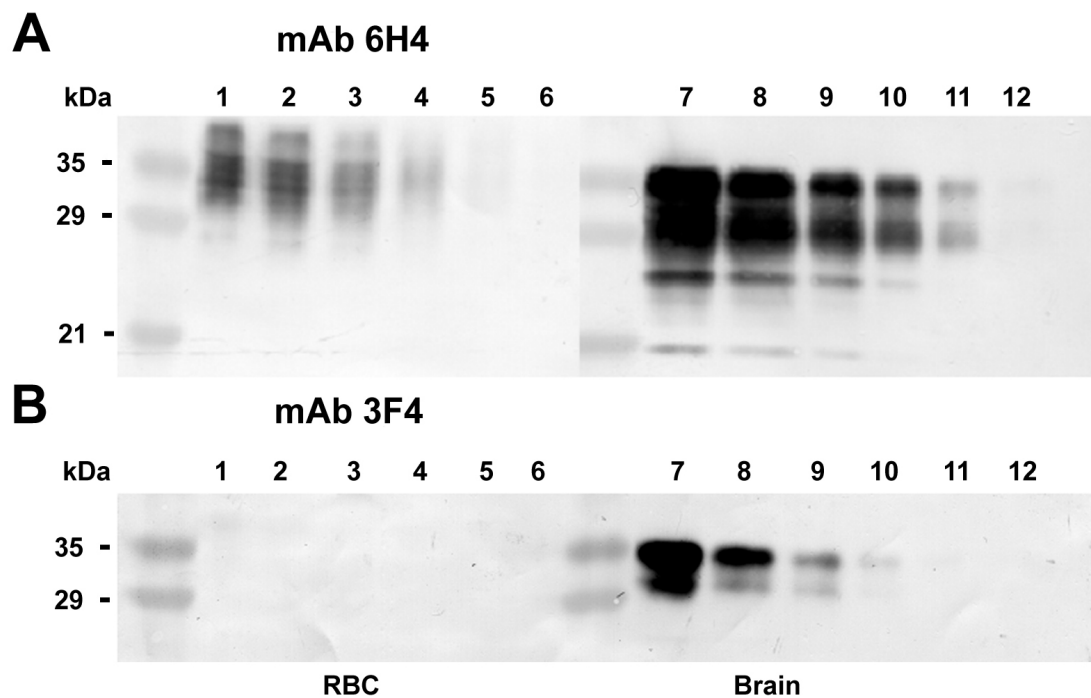


Figure 11: WB comparison of PrP^C detection using mAbs 6H4 and 3F4. WBs of serially twofold diluted samples of 1×10^{10} /mL human erythrocyte ghosts (Lanes 1-6) and 10% normal human brain homogenate (Lanes 7-12) were developed with mAb 6H4 (A) or 3F4 (B). Binding of 3F4 to erythrocyte PrP^C is not improved by denaturation of proteins after boiling with electrophoretic sample buffer, demonstrating that poor binding of 3F4 to human erythrocytes is not caused by blocking of its epitope by conformational change or the interaction of PrP^C with its binding partner on the cell surface. A plausible explanation of poor 3F4 binding is covalent modification of its epitope in red blood cell PrP^C.

The incubation of erythrocyte ghosts with increasing concentrations of proteinase K led to gradual and complete cleavage of PrP^C, demonstrating that erythrocyte PrP^C is similarly as sensitive to proteinase K as PrP^C in equally treated samples of platelets or brain homogenate (not shown). We obtained a similar result after proteinase K treatment of intact erythrocytes and platelets with subsequent FACS analysis of PrP^C (not shown).

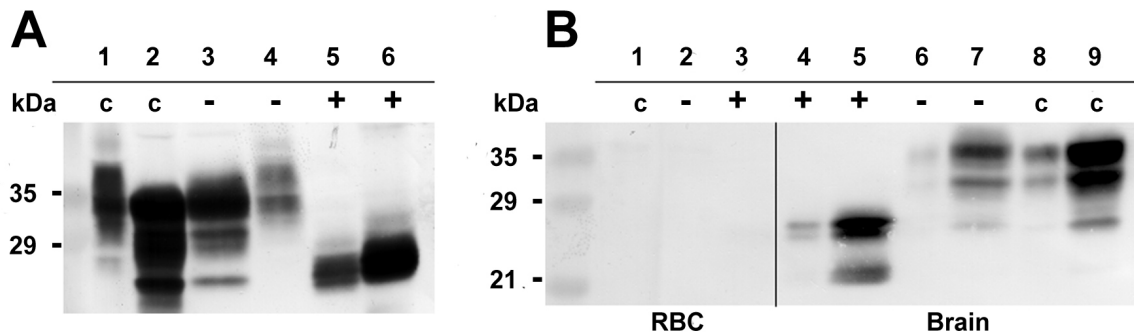


Figure 12: Characterization of basic features of PrP^C on human erythrocytes. **(A)** WB comparison of red blood cells (lanes 1, 4 and 5) and brain (Lanes 2, 3 and 6) PrP^C demonstrate that erythrocyte PrP^C is not significantly truncated. (c) Fresh untreated samples, (+) samples deglycosylated using incubation with PNGase F, and (-) samples incubated without PNGase F. The blot was developed with a mixture of mAbs 6H4 and AG4. **(B)** Deglycosylation of erythrocyte PrP^C does not lead to the restoration of 3F4 binding. Red blood cells (lanes 1-3) and brain (lanes 4-9) samples were (c) fresh untreated, (+) treated with PNGase F, or (-) incubated without PNGase F. Samples 4, 6, and 8 are 10-fold dilutions of Samples 5, 7 and 9, respectively. The blot was developed with mAb 3F4.

4.1.2. The influence of *in vitro* modification of brain PrP^C on the binding of mAb 3F4

The low binding of 3F4 to erythrocyte PrP^C could be caused by modification of its epitope (KTNMKHM). Oxidation of brain PrP^C with increasing concentrations of H₂O₂ up to 130 mmol/L had little effect on the binding of mAb 3F4 or 6H4. At 640 mmol/L, the binding of both 3F4 and 6H4 was diminished (Fig. 13). In contrast, modification of lysine residues to N^ε-(carboxymethyl)lysine (CML) by incubation with increasing concentrations of GA generated complete inhibition of 3F4 binding, while the binding of 6H4 was not affected (Fig. 13). Similarly, incubation with increasing concentrations of Sulfo-NHS-biotin led to a gradual loss of 3F4 binding to PrP^C (Fig. 13).

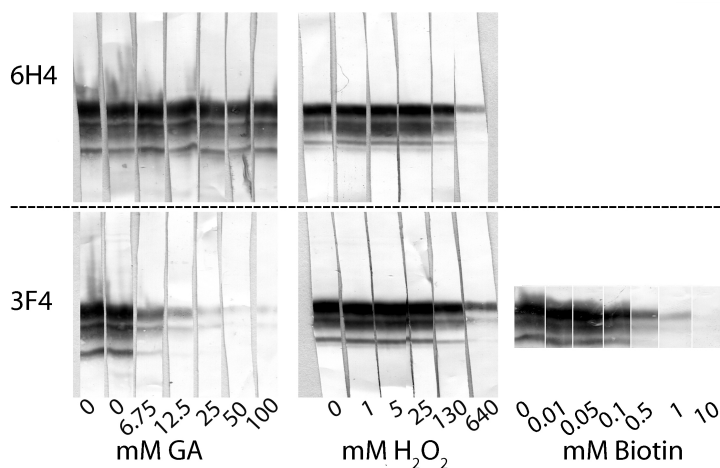


Figure 13: Glycation of PrP^C could be the reason of diminished binding of 3F4 to human erythrocytes. *In vitro* treatment of WBs of normal brain homogenate with increasing concentrations of GA, H₂O₂, or Sulpho-NHS-Biotin. Blots were developed with mAbs 6H4 or 3F4. Modification of lysine residues by GA to CML and Biotin in contrast to oxidation of methionines by H₂O₂ mimics the discrepancy in the binding of mAbs 3F4 and 6H4 found *in vivo* in human red blood cell PrP^C.

4.1.3. FACS analysis of 3F4 and 6H4 binding to CD71⁺ erythroid cells in cord blood

In contrast to peripheral erythrocytes, equal binding of 3F4 and 6H4 to transferrin receptor- positive (CD71⁺) erythroid precursors in cord blood was recorded (Fig. 14).

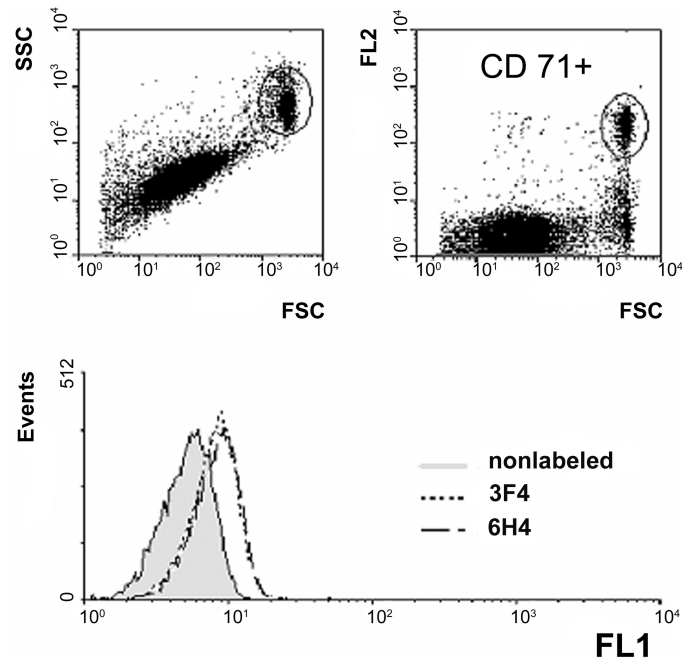


Figure 14: Comparison of 3F4 and 6H4 binding to human cord blood erythrocytes. MAbs 3F4 and 6H4 bind equally well to transferrin receptor- positive erythroid precursors in human cord blood. This suggests that the modification of the 3F4 epitope (KTNMKHM) occurs after the release of red blood cells into circulation. Normal cord blood (n= 3) samples were analyzed using two-color flow cytometry. The logarithmic side scatter/forward scatter (SSC/FSC) plot shows the scatter properties of cord blood and the position of the erythrocyte gate (top left plot). CD71⁺ cells were gated on a FL2/FSC logarithmic plot (top right plot) and their 3F4 and 6H4 fluorescence compared (bottom histogram overlay).

4.2. Expression of PrP^C is regulated during murine erythroid differentiation

4.2.1. Expression of PrP^C differs on individual murine erythroblast subpopulations

Quantitative FACS analysis of PrP^C expression on erythroid subpopulations isolated from BM and spleen (Fig. 15A) showed that the expression of PrP^C is upregulated from proerythroblasts (Pro.E) to basophilic erythroblasts (Ery.A) ~ 2-fold in BM and ~ 3-fold in the spleen cells. Temporal increase is followed by decreasing of membrane bound PrP^C during maturation toward reticulocytes (Ery.C) (Fig. 15B).

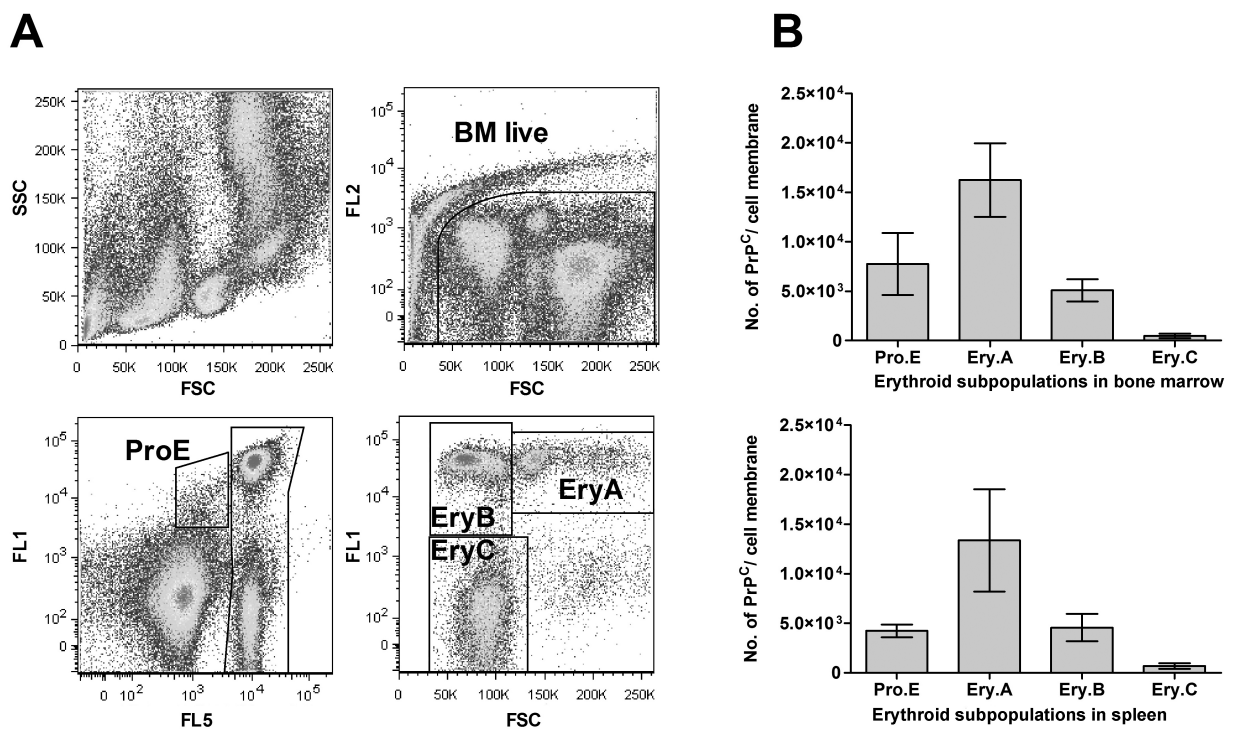


Figure 15: PrP^C is upregulated in early erythroblast precursors and then decreases during their maturation to erythrocytes. (A) Schematic gating strategy of erythroblast precursor: viable cells (7-AAD negative) were labeled with CD71-FITC (FL1) and Ter119-eFluor 450 (FL5). Four populations were identified: proerythroblasts (Pro.E; CD71^{high}Ter119^{medium}) and Ter119^{high} that were gated further on FSC x CD71 to distinguish 3 populations: basophilic erythroblasts (Ery.A; CD71^{high}FSC^{high}), late basophilic and polychromatic erythroblasts (Ery.B; CD71^{high}FSC^{low}), orthochromatic erythroblasts and reticulocytes (Ery.C; CD71^{low}FSC^{low}). (B) Quantitative FACS analysis of PrP^C expression on erythroblast precursors isolated from BM and spleen cells showed that expression of PrP^C is significantly ($p = 0.004$) upregulated from pro.E (7800 ± 3100) to Ery.A (16200 ± 3700). Similarly, in spleen we detected 4200 ± 600 PrP^C molecules on pro.E and 13400 ± 5200 on EryA, ($p = 0.023$). Expression then decreases in Ery.B with 5100 ± 1100 in BM and 4600 ± 1400 on spleen cells. On late precursors (Ery.C) amount of PrP^C is the lowest 470 ± 230 or 680 ± 280 PrP^C molecules. Paired t-test; mean ± SD; n= 5. Number of membrane PrP^C molecules per cell, provided that 1 molecule of anti-PrP^C monoclonal antibody AH6 binds 1 molecule PrP^C.

4.2.2. Differential regulation of PrP^C during inducer mediated erythroid differentiation

MEL cells were grown 5 days in the absence or presence of 5 mM HMBA. In both instances, cells upregulated expression of *Prnp* mRNA. Cells induced to erythroid differentiation upregulated PrP^C protein as early as 6 hours post induction (Fig. 16), with no detectable upregulation of PrP^C in uninduced MEL cells (not shown). Further examination documented that transcription of *Prnp* mRNA in nondifferentiating cells reached maximal expression at 96-120 hours (~ 13-fold expression in comparison with starting point at 0 hours) (Fig. 17A). Similarly, after 24 hours *Prnp* mRNA in differentiating MEL cells raised more than 2-fold, but the peak reached after 120 hours with expression ~ 9-fold compared to time of HMBA addition at 0 hours (Fig. 17B). Expression of PrP^C in untreated cells correlated with mRNA accumulation in later stages (Fig. 17C). Contrary to *Prnp* mRNA in differentiating cells, PrP^C reached the maximal expression in 24 hours with subsequent decrease to almost its basal level (Fig. 17D). Quantitative FACS analysis confirmed observed pattern of PrP^C expression in differentiating cells by WB (Fig. 17E).

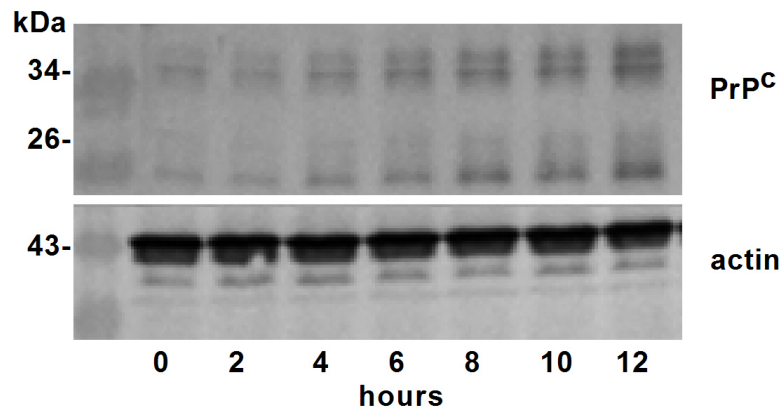


Figure 16: PrP^C upregulation may be recognized ~ 4-6 hours post HMBA induction as shown by WB. MEL cells were harvested in two-hour intervals post induction to differentiation. PrP^C was detected by mix of mAbs 6H4, AG4 and AH6. Actin served as a loading control.

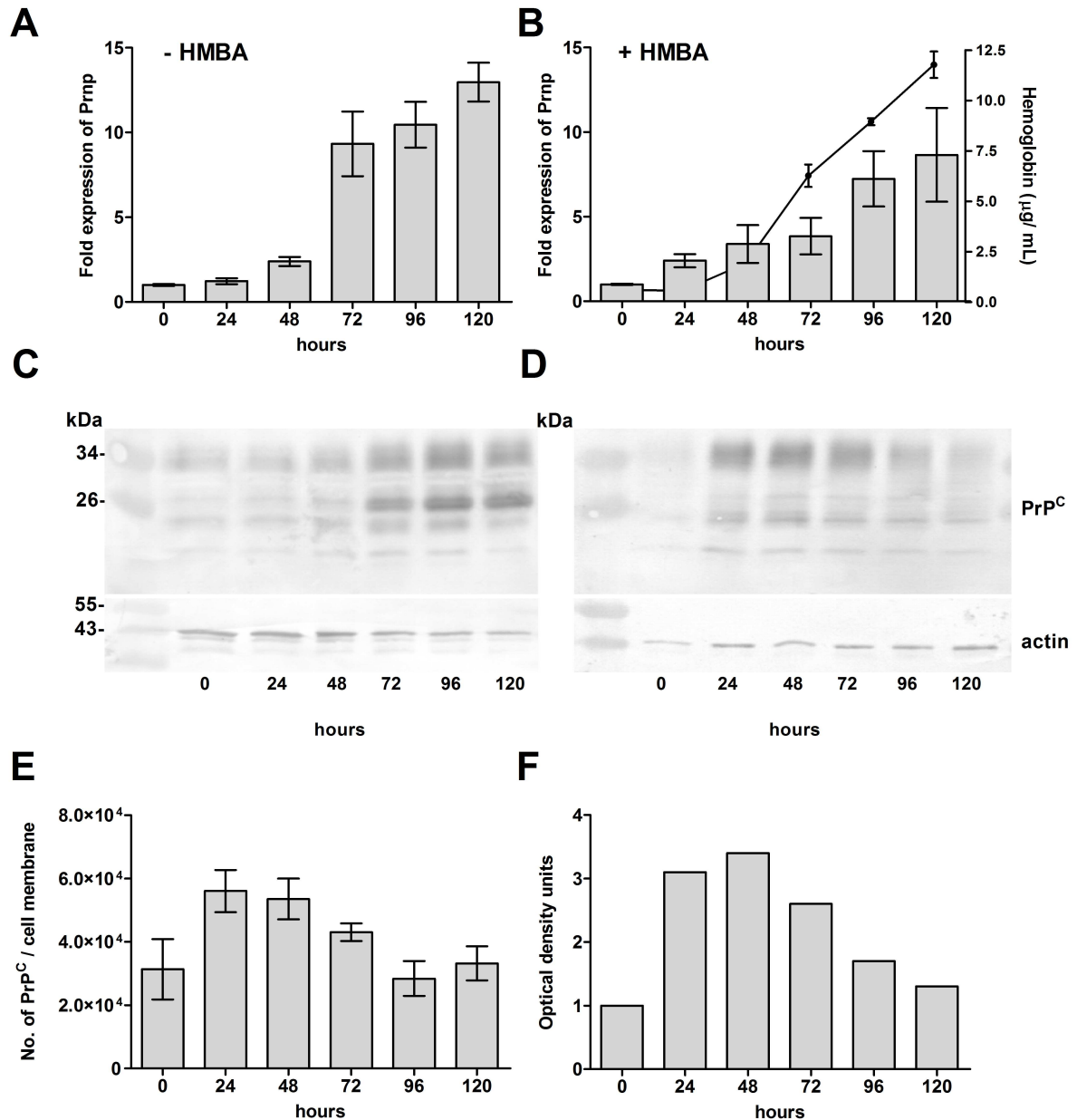


Figure 17: Comparison of PrP^C expression on mRNA and protein level in untreated and differentiating MEL cells. Expression of *Prnp* mRNA increases in uninduced MEL cells (A) similarly like in cells induced to erythroid differentiation (B). Expression was determined as fold difference relative to expression in starting point (mean ± SD). Hemoglobin production illustrates progress of differentiation (B, full line). Increased production of PrP^C protein correlates with elevated mRNA transcription in growth-arrested cells (C), but not in the differentiated cells, where expression of PrP^C protein reaches its maximum 24-48 hours post induction (D). WB was developed by mix of mAbs AH6, AG4 and 6H4. Actin was used for loading control. (E) Number of membrane PrP^C molecules per differentiating cell measured by quantitative FACS, mean ± range. (F) Densitometric analysis of PrP^C expression during erythroid differentiation from picture D.

4.2.3. PrP^C is upregulated after treatment with inhibitor of histone deacetylases

In this experiment, we examined dependence of *Prnp* gene transcription in MEL cells on methylation status of its promoter sequence and chromatin status in *Prnp* locus. For this purpose we treated MEL 707 cells with 5-AzaC an inhibitor of methyltransferases and TSA an inhibitor of histone deacetylases. MEL cells were incubated with 2.5 and 5 ng/mL TSA or 1.25 and 2.5 μ M 5-AzaC. After 24 hours, we monitored transcription of *Prnp* by qRT-PCR. Expression of *Prnp* in TSA treated cells (2.5 ng/mL and 5 ng/mL) was ~ 11-fold or ~ 8-fold higher than in cells at the beginning of treatment (Fig. 18A). Both TSA concentrations led to significantly ($p < 0.0001$) higher *Prnp* transcription than was transcription in control *Prnp* untreated cells. We did not observe any significant *Prnp* upregulation in cells treated with 1.25 or 2.5 μ M 5-AzaC (Fig. 18B). The activation of *Prnp* expression by TSA but not by 5-AzaC was detected also on a protein level by WB (not shown).

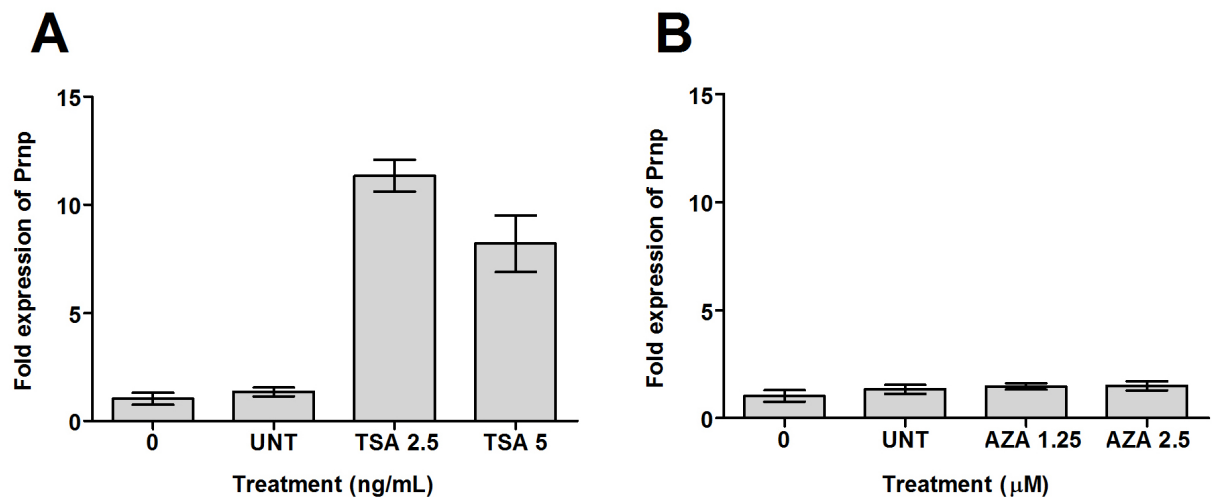


Figure 18: Administration of TSA to growth medium of MEL cells led to the higher *Prnp* gene transcription than treatment with 5-AzaC suggesting that chromatin conformation in *Prnp* locus repress *Prnp* activation. Expression of *Prnp* in MEL cells was examined after 24 hours incubation with 2.5 or 5 ng/mL TSA and 1.25 or 2.5 μ M 5-AzaC, respectively. (A) *Prnp* expression is significantly activated during incubation with TSA an inhibitor of histone deacetylases. (B) Incubation of MEL cells with 5-AzaC an inhibitor of methyltransferases did not lead to *Prnp* activation. *Prnp* expression was quantified by qRT-PCR using *Gapdh* as a reference gene. Expression was determined as a fold difference relative to expression in untreated cells (UNT). Data from two independent experiments; unpaired t-test; mean \pm SD.

4.2.4. Inhibitor of differentiation does not prevent expression of PrP^C

In effort to describe regulation of PrP^C after blocking of erythroid differentiation, we treated MEL cells with Dexamethasone (DEX) an inhibitor of MEL differentiation. In first approach, we changed growth medium 12 hours (early period) post induction (Fig. 19A). After medium exchange cells continued in differentiation in presence of HMBA alone, HMBA and 4 μ M DEX or in growth medium only. Expression of PrP^C was determined by WB after 24 and 120 hours from the beginning of experiment. Degree of differentiation was evaluated by the hemoglobin concentration 120 hours post induction. The highest content of hemoglobin, 17 ± 3 μ g/mL, was in cells continually incubated with HMBA, which hemoglobinized similarly like non-manipulated differentiating cells 17 ± 2.9 μ g/mL (mean \pm SEM). Both lines also expressed elevated levels of PrP^C 24 hours after start of the treatment. At this time, higher level of PrP^C was observed also in cells with medium changed for HMBA/DEX although hemoglobin level was lower, 12.3 ± 3.7 μ g/mL (mean \pm SEM), than in cells with HMBA alone. Cells devoid of HMBA or supplemented with DEX only, produced low levels of hemoglobin comparable to untreated or cells treated with DEX from the beginning. They did not upregulate PrP^C after 24 hours. In second group of cells treated from the beginning with HMBA/DEX, we observed that after medium exchange cells upregulated PrP^C only when HMBA was present in growth medium during 24 hours. If not, the level of PrP^C was lower. PrP^C production after 120 hours was highest in cells that were not treated with HMBA and/or DEX. Cells treated with DEX did not upregulate PrP^C in contrast to untreated confluent cells. Amount of PrP^C in differentiated cells was lower as expected. Cells treated with both agents had level of PrP^C slightly higher than differentiating cells but lower than untreated cells. In second approach, we changed medium 24 hours (late period) after incubation with HMBA or HMBA/DEX when expression of PrP^C was upregulated (Fig. 19B). After medium exchange, the highest hemoglobin production (20 ± 1 μ g/mL) at 120 hours was found in cells with continual presence of HMBA (mean \pm SEM). PrP^C in these cells was downregulated. Similar downregulation was seen in cells incubated with DEX after medium exchange, although their hemoglobin concentration was ~ 3 or 6-fold lower. DEX did not prevent upregulation of PrP^C at 24 hours in presence of HMBA even in higher concentration- 8, 20 and 40 μ M. As well, 120 hours after treatment with increasing concentrations of DEX, no PrP^C upregulation was observed in comparison to DEX untreated cells (not shown). Absence of HMBA and/or DEX upon medium exchange led to PrP^C upregulation with hemoglobin levels ~ 7 -8 μ g/mL.

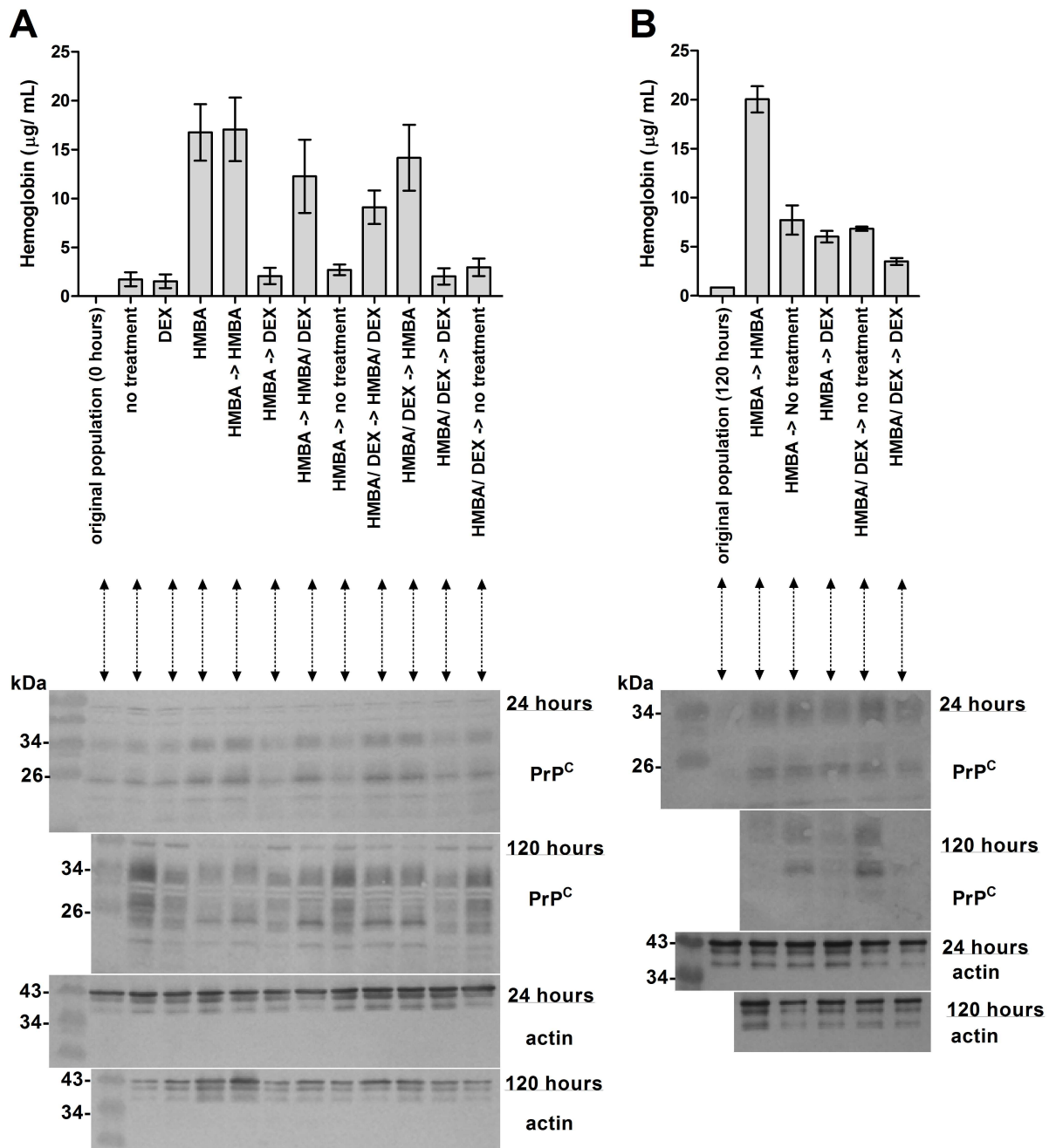


Figure 19: The initial upregulation of PrP^C expression after the induction of differentiation is not affected by DEX. **(A)** Expression of total hemoglobin 120 hours post induction. Induced cells were incubated 12 hours with HMBA and then the medium was changed as shown on x- axis. Expression of PrP^C at 24 hours is highest in cells with HMBA present also after medium exchange. Expression of PrP^C in cells treated with DEX was not similar to untreated cells. Three independent experiments, mean ± SEM. **(B)** Hemoglobin amount 120 hours post induction in cells treated for 24 hours with HMBA when medium was changed as indicated on x- axis. After 120 hours, PrP^C was upregulated only in cells in growth medium without HMBA and/ or DEX. Two independent experiments, mean ± SEM. PrP^C was detected by mix of mAbs AH6, AG4 and 6H4. Hemoglobin was measured by TMB assay.

4.3. Introduction of RNAi methodology and optimization of gene delivery methods for the study of PrP^C role

4.3.1. Transfection of pSilencer 5.1. retro U6 vector coding anti-*Prnp* shRNAs did not lead to PrP^C downregulation

To find out the influence of PrP^C on the process of erythroid differentiation *in vitro* we planned to downregulate its expression. In first approach, we delivered the vectors coding anti-*Prnp* shRNAs by transfection. In that time, there were two published sequences shown to efficiently downregulate PrP^C (Daude et al., 2003), (Tilly et al., 2003). However, only one sequence (here marked as 389) was suitable for cloning to pSilencer 5.1. retro U6 vector. Incorporation of second sequence to retrovector would lead to premature termination of transcription. The reason for premature termination was in the presence of AAAAA (TTTTT) sequence, which is termination site for RNA pol III (Chen et al., 2005). The next 2 sequences (1071 and 1830) were designed and cloned to vector as described above in material and methods part “Cloning- creation of retroviral vectors expressing shRNAs” (Tab. 1).

Selection of MEL cells transfected by pSilencer 5.1. retro U6 vector coding shRNAs led to establishment of puromycin resistant populations. We saw that ratios 3:1 and 4:1 of siPORT XP-1 to DNA were the most effective transfections in cells with starting density 5×10^4 cells per well (Fig 20). However, in selected lines we observed downregulation of PrP^C expression neither on mRNA (Fig. 21A) nor on protein level (Fig. 21B).

Founding of clonal populations did not lead to selection of cell clones with downregulated PrP^C. Attempts to obtain single cells per well (96-well plate) by limited cell dilution of previously selected cells resulted to decreased viability of respective MEL cells. Only cells seeded in a group were proliferating (not shown).

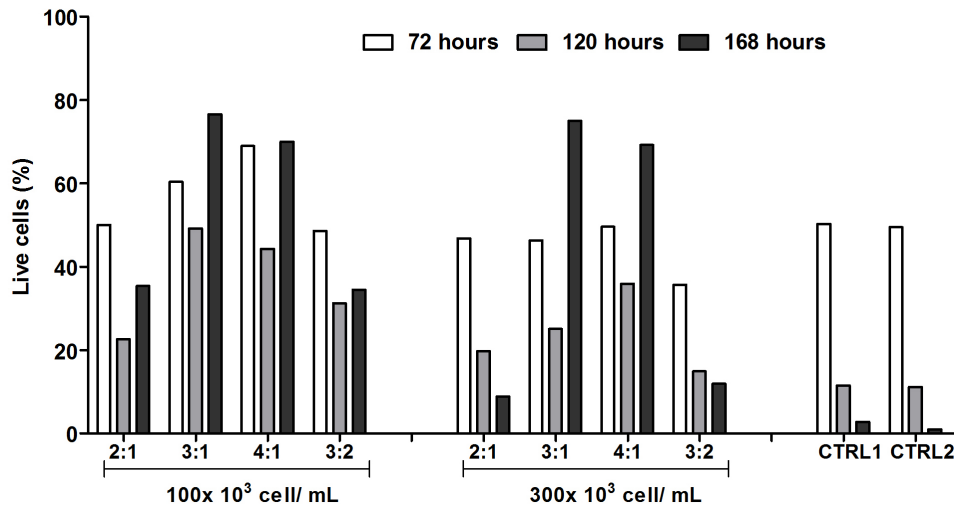


Figure 20: Cell viability after puromycin selection in two groups of MEL cells differing in initial cell density at 24 hours prior to transfection. Percentage of viable cells was determined by Trypan Blue exclusion assay in Bürker chamber at 72, 120, and 168 hours post transfection. CTRL 1 and 2 are control MEL 707 that were not transfected.

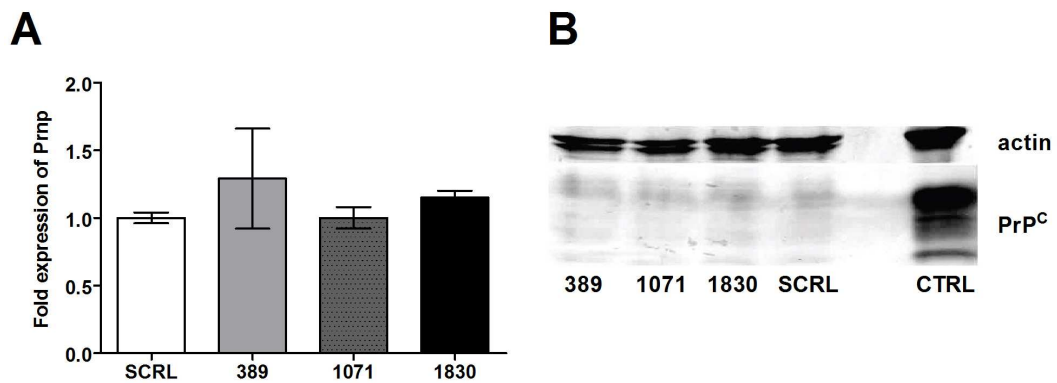


Figure 21: Transfection of pSilencer 5.1. retro U6 vector coding anti-*Prnp* shRNAs did not lead to PrP^C downregulation. (A) Similar expression of *Prnp* gene in MEL cells transfected with pSilencer 5.1. retro U6 vector expressing shRNAs after selection with 0.5 µg/mL puromycin as shown by qRT-PCR using *Gapdh* as a reference gene. Expression in 389, 1071 and 1830 lines was determined as fold difference relative to expression in SCRL cells. (B) Immunoblotting displays similar expression of PrP^C protein in all cells. PrP^C was detected by mix of mAbs AG4 and 6H4. As a loading control polyclonal anti-actin antibody was used. CTRL= positive control for PrP^C detection is represented by 10% murine brain homogenate.

Next, we screened expression of *Prnp* mRNA 12, 24 and 48 hours after transfection to find out if the expression of shRNAs is not inhibited in later stages. We observed mild downregulation (~ 50%) in case of 389-shRNA after 48 hours (Fig. 22A). At that time, second anti-*Prnp* shRNA was shown to be functional upon its transcription from integrated lentivector (Pfeifer et al., 2006). After the cloning of this sequence to our retrovector (marked as 512), we used it in

similar screening as described above. We observed that 512-shRNA expression is downregulated after 48 hours also in this instance but afterwards its level is similar as in SCRL-shRNA (Fig. 22B).

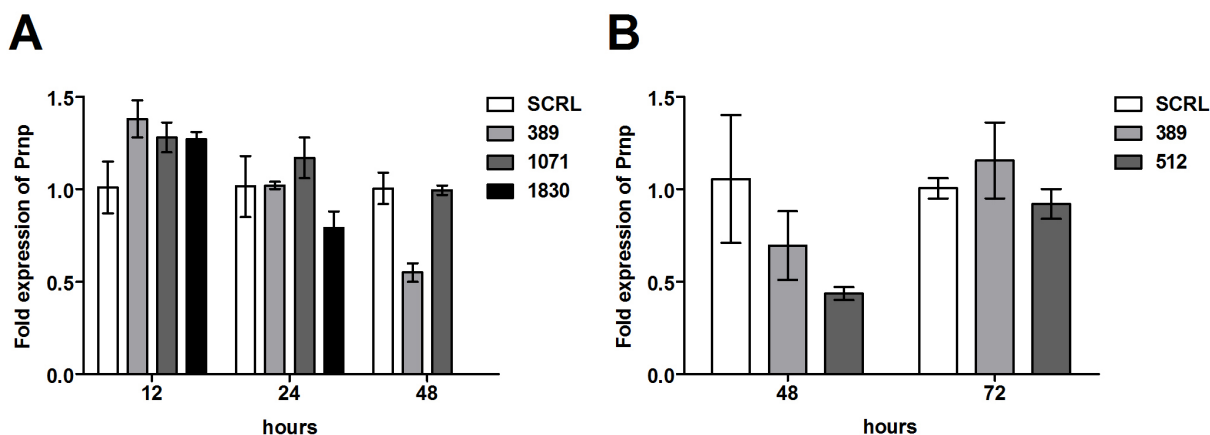


Figure 22: Transcription of *Prnp* gene is partially silenced after 48 hours post transfection with retrovectors coding 389- and 512-shRNAs. **(A)** Expression of *Prnp* mRNA after 12, 24, and 48 hours post transfection. Only 389-shRNA downregulated *Prnp* transcription to ~ 50% after 48 hours. **(B)** Repeated screening 48 hours post transfection showed ~ 40% inhibition of *Prnp* expression transfected with 389-shRNA and ~ 60% inhibition in case of 512-shRNA. After next 24 hours, inhibition was lost and *Prnp* expression in both 389 and 512 lines was similar like in control SCRL line. Quantitative RT-PCR with *Gapdh* as a reference gene. Expression was determined as fold difference relative to expression in SCRL line in specific time points.

Vector integrated to the cell genome may be transcriptionally silenced by DNA methylation and/ or histone modification. Therefore, we treated cells upon selection with mix of 5-AzaC and TSA. Administration of 5-AzaC/TSA may burden cells; therefore, we monitored their viability prior to analysis of *Prnp* expression by qRT-PCR. Cells with stable integrated vectors 389, 512, and SCRL were analyzed by FACS after 14 and 48 hour of 5-AzaC/TSA exposure. Viability was measured by Annexin Vybrant kit (Invitrogen) and 3,3'-dihexyloxycarbocyanine iodide (DiOC₆) (Fig. 23). We saw similar levels of apoptosis/ viability in all lines for respective concentrations of 5-AzaC/TSA. After 14 hours post exposure, average percentage of apoptotic cells increased about 25% alongside increasing 5-AzaC/TSA concentration (Fig. 23A). After additional 34 hours, the percentage of apoptotic cells did not increase proportionally with increasing 5-AzaC/TSA concentration (Fig. 23B). Percentage of viable cells at 14 hours, as stated by DiOC₆ staining, corresponded inversely with percentage of apoptotic cells (Fig. 23C). The same observation after next 34 hours showed disproportions in composition of cell populations based on their viability, suggesting that some cells disintegrated (Fig. 23D).

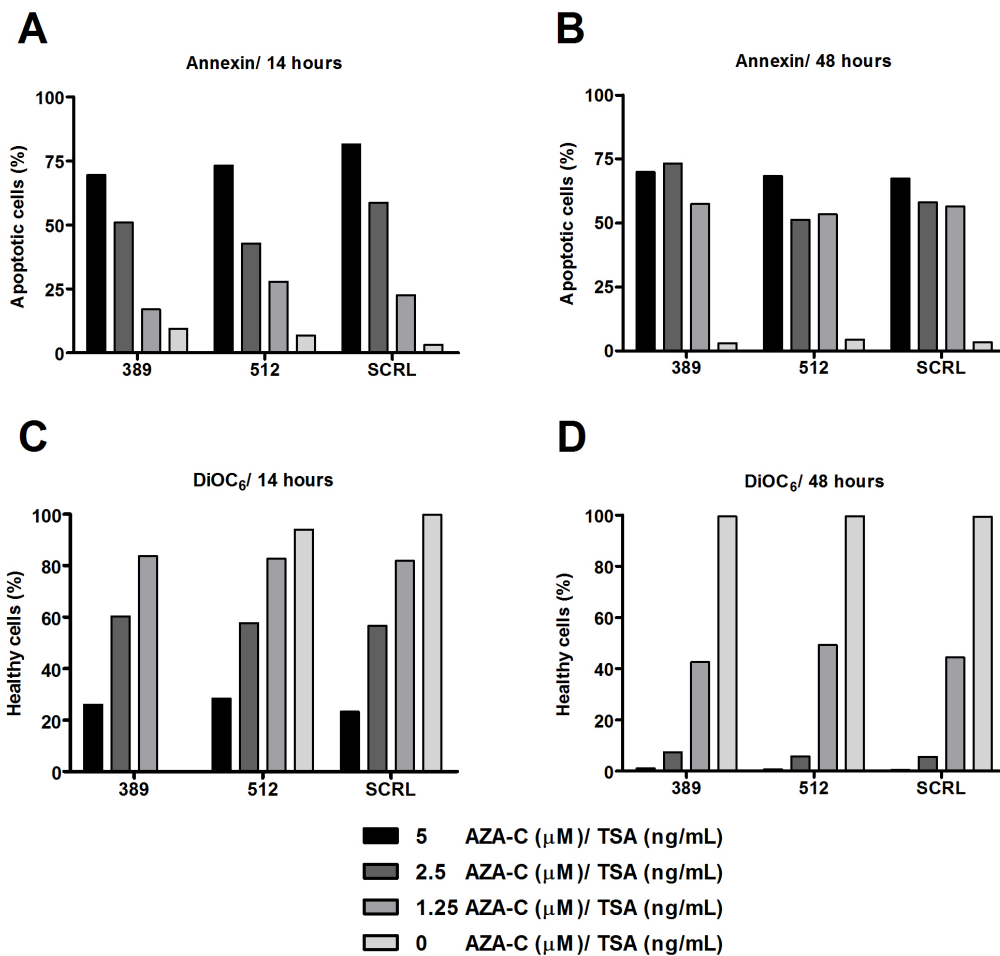


Figure 23: Effect of 5-AzaC/TSA treatment on viability of MEL cells. (A) Cultivation of cells with increasing concentration of 5-AzaC/TSA led after 14 hours to dose response elevation of apoptosis in all lines irrespective of anti-*Prnp* shRNAs. (B) After 48 hours percentage of apoptotic cells rose markedly to 56% only in cells treated by 1.25 5-AzaC (μM)/TSA (ng/mL). (C) Percentage of viable cells after 48 hours. (D) Healthy cells almost disappeared in prolonged incubation with 5 and 2.5 5-AzaC (μM)/TSA (ng/mL).

Based on previous data we analyzed expression of PrP^C just for 389 and SCRL line after 14 hours. We saw increased expression of *Prnp* mRNA after treatment with all 5-AzaC/TSA concentrations (Fig. 24).

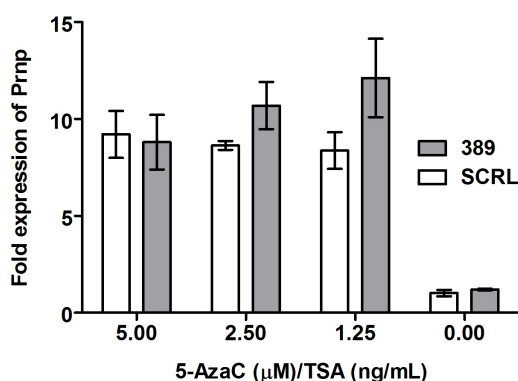


Figure 24: Exposure of MEL cells to increasing concentrations of mixed 5-AzaC (μM)/ TSA (ng/mL) led to upregulation of *Prnp* mRNA transcription after 14 hours. *Prnp* expression was not increased in dose dependent manner. Quantitative RT-PCR with *Gapdh* as a reference gene. Expression was determined as fold difference relative to expression in mock treated SCRL line.

In attempt to resolve why our MEL cells are resistant to puromycin after transfection but do not show any *Prnp* mRNA silencing we decided to test presence of integrated pSilencer 5.1. retro U6 vectors in puromycin resistant cells, we designed set of primers for their PCR detection. However, we did not prove their insertion into genomic DNA (Fig. 25), suggesting that recombination of retrovector during integration to host cell genomic DNA corrupted sequence containing shRNA and its promoter.

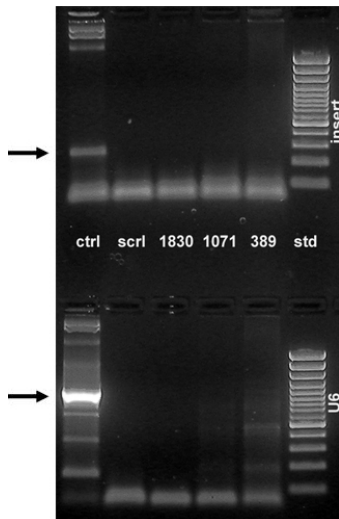


Figure 25: No bands are present in PCR products from genomic DNA of stable transfectants- 389, 1071, 1830, and SCRL MEL cells with supposed incorporated retrovectors as shown by gel electrophoresis after ethidium bromide staining. Expected amplicons-bands should be long 300 bp (insert; detecting presence of cloned shRNA) and 1000 bp (U6; detecting cloned shRNA together with U6 promoter) as was detected (arrows) in control (CTRL) purified retrovector diluted in water.

However, final FACS analysis based on approximative EGFP transfection revealed that transfection efficiency of pSilencer 5.1. retro U6 vectors might vary between ~ 10 and 20% (not shown). This observation hampers our previous findings showing partial *Prnp* silencing in early stages post transfection.

4.3.2. Optimization of retroviral delivery by „packaging cell lines“

Irreproducibility of previous nonviral gene delivery system urged us to employ gene transfer based on retroviral transduction by viral particles produced by „packaging cell lines“.

As a first packaging cell line we used “Phoenix“ cells (Allele Bioscience). Phoenix cells were transfected with transfection agent Arrest-in (Open Biosystems) to DNA of retrovector expressing EGFP (pLEGFP-C1, Clontech) in ratio 8:1 getting ~ 50-70% transfection efficiency. First, to prove functionality of our system we delivered retroviral particles to NIH3T3 cells. We tested two methods- spinfection and co-cultivation. Both ways led to ~ 30-40% positivity for EGFP expression as shown by FACS. After two weeks of selection, EGFP positivity reached ~ 98%. Similar infection of NIH3T3 cells with viral particles coding pSilencer 5.1. retro U6 389, 512 and SCRL shRNAs led to ~ 30-60% inhibition of *Prnp* expression (Fig. 26). Unfortunately, similar approach was not successful in MEL cells (not shown).

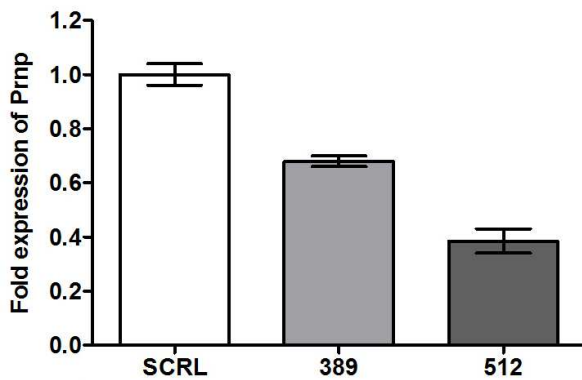


Figure 26: Expression of 389 or 512-shRNAs from integrated retrovirus silenced *Prnp* transcription about 30 or 60%, respectively. Individual shRNAs were delivered to NIH3T3 cells by spinfection of retroviral particles. Quantitative RT-PCR with *Gapdh* as a reference gene. Expression of *Prnp* in 389 and 512 lines was determined as fold difference relative to *Prnp* expression in SCRL line.

4.3.3. RNAi by shRNA of second class led to stable and efficient PrP^C silencing

Finally, we examined the suitability of second generation of shRNAs expressed in context of miRNA (Silva et al., 2005), (Chang et al., 2006) (Fig. 6). In following optimization we changed packaging Phoenix cells for HEK293 GP2 cell line (Clontech). NIH3T3 cells were used as a control for anti-*Prnp* vector delivery and efficiency (Nolan laboratory¹⁰). Based on the FACS analysis of HEK293 GP2 cells transfected by EGFP plasmid, we found out as the most effective 1:9 ratio of DNA to transfection agent. Subsequent optimization showed that we get satisfactory EGFP positivity in target NIH3T3 cells by using the 1:2 ratio of VSV-G plasmid to EGFP retrovector in cells with initial cell density 1×10^5 cells/mL (Fig. 27).

As described in material and methods, we prepared five different anti-*Prnp* shRNAmiR- LP1, LP2, LP5 (the same target sequence as previously used by 512-shRNA), LP6 (the same target sequence as 389-shRNA) and control shRNAmiR LN. In contrast to LP5 shRNAmiR, we failed to prepare correct LP6 shRNAmiR sequence without mutations- deletions of variable length and position in shRNAmiR insert (Tab. 3). Therefore, we excluded LP6 sequence from the next study. Prior to cloning of LP1 and LP2 sequences to LMP vector, we tested their silencing effectivity in pSM2 vectors using NIH3T3 cells as target line (Fig. 28).

	TGCTGTTGACAGTGAGCGAGGGCCCTGGCGGCTACATGCTTAGTGAAGCCACAGATGTAAAGCATGTAGCCGCCAAGGCCCTGCCTACTGCCTCGGA
389/23	GCGGCTA
389/15	GCCAAGGCC
389/03	CTTGGCG
389/08	TGGC
389/05	TGGCG
389/1	CTTGGCGGCTACATGCT
389/A1	GCCGCC
389/A2	TGGCGG
389/B3	GCGGCT

Table 3: After cloning of PCR amplified 389-shRNAmiR (LP6) inserts to LMP retrovector we found various deletions in shRNAmiR sequences isolated from several transformed bacterial colonies (in bold). Blue sequence= expected correct LP6-shRNAmiR; Red sequences= missing sequences.

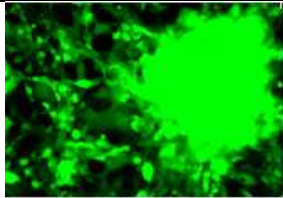
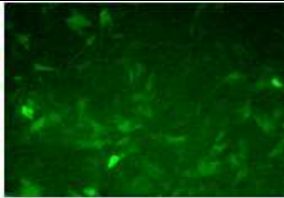
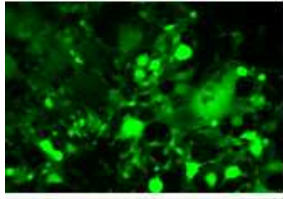
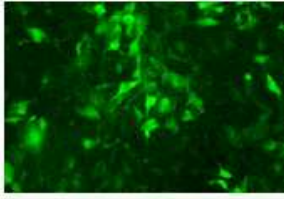
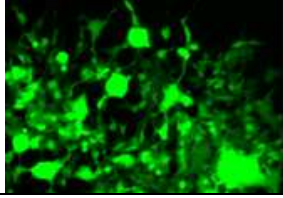
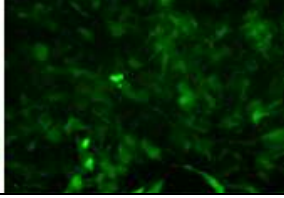
Ratio of vectors	EGFP fluorescence in packaging line:		EGFP fluorescence after retroviral infection-target cells	
	HEK293 GP2	NIH 3T3	*100 x 10 ³	*200 x 10 ³
pVSV-G : pEGFP				
2:1			39	18
1:1			48	24
1:2			54	29

Figure 27: Schematic design of transfection to packaging cell line HEK293 GP2 with various ratios of “vector to envelope plasmid” and following outcome after transduction of target NIH3T3 cells. * Cell density per mL, 24 hours before infection.

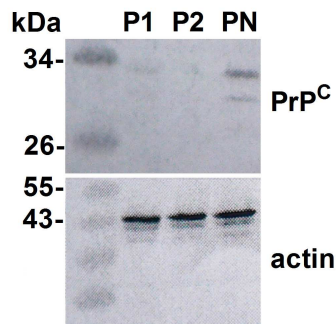


Figure 28: Both anti-*Prnp* shRNAmiRs (P1 and P2) effectively silenced *Prnp* expression in NIH3T3 cells after transduction with pSM2 retrovectors V2MM_66187 or V2MM_63696. PN= control nonsilencing shRNAmiR. PrP^C was detected with mAb AH6. Actin was used as a loading control.

MEL cells were finally infected with LP1, LP2, LP5 and LN retrovectors using both methods of retrovector delivery- spinfection and co-cultivation. Monitoring of EGFP positivity during selection with 0.5 µg/mL puromycin showed rapid increase of EGFP positive cells within one week (NIH3T3) or three weeks (MEL cells) for both retroviral modes of delivery (Fig. 29).

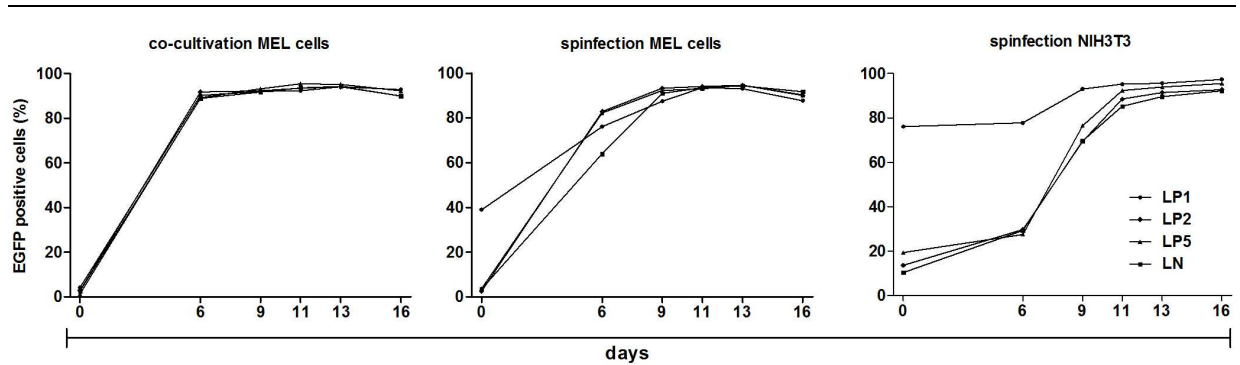


Figure 29: Puromycin treatment of MEL 707 and NIH3T3 cells after retroviral infection led to the selection of cells with integrated retroviral vector within 2 weeks. Efficiency of selection was monitored by presence of retrovector-derived EGFP. Percentage of EGFP positive cells reached > 90% regardless mode of vector delivery and target cell line.

Both, spinfection and co-cultivation, led to efficient silencing of *Prnp* on mRNA and protein level in MEL and NIH3T3 cells using both LP1 and LP2 constructs (Fig. 30A-B). We did not note knockdown of PrP^C in cells transduced with LP5 vector (Fig. 30B). In neither mode of gene delivery RNAi substantially induced cell protective effects as shown by qRT-PCR analysis of chosen interferon stimulated genes (ISGs)- *Eif2ak2*, *Rnase1* and *Oas1a* (Fig. 31).

Silencing of PrP^C in LP1 and LP2 lines is stable during the entire HMBA-mediated erythroid differentiation. In comparison with MEL LN line, PrP^C expression is inhibited from ~ 79% (LP1) to 84% (LP2) at 0 hours to 93% (LP1) and 96% (LP2) after 120 hours, as shown by qRT-PCR (Fig. 32A).

Quantitative FACS analysis confirmed downregulation of PrP^C on cell membranes ~ 83% (LP1) to 88% (LP2) at 0 hours to ~ 92% (LP1) and 95% (LP2) after 48 hours (Fig. 32B). Expression of PrP^C protein in LN lines detected by WB shows similar regulation as observed previously in MEL 707 cells. However, we could barely observe presence of PrP^C in LP1 and LP2 lines only at 24 hours (Fig. 32C) showing effective silencing of total cellular PrP^C protein.

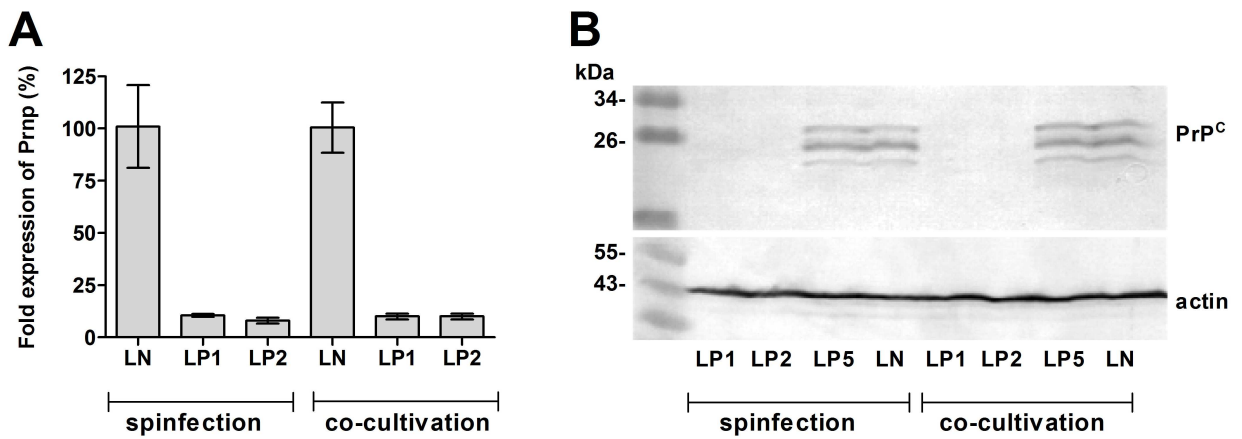


Figure 30: RNAi substantially downregulated PrP^C expression in MEL LP1 and LP2 lines. **(A)** Both methods of retroviral vector delivery led to ~ 90% silencing of *Prnp* mRNA in both lines expressing anti-*Prnp* shRNAmiR (LP1 and LP2) when compared to MEL line expressing nonsilencing shRNAmiR (LN) as shown by qRT-PCR using *Gapdh* as a reference gene; mean \pm SD. **(B)** Confirmation of PrP^C downregulation in LP1 and LP2 on protein level by WB, PrP^C was detected by mAb AH6. No silencing was observed in LP5 cell line. Actin was used as a loading control. Expression of both *Prnp* mRNA and PrP^C protein was evaluated on the end of the selection by puromycin.

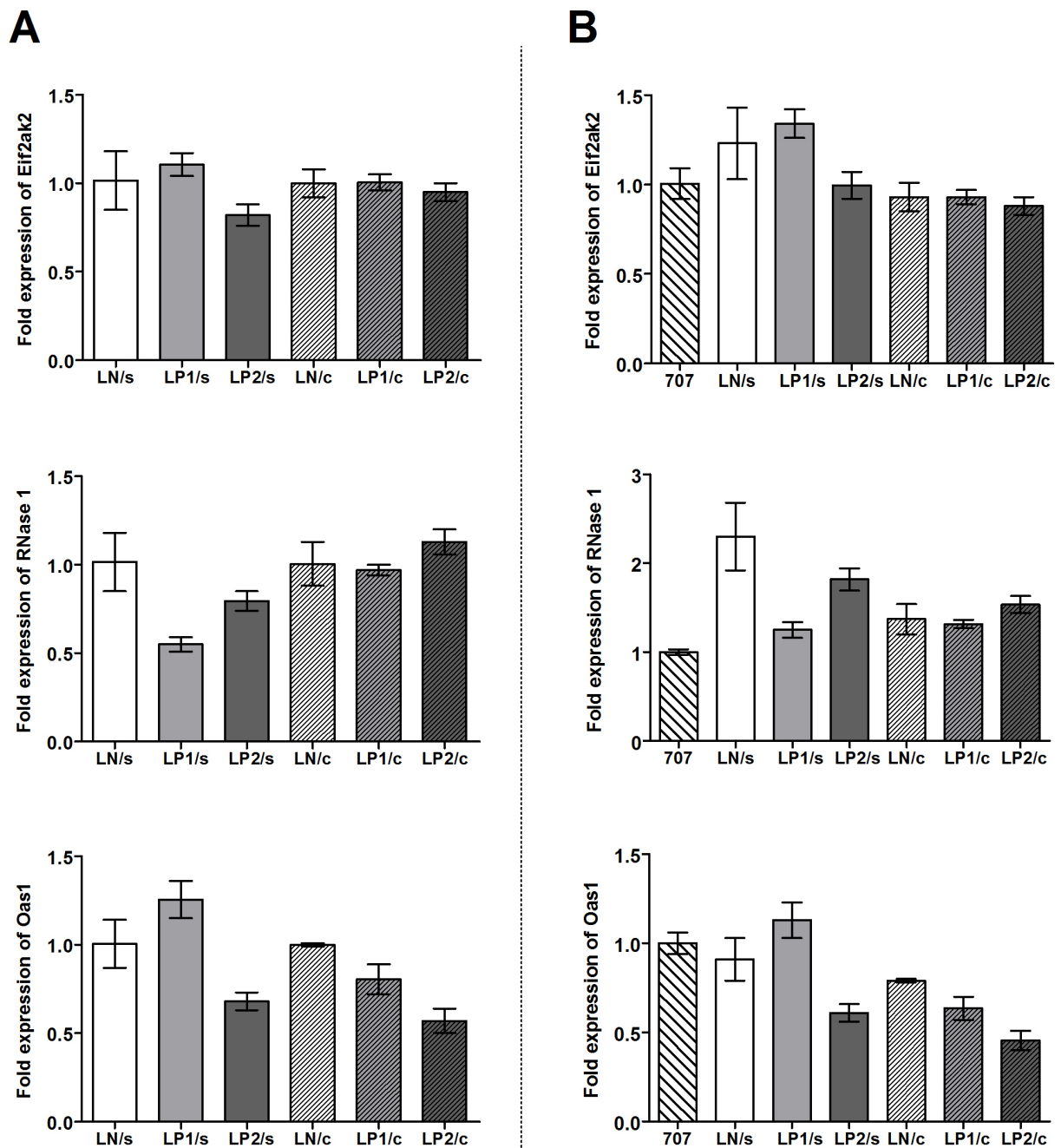


Figure 31: RNAi does not substantially induce interferon response in MEL cells as shown by qRT-PCR following ISGs- *Eif2ak2*, *Rnase1* and *Oas1a*. (A) Left side graphs show transcription of respective genes in lines LP1 and LP2 determined as fold difference relative to expression in LN line separately for both delivery methods. (B) Graphs on the right side show transcription of respective genes in lines LP1, LP2 and LN determined as fold difference relative to expression in retrovirally uninfected MEL 707 line. Cell line name /s or /c denotes method of gene delivery- spinfection or co-cultivation. Transcription of chosen ISGs genes were monitored in cells on the end of the selection. Mean \pm range.

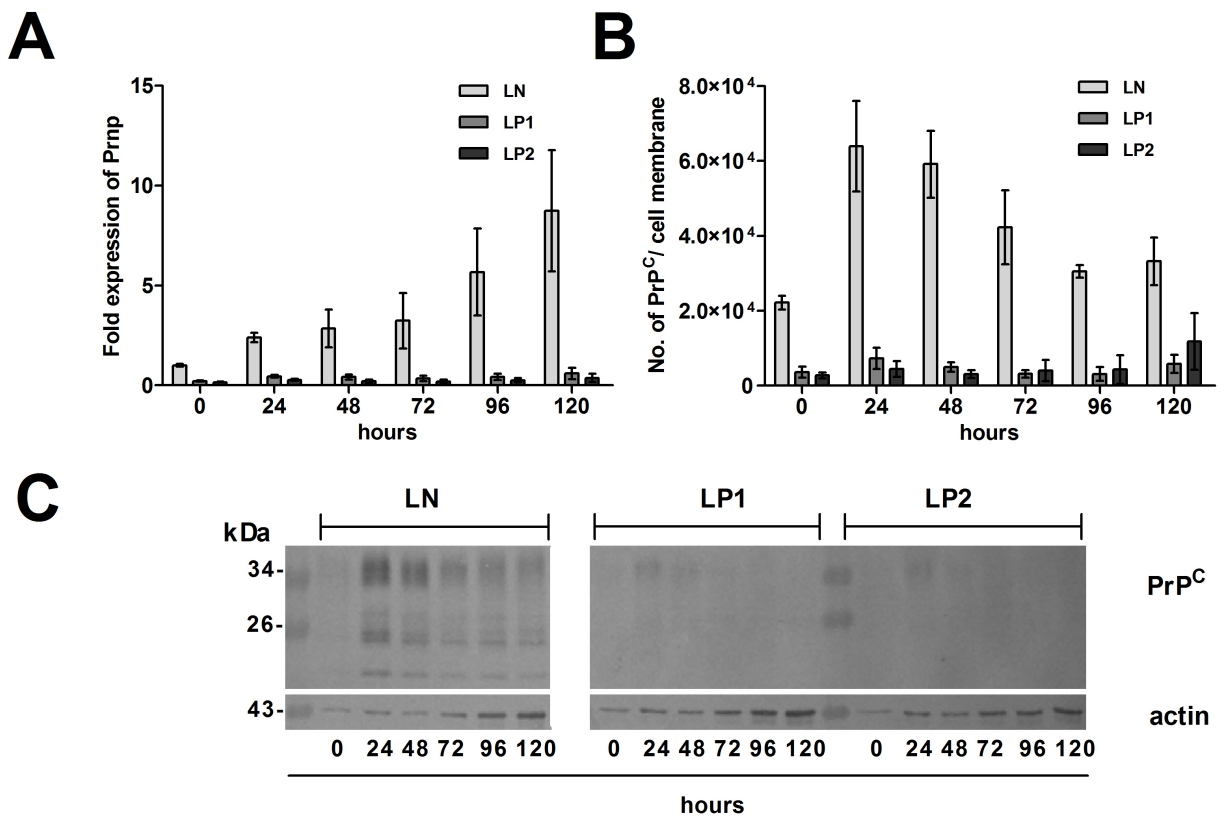


Figure 32: Expression of PrP^C is stably repressed during the course of HMBA-induced erythroid differentiation. (A) Downregulation of *Prnp* on mRNA level; qRT-PCR using *Gapdh* as a reference gene; two independent experiments; mean ± SD. Expression of *Prnp* in lines LP1 and LP2 is determined as fold difference relative to expression in LN cells at 0 hours. (B) Downregulation of PrP^C on cell membranes in LP1 and LP2 lines verified by quantitative FACS, four experiments; mean ± SD. (C) Confirmation of stable PrP^C silencing by WB. PrP^C in LP1 and LP2 cells was hardly detectable at 24 hours post induction to differentiation. PrP^C was detected by mAb mix AH6, AG4 and 6H4. Actin served as a loading control.

4.4. Silencing of *Prnp* gene by RNAi suggests that PrP^C is dispensable for erythroid differentiation *in vitro*

4.4.1. Similar proliferative capacity and viability during differentiation was observed in all MEL lines irrespective of *Prnp* quantity

Cell numbers in LN and LP1 lines similarly increased up to ~ 2.4 × 10⁶ or 2.3 × 10⁶ cells/mL until 72 hours when fall occurred. In LP2 cell line, we noticed higher proliferation activity with maximum of ~ 3 × 10⁶ cells/mL (Fig. 33A). Twenty-four hours post induction *c-myb* transcription was downregulated about ~ 73% in LN line, ~ 78% in LP1 and ~ 88% in LP2 line. After next 24 hours (48 hours post induction), *c-myb* was downregulated to ~ 2% level in comparison to beginning and remained repressed until the end of experiment (Fig. 33B).

Observed reduction of *c-myb* transcription suggests similar loss of proliferative capacity after HMBA induction. In parallel, we monitored percentage of living cells by Trypan Blue exclusion assay estimated by cell-counting machine Countess (Invitrogen). The viability (~94%) did not change during 72 hours post induction. After that, we observed significant but similar drop off in viability in all lines (Fig. 33C). Possible induction to apoptosis by transcriptional increasing of proapoptotic *Bax* was not observed regardless of PrP^C expression (Fig. 33D).

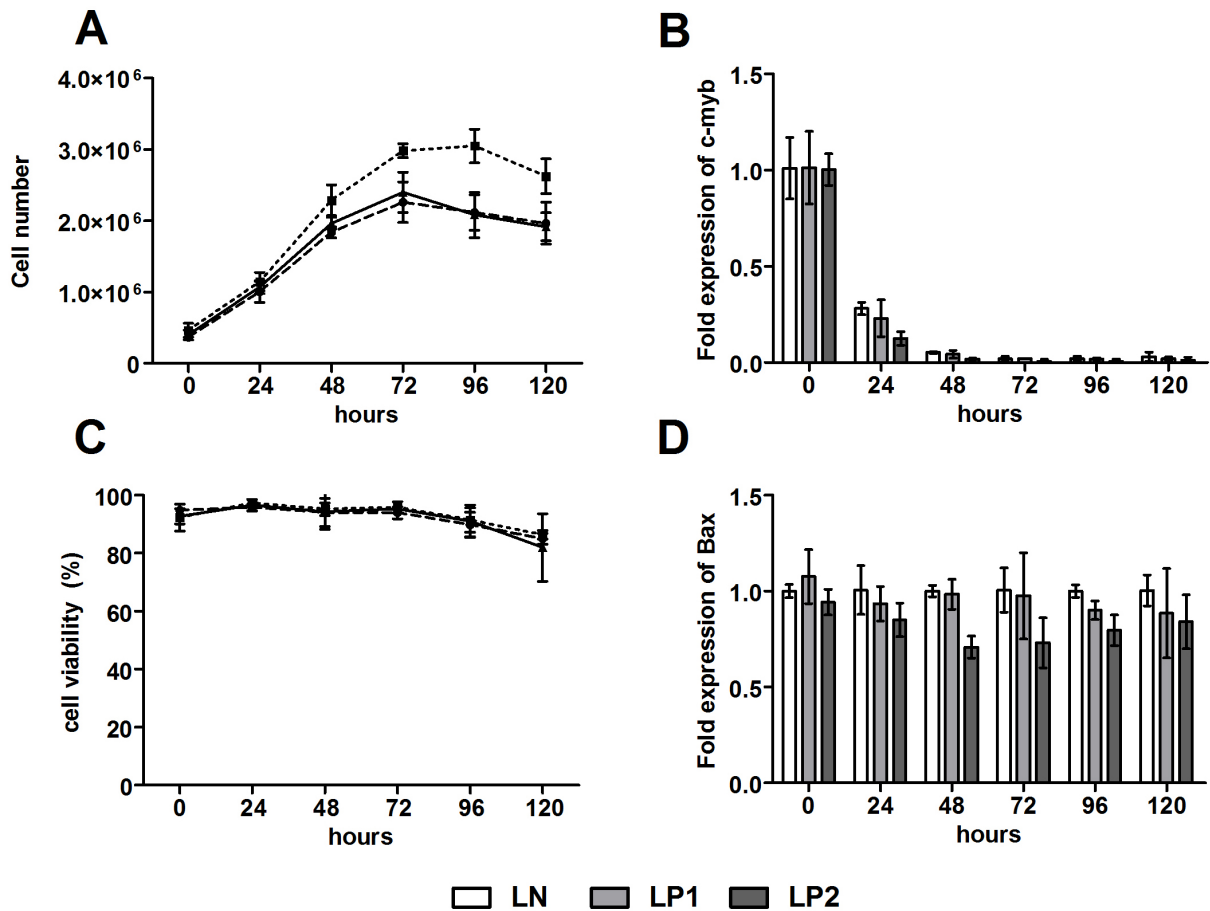


Figure 33: Viability and proliferation of MEL cells during erythroid differentiation shows similar pattern irrespective to PrP^C quantity. **(A)** Cell numbers during erythroid differentiation, counting based on image analysis. **(B)** Transcription of *c-myb* is similarly downregulated in all 3 MEL lines. Expression was determined in each line separately as fold difference relative to expression at 0 hours. **(C)** Cell viability based on Trypan Blue exclusion assay. **(D)** Transcription of *Bax* gene in LP1 and LP2 lines was determined as fold difference to expression in LN cells each day individually. Quantitative RT-PCR using *Gapdh* as a reference gene was used in figures B and D. Data from two independent experiments; mean ± SD.

4.4.2. Silencing of *Prnp* expression does not interfere with erythroid differentiation *in vitro*

Production of hemoglobin was equal irrespective of PrP^C expression (Fig. 34A). In average hemoglobinizing cells produced 14 ± 5 $\mu\text{g/mL}$, 14 ± 4 $\mu\text{g/mL}$ and 17 ± 5 $\mu\text{g/mL}$ of total hemoglobin in LN, LP1 and LP2 line, respectively (mean \pm SD). Similar quantity of transferrin receptor (CD71) molecules per cell was detected in all lines (Fig. 34B). Furthermore, the pattern of its expression during differentiation was similar in all lines as well. Quantity of CD71 was more or less stable during 72 hours, except point at 24 hours when we observed quite high variability. After 96 hours, number of CD71 molecules per cell decreased about 47% (LN), 52% (LP1) and 57% (LP2) in comparison with amount of CD71 at 72 hours. Decrease in CD71 molecules continued next 24 hours in similar manner when we noted fall about 49% (LN), 55% (LP1) and 56% (LP2) from the level of previous day (96 hours).

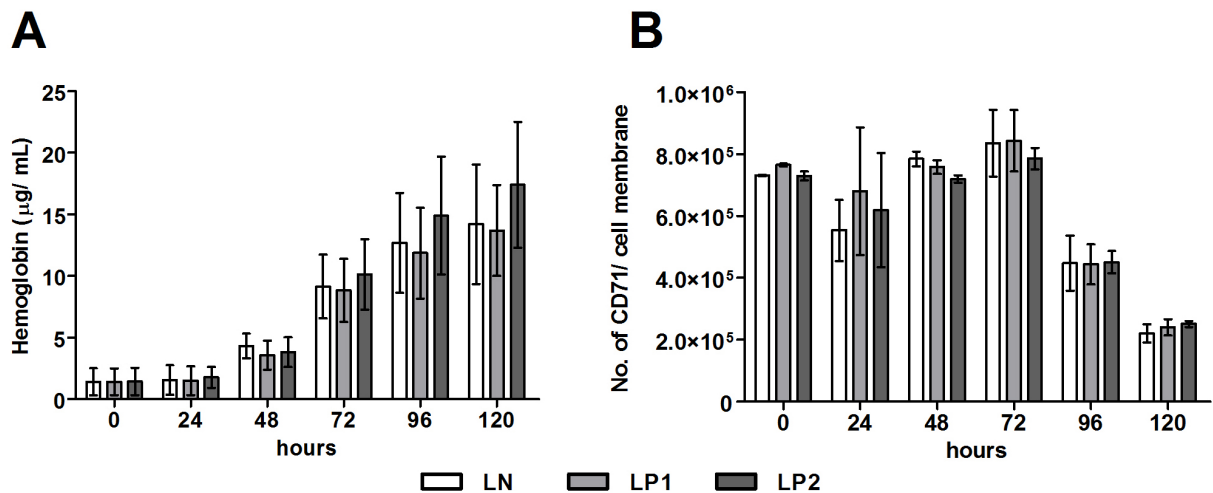


Figure 34: Production of total hemoglobin during differentiation was similar regardless on PrP^C silencing as shown by TMB assay in 100 $\mu\text{g/mL}$ of total proteins; data from four independent experiments; mean \pm SD (A). Pattern of CD71 expression on cell membrane as well as CD71 quantity was similar in all lines (B). Number of CD71 molecules per cell, analyzed by quantitative FACS was based on assumption that one IgG (anti-CD71-PE) molecule binds one molecule of TfR. Data from two independent experiments; mean \pm SD.

Monitoring of selected erythroid specific genes- AHSP (*Eraf*), hemoglobin- α (*Hba*) and *GATA1* (not shown) at transcription level showed also analogical expression in all lines during the differentiation (Fig. 35A-B). Although we noticed that in some time points (24-48 hours) expression of *Eraf* or *Hba* in LP2 line differs in comparison to expression of respective genes in LN line, we cannot assign observed differences solely to PrP^C silencing.

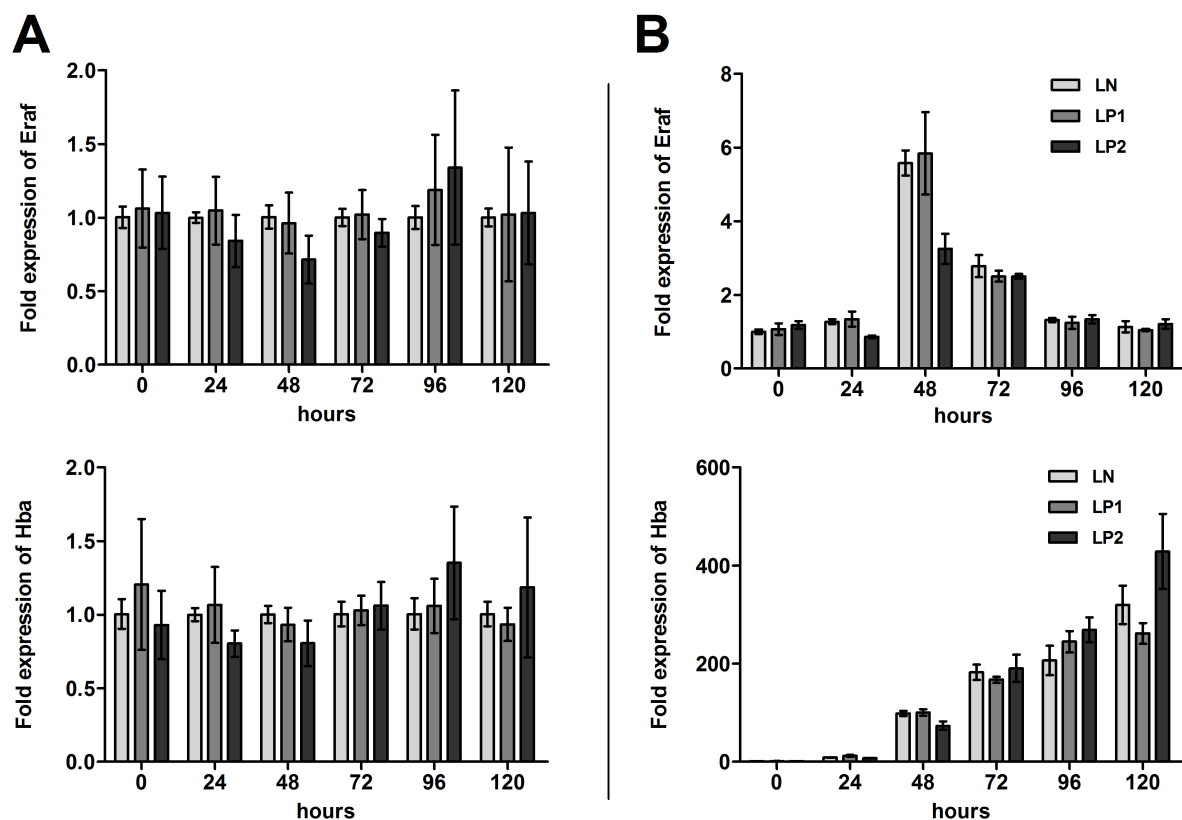


Figure 35: Transcription of selected erythroid markers measured by qRT-PCR shows similar quantity and pattern during erythroid differentiation. Transcription of *Eraf* (α -hemoglobin stabilizing protein) and *Hba* (hemoglobin- α) genes in LP1 and LP2 lines was determined as fold difference relative to expression in LN cells each day individually (A). Quantitative RT-PCR from four independent experiments; mean \pm SD. (B) Representative pattern of transcription was determined in each line separately as fold difference relative to expression in LN at 0 hours.

4.4.3. Low expression of PrP^C does not influence iron uptake in MEL cells

This part of the study was done in collaboration with RNDr. Jiří Petrák, CSc. and Doc. MUDr. Daniel Vyoral, CSc. from Institute of Pathological Physiology, 1. LF UK and Institute of Hematology and Blood Transfusion in Prague, respectively. Besides the quantitation of transferrin receptor by FACS during erythroid differentiation, we also examined uptake of 3 μ M radiolabeled ^{59}Fe bound to transferrin (Tf) with relation to PrP^C expression in MEL cells during normal conditions. MEL absorbed ^{59}Fe -Tf in time dependent manner, but we did not observe any relation of ^{59}Fe -Tf uptake to PrP^C quantity during short time incubation (1, 2 min and 30 sec, 5 and 10 min) (Fig. 36A). On the other side, uptake in MEL 707, LP1 and LP2 cells was significantly lower ($p < 0.0001$) than in LN line during whole prolonged incubation- 10, 30 and 60 min. (Fig. 36B). However, in follow up study we found out that iron uptake in MEL 707 cells was similar to LN cells except the 10 min exposure to ^{59}Fe -Tf when the iron uptake in

MEL 707 was significantly lower ($p = 0.02$). In the rest of the MEL lines with nonsilenced *Prnp* (LMP and LP5) we observed significantly higher ($p < 0.0001$) iron uptake after 10, 30 and 60 min exposure to $^{59}\text{Fe-Tf}$ (Fig. 36C). We also studied $^{59}\text{Fe-Tf}$ uptake in MEL cells 48 hours post induction to erythroid differentiation. In this instance, we saw significant difference between LN and MEL 707 lines in all time points (5, 10 and 15 min) (Fig. 36D). Significant lower iron uptake was observed also in LP2 cells for each time point but uptake in LP1 cells was significantly lower only after 15 min.

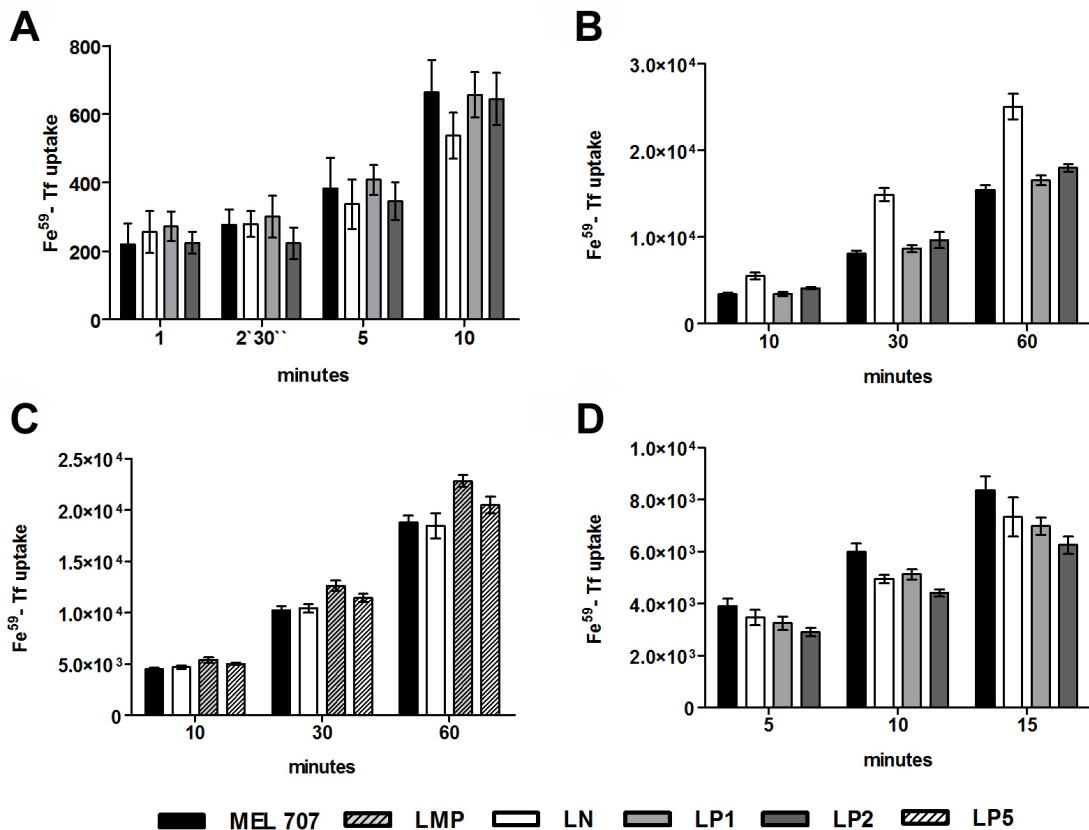


Figure 36: Uptake of $^{59}\text{Fe-Tf}$ by MEL cells tends to be lower in LP1 and LP2 lines in comparison to LN line. However, variability in cells with free *Prnp* expression counteracts to clear decision. (A) Uptake of $^{59}\text{Fe-Tf}$ after short incubation (1, 2 min 30 sec, 5 and 10 min) showed no difference in respect to PrP^C quantity. (B) On the other side, uptake of $^{59}\text{Fe-Tf}$ in longer time points (10, 30 and 60 min) revealed significant difference of LN line from the rest of the lines. (C) Variability in uptakes of $^{59}\text{Fe-Tf}$ among lines with non-silenced PrP^C (MEL707, LMP, LN, and LP5). (D) Uptake of $^{59}\text{Fe-Tf}$ after short time exposure (5, 10 and 15 min) in cells 48 hours post induction to differentiation. Unpaired t-test; mean \pm SD.

4.4.4. All differentiating cells respond similarly to lower level of iron

We compared expression of CD71 in differentiating LN, LP1 and LP2 cells under normal growth conditions and under conditions with lower iron level when iron was chelated by 20 μM Desferral (final concentration). Previously we showed that CD71 expression is

similar during undisturbed differentiation of LP1 and LP2 cells and now we saw similar level of CD71 on membranes of MEL cells even upon treatment with Desferral (Fig. 37A). Addition of Desferral to growth medium simultaneously with HMBA led after 24 hours to the slight but significant ($p = 0.034$) decrease of CD71 in comparison to previous day. At 48 hours expression raised to $\sim 1.1 \pm 1.4 \times 10^6$ IgG/ cell which was significantly ($p = 0.0002$) higher than in untreated group $\sim 7.5 \pm 0.4 \times 10^5$ IgG/ cell (mean \pm SD). Presence of CD71 in untreated group did not show significant difference after 24 or 48 hours. Afterwards, expression of CD71 in all treated and untreated cells decreased similarly. However, significant difference in CD71 expression as seen between Desferral treated and untreated group after 48 hours disappeared, except 120 hours when presence of CD71 was significantly higher on membranes of cells in treated group ($p = 0.003$) (Fig. 37B).

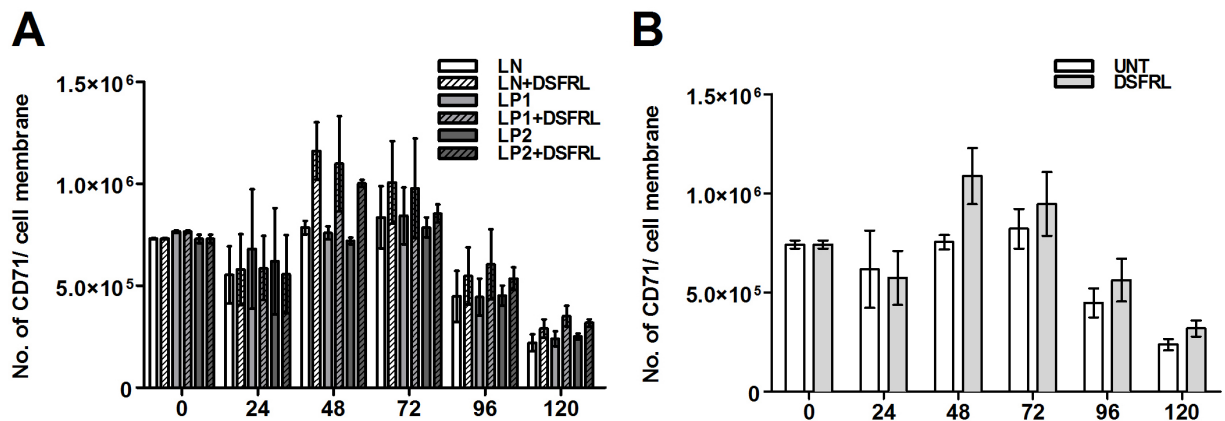


Figure 37: MEL cells in response to iron chelator- Desferral (DSFRL) regulated CD71 expression similarly regardless of PrP^C quantity. **(A)** Expression of CD71 in differentiating MEL lines under normal growth conditions and incubated with DSFRL. **(B)** Presence of CD71 during erythroid differentiation in DSFRL treated and untreated (UNT) group. Data from individual lines are grouped together according the treatment and particular time point. CD71 is significantly upregulated in DSFRL treated group from 48 hours until 120 hours in comparison with UNT. Provided that one molecule of mAb (IgG) binds one molecule of CD71, numbers of IgG/cell equals to numbers of CD71/cell. Quantitative FACS was done using anti-CD71-PE mAb; two independent experiments; unpaired t-test; mean \pm SD.

4.5. Utilization of RNAi in study of infectious prion in cell culture

4.5.1. Preliminary attempts to infect MEL cells with RML infected brain homogenate suggest that MEL cells do not propagate infectious PrP

MEL 707, LN, LP1, and LP2 were left 96 hours to grow until they reached confluence. From this time, cells were incubated for next 24 hours with 0.1 % RML brain homogenate.

After 24 hours, we were able to detect resistant PrP in all MEL cultures, even in cells with minimal expression of PrP^C (Fig 38A). We obtained similar result also after next 96 hours (1st passage) (Fig. 38A). However, signal intensity 120 hours post infection was lower than after 24 hours and completely disappeared after additional 96 hours (2nd passage) (Fig. 38A) suggesting dilution and degradation of resistant PrP. Decreased but still permanent presence of RML signal in LP1 and LP2 lines in RML signal after washing of cells suggests that we detected inoculum (Fig. 38B).

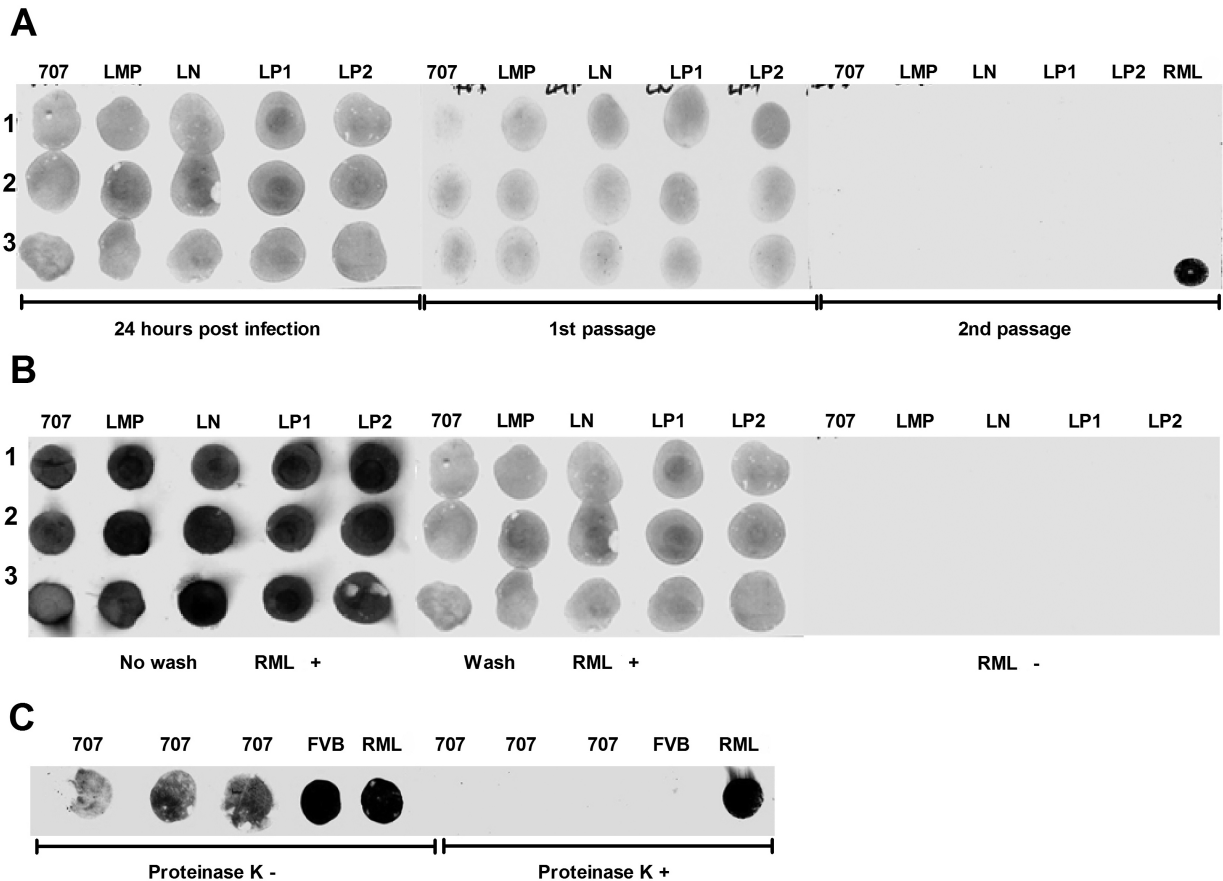


Figure 38: (A) From left to right: RML strain is detected in all MEL cells including LP1, LP2 lines after 24 hours incubation. We can detect resistant PrP after next 96 hours post infection (1st passage) in all MEL cells including LP1, LP2 lines. After next 4 days of growth (2nd passage), we did not detect any positivity for PrP^{TSE}. Cells from all intervals were washed prior to membrane dot blotting. All cell blots were treated with proteinase K. (B) Significant drop off in PrP^{TSE} positivity after washing of infected cells. No PrP^C was detected in RML negative control cells suggesting that we did not observe background signal. Again, all cell blots were treated with proteinase K. (C) Control assay of proteinase K function. PrP^C from MEL 707 cells and normal brain homogenate (FVB) was only detected in untreated cells. Proteinase K effectively degraded all PrP^C in RML uninfected cells/homogenate. PrP^C/PrP^{TSE} was immunoblotted with mix of mAbs- 6H4, AG4 and AH6.

4.5.2. RNAi leads to efficient silencing of *Prnp* gene in CAD5 cells

Transduction of non-infected and also RML propagating CAD5 cells by LP1 and LP2 retrovectors led to efficient silencing of *Prnp* as shown by WB (Fig. 39). Again, LP5 shRNAmiR was not efficient and we excluded LP5 stable integrants from next study. In comparison with LN, expression of *Prnp* mRNA in LP1 and LP2 cells was lower for ~ 86% and ~ 87% respectively (Fig. 40A). As well in CAD5 cells that have been already infected by RML prion strain, we observed downregulation for ~ 77% and 68% in LP1 or LP2 cells, respectively (Fig. 40A). Quantitative FACS analysis confirmed data by qRT-PCR showing corresponding results where LP1 and LP2 were downregulated for ~ 93% and ~ 92%. In RML infected lines, silencing of *Prnp* in LP1 and LP2 was lower for ~ 89% and ~ 87% (Fig. 40B). From three analyzed ISGs genes *Eif2ak2*, *Rnase1* and *Oas1a* we detected by qRT-PCR only *Eif2ak2* and *Rnase1*, although *Rnase1* only in very low detectable level (Fig. 41). Expression of *Eif2ak2* in LMP and LN lines in comparison with CAD5 cells that were not transduced by retroviral vector, did not show significant difference. On the other side, LP1 and LP2 lines in RML uninfected cells showed significantly lower expression of *Eif2ak2* than LN line ($p < 0.0001$ and $p = 0.0004$, respectively) (Fig. 41A). In CAD5 cells infected with RML prion strain, expression of *Eif2ak2* was significantly higher in all cells comparing to LN (Fig. 41B) ($p = 0.0003$ and $p = 0.035$ for LP1 and LP2, respectively). We did not calculate difference in expression of *Rnase1* due to its high variability (not shown).

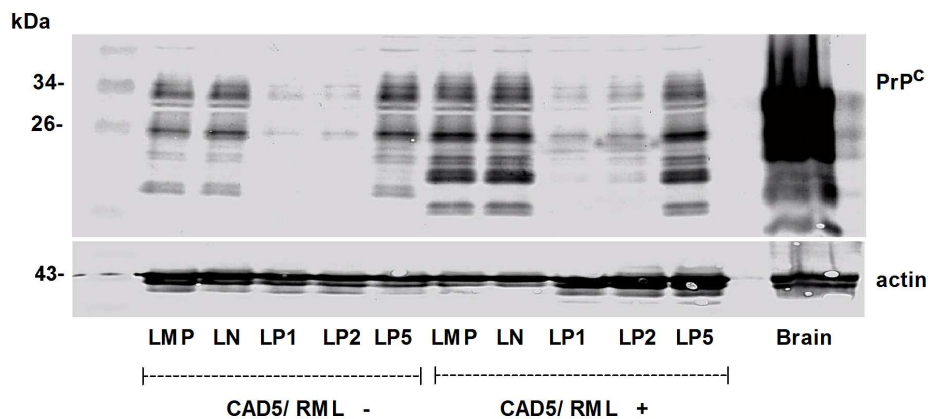


Figure 39: WB shows efficient downregulation of PrP^C expression in CAD5 cells transduced by retroviral vectors expressing shRNAmiRs targeting *Prnp* mRNA (LP1 and LP2). Transduction with LP5 vector did not lead to PrP^C downregulation, which is similar like in nonsilencing LN control and LMP line transduced with empty vector. PrP^C was detected with mix of mAbs - 6H4, AG4 and AH6. Brain= PrP^C positive control- 5% FVB brain homogenate. RML -/+ = susceptible or RML infected CAD5 cells. Actin served as a loading control. WB was done after selection of stable integrants with 1.5 µg/mL puromycin.

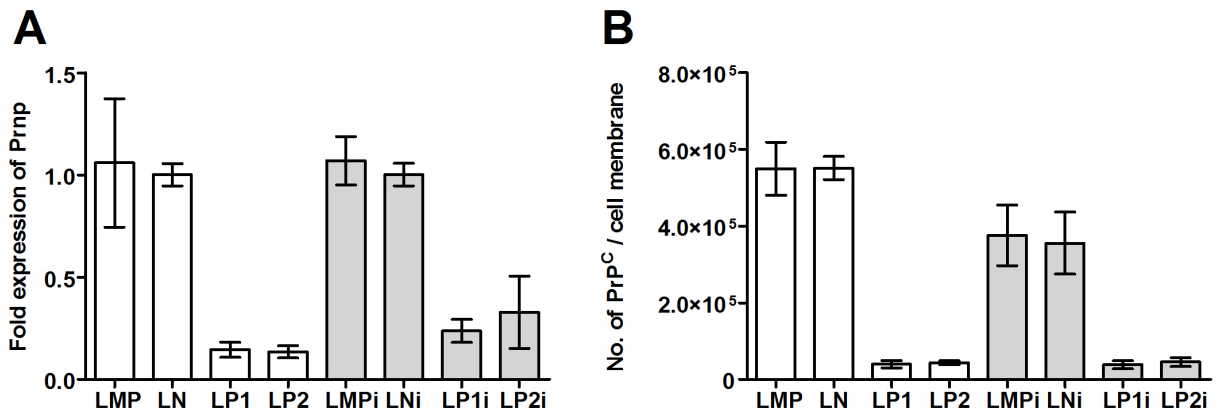


Figure 40: Transcription of *Prnp* is efficiently silenced after selection of CAD5 cells infected with retrovectors coding LP1 and LP2 shRNAmiRs when compared to CAD5 cells expressing nonsilencing LN shRNAmiR. **(A)** *Prnp* silencing in normal CAD5 cells (three independent experiments) and in cells already infected with RML strain (i) prior to *Prnp* silencing (two independent experiments) as shown by qRT-PCR. Expression was determined as fold difference relative to expression in LN cells in each treatment (presence or absence of infectious PrP) individually. **(B)** Number of PrP^C per cell membrane. Quantitative FACS based on assumption that one anti-AH6-PE mAb binds one PrP^C molecule. LMPi, LNⁱ, LP1ⁱ, and LP2ⁱ= RML infected cells. Mean ± SD.

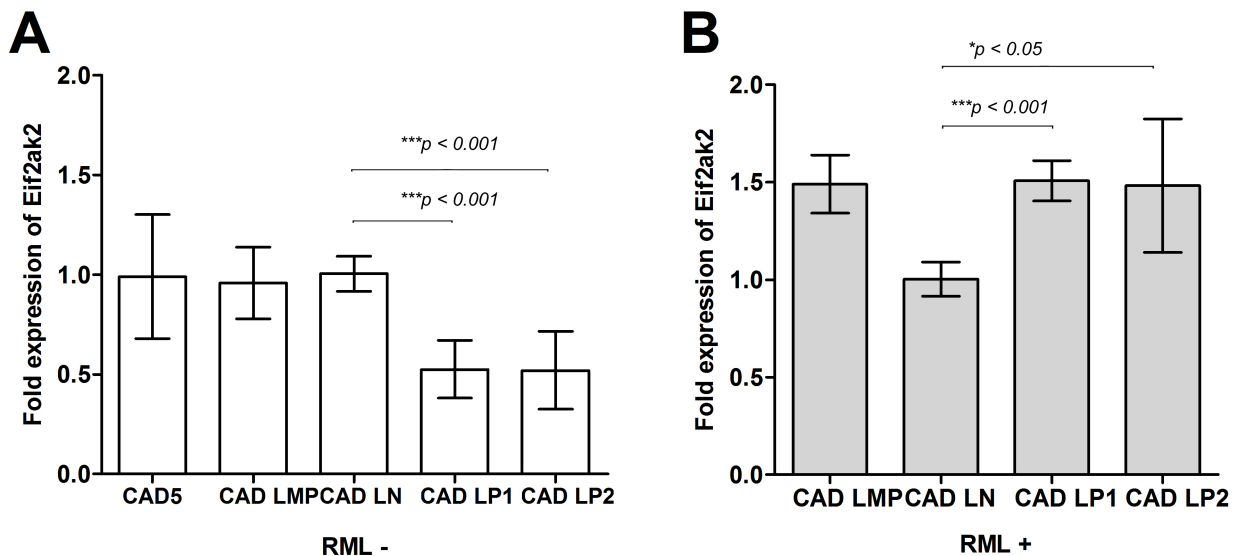


Figure 41: Expression of *Eif2ak2* in CAD5 cells. **(A)** Expression *Eif2ak2* in uninfected LP1 and LP2 lines showed significant lower expression in comparison with LN, LMP or nontransduced CAD5 cells. **(B)** Contrary to uninfected cells, expression of *Eif2ak2* in LP1 and LP2 cells infected with RML was significantly higher in comparison with *de novo* RML infected LN cells but similar to LMP line. Quantitative RT-PCR, *Gapdh* served as reference gene, RML - cells three independent experiments; RML+ two independent experiments; unpaired t-test; mean ± SD. Expression was determined as fold difference relative to expression in LN cells in each treatment (presence or absence of infectious PrP). RML -/+ denotes line uninfected or infected with RML prion strain.

4.5.3. Downregulation of PrP^C expression significantly reduce PrP^{TSE} formation

This part of the study was done in collaboration with Dr. Olga Janouskova from our laboratory. Downregulation of PrP^C expression prior to infection with 0.1% RML containing brain homogenate significantly prevents *de novo* PrP^{TSE} formation in LP1 and LP2 cells as shown by cell blot assay (Fig. 42 A-B). On the other hand, RML infection of control LMP and LN lines with normal PrP^C expression led to propagation of PrP^{TSE} and prion infectivity (Fig. 42A-B). This observation was supported by successful infection of susceptible CAD5 cells with conditioned media harvested either of infected LMP or of LN cells. We detected PrP^{TSE} in CAD5 cells cultivated with infectious medium, diluted at 1:1 ratio with fresh medium, from infected LMP or LN lines. No resistant PrP was seen upon incubation with conditioned growth medium from LP1 and LP2 (Fig. 42C). Similar result, although in lower resolution, was obtained after diluting the infected media with fresh growth medium in ratio 1:4 (Fig. 42C). Analogical incubation of CAD5 cells with lysates from RML infected cells resulted in propagation of PrP^{TSE} only in cells infected with 1% or even 0.1% cell lysate derived from LMP or LN lines but not from LP1 or LP2 lines (Fig. 42D).

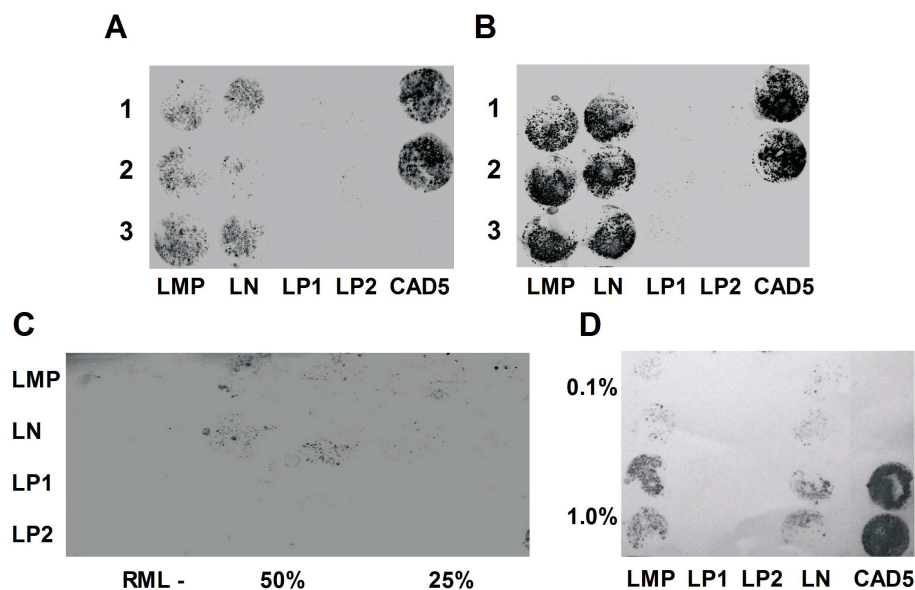


Figure 42: Silencing of *Prnp* gene substantially counteracts to *de novo* propagation of PrP^{TSE}. Detection of PrP^{TSE} after *de novo* infection with 0.1% RML brain homogenate by cell blot assay- 1st passage after infection (A) and 4th passage (B). Infection was carried out in triplicates (1- 3) for transduced cells or in duplicates for nontransduced cells. (C) Detection of PrP^{TSE} after infection of CAD5 cells with 50% or 25% medium harvested from RML infected LMP, LN, LP1 or LP2 cells. (D) PrP^{TSE} after infection of CAD5 cells with 1% or 0.1% cell lysate from LMP, LN, LP1 or LP2 previously infected with 0.1% RML brain homogenate. Infection was performed in duplicates. PrP was detected with mAb AH6.

4.5.4. RNAi of *Prnp* gene does not cure RML infected cells

This part of the study was done in collaboration with Dr. Olga Janouskova from our laboratory. Silencing of PrP^C expression in CAD5 cells, which have been infected with RML prion strain prior to retroviral transduction decreased, but did not prevent propagation of infectious PrP^{TSE} (Fig. 43). This observation suggested that in the case of the established prion infection downregulation of PrP^C- substrate to approximately 10% of its original level is sufficient to sustain PrP^{TSE} multiplication.

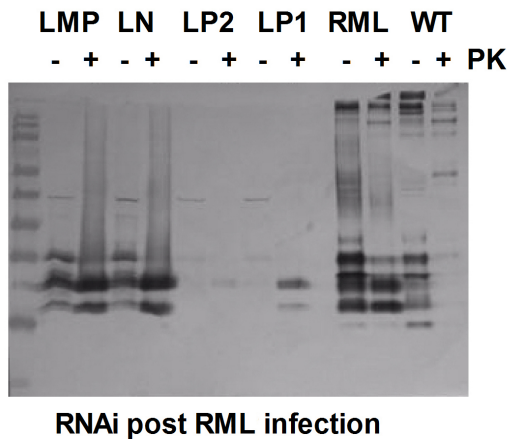


Figure 43: Proteinase K (PK) treatment of CAD5 cells propagating infectious PrP prior to *Prnp* silencing (LP1 and LP2) demonstrates presence of PK resistant PrP. Such latent propagation of PrP^{TSE} was observed after 10 passages. PK-/+ = treatment without or with proteinase K. Individual lanes were loaded with 30 µg (PK-) or 300 µg (PK+) of total proteins. PrP^C/PrP^{TSE} were detected with mAb AH6.

4.5.5. Expression of endogenous retroviruses in CAD5 cells

This part of the study was done in collaboration with Dr. Olga Janouskova from our laboratory. We screened transcription of selected endogenous retroviruses in CAD5 cells in dependence of PrP^C expression and presence of infectious PrP. From panel of monitored ERVs (*IAP-1*, *MLV*, *ERV-L*, *MuRRS*, *VL30-1* and *VL30-2*) we detected expression only of *IAP-1*, *MLV* and *VL30-2*. In RML uninfected LP1 and LP2 CAD5 cells expression of *IAP-1*, *MLV* and *VL30-2* had trend to decrease (Fig. 44A). Expression of ERVs in LP1 and LP2 was significantly lower than in LN as follows: *IAP-1* was lower for ~ 43% ($p = 0.006$) in LP1 line and for ~ 37 % ($p = 0.03$) in LP2 line. Expression of *MLV* in LP1 was not significantly different but in LP2 cells decreased over ~ 36 % ($p = 0.002$). In case of *VL30-2* transcription in both LP1 and LP2 had significantly lower expression ~ 58% ($p = 0.0006$) and ~ 63% ($p = 0.0009$), respectively. No significant difference was seen for any ERV between LMP and LN line. On the other side, expression of ERVs in LP1 and LP2 cells incubated with RML strain was largely higher than in RML infected LN line (Fig. 44B). Difference in expression of *IAP-1* between LP1/LP2 and LN was significantly higher over ~ 25% ($p = 0.025$) in LP1, and ~ 34% ($p = 0.042$) in LP2 cells. The upregulation of *MLV* transcription was as well higher over ~ 56% ($p = 0.0006$) and ~ 71% ($p = 0.002$) for LP1 or LP2 cells, respectively. Difference in

expression of *VL30-2* was significantly higher only in LP2 line, although the mean of expression in LP1 was also higher but due to the variability was not significant. Furthermore, transcription of *MLV* and *VL30-2* in LMP line was also significantly higher than in LN cells. Comparison of ERV transcriptions in LN/RML + line to expression of respective genes in LN/RML - cells revealed that expression of all analyzed ERVs in LN/RML + line were significantly downregulated (not shown). The same comparison in LMP lines showed that expression of ERVs is similar irrespective of presence of infectious PrP. In LP1 and LP2 cells incubated with RML brain homogenate, ERV expression was significantly higher only for *MLV* ($p = 0.032$, $p = 0.009$ for LP1 and P2, respectively). Transcription of *IAP-1* and *VL30-2* was similar for both treatments or was different only in one cell line (not shown).

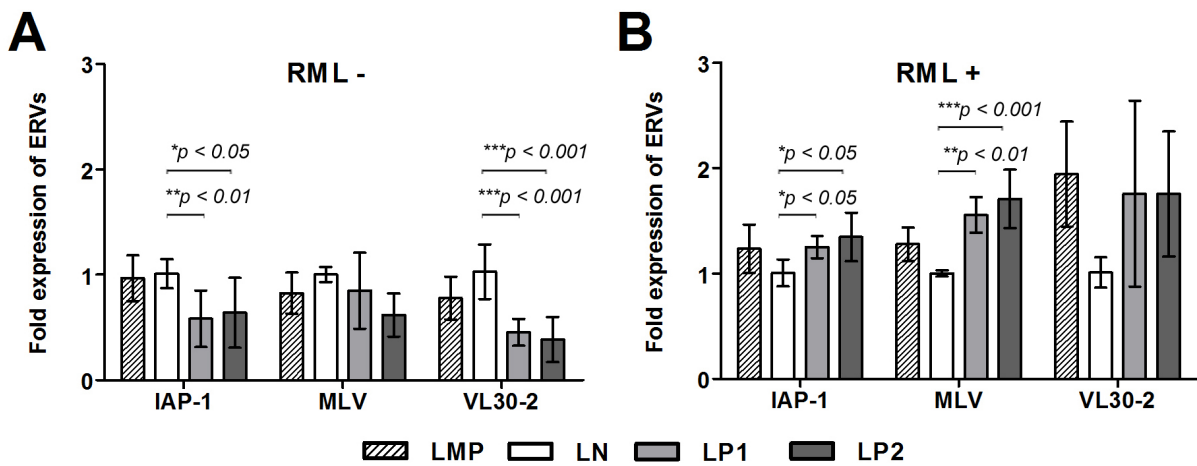


Figure 44: Transcription of ERVs tends to decrease in uninfected LP1 and LP2 cells contrary to RML treated cells where transcription of ERVs has ascending tendency. Expression of individual ERVs (*IAP-1*, *MLV* and *VL30-2*) in noninfected (RML-) cells (A) and in cells incubated with RML prion strain (RML +) (B), as shown by qRT-PCR using *Gapdh* as a reference gene. Expression was determined as fold difference relative to expression in LN cells in each treatment; RML- cells three independent experiments; RML+ two independent experiments; unpaired t-test; mean \pm SD.

5. Discussion

5.1. Characterization of human erythrocyte-associated PrP^C

The presence of TSE infectivity in blood has repeatedly been demonstrated in various species, including mouse, hamster, sheep, deer, and nonhuman primates (Brown, 2005), (Mathiason et al., 2010). In addition, the presence of infectivity in the blood of donors incubating vCJD was revealed by the transmission of the disease to three transfusion recipients (Gillies et al., 2009). All of them received nonleukoreduced erythrocytes. The nature of cells associated with TSE infectivity in blood remains unclear. In rodents, infectivity seems to be concentrated in leukocytes, while both platelets and erythrocytes are devoid of significant infectivity (Cervenakova et al., 2003), (Holada et al., 2002). Interestingly, platelets harbor infectivity in the blood of infected deer, suggesting that association of prions with blood cells could be species and prion strain dependent. The expression of PrP^C may play a role in this discrepancy because rodent platelets, in contrast to deer platelets, do not express the protein (Barclay et al., 2002), (Holada and Vostal, 2000). Considering the importance of PrP^C expression in many aspects of prion pathogenesis, our study was aimed at the elucidation of controversies surrounding its expression in human red blood cells. PrP^C is present on CD34+ marrow stem cells, and its expression is regulated in different cell lineages (Dodelet and Cashman, 1998) (Risitano et al., 2003). Griffiths and colleagues demonstrated that PrP^C expression in cultured human erythroblasts was mostly intracellular, with faint membrane staining, and it was downregulated during their *in vitro* differentiation to more mature erythroid cells (Griffiths et al., 2007). This finding is compatible with the low expression of the protein on the membrane of circulating erythrocytes detected in previous study (Holada and Vostal, 2000). However, this finding was contradicted by several studies reporting no expression of PrP^C on human red blood cells (Barclay et al., 1999), (MacGregor et al., 1999), (Dodelet and Cashman, 1998), (Antoine et al., 2000), (Li et al., 2001). Most of those studies utilized probably the best characterized prion mAb 3F4 (Kascsak et al., 1987). The antibody was developed against hamster scrapie-associated fibrils; however, it also cross-react with human PrP^C. The epitope of the 3F4 (KTNMKHM) is located in the central part of the molecule (PrP₁₀₆₋₁₁₂), which is known to undergo conformational change into infectious PrP, resulting in epitope inaccessibility (Lund et al., 2007), (Safar et al., 1998). To elucidate the controversies surrounding the expression of PrP^C on human erythrocytes, we first repeated the quantitative flow cytometry study utilizing mAb 6H4 and two mAbs that were used in previous negative

reports: FH11 and 3F4. Indeed, both antibodies bound to human erythrocytes substantially less than 6H4: 8.3-fold lower for FH11 and 3.6-fold lower for 3F4. This result was puzzling, especially for 3F4, as its binding to platelets in the same tube was equivalent to 6H4. The overall lower binding of FH11 to a variety of blood cells has been previously described and can be caused by a proteolytic loss of its epitope (PrP₅₁₋₅₅) located on the sensitive N-terminus of PrP^C (Holada et al., 2007), (Leclerc et al., 2003). A similar mechanism could also be responsible for the lower binding of 3F4, although its epitope (PrP₁₀₆₋₁₁₂) is located close to the center of the molecule. The presence of a substantial amount of the stable C1 fragment of PrP^C lacking the 3F4 epitope has been described in the normal brain tissue of man and other mammalian species (Chen et al., 1995), (Laffont-Proust et al., 2006). In contrast, we did not find similar fragments in blots of human erythrocyte ghosts, demonstrating that truncation was not the cause of the decreased 3F4 binding. The red blood cell PrP^C band had slightly lower electrophoretic mobility and was more diffuse than PrP^C in the brain. This could be caused by its different glycosylation pattern, which in theory may contribute to the inaccessibility of the 3F4 epitope. However, enzymatic deglycosylation of erythrocyte PrP^C did not restore its recognition by 3F4. Considering that the binding of 3F4 is prevented by the change in the conformation of protease-resistant PrP, we tested the sensitivity of PrP^C on erythrocytes to proteolysis. However, we did not detect any protease-resistant PrP^C. This, together with the fact that low binding of 3F4 was also recorded on blots after denaturation of proteins by boiling in SDS suggests that the low binding is not caused by the conformation of the protein. On the same basis, the hypothesis that the low binding of 3F4 is caused by the shielding effect of an unknown binding partner of PrP^C on the membrane of erythrocytes can be rejected. Taken together, our results suggest that the reason for decreased binding of 3F4 to erythrocyte PrP^C is posttranslational modification of its epitope KTNMKHM. This modification is apparently introduced after the maturation and release of erythrocytes into circulation as CD71⁺ erythroid precursors in cord blood bound antibodies 3F4 and 6H4 equally well. The modification does not significantly change the electrophoretic mobility of erythrocyte PrP^C because after its deglycosylation, it has similar mobility to deglycosylated brain PrP^C. The importance of both methionine and lysine residues in the 3F4 epitope for binding of the antibody has been previously demonstrated (Lund et al., 2007), (Rubenstein et al., 1999). Methionine residues in the 3F4 epitope have been shown to be sensitive to oxidation and may serve as internal antioxidants, protecting the PrP^C molecule from oxidative damage (Requena et al., 2004). However, in our hands, oxidation of PrP^C with H₂O₂ did not diminish binding of 3F4 relative to 6H4, suggesting that oxidation is not the cause of the low binding of 3F4 to erythrocyte PrP^C.

In contrast, modification of lysine residues by sulfo-NHS-biotin readily led to the loss of 3F4 binding, confirming a previous report by Bolton and coworkers (Bolton et al., 1991). One physiologically occurring modification of lysine residues in proteins is glycation. The treatment of prion protein with glyoxylic acid, which modifies lysine residues to the major advanced glycation end products constituent *N*^ε-(carboxymethyl)lysine, led to a dose-dependent decrease of 3F4 binding, while the binding of 6H4 was unaffected. The modification of membrane proteins by CML in human erythrocytes during their aging in circulation has been previously reported (Ando et al., 1999). This is in agreement with our observation that the epitope of 3F4 in erythroid precursors in cord blood as well as in platelets in circulation is not modified. Obviously, time is needed for the modification to occur, so for erythrocytes, with their life span reaching 120 days compared to the 10 days of platelets, it is more probable that will be modified. Interestingly, glycation of lysine residues on the N-terminal of infectious PrP has already been demonstrated in brains of TSE-infected rodents (Choi et al., 2004). Despite the lack of direct proof, our data suggest that the diminished binding of 3F4 to PrP^C on erythrocytes may be caused by glycation. In effort to prove it directly, we are developing monoclonal antibodies targeting AGEs on PrP^C (Dvorakova et al., 2011). This project is subject of Eva Dvořáková's dissertation thesis, therefore it is not discussed here. The hypothetical existence of a similar modification of blood infectious PrP would prevent its detection using the conformation-dependent immunoassay and other assays that use 3F4 (Safar et al., 1998). In addition, it is likely that the use of the 3F4 antibody was the reason for the underestimation of the overall amount of the PrP^C pool associated with human erythrocytes in some previous studies. All three methods employed in our study to estimate the amount of PrP^C in erythrocytes relative to platelets gave convergent results. Using quantitative flow cytometry, approximately 300 IgG molecules of mAb 6H4 bound to one erythrocyte, while the binding to resting platelets in identical samples was only twice as high. Approximately 70% of PrP^C is localized inside of resting platelets (Holada et al., 2006), which suggests that the amount of PrP^C per platelet, including its intracellular pool, is roughly 7-fold higher than in one erythrocyte. Conformation independent WB analysis of PrP^C levels in carefully isolated platelets and erythrocyte ghosts indicated that the amount of PrP^C per platelet is just 4-fold higher than in one red blood cell. An even lower difference was detected using sandwich ELISA. Taken together, our data demonstrate that the difference in the level of PrP^C between one platelet and one erythrocyte is less than 10-fold, while the normal amount of erythrocytes ($5 \times 10^9/\text{mL}$) in man is about 20-fold higher than the amount of platelets ($2.5 \times 10^8/\text{mL}$). This result implies that erythrocytes should carry at least twice as much PrP^C than platelets, which

makes erythrocytes the main source of cell-associated PrP^C in human blood. Previous studies have described the release of up to 45% of platelet PrP^C after their *in vitro* activation by agonists or during the 5-day storage of platelet concentrates (Bessos et al., 2001), (Robertson et al., 2006). Although we consider it unlikely, we cannot exclude that some release of PrP^C also occurred during the isolation of platelets used in our WB and ELISA studies. However, even if we underestimated the physiological amount of platelet PrP^C by approximately 50%, the overall amount of PrP^C associated with erythrocytes would still surpass the PrP^C platelet pool. Despite this observation, erythrocytes remain an unlikely source of prions in blood because they do not have the ability to supplement their propagation with new molecules of PrP^C. However, the existence of posttranslational modification in the critical part of the molecule may give erythrocyte PrP^C unique properties and favor their binding of prions released to blood by other cells. Further studies aimed on the molecular characterization of this modification and its influence on the interaction of PrP^C with prion particles should clarify if our current view neglects the role of erythrocytes in the blood pathogenesis of prion diseases.

5.2. Expression of PrP^C is regulated during murine erythroid differentiation

Involvement of PrP^C in cellular physiology was proposed for several apparently various processes but so far without any prevailing consensus. Published works reported its attribution to functions, which could be found also during erythroid differentiation, e.g. iron uptake, proliferation and cell protection. Downregulation of several erythroid genes during prion infection was first observation that peripheral pathogenesis of prion diseases is linked to erythropoiesis (Miele et al., 2001), (Brown et al., 2007). However, it is not clear if the effect was caused by direct interaction of prion particles with erythroid cells, or it is side effect of prion infection. Griffiths et al. demonstrated the regulation of PrP^C expression during the differentiation of cultured human erythroblasts *ex vivo* indicating that it may play a role in the differentiation of erythroid precursors (Griffiths et al., 2007). PrP^C was found mostly in the perinuclear region of proerythroblasts, and the amount of PrP^C declined as erythroid cells matured. In our study, we demonstrated that the surface expression of PrP^C on erythroid precursors in the mouse bone marrow and spleen follows a similar pattern as the cells mature. The protein's levels first increase with basophilic erythroblasts, expressing more than twice as much PrP^C as proerythroblasts, and then declines significantly in late basophilic and polychromatic erythroblasts, with most mature small erythroid precursors expressing only around 500 PrP^C molecules per cell. This pattern of expression is suggestive of PrP^C's involvement in the early stages of erythroid differentiation. The differentiation of MEL cells in

culture is known to resemble the *in vivo* process, with similar maturation stages: proerythroblast-like, erythroblasts-like and, occasionally, reticulocyte-like (Hyman et al., 2001). The surface expression of PrP^C on uninduced MEL cells in the exponential phase of growth was approximately six times higher than that observed on proerythroblasts in the mouse bone marrow or spleen. However, the induction of differentiation led nearly to doubling of the PrP^C number on MEL cell membranes within 24 h, which resembled a similar increase of PrP^C expression on basophilic erythroblasts *in vivo*. In agreement with previous observations *in vivo*, we found that this initial upregulation was followed by a gradual downregulation of PrP^C surface levels along with the progression of MEL cells' differentiation. This decrease did not reach the degree observed in small Ter119^{high}CD71^{low} erythroid precursors *in vivo*, which is in line with the limited ability of differentiating MEL cells to reach this stage of maturation. The differentiation of MEL cells is composed of two separate events, growth arrest and terminal differentiation. Both processes are characterized by the activation of early (cell-cycle control) and late (morphological changes) genes (Hyman et al., 2001). The first period lasts approximately 12 hours, after which the first committed cells occur. The majority of cells are terminally differentiated between 24 and 50 hours (Fibach et al., 1977). In agreement with previous studies by Gougomas et al. (Gougomas et al., 2001), we found that the *Prnp* gene in MEL cells is transcriptionally activated both during inducer-mediated differentiation and in confluent cells undergoing cell cycle arrest. In addition, we were able to demonstrate the regulation of PrP^C at the protein level by western blot. Interestingly and in accordance with the flow cytometry results, in differentiating cells, the expression of the protein was downregulated after an initial increase, even though the level of PrP mRNA continued to rise. This result suggests that MEL cells' differentiation leads to a translational regulation of PrP^C levels (Schröder et al., 2002) not seen in uninduced cells undergoing cell-cycle arrest. Alternatively more differentiated cells could degrade PrP^C at an increased rate as has been proposed to explain the disparity between PrP^C protein and mRNA levels in different types of neuronal cells (Ford et al., 2002a). Otsuka et al. recently reported downregulation of PrP^C protein during differentiation of highly responsive subclone of MEL cells (Otsuka et al., 2008). However, their study did not detect an initial increase of PrP^C expression most likely due to the different growing phase of cells at the point of induction. Transcription of *Prnp* gene in proliferating cells (in exponential growth phase) may be repressed by inaccessibility of *Prnp* promoter for transcription factors. After induction to growth arrest, *Prnp* transcription is probably activated by chromatin relaxation as we show here by treatment of MEL cells with TSA- an inhibitor of histone deacetylases. Although regulation sequences of *Prnp* gene contain CpG islands

(Schröder et al., 2002) which may potentially serve for methylation, thus repressing transcription, we did not see any *Prnp* upregulation after blockade of DNA methyltransferases with 5-AzaC. Our data are in agreement with Cabral et al., who reported that regulation of the *Prnp* gene expression depends on chromatin conformation (Cabral et al., 2002).

Stimulation of the glucocorticoid receptor by DEX induces the proliferation and expansion of erythroid progenitors and delays the terminal differentiation of erythrocytes (Chute et al., 2010). In our hands DEX did not prevent the HMBA-induced initial upregulation of PrP^C in MEL cells (even in 10-fold higher concentration) suggesting that it precedes the effect of DEX which is known to suppress the HMBA-mediated commitment to terminal cell division at a relatively late step in this process (Kaneda et al., 1985). However, DEX prevented the increase of PrP^C protein levels in confluent MEL cells after 120 hours of culture demonstrating that the activation of glucocorticoid receptor can interfere with the transcriptional activation of the *Prnp* gene mediated by cell-cycle arrest. The mechanism of DEX's action on the prevention PrP^C protein upregulation in confluent MEL cells is unknown at present. DEX has been shown to induce cell-cycle arrest in number of various cell lines (Mattern et al., 2007), but not in MEL cells, in which it increases cell viability (Osborne et al., 1982), both in induced and uninduced culture. In summary, our results demonstrate that the regulation of PrP^C levels in differentiating MEL cells resembles, at least in part, its regulation in maturing mouse erythroid precursors *in vivo*. To learn more about the importance of PrP^C in the process of MEL cells' differentiation, we created cell lines using RNAi to stably inhibit its expression.

5.2.1. Establishment of cell lines with stable silenced *Prnp* expression

The nature of our *in vitro* model of erythroid differentiation put in the consideration for RNAi gene targeting several complications. Our experiment with *in vitro* erythroid differentiation takes six days. Furthermore, MEL cells are rapidly dividing (~12 hours doubling time), therefore it is not suitable to use temporary siRNA transfection. Otherwise, siRNA transfection could lead to rapid dissolving of transfected siRNA and diminishing of silencing. Considerable problem could be also caused by the low transfection effectivity hampering thus subsequent analysis. These potential problems led us rather to establish the cell culture with stable silenced *Prnp* transcription. The incorporation of retroviral vector expressing anti-*Prnp* shRNA, to host genome, seemed to be the most appropriate approach. Our first model utilized the retrovector coding shRNA of first generation transcribed by RNA pol III. We used three different anti-*Prnp* shRNAs to minimize the side-effects caused by possible unspecific downregulation. However, after the selection of cells with the stable integrated shRNA

expressing retrovectors we did not observe any PrP^C downregulation. Since selected cells may be the heterogeneous population expressing variable levels of the PrP^C (Bengtsson et al., 2005), we tried to isolate single cell clones. We found out that limiting dilution approaching one cell per well (in 96-well plate) interfered with their survival, suggesting the deprivation of cell-cell contacts or special growth metabolites. The requirements for cell-to-cell contact or close proximity of sister cells may be the remnants conserved from *in vivo* erythroblast islands (Chasis and Mohandas, 2008). Nevertheless, even conditioned medium harvested from exponentially growing MEL cells did not lead to enhanced proliferation of isolated single cells. One of the possible explanations why we did not observe *Prnp* silencing is that retrovector-genes, except the gene for puromycin resistance, are transcriptionally repressed during the selection. This was supported by transitional downregulation of *Prnp* transcription in 389 line, at 48 hours post transfection, which faded after next 24 hours to level comparable in SCRL line. We speculated that lack of downregulation in lines 1071 and 1830 was caused by several factors. Occupation of shRNA-target site by proteins is one of the possible explanations since both shRNAs were targeted to 3' UTR in contrast to 389 that was targeted to coding mRNA region. Although 3' UTR is common target for endogenous miRNAs, this sequence may be blocked by proteins regulating translation (Wilkie et al., 2003), (Mazumder et al., 2003). On the other side, Reynolds et al. suggests that functionality of siRNA is rather determined by its properties, than by properties of target mRNA region (Reynolds et al., 2004). We abandoned both sequences and employed new shRNA- 512 (Pfeifer et al., 2006). As well in this instance, we observed partial *Prnp* downregulation after 48 hours post transfection, which disappeared in next 24 hours.

Subsequently we investigated fate of the vector after transfection. We speculated about two most probable scenarios. In first scenario, we hypothesized that expression from our plasmid is epigenetically controlled. Plasmid sequences characteristic by unmethylated CpG motifs, which are prevalent in bacterial, but not vertebrate genomic DNA are recognized in the vector backbone and whole plasmid is repressed (Komura et al., 1995) or transcriptional inhibition is caused by formation of repressive heterochromatin on the plasmid DNA backbone, which then spreads and inactivates the transgene (Chen et al., 2008). In second scenario, we hypothesized that vector recombines while integrating to host genomic DNA destroying thus shRNA expression sequences (Murnane et al., 1990). Treatment with inhibitors of methyltransferases (5-AzaC) and histone deacetylases (TSA) may abolish the possible transcriptional silencing by methylation and/ or chromatin condensation. Using mixture of both compounds, we expected

activation of shRNA transcription upon the treatment, resulting to *Prnp* downregulation. However, after 14 hours we saw upregulation of *Prnp* transcription instead of downregulation. Resistance to puromycin supported the notion that transfected vector must be present in cells. Its maintenance in extrachromosomal state was highly unlikely. To support our hypothesis we designed primers and reaction conditions for PCR detection of particular vector sequences. Our two primer pairs were designed to amplify sequences containing shRNA insert or shRNA together with its promoter. Although we were able to amplify desired fragments from purified vectors, we failed to detect them from the isolated genomic DNA, suggesting that vectors were recombined during the integration.

To gain complex insight into the preparation of stable transfectant MEL cells, we analyzed effectivity of the transfection. Since our retrovector pSilencer does not code for easily recognizable selection marker, we transfected MEL cells with plasmid coding EGFP under similar transfection conditions like for pSilencer bearing shRNAs. FACS analysis showed that EGFP positivity is less than 20%. Such low transfection effectivity suggests that our observations of *Prnp* downregulation in short intervals post transfection were probably overestimated.

In attempt to insert intact shRNA to host genomic DNA, we finally utilized gene delivery system using recombinant retroviral particles. The core of the process lays in using so called „packaging cell lines“, cells that had been already prepared to produce retroviral particles under special circumstances. The packaging cell line expresses all or part of the necessary genes (*gag*, *pol* and *env*) for a virion assembling. Transfection of retroviral plasmid should provide the rest of the important retroviral parts- 5' and 3' LTRs that are used by viruses to insert their genetic sequence into the host genomes and ψ sequence responsible for packaging the genome into the viral particles. After their import to packaging cells, growing viral particles build in the DNA sequence coding resistance gene, shRNA with promoter and ψ sequence flanking with 5' and 3' LTR as its genome. Subsequently virions are released to growth medium.

Initially we used packaging cell line „Phoenix“, which is derived from HEK293 cells. Successful production of retroviral particles was shown by transduction of NIH3T3 cells reaching ~ 30-40% EGFP positivity with maximum ~ 98% after 2 weeks of selection. NIH3T3 cells were used as a test of the principle for delivery system as suggested by [Nolan laboratory](#)¹⁰. We examined two different retroviral delivery methods. In first mode- spinfection, we harvested growth medium from packaging cells after 48 hours post transfection when the virion production should reach the maximum. Retroviral transduction was also enhanced by addition of the cationic polymer Polybrene, which neutralizes charge repulsion between virions and the

cell surface (Davis et al., 2004). Retroviral delivery by the spinfection is based on immediate centrifugation of retroviral particles with target cells. Spinning cells at 500 x g, 90 min is not enough to sediment viral particles in medium but it is thought that virus on membrane fragments is spun onto target cells enhancing thus effectivity of infection (Nolan laboratory¹⁰). In the second approach, co-cultivation, we cultivated transfected Phoenix cells with target cells for 72 hours. We separated both cell cultures by inserts with 0.4 µm pore membrane, allowing transfer of subcellular material. In similar manner, we transduced NIH3T3 cells with retroviral particles produced by Phoenix cells after transfection with the pSilencer vectors 389, 512 and SCRL. After selection, we obtained cell lines with downregulated *Prnp* expression from ~ 40 to 70% by 389- or 512-shRNA, respectively. However, analogical protocol did not lead to establishment of MEL cells with stably downregulated *Prnp*. Since selection led to overall cell death, we concluded that viral particles probably did not enter the MEL cells.

To overcome possible problems with virus entry to target cell we changed Phoenix line for HEK293 GP2 cells. The HEK293 GP2 cells also express necessary genes for virion production except the envelope protein, which has to be cotransfected with retrovector. An advantage of this setup is based on the possibility to use envelope protein specific for target line or pantropic protein with an affinity for indiscriminately many cells. In our set up, we used the G glycoprotein of the vesicular stomatitis virus. VSV-G does not require a cell surface receptor but interacts with phospholipid components of the target cell membrane and mediates the fusion of viral and cellular membranes (Emi et al., 1991). Second improvement of our gene delivery system was based on the use of the retrovector expressing shRNA in context of endogenous miRNA. Expressed construct resembles pre-miRNA and enters the RNAi pathway at the beginning, raising thus effectivity of silencing (Fig. 2) (Silva et al., 2005), (Chang et al., 2006). Complementary to previous anti-*Prnp* shRNA sequences 389 and 512 we adopted commercially available sequences designed here as LP1 and LP2. However, in our system only LP1 and LP2 sequences downregulated *Prnp* gene.

5.2.2. Influence of *Prnp* silencing by RNAi on erythroid differentiation *in vitro*

RNAi administered by shRNA from a retrovector had been previously employed efficiently to inhibit PrP^C expression *in vitro* and *in vivo* (Tilly et al., 2003), (Pfeifer et al., 2006). The main objective for using RNAi to suppress PrP^C was to study of its therapeutic potential in preventing propagation of infectious prions. To the best of our knowledge, our model is the first murine cell line of non-neuronal origin with stably silenced PrP^C expression. Inhibition of the protein's expression at both the mRNA and protein levels was efficiently

maintained during the differentiation of MEL cells, although it varied between 75 and 95 % in individual time points. Despite the silencing, the induction of differentiation led to a slight but detectable increase of PrP^C signal on blots after 24 hours, suggesting that the regulation of the protein's expression in LP1- and LP2-transduced cell lines follows similar pattern as in unmodified MEL cells, although at a suppressed level. Growth curve of LP1-, LP2- and control LN-transduced cell lines after the induction of differentiation was similar, although the LP2 cell line exhibited a higher proliferation capacity. Since the LP1 line did not differ from the control LN line, we could not assign the LP2 cell line's divergence solely to PrP^C silencing. Similarly, the level of the proto-oncogene *c-myb*, expression of which is characteristic of the proliferative state and its constitutive expression has been demonstrated to block MEL cells' differentiation (Clarke et al., 1988), (Chen et al., 2002), decreased upon induction similarly in all created cell lines and remained low during the entire course of the experiment. All cell lines observed here demonstrated similar dynamics and level of hemoglobinization and regulation of the transferrin receptor on their cell membranes. Even under the iron deprivation, expression of transferrin receptor was similarly upregulated in all lines. Furthermore, we did not observe reliable difference in uptake of transferrin coupled with radiolabeled iron. This finding suggested that silencing of PrP^C in MEL cells does not lead to gross perturbation of iron homeostasis, although the involvement of PrP^C in iron-cell uptake was described recently *in vitro* and *in vivo* (Singh et al., 2009a), (Singh et al., 2009b). Monitoring of selected erythroid markers (*Eraf*, *Hba* and *GATA1*) on the transcriptional level also did not reveal significant differences among LP1-transduced, LP2-transduced and LN-transduced cell lines, confirming that PrP^C silencing does not appear to disturb the differentiation of MEL cells. In many cell cultures, the enhanced expression of PrP^C was proposed to facilitate cytoprotective effects (Lo et al., 2007). However, overexpression of exogenously delivered PrP^C in MEL cells did not protect the cells against apoptosis initiated by serum withdrawal (Gougoumas et al., 2007). We also found that silencing of PrP^C did not seem to sensitize cells to apoptosis during differentiation, as demonstrated by a Trypan Blue exclusion assay and by monitoring of *Bax* expression by qRT-PCR. This result is concurrent with Christensen and Harris, who reevaluated former assays reporting a protective activity of PrP^C and suggested that the presence of PrP^C has only a modest effect in cytoprotection *in vitro* (Christensen and Harris, 2008). Taken together, our results imply that, under normal conditions, PrP^C seems dispensable for the erythroid differentiation of MEL cells.

The pattern of PrP^C regulation on erythroid precursors *in vivo* suggests that PrP^C may play a role in the maturation of erythroblasts in erythroblastic islands. We can speculate that PrP^C,

which was shown to bind both laminin and the laminin receptor, can be involved in cell-cell contacts in an erythroblastic niche, or with a surrounding extracellular matrix (Graner et al., 2000), (Gauczynski et al., 2001). Downregulation of PrP^C then could play a role in the dissociation of matured reticulocytes from the erythroblastic niche. Such a role for PrP^C is unlikely to be detected by the MEL cell model. Another explanation could be that PrP^C exerts its function only under stress conditions. This hypothesis is consistent with the documented poor recovery of PrP^{-/-} mice from experimental anemia (Zivny et al., 2008). Finally, it is possible that the effect of PrP^C silencing was compensated for by an unknown pathway or that the remaining expression is sufficient to sustain its role.

5.3. Effect of *Prnp* downregulation on propagation of infectious prion protein in cell culture and expression of endogenous retroviruses

The RNAi was believed to have a great potential in developing a versatile method to treat prion diseases, because RNAi downregulate *Prnp* mRNA and thus PrP^C protein, the common substrate for all types of prion diseases. This approach overcomes many obstacles, which may encounter anti-prion protein agents directly targeting PrP^{TSE} or its propagation. These obstacles likely originate from the specificity of individual PrP^{TSE} strains (Kim et al., 2009). Correlation between anti-prion activity and prion strain was described by several groups recently e.g. Kawasaki with colleagues (Kawasaki et al., 2007). Despite the many advantages for therapy provided by RNAi at first glance, RNAi has three main drawbacks- mean of delivery, side effects and effectivity (Gallozzi et al., 2008), (White et al., 2008). However, RNAi provides important research tool for study of prion pathogenesis *in vitro* and *in vivo*.

We believed that erythroid differentiation of MEL cells could provide an *in vitro* model for previously observed deregulation of selected erythroid genes during progression of prion disease (Miele et al., 2001), (Brown et al., 2007). Therefore, we employed RNAi to create control lines for the study of influence of prion infection on *in vitro* erythroid differentiation. Furthermore, as far as we know, establishment of infectious prion propagation in MEL cells would present the first suspension cell culture propagating PrP^{TSE}. However, infection of MEL cells with 0.1% brain homogenate harboring RML prion strain led after 24 hours post inoculation to the similar detection of PrP^{TSE} in all cells regardless the level of PrP^C expression. Subsequent cell passaging revealed that signal from proteinase K resistant PrP diminishes mostly due to the dilution of inoculum. Our observation suggests that detected signal comes from MEL-attached inoculum as was supported by significant decrease decrease of PrP^{TSE} signal after cell wash. Inability of MEL cells to propagate infectious PrP may be caused by the

relative low number of PrP^C molecules on cell membrane with approximately 10-fold lower level in comparison with CAD5 cells. In addition, exponentially growing MEL cells express even lower number of PrP^C. Additive blocking event for PrP^{TSE} propagation in MEL cells may be provided by the presence of HEPES in growth medium, which was recently shown to inhibit accumulation of the PrP^{TSE} in neural stem cells and N2a cell culture infected with 22L prion strain (Delmouly et al., 2011). Furthermore, rapid cell division acts as a constant diluting factor, halving the amount of PrP^{TSE} per cell at each division cycle (Ghaemmaghami et al., 2007). Thus, even the cell proliferation impedes prion propagation in MEL cell culture with doubling time ~ 12 hours in comparison with CAD5 cells doubling each ~ 20 hours (Qi et al., 1997). Although now we are struggling to create MEL lines propagating PrP^{TSE}, we showed that infectious inoculum resists complete degradation at least 120 hours post application, sufficient time for possible interaction with erythroid differentiation. The question if the PrP^{TSE} may influence erythroid differentiation of MEL cells is under investigation.

On the other side, we introduced *de novo* prion infection in susceptible CAD5 lines, but not in cells with stable downregulated PrP^C. We confirmed data presented by Kim et al. reporting the inability of RNAi to clear pre-existing PrP^{TSE} *in vitro* (Kim et al., 2009). Similar drawback of RNAi approach was described also *in vivo* (Pfeifer et al., 2006), (White et al., 2008).

To our best knowledge, we do not know any publication describing the influence of PrP^C silencing on expression of ERVs. Therefore, besides the study of prion propagation in cell culture, our aim was to extend the observation of Stengel et al., who described that chronic prion infection of hypothalamic neuronal (GT1) and neuroblastoma (N2a) cells affected expression of endogenous retroviruses (Stengel et al., 2006). In our hands, we observed in RML negative LP1 and LP2 cell lines significant downregulation of *IAP-1* and *VL30-2*. In cells *de novo* infected with RML prion strain, we saw opposite situation, LP1 and LP2 lines had significantly higher *IAP-1* and *MLV* levels in comparison to LN. *VL30-2* mean expression in LP1 and LP2 was also higher, but was not significant. Routinely, we also examined expression of several interferon stimulated genes, notably *Eif2ak2*, one of the prominent genes activated during the stress conditions (Williams, 1999), (Wek et al., 2006). Quantitative RT-PCR did not reveal upregulation of interferon stimulated genes in transduced lines over control cells. Surprisingly, transcription of *Eif2ak2* gene correlated with the expression of ERVs. In uninfected cells, *Eif2ak2* was significantly downregulated contrary to infected cells where mean of its expression was significantly higher in both lines with downregulated PrP^C. However, implication of such regulation is currently unclear. Although it could suggest involvement of PrP^C in regulation of ERVs transcription, it is questionable if observed

differences are also biologically meaningful since Stengel et al. considered only 2-fold change in transcription as biologically relevant (Stengel et al., 2006). Molecules of dsRNA are one of the main triggers of *Eif2ak2*; dsRNA may also arise during ERVs biogenesis as was shown for *IAPs* (Kramerov et al., 1985). Murine *Prnp* gene has two well characterized alleles- *Prnp^a* and *Prnp^b* of which sequences differs only in two amino acids at codons 108 and 189 (Brown et al., 2000a). Of note is the finding of Lee et al. who reported that mouse *Prnp^a* but not *Prnp^b* allele contains *IAP* insertion in the anticoding strand of intron 2 (Lee et al., 1998). If *Prnp^a* allele is present in CAD5 cells is unknown, but it would be plausible to speculate about coupled transcriptional activation of both *Prnp* and *IAP* gene. Moreover, it remains to further investigation how prion infection could modify gene regulation in target cells with repressed *Prnp* transcription. It is probable that minimal expression of PrP^C allows prion propagation which could affect transcription by unknown mechanism, but supposed process should be different from the cells with normal level of PrP^C. If our observation that prion infection affects expression of *Eif2ak2* gene and ERVs truly reflects situation in CAD cells, then our data are contradicted by Julius et al., who did not find by microarray analysis any statistically significant and/or biologically convincing, differentially expressed gene in N2aPK1, CAD, and GT1 cells as a response to RML prion infection (Julius et al., 2008). This work also challenges previous work reporting several hundred differentially expressed sequences in the ScN2a and ScGT1 cell lines infected with prion strain RML. These cells demonstrated unique changes in RNA profiles with only minimal overlap in differential gene regulation between the two cell types (Greenwood et al., 2005). To further strengthen our data, we used also second control line transduced by empty retrovector (LMP). In RML negative LMP culture expression of *IAP-1*, *VL30-2* and *Eif2ak2* was similar like in LN and nontransduced cells, but in LMP RML infected cells expression of all analyzed ERVs and *Eif2ak2* was higher than in LN line. Why the expression of ERVs in LN RML positive cells is lower than in LN RML negative is intriguing since expression in LMP cells is similar in both RML positive and RML negative cells. It is unlikely that prion infection would selectively downregulate ERV genes only in LN line.

6. Conclusion

Our data show that erythrocytes are the main source of cell-associated PrP^C in human blood. Furthermore, we emphasize that PrP^C associated with human erythrocytes may differ from PrP^C associated with other blood cells and as such might play significant role in prion pathogenesis.

We found out that expression of PrP^C is regulated during erythroid differentiation of murine erythroid precursors *in vivo* and *in vitro*. Using RNAi, we created murine *in vitro* cell culture model for erythroid differentiation with downregulated PrP^C expression. To the best of our knowledge, our model is the first murine cell line of non-neuronal origin with stably silenced PrP^C expression. We showed that under unchallenged growth condition PrP^C is dispensable for erythroid differentiation *in vitro*.

MEL cells seem to be resistant to propagation of the infectious prion protein. However, RML inoculum is sustained in cell culture at sufficient time required for erythroid differentiation. *De novo* propagation of PrP^{TSE} in CAD5 cells with downregulated PrP^C is effectively abrogated. However, downregulation of PrP^C post PrP^{TSE} infection does not eliminated prion infection.

We found differential regulation of several endogenous retroviruses in CAD5 cells in dependence on the level of PrP^C expression and the presence of prion infection. However, biological relevance of our findings remains for future clarification.

7. References

1. Adler, V., Zeiler, B., Kryukov, V., Kascsak, R., Rubenstein, R., Grossman, A., 2003. Small, highly structured RNAs participate in the conversion of human recombinant PrP(Sen) to PrP(Res) in vitro. *J. Mol. Biol* 332, 47-57.
2. Aguzzi, A., Baumann, F., Bremer, J., 2008. The prion's elusive reason for being. *Annu. Rev. Neurosci* 31, 439-477.
3. Aguzzi, A., Sigurdson, C., Heikenwaelder, M., 2008. Molecular mechanisms of prion pathogenesis. *Annu Rev Pathol* 3, 11-40.
4. Akowitz, A., Manuelidis, E.E., Manuelidis, L., 1993. Protected endogenous retroviral sequences copurify with infectivity in experimental Creutzfeldt-Jakob disease. *Arch. Virol* 130, 301-316.
5. de Almeida, C.J.G., Chiarini, L.B., da Silva, J.P., E Silva, P.M.R., Martins, M.A., Linden, R., 2005. The cellular prion protein modulates phagocytosis and inflammatory response. *J. Leukoc. Biol* 77, 238-246.
6. An, S.S.A., Lim, K.T., Oh, H.J., Lee, B.S., Zukic, E., Ju, Y.R., Yokoyama, T., Kim, S.Y., Welker, E., 2010. Differentiating scrapie-infected blood by detecting disease-associated prion proteins by Multimer Detection System. *Biochem Biophys Res Commun.* 392, 505-509.
7. Ando, K., Beppu, M., Kikugawa, K., Nagai, R., Horiuchi, S., 1999. Membrane proteins of human erythrocytes are modified by advanced glycation end products during aging in the circulation. *Biochem. Biophys. Res. Commun* 258, 123-127.
8. Antoine, N., Cesbron, J.Y., Coumans, B., Jolles, O., Zorzi, W., Heinen, E., 2000. Differential expression of cellular prion protein on human blood and tonsil lymphocytes. *Haematologica* 85, 475-480.
9. Barclay, G.R., Hope, J., Birkett, C.R., Turner, M.L., 1999. Distribution of cell-associated prion protein in normal adult blood determined by flow cytometry. *Br. J. Haematol* 107, 804-814.
10. Barclay, G.R., Houston, E.F., Halliday, S.I., Farquhar, C.F., Turner, M.L., 2002. Comparative analysis of normal prion protein expression on human, rodent, and ruminant blood cells by using a panel of prion antibodies. *Transfusion* 42, 517-526.
11. Behrens, A., Genoud, N., Naumann, H., Rüllicke, T., Janett, F., Heppner, F.L., Ledermann, B., Aguzzi, A., 2002. Absence of the prion protein homologue Doppel causes male sterility. *EMBO J* 21, 3652-3658.
12. Bengtsson, M., Ståhlberg, A., Rorsman, P., Kubista, M., 2005. Gene expression profiling in single cells from the pancreatic islets of Langerhans reveals lognormal distribution of mRNA levels. *Genome Res* 15, 1388-1392.

-
13. Bessos, H., Drummond, O., Prowse, C., Turner, M., MacGregor, I., 2001. The release of prion protein from platelets during storage of apheresis platelets. *Transfusion* 41, 61-66.
 14. Bolton, D.C., Seligman, S.J., Bablanian, G., Windsor, D., Scala, L.J., Kim, K.S., Chen, C.M., Kascsak, R.J., Bendheim, P.E., 1991. Molecular location of a species-specific epitope on the hamster scrapie agent protein. *J. Virol* 65, 3667-3675.
 15. Bosque, P.J., Prusiner, S.B., 2000. Cultured cell sublines highly susceptible to prion infection. *J. Virol* 74, 4377-4386.
 16. Botto, L., Masserini, M., Cassetti, A., Palestini, P., 2004. Immunoseparation of Prion protein-enriched domains from other detergent-resistant membrane fractions, isolated from neuronal cells. *FEBS Lett* 557, 143-147.
 17. Bounhar, Y., Zhang, Y., Goodyer, C.G., LeBlanc, A., 2001. Prion protein protects human neurons against Bax-mediated apoptosis. *J. Biol. Chem* 276, 39145-39149.
 18. Brouckova, A., Holada, K., 2009. Cellular prion protein in blood platelets associates with both lipid rafts and the cytoskeleton. *Thromb. Haemost* 102, 966-974.
 19. Brown, A.R., Blanco, A.R.A., Miele, G., Hawkins, S.A., Hopkins, J., Fazakerley, J.K., Manson, J., Clinton, M., 2007. Differential expression of erythroid genes in prion disease. *Biochem. Biophys. Res. Commun* 364, 366-371.
 20. Brown, D.R., 1999. Prion protein peptide neurotoxicity can be mediated by astrocytes. *J. Neurochem* 73, 1105-1113.
 21. Brown, D.R., Besinger, A., 1998. Prion protein expression and superoxide dismutase activity. *Biochem. J* 334 (Pt 2), 423-429.
 22. Brown, D.R., Iordanova, I.K., Wong, B.S., Vénien-Bryan, C., Hafiz, F., Glasssmith, L.L., Sy, M.S., Gambetti, P., Jones, I.M., Clive, C., Haswell, S.J., 2000a. Functional and structural differences between the prion protein from two alleles prnp(a) and prnp(b) of mouse. *Eur. J. Biochem* 267, 2452-2459.
 23. Brown, D.R., Qin, K., Herms, J.W., Madlung, A., Manson, J., Strome, R., Fraser, P.E., Kruck, T., von Bohlen, A., Schulz-Schaeffer, W., Giese, A., Westaway, D., Kretzschmar, H., 1997. The cellular prion protein binds copper in vivo. *Nature* 390, 684-687.
 24. Brown, D.R., Schmidt, B., Kretzschmar, H.A., 1998. Effects of copper on survival of prion protein knockout neurons and glia. *J. Neurochem* 70, 1686-1693.
 25. Brown, D.R., 2004. Role of the prion protein in copper turnover in astrocytes. *Neurobiol. Dis* 15, 534-543.
-

-
26. Brown, K.L., Stewart, K., Ritchie, D.L., Mabbott, N.A., Williams, A., Fraser, H., Morrison, W.I., Bruce, M.E., 1999. Scrapie replication in lymphoid tissues depends on prion protein-expressing follicular dendritic cells. *Nat. Med* 5, 1308-1312.
 27. Brown, P., 2005. Blood infectivity, processing and screening tests in transmissible spongiform encephalopathy. *Vox Sang* 89, 63-70.
 28. Brown, P., Preece, M., Brandel, J.P., Sato, T., McShane, L., Zerr, I., Fletcher, A., Will, R.G., Pocchiari, M., Cashman, N.R., d'Aignaux, J.H., Cervenáková, L., Fradkin, J., Schonberger, L.B., Collins, S.J., 2000b. Iatrogenic Creutzfeldt-Jakob disease at the millennium. *Neurology* 55, 1075-1081.
 29. Büeler, H., Aguzzi, A., Sailer, A., Greiner, R.A., Autenried, P., Aguet, M., Weissmann, C., 1993. Mice devoid of PrP are resistant to scrapie. *Cell* 73, 1339-1347.
 30. Büeler, H., Fischer, M., Lang, Y., Bluethmann, H., Lipp, H.P., DeArmond, S.J., Prusiner, S.B., Aguet, M., Weissmann, C., 1992. Normal development and behaviour of mice lacking the neuronal cell-surface PrP protein. *Nature* 356, 577-582.
 31. Cabral, A.L.B., Lee, K.S., Martins, V.R., 2002. Regulation of the cellular prion protein gene expression depends on chromatin conformation. *J. Biol. Chem* 277, 5675-5682.
 32. Carp, R.I., Meeker, H.C., Caruso, V., Sersen, E., 1999. Scrapie strain-specific interactions with endogenous murine leukaemia virus. *J. Gen. Virol* 80 (Pt 1), 5-10.
 33. Castilla, J., Saá, P., Hetz, C., Soto, C., 2005. In vitro generation of infectious scrapie prions. *Cell* 121, 195-206.
 34. Castilla, J., Saá, P., Soto, C., 2005. Detection of prions in blood. *Nat. Med* 11, 982-985.
 35. Cervenakova, L., Yakovleva, O., McKenzie, C., Kolchinsky, S., McShane, L., Drohan, W.N., Brown, P., 2003. Similar levels of infectivity in the blood of mice infected with human-derived vCJD and GSS strains of transmissible spongiform encephalopathy. *Transfusion* 43, 1687-1694.
 36. Clarke, M.F., Kukowska-Latallo, J.F., Westin, E., Smith, M., Prochownik, E.V., 1988. Constitutive expression of a c-myc cDNA blocks Friend murine erythroleukemia cell differentiation. *Mol. Cell. Biol* 8, 884-892.
 37. Curin Serbec, V., Bresjanac, M., Popovic, M., Pretnar Hartman, K., Galvani, V., Ruprecht, R., Cernilec, M., Vranac, T., Hafner, I., Jerala, R., 2004. Monoclonal antibody against a peptide of human prion protein discriminates between Creutzfeldt-Jacob's disease-affected and normal brain tissue. *J. Biol. Chem* 279, 3694-3698.
-

-
38. Daude, N., Marella, M., Chabry, J., 2003. Specific inhibition of pathological prion protein accumulation by small interfering RNAs. *J Cell Sci* 116, 2775-2779.
 39. Davis, H.E., Rosinski, M., Morgan, J.R., Yarmush, M.L., 2004. Charged polymers modulate retrovirus transduction via membrane charge neutralization and virus aggregation. *Biophys. J* 86, 1234-1242.
 40. Deleault, N.R., Harris, B.T., Rees, J.R., Supattapone, S., 2007. Formation of native prions from minimal components in vitro. *Proc. Natl. Acad. Sci. U.S.A* 104, 9741-9746.
 41. Deleault, N.R., Lucassen, R.W., Supattapone, S., 2003. RNA molecules stimulate prion protein conversion. *Nature* 425, 717-720.
 42. Delmouly, K., Belondrade, M., Casanova, D., Milhavet, O., Lehmann, S., 2011. HEPES inhibits the conversion of the Prion protein in cell culture. *J Gen Virol*. Epub ahead of print.
 43. Diarra-Mehrpour, M., Arrabal, S., Jalil, A., Pinson, X., Gaudin, C., Piétu, G., Pitaval, A., Ripoche, H., Eloit, M., Dormont, D., Chouaib, S., 2004. Prion protein prevents human breast carcinoma cell line from tumor necrosis factor alpha-induced cell death. *Cancer Res* 64, 719-727.
 44. Dodelet, V.C., Cashman, N.R., 1998. Prion protein expression in human leukocyte differentiation. *Blood* 91, 1556-1561.
 45. Dore, L.C., Amigo, J.D., Dos Santos, C.O., Zhang, Z., Gai, X., Tobias, J.W., Yu, D., Klein, A.M., Dorman, C., Wu, W., Hardison, R.C., Paw, B.H., Weiss, M.J., 2008. A GATA-1-regulated microRNA locus essential for erythropoiesis. *Proc. Natl. Acad. Sci. U.S.A* 105, 3333-3338.
 46. Du, J., Pan, Y., Shi, Y., Guo, C., Jin, X., Sun, L., Liu, N., Qiao, T., Fan, D., 2005. Overexpression and significance of prion protein in gastric cancer and multidrug-resistant gastric carcinoma cell line SGC7901/ADR. *Int. J. Cancer* 113, 213-220.
 47. Dvorakova E., Prouza M., Janouskova O., Panigaj M. and Holada K., Development of monoclonal antibodies specific for glycosylated prion protein. *J Toxicol Environ Health A*, (accepted)
 48. Edgeworth, J.A., Farmer, M., Sicilia, A., Tavares, P., Beck, J., Campbell, T., Lowe, J., Mead, S., Rudge, P., Collinge, J., Jackson, G.S., 2011. Detection of prion infection in variant Creutzfeldt-Jakob disease: a blood-based assay. *Lancet*. Epub ahead of print.
 49. Elliott, S.G., Foote, M., Molineux, G., 2009. Erythropoietins, Erythropoietic Factors, and Erythropoiesis: Molecular, Cellular, Preclinical, and Clinical Biology. Springer.
 50. Emi, N., Friedmann, T., Yee, J.K., 1991. Pseudotype formation of murine leukemia virus with the G protein of vesicular stomatitis virus. *J. Virol* 65, 1202-1207.
-

-
51. Ermonval, M., Mouillet-Richard, S., Codogno, P., Kellermann, O., Botti, J., 2003. Evolving views in prion glycosylation: functional and pathological implications. *Biochimie* 85, 33-45.
 52. Feng, L., Gell, D.A., Zhou, S., Gu, L., Kong, Y., Li, J., Hu, M., Yan, N., Lee, C., Rich, A.M., Armstrong, R.S., Lay, P.A., Gow, A.J., Weiss, M.J., Mackay, J.P., Shi, Y., 2004. Molecular mechanism of AHSP-mediated stabilization of alpha-hemoglobin. *Cell* 119, 629-640.
 53. Fibach, E., Reuben, R.C., Rifkind, R.A., Marks, P.A., 1977. Effect of hexamethylene bisacetamide on the commitment to differentiation of murine erythroleukemia cells. *Cancer Res* 37, 440-444.
 54. Fischer, M., Rüllicke, T., Raeber, A., Sailer, A., Moser, M., Oesch, B., Brandner, S., Aguzzi, A., Weissmann, C., 1996. Prion protein (PrP) with amino-proximal deletions restoring susceptibility of PrP knockout mice to scrapie. *EMBO J* 15, 1255-1264.
 55. Ford, M.J., Burton, L.J., Li, H., Graham, C.H., Frobert, Y., Grassi, J., Hall, S.M., Morris, R.J., 2002a. A marked disparity between the expression of prion protein and its message by neurones of the CNS. *Neuroscience* 111, 533-551.
 56. Ford, M.J., Burton, L.J., Morris, R.J., Hall, S.M., 2002b. Selective expression of prion protein in peripheral tissues of the adult mouse. *Neuroscience* 113, 177-192.
 57. Friend, C., Scher, W., Holland, J.G., Sato, T., 1971. Hemoglobin synthesis in murine virus-induced leukemic cells in vitro: stimulation of erythroid differentiation by dimethyl sulfoxide. *Proc. Natl. Acad. Sci. U.S.A* 68, 378-382.
 58. Gabus, C., Auxilien, S., Péchoux, C., Dormont, D., Swietnicki, W., Morillas, M., Surewicz, W., Nandi, P., Darlix, J.L., 2001. The prion protein has DNA strand transfer properties similar to retroviral nucleocapsid protein. *J. Mol. Biol* 307, 1011-1021.
 59. Gabus, C., Derrington, E., Leblanc, P., Chnaiderman, J., Dormont, D., Swietnicki, W., Morillas, M., Surewicz, W.K., Marc, D., Nandi, P., Darlix, J.L., 2001. The prion protein has RNA binding and chaperoning properties characteristic of nucleocapsid protein NCP7 of HIV-1. *J. Biol. Chem* 276, 19301-19309.
 60. Gallozzi, M., Chapuis, J., Le Provost, F., Le Dur, A., Morgenthaler, C., Peyre, C., Daniel-Carlier, N., Pailhoux, E., Vilotte, M., Passet, B., Herzog, L., Beringue, V., Costa, J., Tixador, P., Tilly, G., Laude, H., Vilotte, J.-L., 2008. Prnp knockdown in transgenic mice using RNA interference. *Transgenic Res* 17, 783-791.
 61. Gauczynski, S., Peyrin, J.M., Haïk, S., Leucht, C., Hundt, C., Rieger, R., Krasemann, S., Deslys, J.P., Dormont, D., Lasmézas, C.I., Weiss, S., 2001. The 37-kDa/67-kDa laminin receptor acts as the cell-surface receptor for the cellular prion protein. *EMBO J* 20, 5863-5875.
-

-
62. Ghaemmaghami, S., Phuan, P.-W., Perkins, B., Ullman, J., May, B.C.H., Cohen, F.E., Prusiner, S.B., 2007. Cell division modulates prion accumulation in cultured cells. *Proc. Natl. Acad. Sci. U.S.A* 104, 17971-17976.
 63. Gillies, M., Chohan, G., Llewelyn, C.A., MacKenzie, J., Ward, H.J.T., Hewitt, P.E., Will, R.G., 2009. A retrospective case note review of deceased recipients of vCJD-implicated blood transfusions. *Vox Sang* 97, 211-218.
 64. Golding, M.C., Long, C.R., Carmell, M.A., Hannon, G.J., Westhusin, M.E., 2006. Suppression of prion protein in livestock by RNA interference. *Proc. Natl. Acad. Sci. U.S.A* 103, 5285-5290.
 65. Gougoumas, D.D., Vizirianakis, I.S., Tsiftoglou, A.S., 2001. Transcriptional activation of prion protein gene in growth-arrested and differentiated mouse erythroleukemia and human neoplastic cells. *Exp Cell Res* 264, 408-417.
 66. Gougoumas, D.D., Vizirianakis, I.S., Triviai, I.N., Tsiftoglou, A.S., 2007. Activation of Prn-p gene and stable transfection of Prn-p cDNA in leukemia MEL and neuroblastoma N2a cells increased production of PrP(C) but not prevented DNA fragmentation initiated by serum deprivation. *J Cell Physiol* 211, 551-559.
 67. Graner, E., Mercadante, A.F., Zanata, S.M., Forlenza, O.V., Cabral, A.L., Veiga, S.S., Juliano, M.A., Roesler, R., Walz, R., Minetti, A., Izquierdo, I., Martins, V.R., Brentani, R.R., 2000. Cellular prion protein binds laminin and mediates neuritogenesis. *Brain Res. Mol. Brain Res* 76, 85-92.
 68. Graner, E., Mercadante, A.F., Zanata, S.M., Martins, V.R., Jay, D.G., Brentani, R.R., 2000. Laminin-induced PC-12 cell differentiation is inhibited following laser inactivation of cellular prion protein. *FEBS Lett* 482, 257-260.
 69. Greenwood, A.D., Horsch, M., Stengel, A., Vorberg, I., Lutzny, G., Maas, E., Schädler, S., Erfle, V., Beckers, J., Schätzl, H., Leib-Mösch, C., 2005. Cell line dependent RNA expression profiles of prion-infected mouse neuronal cells. *J. Mol. Biol* 349, 487-500.
 70. Greig, K.T., Carotta, S., Nutt, S.L., 2008. Critical roles for c-Myb in hematopoietic progenitor cells. *Semin. Immunol* 20, 247-256.
 71. Griffiths, R.E., Heesom, K.J., Anstee, D.J., 2007. Normal prion protein trafficking in cultured human erythroblasts. *Blood* 110, 4518-4525.
 72. Haase, V.H., 2010. Hypoxic regulation of erythropoiesis and iron metabolism. *Am. J. Physiol. Renal Physiol* 299, F1-13.
 73. Haigh, C.L., Wright, J.A., Brown, D.R., 2007. Regulation of prion protein expression by noncoding regions of the Prnp gene. *J. Mol. Biol* 368, 915-927.
-

-
74. Hewitt, P.E., Llewelyn, C.A., Mackenzie, J., Will, R.G., 2006. Creutzfeldt-Jakob disease and blood transfusion: results of the UK Transfusion Medicine Epidemiological Review study. *Vox Sang* 91, 221-230.
 75. Hoessli, D.C., Ilangumaran, S., Soltermann, A., Robinson, P.J., Borisch, B., Nasir-Ud-Din, 2000. Signaling through sphingolipid microdomains of the plasma membrane: the concept of signaling platform. *Glycoconj. J* 17, 191-197.
 76. Holada, K., Vostal, J.G., 2000. Different levels of prion protein (PrP^c) expression on hamster, mouse and human blood cells. *Br. J. Haematol* 110, 472-480.
 77. Holada, K., Glierova, H., Simak, J., Vostal, J.G., 2006. Expression of cellular prion protein on platelets from patients with gray platelet or Hermansky-Pudlak syndrome and the protein's association with alpha-granules. *Haematologica* 91, 1126-1129.
 78. Holada, K., Simak, J., Brown, P., Vostal, J.G., 2007. Divergent expression of cellular prion protein on blood cells of human and nonhuman primates. *Transfusion* 47, 2223-2232.
 79. Holada, K., Vostal, J.G., Theisen, P.W., MacAuley, C., Gregori, L., Rohwer, R.G., 2002. Scrapie infectivity in hamster blood is not associated with platelets. *J. Virol* 76, 4649-4650.
 80. Horejsí, V., Drbal, K., Cebecauer, M., Cerný, J., Brdicka, T., Angelisová, P., Stockinger, H., 1999. GPI-microdomains: a role in signalling via immunoreceptors. *Immunol. Today* 20, 356-361.
 81. Hu, W., Rosenberg, R.N., Stüve, O., 2007. Prion proteins: a biological role beyond prion diseases. *Acta Neurol. Scand* 116, 75-82.
 82. Hutter, G., Heppner, F.L., Aguzzi, A., 2003. No superoxide dismutase activity of cellular prion protein in vivo. *Biol. Chem* 384, 1279-1285.
 83. Hyman, T., Rothmann, C., Heller, A., Malik, Z., Salzberg, S., 2001. Structural characterization of erythroid and megakaryocytic differentiation in Friend erythroleukemia cells. *Exp. Hematol* 29, 563-571.
 84. Chang, K., Elledge, S.J., Hannon, G.J., 2006. Lessons from Nature: microRNA-based shRNA libraries. *Nat. Methods* 3, 707-714.
 85. Chasis, J.A., Mohandas, N., 2008. Erythroblastic islands: niches for erythropoiesis. *Blood* 112, 470-8.
 86. Chen, J., Kremer, C.S., Bender, T.P., 2002. A Myb dependent pathway maintains Friend murine erythroleukemia cells in an immature and proliferating state. *Oncogene* 21, 1859-1869.
 87. Chen, M., Zhang, L., Zhang, H.-Y., Xiong, X., Wang, B., Du, Q., Lu, B., Wahlestedt, C., Liang, Z., 2005. A universal plasmid library encoding all permutations of small interfering RNA. *Proc. Natl. Acad. Sci. U.S.A* 102, 2356-2361.
-

-
88. Chen, S.G., Teplow, D.B., Parchi, P., Teller, J.K., Gambetti, P., Autilio-Gambetti, L., 1995. Truncated forms of the human prion protein in normal brain and in prion diseases. *J. Biol. Chem* 270, 19173-19180.
 89. Chen, S.-Y., Wang, Y., Telen, M.J., Chi, J.-T., 2008. The genomic analysis of erythrocyte microRNA expression in sickle cell diseases. *PLoS ONE* 3, e2360.
 90. Chen, Z., Banks, J., Rifkind, R.A., Marks, P.A., 1982. Inducer-mediated commitment of murine erythroleukemia cells to differentiation: a multistep process. *Proc. Natl. Acad. Sci. U.S.A* 79, 471-475.
 91. Chen, Z.-Y., Riu, E., He, C.-Y., Xu, H., Kay, M.A., 2008. Silencing of episomal transgene expression in liver by plasmid bacterial backbone DNA is independent of CpG methylation. *Mol. Ther* 16, 548-556.
 92. Chiarini, L.B., Freitas, A.R.O., Zanata, S.M., Brentani, R.R., Martins, V.R., Linden, R., 2002. Cellular prion protein transduces neuroprotective signals. *EMBO J* 21, 3317-3326.
 93. Choi, Y.-G., Kim, J.-I., Jeon, Y.-C., Park, S.-J., Choi, E.-K., Rubenstein, R., Kascsak, R.J., Carp, R.I., Kim, Y.-S., 2004. Nonenzymatic glycation at the N terminus of pathogenic prion protein in transmissible spongiform encephalopathies. *J. Biol. Chem* 279, 30402-30409.
 94. Christensen, H.M., Harris, D.A., 2008. Prion protein lacks robust cytoprotective activity in cultured cells. *Mol Neurodegener* 3, 11.
 95. Chute, J.P., Ross, J.R., McDonnell, D.P., 2010. Minireview: Nuclear receptors, hematopoiesis, and stem cells. *Mol. Endocrinol* 24, 1-10.
 96. Ingley, E., Tilbrook, P.A., Klinken, S.P., 2004. New insights into the regulation of erythroid cells. *IUBMB Life* 56, 177-184.
 97. Isaacs, J.D., Jackson, G.S., Altmann, D.M., 2006. The role of the cellular prion protein in the immune system. *Clin. Exp. Immunol* 146, 1-8.
 98. Isaacs, J.D., Garden, O.A., Kaur, G., Collinge, J., Jackson, G.S., Altmann, D.M., 2008. The cellular prion protein is preferentially expressed by CD4+ CD25+ Foxp3+ regulatory T cells. *Immunology* 125, 313-319.
 99. Jelkmann, W., 2004. Molecular biology of erythropoietin. *Intern. Med* 43, 649-659.
 100. Jeong, B.-H., Lee, Y.-J., Carp, R.I., Kim, Y.-S., 2009. The prevalence of human endogenous retroviruses in cerebrospinal fluids from patients with sporadic Creutzfeldt-Jakob disease. *J Clin Virol* 47, 136-142.
 101. Jolicœur, P., Massé, G., Kay, D.G., 1996. The prion protein gene is dispensable for the development of spongiform myeloencephalopathy induced by the neurovirulent Cas-Br-E murine leukemia virus. *J Virol* 70, 9031-9034.
-

-
102. Julius, C., Hutter, G., Wagner, U., Seeger, H., Kana, V., Kranich, J., Klöhn, P.-C., Klöhn, P., Weissmann, C., Miele, G., Aguzzi, A., 2008. Transcriptional stability of cultured cells upon prion infection. *J. Mol. Biol* 375, 1222-1233.
 103. Kaneda, T., Murate, T., Sheffery, M., Brown, K., Rifkind, R.A., Marks, P.A., 1985. Gene expression during terminal differentiation: dexamethasone suppression of inducer-mediated alpha 1- and beta maj-globin gene expression. *Proc. Natl. Acad. Sci. U.S.A* 82, 5020-5024.
 104. Kascsak, R.J., Rubenstein, R., Merz, P.A., Tonna-DeMasi, M., Fersko, R., Carp, R.I., Wisniewski, H.M., Diringer, H., 1987. Mouse polyclonal and monoclonal antibody to scrapie-associated fibril proteins. *J. Virol* 61, 3688-3693.
 105. Kawasaki, Y., Kawagoe, K., Chen, C.-jen, Teruya, K., Sakasegawa, Y., Doh-ura, K., 2007. Orally administered amyloidophilic compound is effective in prolonging the incubation periods of animals cerebrally infected with prion diseases in a prion strain-dependent manner. *J. Virol* 81, 12889-12898.
 106. Kihm, A.J., Kong, Y., Hong, W., Russell, J.E., Rouda, S., Adachi, K., Simon, M.C., Blobel, G.A., Weiss, M.J., 2002. An abundant erythroid protein that stabilizes free alpha-haemoglobin. *Nature* 417, 758-763.
 107. Kim, B.-H., Lee, H.-G., Choi, J.-K., Kim, J.-I., Choi, E.-K., Carp, R.I., Kim, Y.-S., 2004. The cellular prion protein (PrPC) prevents apoptotic neuronal cell death and mitochondrial dysfunction induced by serum deprivation. *Brain Res. Mol. Brain Res* 124, 40-50.
 108. Kim, B.-E., Nevitt, T., Thiele, D.J., 2008. Mechanisms for copper acquisition, distribution and regulation. *Nat. Chem. Biol* 4, 176-185.
 109. Kim, V.N., Han, J., Siomi, M.C., 2009. Biogenesis of small RNAs in animals. *Nat. Rev. Mol. Cell Biol* 10, 126-139.
 110. Kim, Y., Lee, J., Lee, C., 2008. In silico comparative analysis of DNA and amino acid sequences for prion protein gene. *Transbound Emerg Dis* 55, 105-114.
 111. Kim, Y., Han, B., Titlow, W., Mays, C.E., Kwon, M., Ryou, C., 2009. Utility of RNAi-mediated prnp gene silencing in neuroblastoma cells permanently infected by prions: Potentials and limitations. *Antiviral Res.* 84, 185-193.
 112. Kimelberg, H.K., 2010. Functions of mature mammalian astrocytes: a current view. *Neuroscientist* 16, 79-106.
 113. Komura, J., Okada, T., Ono, T., 1995. Repression of transient expression by DNA methylation in transcribed regions of reporter genes introduced into cultured human cells. *Biochim. Biophys. Acta* 1260, 73-78.
-

-
114. Korth, C., Stierli, B., Streit, P., Moser, M., Schaller, O., Fischer, R., Schulz-Schaeffer, W., Kretzschmar, H., Raeber, A., Braun, U., Ehrensperger, F., Hornemann, S., Glockshuber, R., Riek, R., Billeter, M., Wüthrich, K., Oesch, B., 1997. Prion (PrP^{Sc})-specific epitope defined by a monoclonal antibody. *Nature* 390, 74-77.
 115. Kramerov, D.A., Bukrinsky, M.I., Ryskov, A.P., 1985. DNA sequences homologous to long double-stranded RNA. Transcription of intracisternal A-particle genes and major long repeat of the mouse genome. *Biochim. Biophys. Acta* 826, 20-29.
 116. Kubosaki, A., Nishimura-Nasu, Y., Nishimura, T., Yusa, S., Sakudo, A., Saeki, K., Matsumoto, Y., Itohara, S., Onodera, T., 2003. Expression of normal cellular prion protein (PrP(c)) on T lymphocytes and the effect of copper ion: Analysis by wild-type and prion protein gene-deficient mice. *Biochem. Biophys. Res. Commun* 307, 810-813.
 117. Kupfer, L., Hinrichs, W., Groschup, M.H., 2009. Prion protein misfolding. *Curr. Mol. Med* 9, 826-835.
 118. Kuwahara, C., Takeuchi, A.M., Nishimura, T., Haraguchi, K., Kubosaki, A., Matsumoto, Y., Saeki, K., Matsumoto, Y., Yokoyama, T., Itohara, S., Onodera, T., 1999. Prions prevent neuronal cell-line death. *Nature* 400, 225-226.
 119. Laffont-Proust, I., Hässig, R., Haïk, S., Simon, S., Grassi, J., Fonta, C., Faucheux, B.A., Moya, K.L., 2006. Truncated PrP(c) in mammalian brain: interspecies variation and location in membrane rafts. *Biol. Chem* 387, 297-300.
 120. Lasmézas, C.I., Cesbron, J.Y., Deslys, J.P., Demaimay, R., Adjou, K.T., Rioux, R., Lemaire, C., Loch, C., Dormont, D., 1996. Immune system-dependent and -independent replication of the scrapie agent. *J. Virol* 70, 1292-1295.
 121. Lawrie, C.H., 2010. microRNA expression in erythropoiesis and erythroid disorders. *Br. J. Haematol* 150, 144-151.
 122. Leblanc, P., Alais, S., Porto-Carreiro, I., Lehmann, S., Grassi, J., Raposo, G., Darlix, J.L., 2006. Retrovirus infection strongly enhances scrapie infectivity release in cell culture. *EMBO J* 25, 2674-2685.
 123. Leblanc, P., Baas, D., Darlix, J.-L., 2004. Analysis of the interactions between HIV-1 and the cellular prion protein in a human cell line. *J. Mol. Biol* 337, 1035-1051.
 124. Leclerc, E., Peretz, D., Ball, H., Solfrosi, L., Legname, G., Safar, J., Serban, A., Prusiner, S.B., Burton, D.R., Williamson, R.A., 2003. Conformation of PrP(C) on the cell surface as probed by antibodies. *J. Mol. Biol* 326, 475-483.
 125. Lee, I.Y., Westaway, D., Smit, A.F., Wang, K., Seto, J., Chen, L., Acharya, C., Ankener, M., Baskin, D., Cooper, C., Yao, H., Prusiner, S.B., Hood, L.E., 1998. Complete genomic sequence and analysis of the prion protein gene region from three mammalian species. *Genome Res* 8, 1022-1037.
-

-
126. Lee, K.-H., Jeong, B.-H., Jin, J.-K., Meeker, H.C., Kim, J.-I., Carp, R.I., Kim, Y.-S., 2006. Scrapie infection activates the replication of ecotropic, xenotropic, and polytropic murine leukemia virus (MuLV) in brains and spinal cords of senescence-accelerated mice: implication of MuLV in progression of scrapie pathogenesis. *Biochem. Biophys. Res. Commun* 349, 122-130.
 127. Li, G., Bolton, D.C., 1997. A novel hamster prion protein mRNA contains an extra exon: increased expression in scrapie. *Brain Res* 751, 265-274.
 128. Li, R., Liu, D., Zanusso, G., Liu, T., Fayen, J.D., Huang, J.H., Petersen, R.B., Gambetti, P., Sy, M.S., 2001. The expression and potential function of cellular prion protein in human lymphocytes. *Cell. Immunol* 207, 49-58.
 129. Liu, Y., Pop, R., Sadegh, C., Brugnara, C., Haase, V.H., Socolovsky, M., 2006. Suppression of Fas-FasL coexpression by erythropoietin mediates erythroblast expansion during the erythropoietic stress response in vivo. *Blood* 108, 123-133.
 130. Livak, K.J., Schmittgen, T.D., 2001. Analysis of relative gene expression data using real-time quantitative PCR and the $2^{-\Delta\Delta C(T)}$ Method. *Methods* 25, 402-408.
 131. Llewelyn, C.A., Hewitt, P.E., Knight, R.S.G., Amar, K., Cousens, S., Mackenzie, J., Will, R.G., 2004. Possible transmission of variant Creutzfeldt-Jakob disease by blood transfusion. *Lancet* 363, 417-421.
 132. Lo, R.Y.-Y., Shyu, W.-C., Lin, S.-Z., Wang, H.-J., Chen, S.-S., Li, H., 2007. New molecular insights into cellular survival and stress responses: neuroprotective role of cellular prion protein (PrPC). *Mol. Neurobiol* 35, 236-244.
 133. Loeuillet, C., Lemaire-Vieille, C., Naquet, P., Cesbron-Delauw, M.-F., Gagnon, J., Cesbron, J.-Y., 2010. Prion replication in the hematopoietic compartment is not required for neuroinvasion in scrapie mouse model. *PLoS ONE* 5. e13166.
 134. Lu, J., Getz, G., Miska, E.A., Alvarez-Saavedra, E., Lamb, J., Peck, D., Sweet-Cordero, A., Ebert, B.L., Mak, R.H., Ferrando, A.A., Downing, J.R., Jacks, T., Horvitz, H.R., Golub, T.R., 2005. MicroRNA expression profiles classify human cancers. *Nature* 435, 834-838.
 135. Lund, C., Olsen, C.M., Tveit, H., Tranulis, M.A., 2007. Characterization of the prion protein 3F4 epitope and its use as a molecular tag. *J. Neurosci. Methods* 165, 183-190.
 136. Mabbott, N.A., Brown, K.L., Manson, J., Bruce, M.E., 1997. T-lymphocyte activation and the cellular form of the prion protein. *Immunology* 92, 161-165.
 137. MacGregor, I.R., Drummond, O., 2001. Species differences in the blood content of the normal cellular isoform of prion protein, PrP(c), measured by time-resolved fluoroimmunoassay. *Vox Sang* 81, 236-240.
-

-
138. MacGregor, I., Hope, J., Barnard, G., Kirby, L., Drummond, O., Pepper, D., Hornsey, V., Barclay, R., Bessos, H., Turner, M., Prowse, C., 1999. Application of a time-resolved fluoroimmunoassay for the analysis of normal prion protein in human blood and its components. *Vox Sang* 77, 88-96.
139. Mallucci, G., Dickinson, A., Linehan, J., Klöhn, P.-C., Brandner, S., Collinge, J., 2003. Depleting neuronal PrP in prion infection prevents disease and reverses spongiosis. *Science* 302, 871-874.
140. Manson, J.C., Clarke, A.R., Hooper, M.L., Aitchison, L., McConnell, I., Hope, J., 1994. 129/Ola mice carrying a null mutation in PrP that abolishes mRNA production are developmentally normal. *Mol. Neurobiol* 8, 121-127.
141. Manuelidis, L., 2010. Nuclease resistant circular DNAs copurify with infectivity in scrapie and CJD. *J Neurovirol*. Epub ahead of print.
142. Mathiason, C.K., Hayes-Klug, J., Hays, S.A., Powers, J., Osborn, D.A., Dahmes, S.J., Miller, K.V., Warren, R.J., Mason, G.L., Telling, G.C., Young, A.J., Hoover, E.A., 2010. B cells and platelets harbor prion infectivity in the blood of deer infected with chronic wasting disease. *J. Virol* 84, 5097-5107.
143. Mattern, J., Büchler, M.W., Herr, I., 2007. Cell cycle arrest by glucocorticoids may protect normal tissue and solid tumors from cancer therapy. *Cancer Biol. Ther* 6, 1345-1354.
144. Mazumder, B., Seshadri, V., Fox, P.L., 2003. Translational control by the 3'-UTR: the ends specify the means. *Trends Biochem. Sci* 28, 91-98.
145. Miele, G., Manson, J., Clinton, M., 2001. A novel erythroid-specific marker of transmissible spongiform encephalopathies. *Nat. Med* 7, 361-364.
146. Miele, G., Seeger, H., Marino, D., Eberhard, R., Heikenwalder, M., Stoeck, K., Basagni, M., Knight, R., Green, A., Chianini, F., Wüthrich, R.P., Hock, C., Zerr, I., Aguzzi, A., 2008. Urinary alpha1-antichymotrypsin: a biomarker of prion infection. *PLoS ONE* 3, e3870.
147. Moore, R.C., Lee, I.Y., Silverman, G.L., Harrison, P.M., Strome, R., Heinrich, C., Karunaratne, A., Pasternak, S.H., Chishti, M.A., Liang, Y., Mastrangelo, P., Wang, K., Smit, A.F., Katamine, S., Carlson, G.A., Cohen, F.E., Prusiner, S.B., Melton, D.W., Tremblay, P., Hood, L.E., Westaway, D., 1999. Ataxia in prion protein (PrP)-deficient mice is associated with upregulation of the novel PrP-like protein doppel. *J. Mol. Biol* 292, 797-817.
148. Moore, R.C., Mastrangelo, P., Bouzamondo, E., Heinrich, C., Legname, G., Prusiner, S.B., Hood, L., Westaway, D., DeArmond, S.J., Tremblay, P., 2001. Doppel-induced cerebellar degeneration in transgenic mice. *Proc. Natl. Acad. Sci. U.S.A* 98, 15288-15293.
149. Moreau-Gachelin, F., 2008. Multi-stage Friend murine erythroleukemia: molecular insights into oncogenic cooperation. *Retrovirology* 5, 99.
-

-
150. Morel, E., Fouquet, S., Chateau, D., Yvernauld, L., Frobert, Y., Pincon-Raymond, M., Chambaz, J., Pillot, T., Rousset, M., 2004. The cellular prion protein PrP^c is expressed in human enterocytes in cell-cell junctional domains. *J. Biol. Chem* 279, 1499-1505.
151. Mouillet-Richard, S., Ermonval, M., Chebassier, C., Laplanche, J.L., Lehmann, S., Launay, J.M., Kellermann, O., 2000. Signal transduction through prion protein. *Science* 289, 1925-1928.
152. Murate, T., Kaneda, T., Rifkind, R.A., Marks, P.A., 1984. Inducer-mediated commitment of murine erythroleukemia cells to terminal cell division: the expression of commitment. *Proc. Natl. Acad. Sci. U.S.A* 81, 3394-3398.
153. Murnane, J.P., Yezzi, M.J., Young, B.R., 1990. Recombination events during integration of transfected DNA into normal human cells. *Nucleic Acids Res* 18, 2733-2738.
154. Nemeth, E., 2008. Iron regulation and erythropoiesis. *Curr Opin Hematol* 15, 169-175.
155. Nico, P.B.C., de-Paris, F., Vinadé, E.R., Amaral, O.B., Rockenbach, I., Soares, B.L., Guarnieri, R., Wichert-Ana, L., Calvo, F., Walz, R., Izquierdo, I., Sakamoto, A.C., Brentani, R., Martins, V.R., Bianchin, M.M., 2005. Altered behavioural response to acute stress in mice lacking cellular prion protein. *Behav. Brain Res* 162, 173-181.
156. Nishigaki, K., Thompson, D., Hanson, C., Yugawa, T., Ruscetti, S., 2001. The envelope glycoprotein of friend spleen focus-forming virus covalently interacts with and constitutively activates a truncated form of the receptor tyrosine kinase Stk. *J. Virol* 75, 7893-7903.
157. Nishihara, E., Furuyama, T., Yamashita, S., Mori, N., 1998. Expression of copper trafficking genes in the mouse brain. *Neuroreport* 9, 3259-3263.
158. Nixon, R.R., 2005. Prion-associated increases in Src-family kinases. *J. Biol. Chem* 280, 2455-2462.
159. O'Carroll, D., Mecklenbrauker, I., Das, P.P., Santana, A., Koenig, U., Enright, A.J., Miska, E.A., Tarakhovsky, A., 2007. A Slicer-independent role for Argonaute 2 in hematopoiesis and the microRNA pathway. *Genes Dev* 21, 1999-2004.
160. Oesch, B., Westaway, D., Wälchli, M., McKinley, M.P., Kent, S.B., Aebersold, R., Barry, R.A., Tempst, P., Teplow, D.B., Hood, L.E., 1985. A cellular gene encodes scrapie PrP 27-30 protein. *Cell* 40, 735-746.
161. Osborne, H.B., Bakke, A.C., Yu, J., 1982. Effect of dexamethasone on hexamethylene bisacetamide-induced Friend cell erythrodifferentiation. *Cancer Res* 42, 513-518.
-

-
162. Otsuka, Y., Ito, D., Katsuoka, K., Arashiki, N., Komatsu, T., Inaba, M., 2008. Expression of alpha-hemoglobin stabilizing protein and cellular prion protein in a subclone of murine erythroleukemia cell line MEL. *Jpn J Vet Res* 56, 75-84.
 163. Paddison, P.J., Cleary, M., Silva, J.M., Chang, K., Sheth, N., Sachidanandam, R., Hannon, G.J., 2004. Cloning of short hairpin RNAs for gene knockdown in mammalian cells. *Nat. Methods* 1, 163-167.
 164. Pan, T., Li, R., Wong, B.-S., Liu, T., Gambetti, P., Sy, M.-S., 2002. Heterogeneity of normal prion protein in two-dimensional immunoblot: presence of various glycosylated and truncated forms. *J. Neurochem* 81, 1092-1101.
 165. Panigaj, M., Brouckova, A., Glierova, H., Dvorakova, E., Simak, J., Vostal, J.G., Holada, K., 2010. Underestimation of the expression of cellular prion protein on human red blood cells. *Transfusion*. 51, 1012-1021.
 166. Papapetrou, E.P., Korkola, J.E., Sadelain, M., 2010. A genetic strategy for single and combinatorial analysis of miRNA function in mammalian hematopoietic stem cells. *Stem Cells* 28, 287-296.
 167. Pattison, I.H., Jones, K.M., Jebbett, J.N., 1971. Detection of the scrapie agent in tissues of normal mice with special reference to the possibility of accidental laboratory contamination. *Res. Vet. Sci* 12, 30-39.
 168. Pauly, P.C., Harris, D.A., 1998. Copper stimulates endocytosis of the prion protein. *J. Biol. Chem* 273, 33107-33110.
 169. Perry, C., Soreq, H., 2002. Transcriptional regulation of erythropoiesis. Fine tuning of combinatorial multi-domain elements. *Eur. J. Biochem* 269, 3607-3618.
 170. Peters, P.J., Mironov, A., Peretz, D., van Donselaar, E., Leclerc, E., Erpel, S., DeArmond, S.J., Burton, D.R., Williamson, R.A., Vey, M., Prusiner, S.B., 2003. Trafficking of prion proteins through a caveolae-mediated endosomal pathway. *J. Cell Biol* 162, 703-717.
 171. Petrak, J., Myslivcova, D., Man, P., Cmejlova, J., Cmejla, R., Vyoral, D., 2007. Proteomic analysis of erythroid differentiation induced by hexamethylene bisacetamide in murine erythroleukemia cells. *Exp. Hematol* 35, 193-202.
 172. Pfeifer, A., Eigenbrod, S., Al-Khadra, S., Hofmann, A., Mitteregger, G., Moser, M., Bertsch, U., Kretzschmar, H., 2006. Lentivector-mediated RNAi efficiently suppresses prion protein and prolongs survival of scrapie-infected mice. *J. Clin. Invest* 116, 3204-3210.
 173. Prusiner, S.B., Scott, M.R., DeArmond, S.J., Cohen, F.E., 1998. Prion protein biology. *Cell* 93, 337-348.
 174. Qi, Y., Wang, J.K., McMillian, M., Chikaraishi, D.M., 1997. Characterization of a CNS cell line, CAD, in which morphological differentiation is initiated by serum deprivation. *J. Neurosci* 17, 1217-1225.
-

-
175. Qin, K., Zhao, L., Ash, R.D., McDonough, W.F., Zhao, R.Y., 2009. ATM-mediated transcriptional elevation of prion in response to copper-induced oxidative stress. *J. Biol. Chem* 284, 4582-4593.
176. Ramsay, R.G., Ikeda, K., Rifkind, R.A., Marks, P.A., 1986. Changes in gene expression associated with induced differentiation of erythroleukemia: protooncogenes, globin genes, and cell division. *Proc. Natl. Acad. Sci. U.S.A* 83, 6849-6853.
177. Requena, J.R., Dimitrova, M.N., Legname, G., Teijeira, S., Prusiner, S.B., Levine, R.L., 2004. Oxidation of methionine residues in the prion protein by hydrogen peroxide. *Arch. Biochem. Biophys* 432, 188-195.
178. Reuben, R.C., Wife, R.L., Breslow, R., Rifkind, R.A., Marks, P.A., 1976. A new group of potent inducers of differentiation in murine erythroleukemia cells. *Proc. Natl. Acad. Sci. U.S.A* 73, 862-866.
179. Reynolds, A., Leake, D., Boese, Q., Scaringe, S., Marshall, W.S., Khvorova, A., 2004. Rational siRNA design for RNA interference. *Nat Biotechnol* 22, 326-330.
180. Rieger, R., Edenhofer, F., Lasmézas, C.I., Weiss, S., 1997. The human 37-kDa laminin receptor precursor interacts with the prion protein in eukaryotic cells. *Nat. Med* 3, 1383-1388.
181. Risitano, A.M., Holada, K., Chen, G., Simak, J., Vostal, J.G., Young, N.S., Maciejewski, J.P., 2003. CD34+ cells from paroxysmal nocturnal hemoglobinuria (PNH) patients are deficient in surface expression of cellular prion protein (PrP_c). *Exp. Hematol* 31, 65-72.
182. Robertson, C., Booth, S.A., Beniac, D.R., Coulthart, M.B., Booth, T.F., McNicol, A., 2006. Cellular prion protein is released on exosomes from activated platelets. *Blood* 107, 3907-3911.
183. Rönstrand, L., 2004. Signal transduction via the stem cell factor receptor/c-Kit. *Cell. Mol. Life Sci* 61, 2535-2548.
184. Rossi, D., Cozzio, A., Flechsig, E., Klein, M.A., Rüllicke, T., Aguzzi, A., Weissmann, C., 2001. Onset of ataxia and Purkinje cell loss in PrP null mice inversely correlated with Dpl level in brain. *EMBO J* 20, 694-702.
185. Rubenstein, R., Kascsak, R.J., Papini, M., Kascsak, R., Carp, R.I., LaFauci, G., Melen, R., Langeveld, J., 1999. Immune surveillance and antigen conformation determines humoral immune response to the prion protein immunogen. *J. Neurovirol* 5, 401-413.
186. Rudd, P.M., Wormald, M.R., Wing, D.R., Prusiner, S.B., Dwek, R.A., 2001. Prion glycoprotein: structure, dynamics, and roles for the sugars. *Biochemistry* 40, 3759-3766.
187. Ruscetti, S.K., 1999. Deregulation of erythropoiesis by the Friend spleen focus-forming virus. *Int. J. Biochem. Cell Biol* 31, 1089-1109.
-

-
188. Saborio, G.P., Permanne, B., Soto, C., 2001. Sensitive detection of pathological prion protein by cyclic amplification of protein misfolding. *Nature* 411, 810-813.
189. Safar, J., Wille, H., Itri, V., Groth, D., Serban, H., Torchia, M., Cohen, F.E., Prusiner, S.B., 1998. Eight prion strains have PrP(Sc) molecules with different conformations. *Nat. Med* 4, 1157-1165.
190. Sakaguchi, S., Katamine, S., Nishida, N., Moriuchi, R., Shigematsu, K., Sugimoto, T., Nakatani, A., Kataoka, Y., Houtani, T., Shirabe, S., Okada, H., Hasegawa, S., Miyamoto, T., Noda, T., 1996. Loss of cerebellar Purkinje cells in aged mice homozygous for a disrupted PrP gene. *Nature* 380, 528-531.
191. Sandberg, M.K., Al-Doujaily, H., Sharps, B., Clarke, A.R., Collinge, J., 2011. Prion propagation and toxicity in vivo occur in two distinct mechanistic phases. *Nature* 470, 540-542.
192. dos Santos, C.O., Dore, L.C., Valentine, E., Shelat, S.G., Hardison, R.C., Ghosh, M., Wang, W., Eisenstein, R.S., Costa, F.F., Weiss, M.J., 2008. An iron responsive element-like stem-loop regulates alpha-hemoglobin-stabilizing protein mRNA. *J. Biol. Chem* 283, 26956-26964.
193. Santuccione, A., Sytnyk, V., Leshchyn's'ka, I., Schachner, M., 2005. Prion protein recruits its neuronal receptor NCAM to lipid rafts to activate p59fyn and to enhance neurite outgrowth. *J. Cell Biol* 169, 341-354.
194. Sato, T., Friend, C., De Harven, E., 1971. Ultrastructural changes in Friend erythroleukemia cells treated with dimethyl sulfoxide. *Cancer Res* 31, 1402-1417.
195. Shyng, S.L., Heuser, J.E., Harris, D.A., 1994. A glycolipid-anchored prion protein is endocytosed via clathrin-coated pits. *J. Cell Biol* 125, 1239-1250.
196. Schröder, B., Nickodemus, R., Jürgens, T., Bodemer, W., 2002. Upstream AUGs modulate prion protein translation in vitro. *Acta Virol* 46, 159-167.
197. Silva, J.M., Li, M.Z., Chang, K., Ge, W., Golding, M.C., Rickles, R.J., Siolas, D., Hu, G., Paddison, P.J., Schlabach, M.R., Sheth, N., Bradshaw, J., Burchard, J., Kulkarni, A., Cavet, G., Sachidanandam, R., McCombie, W.R., Cleary, M.A., Elledge, S.J., Hannon, G.J., 2005. Second-generation shRNA libraries covering the mouse and human genomes. *Nat. Genet* 37, 1281-1288.
198. Singh, A., Mohan, M.L., Isaac, A.O., Luo, X., Petrak, J., Vyoral, D., Singh, N., 2009a. Prion protein modulates cellular iron uptake: a novel function with implications for prion disease pathogenesis. *PLoS ONE* 4, e4468.
199. Singh, A., Kong, Q., Luo, X., Petersen, R.B., Meyerson, H., Singh, N., 2009b. Prion protein (PrP) knock-out mice show altered iron metabolism: a functional role for PrP in iron uptake and transport. *PLoS ONE* 4, e6115.
-

-
200. Solfrosi, L., Criado, J.R., McGavern, D.B., Wirz, S., Sánchez-Alavez, M., Sugama, S., DeGiorgio, L.A., Volpe, B.T., Wiseman, E., Abalos, G., Masliah, E., Gilden, D., Oldstone, M.B., Conti, B., Williamson, R.A., 2004. Cross-linking cellular prion protein triggers neuronal apoptosis in vivo. *Science* 303, 1514-1516.
 201. Spielhauer, C., Schätzl, H.M., 2001. PrPC directly interacts with proteins involved in signaling pathways. *J. Biol. Chem* 276, 44604-44612.
 202. Stahl, N., Borchelt, D.R., Hsiao, K., Prusiner, S.B., 1987. Scrapie prion protein contains a phosphatidylinositol glycolipid. *Cell* 51, 229-240.
 203. Stengel, A., Bach, C., Vorberg, I., Frank, O., Gilch, S., Lutzny, G., Seifarth, W., Erfle, V., Maas, E., Schätzl, H., Leib-Mösch, C., Greenwood, A.D., 2006. Prion infection influences murine endogenous retrovirus expression in neuronal cells. *Biochem. Biophys. Res. Commun* 343, 825-831.
 204. Stöckel, J., Safar, J., Wallace, A.C., Cohen, F.E., Prusiner, S.B., 1998. Prion protein selectively binds copper(II) ions. *Biochemistry* 37, 7185-7193.
 205. Stocking, C., Kozak, C.A., 2008. Murine endogenous retroviruses. *Cell. Mol. Life Sci* 65, 3383-3398.
 206. Svoboda, P., 2007. Off-targeting and other non-specific effects of RNAi experiments in mammalian cells. *Curr Opin Mol Ther* 9, 248-257.
 207. Szurek, P.F., Yuen, P.H., Jerzy, R., Wong, P.K., 1988. Identification of point mutations in the envelope gene of Moloney murine leukemia virus TB temperature-sensitive paralytogenic mutant ts1: molecular determinants for neurovirulence. *J. Virol* 62, 357-360.
 208. Tamir, A., Petrocelli, T., Stetler, K., Chu, W., Howard, J., Croix, B.S., Slingerland, J., Ben-David, Y., 2000. Stem cell factor inhibits erythroid differentiation by modulating the activity of G1-cyclin-dependent kinase complexes: a role for p27 in erythroid differentiation coupled G1 arrest. *Cell Growth Differ* 11, 269-277.
 209. Taruscio, D., Mantovani, A., 2004. Factors regulating endogenous retroviral sequences in human and mouse. *Cytogenet. Genome Res* 105, 351-362.
 210. Tattum, M.H., Jones, S., Pal, S., Collinge, J., Jackson, G.S., 2010. Discrimination between prion-infected and normal blood samples by protein misfolding cyclic amplification. *Transfusion* 50, 996-1002.
 211. Telling, G.C., Scott, M., Mastrianni, J., Gabizon, R., Torchia, M., Cohen, F.E., DeArmond, S.J., Prusiner, S.B., 1995. Prion propagation in mice expressing human and chimeric PrP transgenes implicates the interaction of cellular PrP with another protein. *Cell* 83, 79-90.
 212. Tilly, G., Chapuis, J., Vilette, D., Laude, H., Vilotte, J.L., 2003. Efficient and specific down-regulation of prion protein expression by RNAi. *Biochem Biophys Res Commun* 305, 548-551.
-

-
213. Tobler, I., Gaus, S.E., Deboer, T., Achermann, P., Fischer, M., Rülicke, T., Moser, M., Oesch, B., McBride, P.A., Manson, J.C., 1996. Altered circadian activity rhythms and sleep in mice devoid of prion protein. *Nature* 380, 639-642.
214. Tsiftoglou, A.S., Vizirianakis, I.S., Strouboulis, J., 2009. Erythropoiesis: model systems, molecular regulators, and developmental programs. *IUBMB Life* 61, 800-830.
215. Vey, M., Pilkuhn, S., Wille, H., Nixon, R., DeArmond, S.J., Smart, E.J., Anderson, R.G., Taraboulos, A., Prusiner, S.B., 1996. Subcellular colocalization of the cellular and scrapie prion proteins in caveolae-like membranous domains. *Proc. Natl. Acad. Sci. U.S.A* 93, 14945-14949.
216. Wadsworth, J.D., Joiner, S., Hill, A.F., Campbell, T.A., Desbruslais, M., Luthert, P.J., Collinge, J., 2001. Tissue distribution of protease resistant prion protein in variant Creutzfeldt-Jakob disease using a highly sensitive immunoblotting assay. *Lancet* 358, 171-180.
217. Wek, R.C., Jiang, H.-Y., Anthony, T.G., 2006. Coping with stress: eIF2 kinases and translational control. *Biochem. Soc. Trans* 34, 7-11.
218. White, M.D., Farmer, M., Mirabile, I., Brandner, S., Collinge, J., Mallucci, G.R., 2008. Single treatment with RNAi against prion protein rescues early neuronal dysfunction and prolongs survival in mice with prion disease. *Proc. Natl. Acad. Sci. U.S.A* 105, 10238-10243.
219. Wickrema, A., Kee, B., 2009. *Molecular basis of hematopoiesis*. Springer.
220. Wilkie, G.S., Dickson, K.S., Gray, N.K., 2003. Regulation of mRNA translation by 5'- and 3'-UTR-binding factors. *Trends Biochem. Sci* 28, 182-188.
221. Williams, B.R., 1999. PKR; a sentinel kinase for cellular stress. *Oncogene* 18, 6112-6120.
222. Winter, J., Jung, S., Keller, S., Gregory, R.I., Diederichs, S., 2009. Many roads to maturity: microRNA biogenesis pathways and their regulation. *Nat. Cell Biol* 11, 228-234.
223. Zhang, C.C., Lodish, H.F., 2008. Cytokines regulating hematopoietic stem cell function. *Curr. Opin. Hematol* 15, 307-311.
224. Zhang, C.C., Lodish, H.F., 2005. Murine hematopoietic stem cells change their surface phenotype during ex vivo expansion. *Blood* 105, 4314-4320.
225. Zhang, C.C., Steele, A.D., Lindquist, S., Lodish, H.F., 2006. Prion protein is expressed on long-term repopulating hematopoietic stem cells and is important for their self-renewal. *Proc. Natl. Acad. Sci. U.S.A* 103, 2184-2189.
226. Zhao, G., Yu, D., Weiss, M.J., 2010. MicroRNAs in erythropoiesis. *Curr. Opin. Hematol* 17, 155-162.
-

-
227. Zivny, J.H., Gelderman, M.P., Xu, F., Piper, J., Holada, K., Simak, J., Vostal, J.G., 2008. Reduced erythroid cell and erythropoietin production in response to acute anemia in prion protein-deficient (Prnp^{-/-}) mice. *Blood Cells Mol. Dis* 40, 302-307.
 228. Zou, W.-Q., Zheng, J., Gray, D.M., Gambetti, P., Chen, S.G., 2004. Antibody to DNA detects scrapie but not normal prion protein. *Proc. Natl. Acad. Sci. U.S.A* 101, 1380-1385.

7.1. Online URL references

1. <http://www.cjd.ed.ac.uk/figures.htm>
2. http://www.ambion.com/techlib/misc/siRNA_finder.html
3. <http://www.ncbi.nlm.nih.gov/BLAST>
4. http://www.ambion.com/techlib/misc/psilencer_converter.html
5. http://www.ambion.com/techlib/misc/vectors/5.1_u6.html
6. <http://www.openbiosystems.com/ProductLiterature.aspx?AliasPath=/RNAi/RetroviralCloningVectors&CatalogNumber=EAV4679>
7. <http://cancan.cshl.edu/cgi-bin/Codex/Codex.cgi>
8. <http://www.openbiosystems.com/RNAi/shRNAMirLibraries/pSM2Retroviral/>
9. <http://www.openbiosystems.com/RNAi/RetroviralCloningVectors/>
10. http://www.stanford.edu/group/nolan/protocols/pro_optimiz.html

8. Supplements

Articles:

1. Panigaj M., Brouckova A., Glierova H., Dvorakova E., Simak J., Vostal J.G., Holada K., 2011. Underestimation of the expression of cellular prion protein on human red blood cells, *Transfusion* 51, 1012-1021.
IF= 2.982
2. Panigaj M., Glierova H. and Holada K., Expression of prion protein in mouse erythroid progenitors and differentiating murine erythroleukemia cells, (submitted).

Underestimation of the expression of cellular prion protein on human red blood cells

Martin Panigaj, Adela Brouckova, Hana Glierova, Eva Dvorakova, Jan Simak, Jaroslav G. Vostal, and Karel Holada

BACKGROUND: Recent transmissions of variant Creutzfeldt-Jakob disease by blood transfusion emphasize the need for the development of prion screening tests. The detection of prions in blood is complicated by the presence of poorly characterized cellular prion protein (PrP^C) in both plasma and blood cells. According to published studies, most of PrP^C in blood cells resides in platelets (PLTs) and white blood cells.

STUDY DESIGN AND METHODS: To clarify conflicting reports about the quantity of PrP^C associated with human red blood cells (RBCs), quantitative flow cytometry, Western blot (WB), and enzyme-linked immunosorbent assay (ELISA) were used to measure protein levels in healthy donors.

RESULTS: RBCs expressed 290 ± 140 molecules of PrP^C per cell, assuming equimolar binding of monoclonal antibody (MoAb) 6H4 to PrP^C. Binding of alternate PrP^C MoAbs, FH11 and 3F4, was substantially lower. WB estimated the level of PrP^C per cell on RBCs to be just four times lower than in PLTs. A similar level of PrP^C was detected using ELISA. The weak binding of commonly used MoAb 3F4 was not caused by PrP^C conformation, truncation, or glycosylation, suggesting a covalent modification, likely glycation, of the 3F4 epitope.

CONCLUSIONS: Taken together, human RBCs express low but significant amounts of PrP^C/cell, which makes them, due to high RBC numbers, major contributors to the pool of cell-associated PrP^C in blood. Previous reports utilizing MoAb 3F4 may have underestimated the amount of PrP^C in RBCs. Likewise, screening tests for the presence of the abnormal prion protein in blood may be difficult if the abnormal protein is modified similar to RBC PrP^C.

Cellular prion protein (PrP^C) is expressed in various cell types and tissues, including blood cells. The physiological function of PrP^C remains unclear. Together with its conformationally altered form, PrP^{TSE}, it plays a crucial role in prion diseases.¹ Prion diseases, or transmissible spongiform encephalopathies (TSEs), are neurodegenerative disorders affecting a broad spectrum of mammalian species. The common trait of TSEs is a long subclinical period with a final rapid deterioration of cerebral function followed by inevitable death. Until recently, in modern societies, the only documented mode of transmission from human to human was iatrogenic cases in which disease was spread

ABBREVIATIONS: CML = N^ε-(carboxymethyl)lysine; GA = glyoxylic acid; PBST = phosphate-buffered saline with Tween 20; PK = proteinase K; PMSF = phenylmethylsulfonyl fluoride; PRP = platelet-rich plasma; PrP^C = cellular prion protein; PWB = platelet wash buffer; RT = room temperature; sulfo-NHS-biotin = N-hydroxysulfosuccinimide biotin; TBS = Tris-buffered saline; TSE(s) = transmissible spongiform encephalopathy(-ies); vCJD = variant Creutzfeldt-Jakob disease; WB = Western blot.

From the Institute of Immunology and Microbiology, 1st Faculty of Medicine, Charles University, Prague, Czech Republic; and the Division of Hematology, Center for Biologics Evaluation and Research, FDA, Bethesda, Maryland.

Address reprint requests to: Karel Holada, PhD, Institute of Immunology and Microbiology, 1st Faculty of Medicine, Charles University in Prague, Studnickova 7, 128 20 Prague 2, Czech Republic; e-mail: karel.holada@lf1.cuni.cz.

This work was supported by Grants GACR 310/08/0878, GACR 203/07/1517, MSM0021620806, and SVV-2010-260506.

The findings and conclusions in this article have not been formally disseminated by the Food and Drug Administration and should not be construed to represent any Agency determination or policy.

Received for publication July 23, 2010; revision received September 13, 2010, and accepted September 15, 2010.

doi: 10.1111/j.1537-2995.2010.02924.x

TRANSFUSION 2011;51:1012-1021.

via contaminated neurosurgical instruments, tissue grafts, or hormones.² Despite the proven transmissibility of prion diseases via blood transfusion in laboratory animals, such cases in humans remained undetected until recently.³ As of this year, four cases of variant Creutzfeldt-Jakob disease (vCJD) transmission by blood transfusion, including one asymptomatic vCJD carrier, have been described in the United Kingdom.⁴ All of the patients received nonleukoreduced red blood cells (RBCs) from apparently healthy donors who developed vCJD symptoms many months after the donation. Recently, vCJD PrP^{TSE} was found in the spleen of a UK hemophilia patient who died from reasons not related to TSE.⁵ While the annual number of vCJD victims remains low, the number of asymptotically infected individuals may be significantly higher.^{6,7} These subclinical cases can pose a serious threat of vCJD iatrogenic transmission. In this situation, the development of a fast, sensitive, and noninvasive donor screening test for prion diseases remains an important and controversial issue.^{8,9} Unfortunately, PrP^{TSE} is currently the only known specific molecular marker of the disease, and its detection in blood is challenging.¹⁰ The nature and properties of blood PrP^{TSE} are not known, and the availability of PrP^{TSE}-specific antibodies is limited. Commercial diagnostic tests usually depend on proteinase K (PK) treatment to distinguish partially resistant PrP^{TSE} from sensitive PrP^C. Another principle is used in the conformation-dependent immunoassay developed by Safar and colleagues¹¹ that utilizes the difference in the affinity of monoclonal antibody (MoAb) 3F4 to native and denatured PrP^{TSE}. The 3F4 epitope is buried in the PrP^{TSE} molecule and becomes accessible after denaturation. Thus, the comparison of signals between native and denatured sample allows for the detection of PrP^{TSE}. Human blood contains a substantial amount of poorly characterized PrP^C, complicating the detection of PrP^{TSE} by providing heterogeneous background. According to published studies, most of PrP^C in the cellular compartment of blood resides in platelets (PLTs) and on white blood cells (WBCs).^{12,13} Opinions on the expression of PrP^C on RBCs differ significantly. A number of studies have reported no or insignificant expression of PrP^C. Dodelet and Cashman¹⁴ have reported the absence of PrP^C expression on RBCs using flow cytometry with MoAb 3F4. Similarly, Barclay and coworkers¹² did not detect any PrP^C on RBCs using flow cytometry with MoAbs 3F4 and FH11. In addition, no expression was reported in flow cytometry studies of Antoine and colleagues¹⁵ and Li and colleagues¹⁶ using different PrP antibodies (8G8, 3B5, and 8H4). MacGregor and colleagues¹³ used time-resolved dissociation-enhanced fluoroimmunoassay with FH11 as the capture antibody and 3F4 as the detecting antibody to measure the amount of PrP^C in separated human blood cells. They estimated that 84% of PrP^C levels were associated with PLTs, 10% with WBCs, and only 5.7% with RBCs. This observation was in accordance

with the negligible PrP^C expression reported by the above-mentioned flow cytometry studies. Later, Barclay and colleagues¹⁷ used a panel of 12 MoAbs to compare the expression of PrP^C on blood cells using flow cytometry. Out of 12 antibodies, only three (6H4, 4F2, and 8G8) demonstrated weak but clearly distinct binding to human RBCs. We first observed the expression of a minute amount of PrP^C on human RBCs using flow cytometry with the 6H4 antibody.¹⁸ Our finding was questioned by some authors, particularly due to the single-antibody approach.¹⁹ In view of the above controversial reports, the question of the presence of PrP^C on circulating human RBCs has remained uncertain. This uncertainty has been furthered by the repeated failure of MoAb 3F4, one of the most trusted prion antibodies, to detect a significant level of RBC PrP^C.^{12-14,17} Here, we provide a conclusive study demonstrating the expression of PrP^C on circulating human RBCs using various antibodies and different methods. In addition, we provide an explanation for the weak binding of 3F4 to human RBC PrP^C and discuss possible implications of this phenomenon for the development of a PrP^{TSE} detection test.

MATERIALS AND METHODS

Samples

Citrate-anticoagulated blood of healthy volunteers was provided by the Transfusion Department of Institute of Hematology and Blood Transfusion in Prague. Samples of cord blood were provided by the Institute for the Care of Mother and Child in Prague. Normal brain samples (lobus frontalis) were provided by the Institute of Pathological Medicine (1st Faculty of Medicine, Charles University, Prague, Czech Republic). The collection of samples was conducted in accordance with the Helsinki Declaration.

Flow cytometry

Quantitative fluorescence-activated cell sorting (FACS) analysis with fluorescein isothiocyanate (FITC)-labeled MoAbs FH11 (TSE Resource Centre, Compton, UK), 3F4 (MAB1562, Chemicon, Inc., Temecula, CA), and 6H4 (Prionics AG, Zürich, Switzerland) against different epitopes of human PrP^C- PrP₅₁₋₅₅, PrP₁₀₆₋₁₁₂, and PrP₁₄₄₋₁₅₂ (Fig. 1) was performed on RBCs of eight healthy donors as described previously.¹⁸ Standard beads (Quantum 24, Bangs Laboratories, Inc., Fishers, IN) were used for construction of calibration regression line, and the number of immunoglobulin (Ig)G molecules bound per cell was calculated. Two-color flow cytometry was used for the comparison of MoAb 3F4 and 6H4 binding to transferrin receptor-positive (CD71+) erythroid cells in cord blood. RBCs were sedimented (1 × g, 45 min, room temperature [RT]) on Ficoll-Hypaque. Cells in the supernatant were incubated

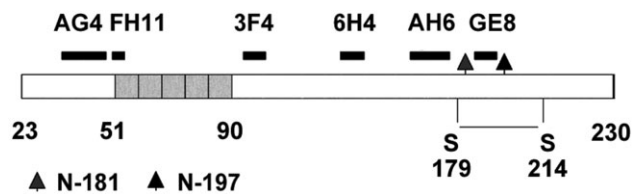


Fig. 1. Schematic structure of human PrP^c with the location of epitopes of MoAbs used in the study. MoAbs FH11, 3F4, and 6H4 were used in the flow cytometry study of its expression on human RBCs. MoAbs AG4 and GE8 were used for measurement of PrP^c content in RBCs and PLTs by ELISA and together with AH6 in WB studies. The mixtures of MoAbs AG4 and 6H4 or AG4, AH6, and GE8 were used in attempts to detect truncated forms of RBC PrP^c. The octarepeats region (51-90), two N-glycosylation sites (181, 197), and the disulfide bridge (179-214) are shown.

with saturating concentrations of MoAb 3F4 or 6H4, fixed with 1% paraformaldehyde, and after washing, incubated with FITC-labeled anti-mouse immunoglobulin (Ig)G goat secondary antibody (Beckman Coulter, Inc., Brea, CA) followed by phycoerythrin-conjugated CD71 MoAb (MEM-75, Exbio, Prague, Czech Republic). CD71-positive cells were gated on FL2/forward scatter plot, and their FITC fluorescence was compared.

Preparation of brain homogenate

Brain tissue was homogenized (1:9) in ice-cold Tris-buffered saline (TBS; 20 mmol/L Tris and 145 mmol/L NaCl, pH 7.4) with 1 mmol/L ethylenediaminetetraacetate (EDTA) and 1 mmol/L phenylmethylsulfonyl fluoride (PMSF). Coarse fragments were removed (4000 × g, 10 min, 4°C), and the supernatant was stored frozen in aliquots at –80°C.

Simultaneous isolation of PLTs and RBC ghosts

Blood was diluted 1:1 with PLT wash buffer (PWB; 12.9 mmol/L citrate, 30 mmol/L glucose, 120 mmol/L NaCl, and 5 mmol/L EDTA, pH 6.5) and centrifuged (300 × g, 15 min, RT). PLT-rich plasma (PRP) was transferred into a new tube, and sedimented cells were resuspended in PWB. This step was repeated three times to remove the majority of PLTs and plasma. The numbers of blood cells in individual stages of separation were monitored using a cell counter (ADVIA 60, Bayer, Leverkusen, Germany) and served as a base for estimation of numbers of contaminating cells in separated blood fractions. RBCs were resuspended in cold phosphate-buffered saline (PBS; pH 7.4) and centrifuged (1500 × g, 10 min, 4°C). The supernatant and the buffy coat containing WBCs were discarded together with the upper quarter of the RBC phase. The middle half of the RBC phase was diluted with the

same volume of PBS and RBCs were lysed with 14 volumes of ice-cold lysis buffer (5 mmol/L sodium phosphate and 1 mmol/L EDTA, pH 7.4). The remaining contaminating PLTs and WBCs were removed using centrifugation (2000 × g, 5 min, 4°C). RBC ghosts were sedimented at 20,000 × g (40 min, 4°C), washed three times with lysis buffer, resuspended in TBS, and stored frozen at –80°C. PLTs were isolated from PRP combined with washing RBC PLT-containing fractions. PLTs were sedimented in one tube (1500 × g, 10 min, RT) and resuspended in PWB. Contaminating WBCs and RBCs were centrifuged (300 × g, 15 min, RT), and the supernatant containing pure PLTs was transferred to a new tube. The PLTs were washed twice with PWB, resuspended (5 × 10⁹ PLT/mL) in TBS (pH 7.4), and stored frozen at –80°C.

Electrophoresis and Western blot

Proteins were separated on a 10% sodium dodecyl sulfate-polyacrylamide gel electrophoresis (SDS-PAGE) gel and transferred to a 0.2- μ m nitrocellulose membrane. The membrane was blocked with TBS with 0.05 % Tween 20, pH 7.4, followed by TBST with 5% dry nonfat milk and incubated with appropriate MoAb (0.5 μ g/mL 6H4, 1 μ g/mL AG4, or 0.5 μ g/mL 3F4) diluted in TBST. After being washed, the membrane was incubated with anti-mouse IgG goat F(ab)2 linked to alkaline phosphatase (Biosource International, Camarillo, CA) and bands were visualized with a 5-bromo-4-chloro-3-indolyl-phosphate/nitroblue tetrazolium phosphatase substrate.

Comparison of the amount of PrP^c on PLTs and RBCs using Western blot

Cells were isolated as described above. Care was taken to avoid contamination of RBC ghosts and PLTs by other cells. The comparison was performed by comparing the intensity of PrP^c bands on blots between samples prepared from 1 × 10¹⁰ RBCs/mL and serial dilutions of sample containing 5 × 10⁹ PLTs/mL. PrP^c was detected using MoAb 6H4 or a mixture of MoAbs AG4, AH6, and GE8 (epitopes PrP₃₇₋₅₀, PrP₁₅₉₋₁₇₄, and PrP₁₈₃₋₁₉₁, respectively; 1 μ g/mL of each, TSE Resource Centre, Compton, UK). In the first round of experiments, the comparison was performed between homologous PLTs and RBCs and repeated three times on cells from three donors. The final experiment was performed with homologous PLTs and RBC ghosts isolated from five individual donors. The density of bands on blots was quantified using densitometer software (MiniLumi, DNR Bio-Imaging Systems Ltd, Jerusalem, Israel).

Production of recombinant human prion protein

The pRSET A plasmid with the full-length human prion protein sequence 23-230 (hrPrP) was provided by Prof.

Wüthrich (Institute of Molecular Biology and Biophysics, ETH Zurich, Switzerland). Transformed bacteria (*Escherichia coli* BL21 [DE3]) were grown at 37°C in Luria-Bertani medium until the cell density was approximately 0.6 OD₆₀₀ units. hrPrP expression was then induced using 1 mmol/L isopropyl β-D-1-thiogalactopyranoside and the cultures were grown for an additional 4 hours. The cells were harvested using centrifugation and sonicated in PBS with 1 mmol/L PMSF. Inclusion bodies were solubilized in 8 mol/L urea and the prion protein was purified on metal affinity resin (TALON, Clontech, Saint-Germain-en-Laye, France) and oxidized to form intramolecular disulfide bonds, as previously described.²⁰

Comparison of the amount of PrP^C on PLTs and RBCs using enzyme-linked immunosorbent assay

Homologous PLTs and RBC ghosts of healthy donors (n = 5) were isolated as described above. A microtitration plate (MaxiSorp, Nunc, Roskilde, Denmark) was coated overnight with MoAb AG4 (1 μg/mL) in carbonate buffer, pH 9.6, at 4°C. The plate was washed with PBS with 0.05% Tween 20 (PBST) and blocked for 1 hour at RT in 5% nonfat milk in PBST. Samples of PLTs, RBC ghosts, and hrPrP were diluted in PBS with 1% Triton X-100 and incubated overnight at 4°C (50 μL/well). The plate was washed and incubated for 2 hours at 37°C with custom biotinylated MoAb GE8. After being washed with PBST, streptavidin-horseradish peroxidase (Invitrogen) diluted 1:10,000 was added to wells and incubated for 1 hour at 37°C. The plate was washed and developed with TMB substrate for 4 minutes. The reaction was stopped with the addition of 1 mol/L H₂SO₄, and absorbance was measured at 405 nm.

Deglycosylation

RBC ghosts and brain samples were deglycosylated using PNGase F (New England Biolabs, Ipswich, MA) according to the manufacturer's protocol. The samples were denatured, supplemented with complete protease inhibitor (Roche, Mannheim, Germany), Triton X-100, incubated overnight at 37°C with 100 U/mL PNGase F, and analyzed using immunoblotting. Fresh untreated RBC ghosts and brain samples and their aliquots incubated overnight without PNGase F served as controls.

PK resistance assay on intact cells

Nine volumes of PRP were mixed with 1 volume of whole blood to obtain similar numbers of PLTs and RBCs in the sample. Cells were diluted 10-fold in *N*-(2-hydroxyethyl)piperazine-*N'*-(2-ethanesulfonic acid)-bovine serum albumin (HEPES-BSA; 4 mmol/L HEPES, 137 mmol/L NaCl, 2.7 mmol/L KCl, 1 mmol/L MgCl₂,

5.5 mmol/L glucose, 3 mmol/L NaH₂PO₄ with 0.1% BSA, pH 7.4) and treated for 15 minutes with increasing concentrations (0, 1, 5, 10, and 50 μg/mL) of PK at 30°C. Proteolysis was terminated using 2 mmol/L PMSF and aliquots of samples were labeled with FITC-conjugated MoAbs 3F4 or 6H4. After incubation, the cells were sedimented (2000 × g, 5 min), resuspended in HEPES-BSA, and analyzed using FACS.

PK resistance assay on cell lysates

Homologous RBC ghosts and PLTs and normal brain homogenate were lysed using 1% Triton X-100 and treated for 30 minutes on ice with 0, 2.5, 5, 50, and 100 μg/mL PK. The incubation was terminated using 2 mmol/L PMSF, and samples were analyzed using immunoblotting with MoAbs 6H4 and AG4.

In vitro modification of brain PrP^C by hydrogen peroxide, *N*-hydroxysulfosuccinimide biotin, and glyoxylic acid

Samples of normal brain homogenate were separated using SDS-PAGE and blotted, and the membrane was cut into strips. Individual strips were treated with increasing concentrations of hydrogen peroxide (0, 1, 5, 25, 130, and 640 mmol/L) in PBS for 30 minutes at RT or with increasing concentrations of *N*-hydroxysulfosuccinimide biotin (sulfo-NHS-biotin, Thermo Fischer Scientific, Rockford, IL; 0, 0.01, 0.05, 0.1, 0.5, 1, and 10 mmol/L) in PBS (1 hr, 37°C). Incubation with increasing concentrations (0, 6.75, 12.5, 25, 50, and 100 mmol/L) of glyoxylic acid (GA) was performed in 0.2 mol/L phosphate buffer (pH 7.4) containing 150 mmol/L sodium cyanoborohydride for 24 hours at 37°C.²¹ After incubation, the strips were washed three times with PBS and then developed with MoAb 3F4 or 6H4 as described above.

In vitro modification of recombinant human prion protein by GA

Oxidized hrPrP was diluted to 1 μg/mL in carbonate buffer (15 mmol/L Na₂CO₃ and 35 mmol/L NaHCO₃, pH 9.6) and used for coating an enzyme-linked immunosorbent assay (ELISA; MaxiSorp, Nunc) plate (3 hr, 37°C). After being washed with PBST, the wells were incubated overnight at 4°C with increasing concentrations of GA (0, 6.75, 12.5, 25, 50, and 100 mmol/L) in 0.2 mol/L phosphate buffer (pH 7.4) containing 150 mmol/L sodium cyanoborohydride. The plate was washed, blocked, and developed with MoAb 3F4 or AG4 (0.1 μg/mL in PBST) as described above.

RESULTS

Quantitative FACS analysis of PrP^C expression on RBCs

Notable differences in the binding of antibodies to human RBCs were found. One RBC bound 290 ± 140

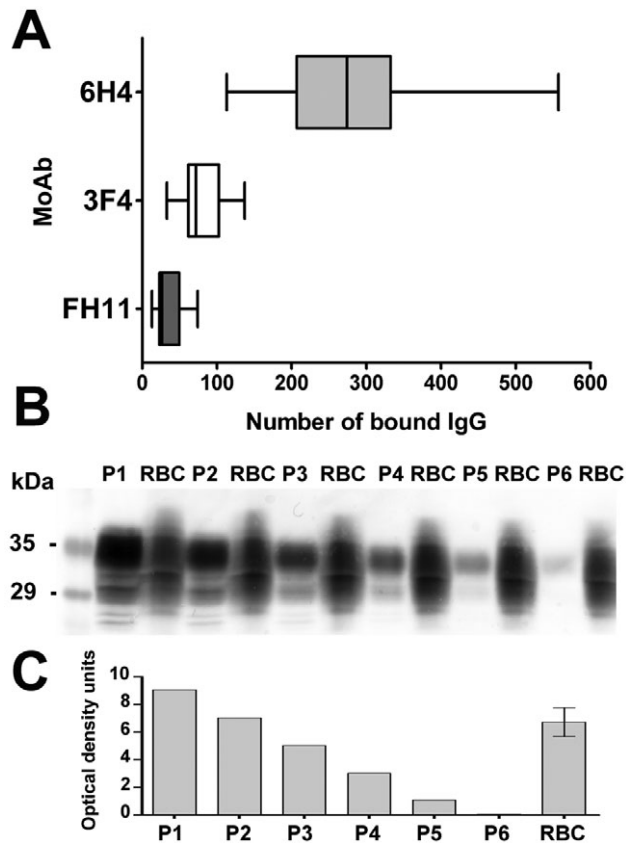


Fig. 2. Quantification of PrP^C expression on human RBCs using flow cytometry and WB. (A) Binding of MoAbs to RBCs of healthy donors measured using quantitative flow cytometry (n = 8). The range of the data, 50% percentile (box), and median are shown. (B) WB comparison of PrP^C levels in representative standardized samples of RBC ghosts (1×10^{10} RBC/mL) and PLTs (P1-P6 = 5×10^9 , 2.5×10^9 , 1.25×10^9 , 6.25×10^8 , 3.13×10^8 , and 1.56×10^8 PLT/mL) developed with MoAb 6H4. (C) Densitometry of bands on blot (B) demonstrates that RBCs contain four times less PrP^C levels than an equal number of PLTs.

(median \pm SD) IgG molecules of 6H4. The binding of 3F4 and FH11 was much lower: 80 ± 35 and 35 ± 20 (median \pm SD) IgG molecules per cell, respectively (Fig. 2A). In contrast, the binding of 3F4 and 6H4 to PLTs in identical samples was roughly equivalent: 630 ± 150 and 635 ± 280 (median \pm SD) IgG molecules per cell, respectively (not shown).

Purity of homologous simultaneously isolated PLTs and RBC ghosts

The isolation procedure led to the preparation of pure cell fractions. Isolated PLTs contained a mean of 1 WBC per 680 ± 270 (mean \pm SD, n = 6) PLTs, and contamination with RBCs in this fraction was below the limit of the cell

counter. Isolated RBCs before hypotonic lysis contained 1 WBC per 1360 ± 280 (mean \pm SD, n = 6) RBCs, and the PLT count was below the limit of the cell counter. In addition, the subsequent centrifugation step after the lysis of RBCs removed virtually all remaining nonlysed cells, leaving RBC ghosts free of cell contamination.

Western blot comparison of PrP^C amount in RBCs and PLTs

In the first set of Western blot (WB) experiments in three separate donors, one PLT contained two- to fourfold more PrP^C than one RBC ghost when measured with MoAb 6H4 and four- to eightfold more when measured with a mixture of PrP MoAbs GE8, AG4, and AH6 (not shown). In the second set of experiments, PLTs and RBC ghosts were prepared from the blood of five separate donors and then pooled to obtain representative mixed PLT and RBC ghost samples. Densitometry analysis of the blot developed with 6H4 confirmed that one PLT contained approximately four times more PrP^C than one RBC ghost (Figs. 2B and 2C).

ELISA comparison of PrP^C amount in RBCs and PLTs

Recombinant human prion protein was used for the construction of the calibration curve in a sandwich ELISA using MoAbs AG4 and GE8. The assay gave a linear response in the range of 2 to 25 ng hrPrP/mL (not shown). Isolated homologous PLTs and RBC ghosts of five separate donors were assayed in triplicate in serial dilutions containing 1×10^9 , 5×10^8 , 2.5×10^8 , and 1.25×10^8 cells/mL. The mean level of PrP^C per 1×10^9 PLTs was 8.2 ± 1.6 ng (mean \pm SD, n = 5) and 2.9 ± 0.6 ng (mean \pm SD, n = 5) per 1×10^9 RBC ghosts. This result estimates the mean amount of PrP^C per PLT to be approximately three times higher than one RBC ghost.

Characterization of RBC PrP^C using WB

Little to no 3F4 bound to PrP^C in serially diluted RBC ghost samples after blotting, while 3F4 binding to brain PrP^C was readily detected (Fig. 3B). At the same time, 6H4 detected RBC PrP^C on blots with similar sensitivity to brain PrP^C (Fig. 3A). WB analysis revealed that RBC PrP^C was present mainly in its diglycosylated form, detected as a diffuse band with a molecular weight slightly higher (35-38 kDa) than brain PrP^C (Fig. 4A). Deglycosylation of PrP^C with PNGase F led to the detection of a single band with a molecular weight similar to deglycosylated brain PrP^C. No major fragments suggesting a significant presence of truncated forms of PrP^C in human RBCs were detected. Denaturation of the sample by boiling with SDS or its deglycosylation did not improve the binding of MoAb 3F4 to RBC PrP^C (Fig. 4B).

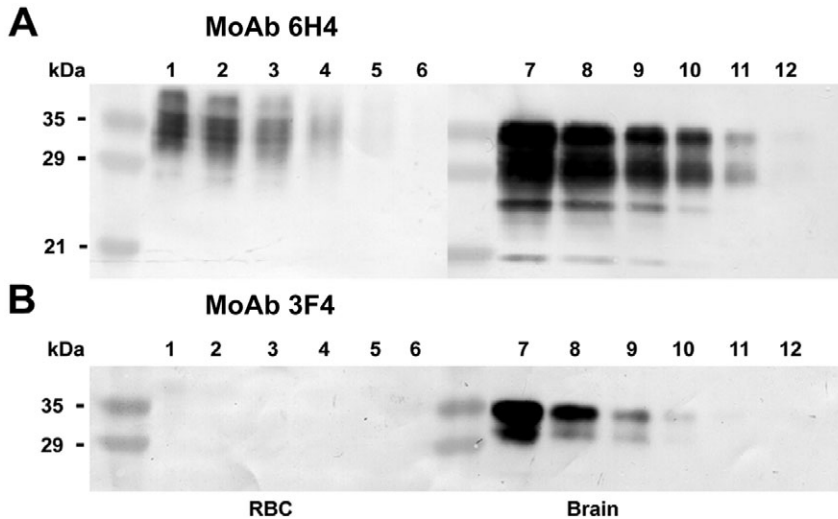


Fig. 3. WB comparison of PrP^C detection using MoAbs 6H4 and 3F4. WBs of serially twofold diluted samples of 1×10^{10} /mL human RBC ghosts (Lanes 1-6) and 10% normal human brain homogenate (Lanes 7-12) were developed with MoAb 6H4 (A) or 3F4 (B). Binding of 3F4 to RBC PrP^C is not improved by denaturation of proteins after boiling with electrophoretic sample buffer, demonstrating that poor binding of 3F4 to human RBCs is not caused by occlusion of its epitope by conformational change or the interaction of PrP^C with its binding partner on the surface of cells. A plausible explanation of poor 3F4 binding is covalent modification of its epitope in RBC PrP^C.

Sensitivity of RBC PrP^C to PK

The incubation of solubilized RBC ghosts with increasing concentrations of PK led to gradual and complete cleavage of PrP^C, demonstrating that RBC PrP^C is similarly as sensitive to PK as PrP^C in equally treated samples of PLTs (not shown) or brain homogenate (Fig. 4C). A similar result was obtained after PK treatment of intact RBCs and PLTs with subsequent analysis of the presence of PrP^C using flow cytometry (not shown).

FACS analysis of 3F4 and 6H4 binding to CD71+ erythroid cells in cord blood

In contrast to peripheral RBCs, equal binding of 3F4 and 6H4 to transferrin receptor-positive (CD71+) erythroid precursors in cord blood was recorded (Fig. 5A).

The influence of in vitro modification of brain PrP^C or recombinant human PrP on the binding of MoAb 3F4

The low binding of 3F4 to RBC PrP^C can be caused by modification of its epitope (KTNMKHM). Oxidation of brain PrP^C with increasing concentrations of hydrogen peroxide up to 130 mmol/L had little effect on the binding of 3F4. At 640 mmol/L, the binding of both 3F4 and 6H4 was diminished (Fig. 5B). In contrast, modi-

fication of lysine residues with increasing concentrations of Sulfo-NHS-biotin led to a gradual loss of 3F4 binding to PrP^C (not shown). Similarly, the modification of lysine residues to *N*^ε-(carboxymethyl)lysine (CML) by incubation with increasing concentrations of GA caused complete inhibition of 3F4 binding, while the binding of 6H4 was not affected (Fig. 5B). Similar results were obtained after GA treatment of hrPrP adsorbed on ELISA plates. Concentrations of GA above 50 mmol/L led to the complete loss of 3F4 binding, while the binding of AG4 was not affected (not shown).

DISCUSSION

The presence of TSE infectivity in blood has repeatedly been demonstrated in various species, including mouse, hamster, sheep, deer, and nonhuman primates.^{22,23} In addition, the presence of infectivity in the blood of donors incubating vCJD was revealed by the transmission of the disease to three transfusion recipients.⁴ All of them received nonleukoreduced RBCs. The nature of cells associated with TSE infectivity in blood remains unclear. In rodents, infectivity seems to be concentrated in WBCs, while both PLTs and RBCs are devoid of significant infectivity.^{24,25} Interestingly, PLTs harbor infectivity in the blood of infected deer,²³ suggesting that association of prions with blood cells could be species and prion strain dependent. The expression of PrP^C may play a role in this discrepancy because rodent PLTs, in contrast to deer PLTs, do not express the protein.^{17,18} Considering the importance of PrP^C expression in many aspects of prion pathogenesis, our study was aimed at the elucidation of controversies surrounding its expression in human RBCs. PrP^C is present on CD34+ marrow stem cells, and its expression is regulated in different cell lineages.^{14,26} Griffiths and colleagues²⁷ demonstrated that PrP^C expression in cultured human erythroblasts was mostly intracellular, with faint membrane staining, and it was down regulated during their in vitro differentiation to more mature erythroid cells. This finding is compatible with the low expression of the protein on the membrane of circulating RBCs detected in our previous study.¹⁸ However, our finding was contradicted by several studies reporting no expression of PrP^C on human RBCs.¹²⁻¹⁶ Most of those studies utilized probably the best characterized prion MoAb 3F4.²⁸ The antibody was developed against hamster scrapie-associated fibrils; however, it also crossreacts with human PrP^C. The epitope of the 3F4

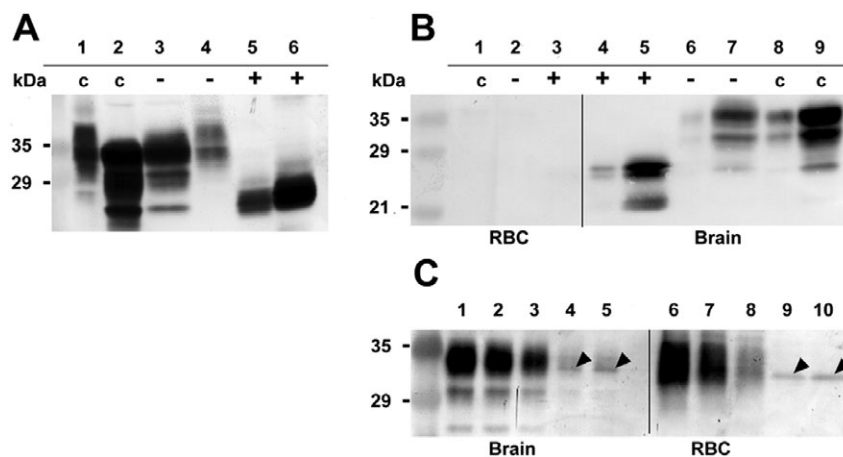


Fig. 4. Characterization of basic features of PrP^C on human RBCs. (A) WB comparison of RBCs (Lanes 1, 4, and 5) and brain (Lanes 2, 3, and 6) PrP^C demonstrate that RBC PrP^C is not significantly truncated. (c) Fresh untreated samples, (+) samples deglycosylated using incubation with PNGase F, and (-) samples incubated without PNGase F. The blot was developed with a mixture of MoAbs 6H4 and AG4. (B) Deglycosylation of RBC PrP^C does not lead to the restoration of 3F4 binding. RBC (Lanes 1-3) and brain (Lanes 4-9) samples were (c) fresh untreated, (+) treated with PNGase F, or (-) incubated without PNGase F. Samples 4, 6, and 8 are 10-fold dilutions of Samples 5, 7, and 9, respectively. The blot was developed with MoAb 3F4. (C) Brain and RBC PrP^C displayed similar sensitivity to proteolysis by increasing concentrations of PK (0, 2.5, 5, 50, and 100 μ g/mL). Lanes 1 through 5 = brain samples; Lanes 6 through 10 = RBC samples. Sharp bands (~33 kDa) in Lanes 4, 5, 9, and 10 represent a nonspecific signal of PK (arrowhead). The blot was developed with MoAb 6H4.

(KTNMKHM) is located in the central part of the molecule (PrP₁₀₆₋₁₁₂),²⁹ which is known to undergo conformational change into PrP^{TSE}, resulting in epitope inaccessibility.¹¹ To elucidate the controversies surrounding the expression of PrP^C on human RBCs, we first repeated the quantitative flow cytometry study utilizing MoAb 6H4 and two MoAbs that were used in previous negative reports: FH11 and 3F4. Indeed, both antibodies bound to RBCs substantially less than 6H4: 8.3-fold lower for FH11 and 3.6-fold lower for 3F4. This result was puzzling, especially for 3F4, as its binding to PLTs in the same tube was equivalent to 6H4. The overall lower binding of FH11 to a variety of blood cells has been previously described³⁰ and can be caused by a proteolytic loss of its epitope (PrP₅₁₋₅₅) located on the sensitive N-terminus of PrP^C.³¹ A similar mechanism could also be responsible for the lower binding of 3F4, although its epitope (PrP₁₀₆₋₁₁₂) is located close to the center of the molecule. The presence of a substantial amount of the stable C1 fragment of PrP^C lacking the 3F4 epitope has been described in the normal brain tissue of man and other mammalian species.^{32,33} In contrast, we did not find similar fragments in blots of human RBC ghosts, demonstrating that truncation was not the cause of the decreased 3F4 binding. The RBC PrP^C band had slightly lower electrophoretic mobility and was more diffuse than PrP^C in the brain. This could be caused by a different glycosylation

pattern of RBC PrP^C, which may in theory contribute to the inaccessibility of the 3F4 epitope. However, enzymatic deglycosylation of RBC PrP^C did not restore its recognition by 3F4. Considering that the binding of 3F4 is prevented by the change in the conformation of protease-resistant PrP^{TSE},¹¹ we tested the sensitivity of PrP^C on RBCs to proteolysis. However, we did not detect any protease-resistant PrP^C on RBCs. This, together with the fact that low binding of 3F4 was also recorded on blots after denaturation of proteins by boiling with SDS suggests that the low binding is not caused by the conformation of the protein. On the same basis, the hypothesis that the low binding of 3F4 is caused by the shielding effect of an unknown binding partner of PrP^C on the membrane of RBCs can be rejected. Taken together, our results suggest that the reason for decreased binding of 3F4 to RBC PrP^C is posttranslational modification of its epitope KTNMKHM. This modification is apparently introduced after the maturation and release of RBCs into circulation as CD71+ erythroid precursors in cord blood bound antibodies

3F4 and 6H4 equally well. The modification does not significantly change the electrophoretic mobility of RBC PrP^C because after its deglycosylation, it has similar mobility to deglycosylated brain PrP^C. The importance of both methionine and lysine residues in the 3F4 epitope for binding of the antibody has been previously demonstrated.^{29,34} Methionine residues in the 3F4 epitope have been shown to be sensitive to oxidation and may serve as internal antioxidants, protecting the PrP^C molecule from oxidative damage.³⁵ However, in our hands, oxidation of PrP^C with H₂O₂ did not diminish binding of 3F4 relative to 6H4, suggesting that oxidation is not the cause of the low binding of 3F4 to RBC PrP^C. In contrast, modification of lysine residues by sulfo-NHS-biotin readily led to the loss of 3F4 binding, confirming a previous report by Bolton and coworkers.³⁶ One physiologically occurring modification of lysine residues in proteins is glycation. The treatment of prion protein with GA, which modifies lysine residues to the major advanced glycation endproducts constituent CML, led to a dose-dependent decrease of 3F4 binding, while the binding of 6H4 was unaffected. The modification of membrane proteins by CML in human RBCs during their aging in circulation has been previously reported.²¹ This is in agreement with our observation that the epitope of 3F4 in erythroid precursors in cord blood as well as in PLTs in circulation is not modified. Obviously, time is needed for

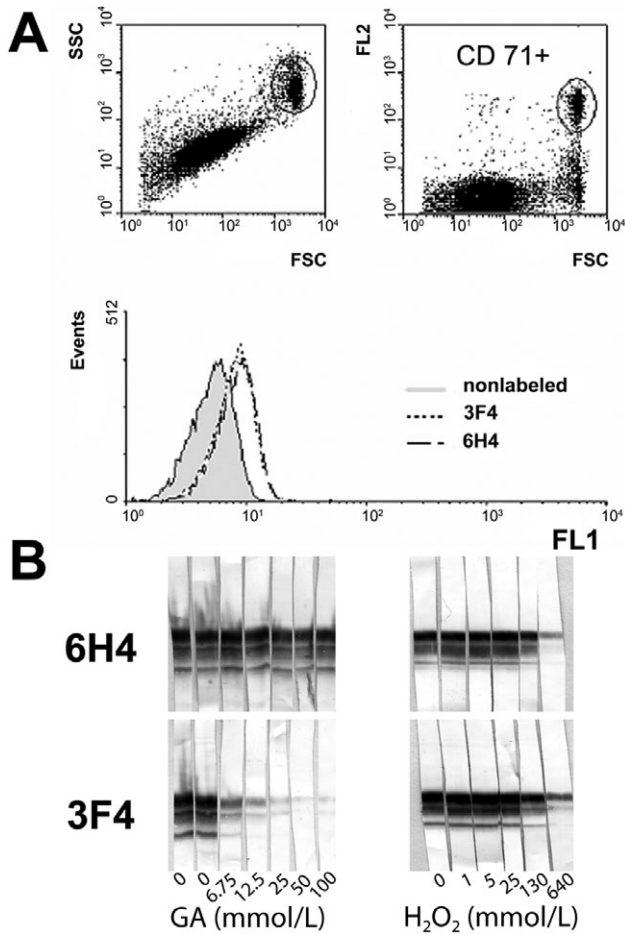


Fig. 5. Glycation of PrP^C could be the reason for diminished binding of 3F4 to human RBCs. (A) MoAbs 3F4 and 6H4 bind equally well to transferrin receptor-positive (CD71+) erythroid precursors in human cord blood. This suggests that the modification of the 3F4 epitope (KTNMKHM) occurs after the release of RBCs into circulation. Normal cord blood ($n = 3$) samples were analyzed using two-color flow cytometry. The logarithmic side scatter/forward scatter (SSC/FSC) plot shows the scatter properties of cord blood and the position of the RBC gate (top left plot). CD71+ cells were gated on a FL2/FSC logarithmic plot (top right plot) and their 3F4 and 6H4 fluorescence compared (bottom histogram overlay). (B) In vitro treatment of WBs of normal brain homogenate with increasing concentrations of GA or hydrogen peroxide (H_2O_2). Blots were developed with 6H4 (top) or 3F4 (bottom). Modification of lysine residues by GA to carboxymethyl lysine in contrast to oxidation of methionines by H_2O_2 readily mimics the discrepancy in the binding of MoAbs 3F4 and 6H4 found in vivo in human RBC PrP^C, suggesting that glycation may be the cause of the modification of its 3F4 epitope.

the modification to occur, and RBCs, with their life span reaching 120 days compared to the 10 days of PLTs, are in a better position to be modified. Interestingly, glycation of lysine residues on the N-terminal of PrP^{TSE} has already

been demonstrated in brains of TSE-infected rodents.³⁷ Despite the lack of direct proof, our data suggest that the diminished binding of 3F4 to PrP^C on RBCs may be caused by glycation. The hypothetical existence of a similar modification of blood PrP^{TSE} would prevent its detection using the conformation-dependent immunoassay¹¹ and other assays that use 3F4. In addition, it is likely that the use of the 3F4 antibody was the reason for the underestimation of the overall amount of the PrP^C pool associated with human RBCs in some previous studies. All three methods employed in our study to estimate the amount of PrP^C in RBCs relative to PLTs gave convergent results. Using quantitative flow cytometry, approximately 300 IgG molecules of antibody 6H4 bound to one RBC, while the binding to resting PLTs in identical samples was only twice as high. We have previously estimated that approximately 70% of PrP^C is localized inside of resting PLTs.³⁸ This suggests that the amount of PrP^C per PLT, including its intracellular pool, is roughly sevenfold higher than in one RBC. Conformation-independent WB analysis of PrP^C levels in carefully isolated PLTs and RBC ghosts indicated that the amount of PrP^C per PLT is just fourfold higher than in one RBC. An even lower difference was detected using sandwich ELISA. Taken together, our data demonstrate that the difference in the level of PrP^C between one PLT and one RBC is less than 10-fold, while the normal amount of RBCs (5×10^9 /mL) in man is about 20-fold higher than the amount of PLTs (2.5×10^8 /mL). This result implies that RBCs should carry at least twice as much PrP^C than PLTs, which makes RBCs the main source of cell-associated PrP^C in human blood. Previous studies have described the release of up to 45% of PLT PrP^C after in vitro activation of PLTs by agonists or during the 5-day storage of PLT concentrates.^{39,40} Although we deem it unlikely, we cannot exclude that some release of PrP^C also occurred during the isolation of PLTs used in our WB and ELISA studies. However, even if we underestimated the physiological amount of PLT PrP^C by approximately 50%, the overall amount of PrP^C associated with RBCs would still surpass the PrP^C PLT pool.

Despite this observation, RBCs remain an unlikely source of prions in blood because they do not have the ability to supplement their propagation with new molecules of PrP^C. However, the existence of posttranslational modification in the critical part of the molecule may give RBC PrP^C unique properties and favor their binding of prions released to blood by other cells. Further studies aimed on the molecular characterization of this modification and its influence on the interaction of PrP^C with prion particles should clarify if our current view neglects the role of RBCs in the blood pathogenesis of prion diseases.

ACKNOWLEDGMENTS

We acknowledge the TSE Resource Centre (The Roslin Institute, University of Edinburgh) for the donation of antibodies FH11,


AG4, AH6, and GE8 and Prof. Kurt Wüthrich (Institute of Molecular Biology and Biophysics, ETH Zurich) for the donation of the pRSET-A-(hrPrP) plasmid.

CONFLICT OF INTEREST

The authors declare no conflict of interest.

REFERENCES

1. Prusiner SB. Prions. *Proc Natl Acad Sci U S A* 1998;95:13363-83.
2. Brown P, Preece M, Brandel JP, Sato T, McShane L, Zerr I, Fletcher A, Will RG, Pocchiari M, Cashman NR, d'Aignaux JH, Cervenakova L, Fradkin J, Schonberger LB, Collins SJ. Iatrogenic Creutzfeldt-Jakob disease at the millennium. *Neurology* 2000;55:1075-81.
3. Llewelyn CA, Hewitt PE, Knight RS, Amar K, Cousens S, Mackenzie J, Will RG. Possible transmission of variant Creutzfeldt-Jakob disease by blood transfusion. *Lancet* 2004;363:417-21.
4. Gillies M, Chohan G, Llewelyn CA, MacKenzie J, Ward HJ, Hewitt PE, Will RG. A retrospective case note review of deceased recipients of vCJD-implicated blood transfusions. *Vox Sang* 2009;97:211-8.
5. Peden A, McCardle L, Head MW, Love S, Ward HJ, Cousens SN, Keeling DM, Millar CM, Hill FG, Ironside JW. Variant CJD infection in the spleen of a neurologically asymptomatic UK adult patient with haemophilia. *Haemophilia* 2010;16:296-304.
6. Hilton DA, Ghani AC, Conyers L, Edwards P, McCardle L, Ritchie D, Penney M, Hegazy D, Ironside JW. Prevalence of lymphoreticular prion protein accumulation in UK tissue samples. *J Pathol* 2004;203:733-9.
7. Lefrere JJ, Hewitt P. From mad cows to sensible blood transfusion: the risk of prion transmission by labile blood components in the United Kingdom and in France. *Transfusion* 2009;49:797-812.
8. Turner ML, Ludlam CA. An update on the assessment and management of the risk of transmission of variant Creutzfeldt-Jakob disease by blood and plasma products. *Br J Haematol* 2009;144:14-23.
9. Dodd RY. Prions and precautions: be careful for what you ask. *Transfusion* 2010;50:956-8.
10. Tattum MH, Jones S, Pal S, Collinge J, Jackson GS. Discrimination between prion-infected and normal blood samples by protein misfolding cyclic amplification. *Transfusion* 2010;50:996-1002.
11. Safar J, Wille H, Itri V, Groth D, Serban H, Torchia M, Cohen FE, Prusiner SB. Eight prion strains have PrP(Sc) molecules with different conformations. *Nat Med* 1998;4:1157-65.
12. Barclay GR, Hope J, Birkett CR, Turner ML. Distribution of cell-associated prion protein in normal adult blood determined by flow cytometry. *Br J Haematol* 1999;107:804-14.
13. MacGregor I, Hope J, Barnard G, Kirby L, Drummond O, Pepper D, Hornsey V, Barclay R, Bessos H, Turner M, Prowse C. Application of a time-resolved fluoroimmunoassay for the analysis of normal prion protein in human blood and its components. *Vox Sang* 1999;77:88-96.
14. Dodelet VC, Cashman NR. Prion protein expression in human leukocyte differentiation. *Blood* 1998;91:1556-61.
15. Antoine N, Cesbron JY, Coumans B, Jolois O, Zorzi W, Heinen E. Differential expression of cellular prion protein on human blood and tonsil lymphocytes. *Haematologica* 2000;85:475-80.
16. Li R, Liu D, Zanusso G, Liu T, Fayen JD, Huang JH, Petersen RB, Gambetti P, Sy MS. The expression and potential function of cellular prion protein in human lymphocytes. *Cell Immunol* 2001;207:49-58.
17. Barclay GR, Houston EF, Halliday SI, Farquhar CF, Turner ML. Comparative analysis of normal prion protein expression on human, rodent, and ruminant blood cells by using a panel of prion antibodies. *Transfusion* 2002;42:517-26.
18. Holada K, Vostal JG. Different levels of prion protein (PrPc) expression on hamster, mouse and human blood cells. *Br J Haematol* 2000;110:472-80.
19. Anstee DJ. Prion protein and the red cell. *Curr Opin Hematol* 2007;14:210-4.
20. Pavlicek A, Bednarova L, Holada K. Production, purification and oxidative folding of the mouse recombinant prion protein. *Folia Microbiol (Praha)* 2007;52:391-7.
21. Ando K, Beppu M, Kikugawa K, Nagai R, Horiuchi S. Membrane proteins of human erythrocytes are modified by advanced glycation end products during aging in the circulation. *Biochem Biophys Res Commun* 1999;258:123-7.
22. Brown P. Blood infectivity, processing and screening tests in transmissible spongiform encephalopathy. *Vox Sang* 2005;89:63-70.
23. Mathiason CK, Hayes-Klug J, Hays SA, Powers J, Osborn DA, Dahmes SJ, Miller KV, Warren RJ, Mason GL, Telling GC, Young AJ, Hoover EA. B cells and platelets harbor prion infectivity in the blood of deer infected with chronic wasting disease. *J Virol* 2010;84:5097-107.
24. Cervenakova L, Yakovleva O, McKenzie C, Kolchinsky S, McShane L, Drohan WN, Brown P. Similar levels of infectivity in the blood of mice infected with human-derived vCJD and GSS strains of transmissible spongiform encephalopathy. *Transfusion* 2003;43:1687-94.
25. Holada K, Vostal JG, Theisen PW, MacAuley C, Gregori L, Rohwer RG. Scrapie infectivity in hamster blood is not associated with platelets. *J Virol* 2002;76:4649-50.
26. Risitano AM, Holada K, Chen G, Simak J, Vostal JG, Young NS, Maciejewski JP. CD34+ cells from paroxysmal nocturnal hemoglobinuria (PNH) patients are deficient in surface expression of cellular prion protein (PrPc). *Exp Hematol* 2003;31:65-72.
27. Griffiths RE, Heesom KJ, Anstee DJ. Normal prion protein trafficking in cultured human erythroblasts. *Blood* 2007;110:4518-25.

28. Kascsak RJ, Rubenstein R, Merz PA, Tonna-DeMasi M, Fersko R, Carp RI, Wisniewski HM, Diringer H. Mouse polyclonal and monoclonal antibody to scrapie-associated fibril proteins. *J Virol* 1987;61:3688-93.
29. Lund C, Olsen CM, Tveit H, Tranulis MA. Characterization of the prion protein 3F4 epitope and its use as a molecular tag. *J Neurosci Methods* 2007;165:183-90.
30. Holada K, Simak J, Brown P, Vostal JG. Divergent expression of cellular prion protein on blood cells of human and nonhuman primates. *Transfusion* 2007;47:2223-32.
31. Leclerc E, Peretz D, Ball H, Solfrosi L, Legname G, Safar J, Serban A, Prusiner SB, Burton DR, Williamson RA. Conformation of PrP(C) on the cell surface as probed by antibodies. *J Mol Biol* 2003;326:475-83.
32. Chen SG, Teplow DB, Parchi P, Teller JK, Gambetti P, Autilio-Gambetti L. Truncated forms of the human prion protein in normal brain and in prion diseases. *J Biol Chem* 1995;270:19173-80.
33. Laffont-Proust I, Hassig R, Haik S, Simon S, Grassi J, Fonta C, Faucheux BA, Moya KL. Truncated PrP(c) in mammalian brain: interspecies variation and location in membrane rafts. *Biol Chem* 2006;387:297-300.
34. Rubenstein R, Kascsak RJ, Papini M, Kascsak R, Carp RI, LaFauci G, Meloen R, Langeveld J. Immune surveillance and antigen conformation determines humoral immune response to the prion protein immunogen. *J Neurovirol* 1999;5:401-13.
35. Requena JR, Dimitrova MN, Legname G, Teijeira S, Prusiner SB, Levine RL. Oxidation of methionine residues in the prion protein by hydrogen peroxide. *Arch Biochem Biophys* 2004;432:188-95.
36. Bolton DC, Seligman SJ, Bablanian G, Windsor D, Scala LJ, Kim KS, Chen CM, Kascsak RJ, Bendheim PE. Molecular location of a species-specific epitope on the hamster scrapie agent protein. *J Virol* 1991;65:3667-75.
37. Choi YG, Kim JI, Jeon YC, Park SJ, Choi EK, Rubenstein R, Kascsak RJ, Carp RI, Kim YS. Nonenzymatic glycation at the N terminus of pathogenic prion protein in transmissible spongiform encephalopathies. *J Biol Chem* 2004;279:30402-9.
38. Holada K, Glierova H, Simak J, Vostal JG. Expression of cellular prion protein on platelets from patients with gray platelet or Hermansky-Pudlak syndrome and the protein's association with alpha-granules. *Haematologica* 2006;91:1126-9.
39. Bessos H, Drummond O, Prowse C, Turner M, MacGregor I. The release of prion protein from platelets during storage of apheresis platelets. *Transfusion* 2001;41:61-6.
40. Robertson C, Booth SA, Beniac DR, Coulthart MB, Booth TF, McNicol A. Cellular prion protein is released on exosomes from activated platelets. *Blood* 2006;107:3907-11. 

Expression of Prion Protein in Mouse Erythroid Progenitors and Differentiating Murine Erythroleukemia Cells

Martin Panigaj, Hana Glierova, Karel Holada*

Institute of Immunology and Microbiology, First Faculty of Medicine, Charles University in Prague, Prague, Czech Republic

* Corresponding author:

Karel Holada, Ph.D., Institute of Immunology and Microbiology, First Faculty of Medicine, Charles University in Prague, Studnickova 7, 128 20 Prague 2, Czech Republic.

Tel./Fax.: +420 22496 8503 / +420 22496 8496

E-mail: Karel.Holada@LF1.cuni.cz

Abstract

Prion diseases have been observed to deregulate the transcription of erythroid genes, and prion protein knockout mice have demonstrated a diminished response to experimental anemia. To investigate the role of the cellular prion protein (PrP^C) in erythropoiesis, we studied the protein's expression on mouse erythroid precursors *in vivo* and utilized an *in vitro* model of the erythroid differentiation of murine erythroleukemia cells (MEL) to evaluate the effect of silencing PrP^C through RNA interference.

The expression of PrP^C and selected differentiation markers was analyzed by quantitative multicolor flow cytometry, western blot analysis and quantitative RT-PCR. The silencing of PrP^C expression in MEL cells was achieved by expression of shRNAmir from an integrated retroviral vector genome. The initial upregulation of PrP^C expression in differentiating erythroid precursors was detected both *in vivo* and *in vitro*, suggesting PrP^C's importance to the early stages of differentiation. The upregulation was highest on early erythroblasts (16200 ± 3700 PrP^C / cell) and was followed by the gradual decrease of PrP^C level with the precursor's maturation reaching 470 ± 230 PrP^C / cell on most mature CD71⁻Ter119⁺ small precursors. Interestingly, the downregulation of PrP^C protein with maturation of MEL cells was not accompanied by the decrease of PrP mRNA. The stable expression of anti-Prnp shRNAmir in MEL cells led to the efficient (>80%) silencing of PrP^C levels. Cell growth, viability, hemoglobin production and the transcription of selected differentiation markers were not affected by the downregulation of PrP^C.

In conclusion, the regulation of PrP^C expression in differentiating MEL cells mimics the pattern detected on mouse erythroid precursors *in vivo*. Decrease of PrP^C protein expression during MEL cell maturation is not regulated on transcriptional level. The efficient silencing of PrP^C levels, despite not affecting MEL cell differentiation, enables created MEL lines to be used for studies of PrP^C cellular function.

Introduction

The cellular prion protein (PrP^C) is expressed in cells of various origins. It is conserved through the whole vertebrate class, suggesting its importance in cellular physiology [1]. However, its role in physiological processes remains enigmatic although PrP^C plays a basic role in the pathogenesis of the fatal neurodegenerative disorders known as Transmissible Spongiform Encephalopathies. Observation of PrP^C deficient mice (PrP^{-/-}) did not reveal significant health problems. On the other hand, experiments in cell cultures suggested that PrP^C is linked to such processes as the prevention of apoptosis, copper metabolism linked to oxidative stress, iron metabolism, signalization and differentiation [2,3,4]. A connection between prion pathogenesis and erythropoiesis was suggested by the downregulation of the α -hemoglobin stabilizing protein (AHSP) mRNA during prion disease [5]. A later study indicated that the disease progression affected the transcription of several other murine erythroid genes, e.g., Kell, GPA, band 3 and ankyrin [6]. A link between PrP^C expression and erythropoiesis was also demonstrated in PrP^{-/-} mice after the experimental induction of hemolytic anemia. Upon treatment with phenylhydrazine, PrP^{-/-} mice produced fewer reticulocytes than did PrP^{+/+} mice. This result was probably due to the reduced level of erythropoietin production and higher percentage of apoptotic erythroid precursors [7]. Apparently, the expression of PrP^C is generally important in hematopoiesis. PrP^C is present on the surface of mouse long-term hematopoietic stem cells (LT-HSCs) and supports their self-renewal and engraftment during serial transplantation. Quantitatively, 40% of mouse bone marrow (BM) cells express PrP^C, and, from this population of cells, 80% are erythroid cells [8]. CD34⁺ human bone marrow stem cells also express PrP^C [9,10], and circulating human and mouse red blood cells have similarly low levels of PrP^C on their cellular membranes [11,12]. A widely used model for the study of erythroid differentiation *in vitro* is presented by murine erythroleukemia (MEL) cells. MEL cells are blocked at the proliferative proerythroblast stage, and, after the addition of polar substances, e.g., hexamethylene bisacetamide (HMBAA), they lose their proliferative capacity and enter cell-cycle arrest. This process is characterized by structural (decreased cell volume and nuclear condensation) and biochemical changes (activation of erythroid genes, hemoglobin accumulation), which resemble those exhibited by natural erythroid differentiation [13]. Gougoumas and colleagues demonstrated transcriptional activation at the mRNA level of the PrP gene in growth-arrested MEL cells [14]. Our study extends their observations by demonstrating divergences in the regulation of PrP^C at the protein and mRNA levels during inducer-mediated erythroid differentiation and cell-growth arrest caused by confluency. In

addition, we exploited MEL cell lines with stably downregulated levels of PrP^C to study its importance in the differentiation of MEL cells.

Results

Regulation of PrP^C expression on mouse bone marrow and spleen erythroid precursors

Erythroid precursors were gated according their Ter119 and CD71 signals and the forward scatter (FSC) signals to the proE, EryA, EryB and EryC subpopulations (Fig. 1 A). CD71⁺Ter119^{+/+} bone marrow proerythroblasts (proE) expressed 7800 ± 3100 PrP^C molecules / cell, assuming that one molecule of mAb AH6 binds one molecule of PrP^C. The expression of CD71⁺Ter119⁺ basophilic erythroblasts (EryA) was elevated to 16200 ± 3700 PrP^C / cell and decreased in late basophilic and polychromatic erythroblasts (EryB) to 5100 ± 1100 PrP^C / cell and was also diminished in late CD71⁻Ter119⁺ small precursors (EryC) (470 ± 230 PrP^C / cell). Corresponding erythroid precursors in the spleen expressed 4200 ± 600 , 13400 ± 5200 , 4600 ± 1400 and 680 ± 280 PrP^C / cell, respectively (Fig. 1 B).

Regulation of PrP^C expression during the erythroid differentiation of MEL cells

MEL cells were grown for five days in the absence or presence of 5 mM HMBA. The cells increased their expression of Prnp mRNA, reaching 13 ± 1.2 -fold and 8.7 ± 2.8 -fold relative expression after 120 hours in uninduced and differentiating cells, respectively (Fig. 2 A and B). While the level of PrP mRNA in the differentiating cells more than doubled within 24 h after induction, a similar increase in the uninduced cells was observed after 48 h in culture when cells were reaching confluency. At the protein level, the uninduced cells increased their PrP^C, reaching a maximum expression in confluent culture at 96 - 120 h (Fig. 2C) which correlated with the expression of Prnp mRNA. In contrast, the expression of the PrP^C protein in differentiating cells peaked at 24 - 48 h post-induction (Fig. 2D) with a subsequent decrease to almost its basal level at 120 h, as demonstrated by densitometry (Fig. 2F). The increased density of the PrP^C band on the WB was already visible within 6 h post-induction (not shown). These results were confirmed by quantitative FACS analysis, which demonstrated approximately twofold increase of PrP^C membrane expression after 24 h of differentiation, with a subsequent return to the basal level after 96 h (Fig. 1E).

Dexamethasone treatment of MEL cells lowers their expression of PrP^C in confluent culture irrespective of production of hemoglobin

Treatment of uninduced MEL cells with 4 μ M dexamethasone (DEX) partially prevented the increase of PrP^C levels after 120 h in confluent culture (Fig. 3 A). The intensity of the PrP^C band in DEX-treated cells was similar to that of HMBA-stimulated, fully hemoglobinized cells. Stimulation of cells with HMBA for 12 h was not sufficient to induce their effective hemoglobinization and led to high levels of PrP^C in confluent culture after 120 h. After 12 h with HMBA, cells were transferred to medium with DEX, and the increase of PrP^C levels at 120 h was inhibited. The stimulation of cells with HMBA in the presence of DEX led to a partial decrease in hemoglobinization and intermediate levels of PrP^C at 120 h. A slight increase in PrP^C levels after 24 h was detected in all treatments in which HMBA was present during the first 12 h and the second 12 h of incubation, irrespective of the presence or absence of DEX (Fig. 3 A). In the second approach, the cells were stimulated with HMBA or HMBA/and DEX for 24 h and then transferred to fresh medium with or without HMBA or DEX (Fig. 3 B). Again, the presence of DEX during first 24 h of cellular stimulation with HMBA did not change the levels of PrP^C after 24 h, even when a concentration of 40 μ M was used (not shown). However, the presence of DEX led to a marked decrease of PrP^C levels after 120 h in comparison with cells cultivated without DEX, although the hemoglobinization of cells was similar. The expression of PrP^C was comparable with that of fully hemoglobinized HMBA-stimulated cells (Fig. 3 B). The detected changes in the levels of PrP^C were not caused by differences in loading, as demonstrated by actin labeling.

Retroviral vector delivery of anti-Prnp shRNAmir leads to stable and efficient PrP^C silencing

Both spinfection and co-cultivation methods led to efficient (~ 90%) silencing of PrP^C at the mRNA (Fig. 4 A) and protein levels (Fig. 4 B) by LP1 and LP2 constructs in comparison with control construct LN. The LP5 construct did not produce any downregulation of PrP^C levels (Fig. 4 B). Retroviral infection of cells did not induce cell-protective effects, as demonstrated by qRT-PCR analysis of chosen interferon-stimulating genes *Oas1a*, *Rnase1* and *Eif2ak2* (not shown). The silencing of PrP^C in LP1 and LP2 lines was stable during the course of HMBA-induced cell differentiation (Fig 5). In comparison with LN, LP1- and LP2-transduced cells exhibited 79% and 84% inhibition of Prnp mRNA expression at the beginning of differentiation and 93% and 96% after 120 h of differentiation, respectively (Fig. 5 A). The

levels of Prnp mRNA and protein during differentiation of the control LN-transduced cells (Fig. 5 A, C) was upregulated similarly as in non-manipulated MEL cells (Fig. 2 B, D). The stability of PrP^C silencing was confirmed by quantitative FACS analysis, which demonstrated downregulation of PrP^C at the cell membrane ranging from 17% (LP1) and 12% (LP2) to 8% (LP1) and 5% (LP2) of its expression (100%) in LN-transduced cells at the beginning of differentiation and after 48 h, respectively (Fig. 5 B). These results were confirmed by western blot analysis in which we could faintly detect PrP^C in LP1 and LP2 cells only after 24 hours, while the protein in LN-transduced cells was readily detected (Fig. 5 C).

Silencing of the Prnp gene by RNAi does not affect HMBA-induced differentiation of MEL cells

Cell numbers in differentiating LN and LP1 lines increased similarly, reaching 2.4×10^6 cells/mL at 72 h. The LP2-transduced cell line produced slightly more cells, with a maximum of 3.0×10^6 cells/mL at 72 h (Fig. 6A). In a Trypan Blue exclusion assay, all cell lines demonstrated a similar viability (~94%) over a 72-h post-induction period and, also, a similar slight decrease of viability after 96 and 120 h (Fig. 6 B). We did not detect any differences in the transcriptional levels of proapoptotic Bax (not shown). The dynamic of hemoglobin production was comparable in all cell lines, irrespective of the level of PrP^C (Fig. 6 C). Similarly, surface expression of the transferrin receptor (CD71) was similarly regulated in all cell lines (Fig. 6 D). Also, no difference was demonstrated in the levels of c-myb mRNA, which were downregulated approximately eightfold after 24 h post-induction in all lines. After 48 h, c-myb mRNA was downregulated to ~ 2% of the starting level and remained silenced until the end of the experiment (not shown). Similarly, monitoring of the erythroid markers Eraf and Hba (Fig. 7A and B) and GATA-1 (not shown) during the differentiation of cells at the transcriptional level indicated analogous expression in all lines, irrespective of PrP^C levels.

Discussion

The role of PrP^C in cellular physiology has been proposed for a variety of processes, but with no prevailing consensus to date [1]. The downregulation of erythroid genes during prion infection has established a link between the peripheral pathogenesis of prion diseases and erythropoiesis. However, it is not clear if the effect is caused by direct interaction of prion particles with erythroid cells or if it is triggered by some yet unknown humoral response to the infection. The expression of PrP^C on circulating red blood cells (RBCs) of closely related nonhuman primates varies from several thousand per cell to zero [15], implying that its function on mature erythrocytes is not conserved. Griffiths et al. demonstrated the regulation of PrP^C expression during the differentiation of cultured human erythroblasts *in vitro*, indicating that it may play a role in the differentiation of erythroid precursors. PrP^C was found mostly in the perinuclear region of proerythroblasts, and the amount of PrP^C declined as erythroid cells matured [16]. Human and mouse RBCs express approximately 200 PrP^C molecules per cell [11], suggesting a similar regulation of its expression in the erythroid lineage in both species. In this study, we demonstrated that the surface expression of PrP^C on erythroid precursors in the mouse bone marrow and spleen follows a similar pattern as the cells mature. The protein's levels first increase with basophilic erythroblasts, expressing more than twice as much PrP^C as proerythroblasts, and then declines significantly in late basophilic and polychromatic erythroblasts, with most mature small erythroid precursors expressing only around 500 PrP^C molecules per cell. This pattern of expression is suggestive of PrP^C's involvement in the early stages of erythroid differentiation. The differentiation of MEL cells in culture is known to resemble the *in vivo* process, with similar maturation stages: proerythroblast-like, erythroblasts-like and, occasionally, reticulocyte-like [16,17]. The surface expression of PrP^C on uninduced MEL cells in the exponential phase of growth was approximately six times higher than that observed on proerythroblasts in the mouse bone marrow or spleen. However, the induction of differentiation led to nearly doubling of the PrP^C number on MEL cell membranes within 24 h, which resembled a similar increase of PrP^C expression on basophilic erythroblasts *in vivo*. In agreement with previous observations *in vivo*, we found that this initial upregulation was followed by a gradual downregulation of PrP^C surface levels along with the progression of MEL cells' differentiation. This decrease did not reach the degree observed in small CD71⁻ Ter119⁺ erythroid precursors *in vivo*, which is in line with the limited ability of differentiating MEL cells to reach this stage of maturation. The differentiation of MEL cells is composed of two separate events, growth arrest and terminal differentiation. Both processes are

characterized by the activation of early (cell-cycle control) and late (morphological changes) genes [17]. The first period lasts approximately 12 hours, after which the first committed cells materialize. The majority of cells are terminally differentiated between 24 and 50 h [18]. In agreement with previous studies by Gougomas et al. [14], we found that the *Prnp* gene in MEL cells is transcriptionally activated both during inducer-mediated differentiation and in confluent cells undergoing cell-cycle arrest. In addition, we were able to demonstrate the regulation of PrP^C at the protein level by western blot. Interestingly and in accordance with the flow cytometry results, in differentiating cells, the expression of the protein was downregulated after an initial increase, even though the level of PrP mRNA continued to rise. This result suggests that MEL cells' differentiation leads to a translational regulation of PrP^C levels [19] not seen in uninduced cells undergoing cell-cycle arrest. Alternatively, more differentiated cells could degrade PrP^C at an increased rate, as has been proposed to explain the disparity between PrP protein and mRNA levels in different types of neuronal cells [20]. The downregulation of PrP^C protein during the differentiation of highly responsive subclones of MEL cells was recently reported by Otsuka et al. [21]; however, their study did not detect an initial increase of PrP^C expression, most likely due to the different status of cells at the point of induction. Stimulation of the glucocorticoid receptor by DEX induces the proliferation and expansion of erythroid progenitors and delays the terminal differentiation of erythrocytes [22]. In our hands, DEX did not prevent the HMBA-induced initial upregulation of PrP^C in MEL cells, suggesting that it precedes the effect of DEX, which is known to suppress the HMBA-mediated commitment to terminal cell division at a relatively late step in this process [23]. However, DEX prevented the increase of PrP^C protein levels in confluent MEL cells after 120 h of culture, demonstrating that the activation of the glucocorticoid receptor can interfere with the transcriptional activation of the *Prnp* gene mediated by cell-cycle arrest. The mechanism of DEX's action on the prevention PrP^C protein upregulation in confluent MEL cells is unknown at present. DEX has been shown to induce cell-cycle arrest in number of various cell lines [24], but not in MEL cells, in which it increases cell viability [25], both in induced and uninduced culture. In summary, our results demonstrate that the regulation of PrP^C levels in differentiating MEL cells resembles, at least in part, its regulation in maturing mouse erythroid precursors *in vivo*. To learn more about the importance of PrP^C in the process of MEL cells' differentiation, we created cell lines using RNAi to stably inhibit expression of the protein. RNAi administered by shRNA from a retrovector had previously been employed efficiently to inhibit PrP^C expression *in vitro* and *in vivo* [26,27]. The main objective for using RNAi to suppress PrP^C was to study its therapeutic potential in preventing propagation of infectious prions. To the best of our knowledge, our

model is the first murine cell line of non-neuronal origin with stably silenced PrP^C expression. Inhibition of the protein's expression at both the mRNA and protein levels was efficiently maintained during the differentiation of MEL cells, although it varied between 75 and 95% in individual time points. Despite the silencing, the induction of differentiation led to a detectable increase of PrP^C signal on blots after 24 h, suggesting that the regulation of the protein's expression in LP1- and LP2-transduced cell lines follows similar pattern as in unmodified MEL cells, although at a suppressed level. Growth curve and viability of LP1-, LP2- and control LN-transduced cell lines after the induction of differentiation was similar, although the LP2-transduced cell line exhibited a higher proliferation capacity. Since the LP1-transduced cell line did not differ from control LN-transduced cell line, we could not assign the LP2-transduced cell line's divergence solely to PrP^C silencing. All cell lines observed here demonstrated similar dynamics and level of hemoglobinization and regulation of the transferrin receptor on their cell membranes. This finding suggested that silencing of PrP^C in MEL cells does not lead to gross perturbation of iron homeostasis, although the involvement of PrP^C in iron-cell uptake was described recently [28,29]. Similarly, the level of the protooncogene c-myc, expression of which is characteristic of the proliferative state and has been demonstrated to block MEL cells' differentiation [30,31], decreased upon induction similarly in all created cell lines and remained low during the entire course of the experiment. Monitoring of selected erythroid markers (AHSP, Hba and GATA-1) on the transcriptional level also did not reveal significant differences among LP1-transduced, LP2-transduced and LN-transduced cell lines, confirming that PrP^C silencing does not appear disturb the differentiation of MEL cells. In many cell cultures, the enhanced expression of PrP^C was proposed to facilitate cytoprotective effects [32]. However, overexpression of exogenously delivered PrP^C in MEL cells did not protect the cells against apoptosis initiated by serum withdrawal [33]. We also found that silencing of PrP^C did not seem to sensitize cells to apoptosis during differentiation, as demonstrated by a Trypan Blue exclusion assay and by monitoring of Bax expression by qRT-PCR. This result is concurrent with Christensen and Harris, who reevaluated former assays reporting a protective activity of PrP^C and suggested that the presence of PrP^C has only a modest effect in cytoprotection *in vitro* [34].

Taken together, our results imply that, under normal conditions, PrP^C seems dispensable for the erythroid differentiation of MEL cells. The pattern of PrP^C regulation on erythroid precursors *in vivo* suggests that PrP^C may play a role in the maturation of erythroblasts in erythroblastic islands. We can speculate that PrP^C, which was shown to bind both laminin and the laminin

receptor [35,36], can be involved in cell-cell contacts in an erythroblastic niche, or with a surrounding extracellular matrix. Downregulation of PrP^C, then, could play a role in the dissociation of matured reticulocytes from the erythroblastic niche. Such a role for PrP^C is unlikely to be detected by the MEL cell model. Another explanation could be that PrP^C exerts its function only under stress conditions. This hypothesis is consistent with the documented poor recovery of PrP^{-/-} mice from experimental anemia [7]. Finally, it is possible that the effect of PrP^C silencing was compensated for by an unknown pathway or that the remaining expression is sufficient to sustain its role.

In conclusion, we created model cell lines with efficiently silenced expression of PrP^C, which are the first of their kind and may serve in subsequent searches for the physiological function of PrP^C and could be utilized as a valuable tool in studies of the connection between prion pathogenesis and the downregulation of erythroid genes.

Materials and Methods

Flow cytometry of mouse bone marrow and spleen erythroid precursors

The study was approved by the Committee on the Ethics of Animal Experiments of the First Faculty of Medicine, Charles University in Prague (Permit Number: 217/07). Bone marrow (BM) cells were isolated from the femurs of PrP^{+/+} mice (C57BL/6x129/SvxCD1 mixed background) by washing with PBS, 1% BSA and 2 mM EDTA, pH 7.4 (PBS-BE). Spleen and BM cells were passed through a 40- μ m cell strainer (Becton Dickinson, San Diego, CA, USA) to eliminate stroma and debris. The cells were labeled (30 min, 4° C) with saturating concentration of monoclonal antibodies (mAbs): anti-mouse Ter-119 eFluor 450, anti-mouse CD71-FITC (both eBioscience, San Diego, CA, USA) and AH6 (TSE Resource Center, Roslin, UK), custom conjugated to PE (Exbio, Vestec, Czech Republic). Labeled cells were washed and resuspended in PBS-BE, and their fluorescence was analyzed on a BD FACSCanto II flow cytometer equipped with BD FACSDiva Software v6.0 (Becton Dickinson). Dead cells were excluded from the analysis by 7-aminoactinomycin D (7-AAD) (Molecular Probes, Eugene, OR, USA) labeling, and the fluorescence of live cells (10^5) was analyzed. Erythroblast subpopulations were resolved according Ter119, CD71 and forward-scatter (FSC) signals. Proerythroblasts (proE) were identified as Ter119^{medium} CD71⁺ cells. Ter119^{high} cells were divided using both the CD71 and FSC parameters into three populations, labeled EryA, EryB and EryC, as described previously [37], and the binding of the prion mAb AH6 was quantified using Standard Quantum R-PE MESF beads (Bangs Laboratories, Fishers, IN, USA) [15].

Flow cytometry of cell cultures

Cells were washed with 1% BSA-PBS, pH 7.4 (PBS-B) and labeled for 20 min at RT with saturating concentrations of the AH6-PE or anti-mouse CD71-PE (eBioscience) mAbs. Next, washed cells were resuspended in PBS-B and analyzed using a flow cytometer to standardize the fluorescence readings and to allow for the quantification of PrP^C and CD71 expression. Standard Quantum R-PE MESF beads were run as a separate sample. Viable cells were identified as a 7-AAD-negative population.

Cell cultures

The MEL cell line (clone 707, ECACC, Salisbury, UK) and packaging cell line HEK293 GP2 (Clontech, Mountain View, CA USA) were maintained in DMEM growth medium containing high glucose (4.5 g/L), L- glutamine, sodium pyruvate, 10% fetal bovine serum and puromycin/ streptomycin (all reagents from PAA, Pasching, Austria). Cells were cultured at 37 °C in a humidified atmosphere containing 5% CO₂. For all experiments, MEL cells between the second and fourth passages were seeded at a density of 10⁵ cells/mL 24 h before induction of differentiation by 5 mM HMBA (final concentration). In some instances, 4 μM dexamethasone (DEX) (Sigma-Aldrich, Prague, Czech Republic) was used to block the commitment of MEL cells. The cells were incubated with either HMBA, HMBA and DEX or DEX alone for 12 h or 24 h, and then the medium was changed, and the cells were grown in the presence of either HMBA, DEX, HMBA and DEX, or in medium only.

Cloning

For the silencing of cellular prion expression, we used shRNAmir sequences HP_285770 (LP1) and HP_288208 (LP2), which are available in the RNAi codex database (<http://cancan.cshl.edu/cgi-bin/Codex/Codex.cgi>). The shRNAs, together with the control nonsilencing shRNAmir (LN), were ordered in the pSM2 retro vectors V2MM_66187, V2MM_63696 and RHS1707 (Open Biosystems, Huntsville, AL, USA)[38]. The third anti-Prnp mRNA sequence (LP5), adopted from Pfeifer et al., was purchased as an oligonucleotide [27]. All sequences were cloned into the LMP retrovector MSCV/LTRmiR30-PIG (Open Biosystems). Constructs created in this study were verified by sequencing.

RNAi of Prnp expression

Packaging HEK293 GP2 cells were seeded at a density of approximately 1.5x 10⁵ cells/well (24-well plate). After 24 h, the cells were transfected with a mixture of the VSV-G plasmid, coding the envelope protein of the vesicular stomatitis virus (Clontech), and the appropriate LMP retrovector (LN, LP1, LP2 or LP5). Plasmids were delivered in a ratio of 9:1 with the Arrest-in transfection agent (Open Biosystems). Three days after transfection, media containing retroviral particles were centrifuged (400 g, 4 °C) to pellet eventual cell contaminants, and the

infectious supernatant, containing 4 µg/mL Polybrene (Sigma-Aldrich), was added to MEL cells in a 1:1 ratio. Subsequently, transduced MEL cells were spun down at 450 g for 90 min at RT (a method known as spinfection). In a second approach, the MEL cells were infected by co-cultivation with a packaging cell line. In this method, medium in HEK293 GP2 cells was aspirated 24 h postinfection, and 2×10^4 MEL cells/well were added inside the 0.4-µm-pore translucent polyphthalate insert (Becton Dickinson) in a 0.7 mL total volume of fresh media containing 4 µg/mL Polybrene. After 48 (co-cultivation) or after 72 (spinfection) hours of incubation, the cells were diluted with fresh medium, and selection started the next day through the addition of puromycin (Sigma) at a final concentration of 0.5 µg/mL. The percentage of cells with an integrated retrovector genome was monitored by FACS utilizing eGFP positivity. Cell lines prepared by both methods were mixed after three weeks after reaching >95% eGFP positivity and were frozen in aliquots.

Western blot

Cells were washed in PBS and lysed with 1% TX-100, 0.5% sodium deoxycholate and 0.1% SDS in 150 mM NaCl, 2 mM MgCl₂ and 50 mM Tris, pH 8.0, supplemented with 12 units/µL benzonase (Sigma) and the EDTA-free protease inhibitor Complete (Roche Diagnostics, Basel, Switzerland). Protein concentration was measured by BCA assay (Thermo Fisher Scientific, Rockford, IL, USA), and 20 µg proteins/lane were loaded for SDS-PAGE analysis. Separated proteins were blotted to nitrocellulose membranes (Bio-Rad, Hercules, CA, USA) and PrP^C detected with a mix of the mAbs AH6, AG4 (both 1 µg/mL, TSE resource center) and 6H4 (0.05 µg/mL, Prionics AG, Zurich, Switzerland). The anti-actin polyclonal Ab I-19 (Santa Cruz, Santa Cruz, CA, USA) (0.5 µg/mL) was used as a loading control. Secondary antibodies were goat anti mouse IgG F(ab)₂ alkaline phosphatase (Biosource) and goat anti rabbit IgG F(ab)₂ alkaline phosphatase (Caltag, Buckingham, UK), both at a dilution of 1: 4000. BCIP/NBT (Caltag) was used as a chromogen.

Reverse transcription and quantitative PCR

RNA was isolated using the RNA Blue solution according to the manufacturer's manual (Top-Bio, Prague, Czech Republic). Contaminating genomic DNA was degraded by treatment with TURBO DNase (Ambion, Austin, TX, USA). RNA integrity was evaluated by electrophoresis, and 0.5 µg RNA was reverse-transcribed with the RevertAid first-strand cDNA synthesis kit (Fermentas, Burlington, ON, Canada) according to the manufacturer's manual. Complementary DNA was tenfold diluted, and 2 µL were used for qRT-PCR performed in an ABI 7300 PCR System using TaqMan primers, probes and the Universal PCR Master Mix (Applied Biosystems, Carlsbad, CA, USA). We monitored the expression of the following genes: glyceraldehyde-3-phosphate dehydrogenase (*Gapdh*), the prion protein (*Prnp*), the hemoglobin alpha adult chain 1 (*Hba-a1*), the myeloblastosis oncogene (*Myb*), the α -hemoglobin stabilizing protein (*Eraf*), the GATA-binding protein 1 (*GATA-1*), 2'-5' oligoadenylate synthetase 1A (*Oas1a*), ribonuclease L (*Rnase1*), the eukaryotic translation initiation factor 2-alpha kinase 2 (*Eif2ak2*) and the BCL2-associated X protein (*Bax*). Relative expression levels were calculated using the $2^{-\Delta\Delta CT}$ method [39] and normalized to the reference *Gapdh* gene. Expression quantities were normalized as described in results.

Spectrophotometric determination of hemoglobin content

The hemoglobin concentration in MEL cell lysates was measured with the TMB assay as described previously, with adjustments for 96-well plates [40]. The cell lysates were diluted to contain 100 µg of protein per mL, and their absorbance at 660 nm was measured using a VICTOR² D fluorometer (PerkinElmer, Waltham, Massachusetts, USA). The amount of hemoglobin was subtracted from the calibration curve composed of serial dilutions of purified hemoglobin (Sigma).

Acknowledgments

We would like to thank Jana Cmejlova, Ph.D. and Radek Cmejla, Ph.D. (Institute of Hematology and Blood Transfusion, Prague) and Peter Svoboda, Ph.D. (Institute of Molecular Genetics of the ASCR, Prague) for helpful discussions. We acknowledge the TSE Resource Centre (The Roslin Institute, University of Edinburgh) for the donation of the antibodies AG4 and AH6.

References

1. Linden R, Martins VR, Prado MA, Cammarota M, Izquierdo I, et al. (2008) Physiology of the prion protein. *Physiol Rev* 88: 673-728.
2. Roucou X, Gains M, LeBlanc AC (2004) Neuroprotective functions of prion protein. *J Neurosci Res* 75: 153-161.
3. Singh A, Kong Q, Luo X, Petersen RB, Meyerson H, et al. (2009) Prion protein (PrP) knock-out mice show altered iron metabolism: a functional role for PrP in iron uptake and transport. *PLoS One* 4: e6115.
4. Nicolas O, Gavin R, del Rio JA (2009) New insights into cellular prion protein (PrP^c) functions: the "ying and yang" of a relevant protein. *Brain Res Rev* 61: 170-184.
5. Miele G, Manson J, Clinton M (2001) A novel erythroid-specific marker of transmissible spongiform encephalopathies. *Nat Med* 7: 361-364.
6. Brown AR, Blanco AR, Miele G, Hawkins SA, Hopkins J, et al. (2007) Differential expression of erythroid genes in prion disease. *Biochem Biophys Res Commun* 364: 366-371.
7. Zivny JH, Gelderman MP, Xu F, Piper J, Holada K, et al. (2008) Reduced erythroid cell and erythropoietin production in response to acute anemia in prion protein-deficient (Prnp^{-/-}) mice. *Blood Cells Mol Dis* 40: 302-307.
8. Zhang CC, Steele AD, Lindquist S, Lodish HF (2006) Prion protein is expressed on long-term repopulating hematopoietic stem cells and is important for their self-renewal. *Proc Natl Acad Sci U S A* 103: 2184-2189.
9. Dodelet VC, Cashman NR (1998) Prion protein expression in human leukocyte differentiation. *Blood* 91: 1556-1561.
10. Risitano AM, Holada K, Chen G, Simak J, Vostal JG, et al. (2003) CD34⁺ cells from paroxysmal nocturnal hemoglobinuria (PNH) patients are deficient in surface expression of cellular prion protein (PrP^c). *Exp Hematol* 31: 65-72.
11. Holada K, Vostal JG (2000) Different levels of prion protein (PrP^c) expression on hamster, mouse and human blood cells. *Br J Haematol* 110: 472-480.
12. Panigaj M, Brouckova A, Glierova H, Dvorakova E, Simak J, et al. (2010) Underestimation of the expression of cellular prion protein on human red blood cells. *Transfusion*.
13. Marks PA, Rifkind RA (1989) Induced differentiation of erythroleukemia cells by hexamethylene bisacetamide: a model for cytodifferentiation of transformed cells. *Environ Health Perspect* 80: 181-188.
14. Gougoumas DD, Vizirianakis IS, Tsiftoglou AS (2001) Transcriptional activation of prion protein gene in growth-arrested and differentiated mouse erythroleukemia and human neoplastic cells. *Exp Cell Res* 264: 408-417.
15. Holada K, Simak J, Brown P, Vostal JG (2007) Divergent expression of cellular prion protein on blood cells of human and nonhuman primates. *Transfusion* 47: 2223-2232.

16. Griffiths RE, Heesom KJ, Anstee DJ (2007) Normal prion protein trafficking in cultured human erythroblasts. *Blood* 110: 4518-4525.
17. Hyman T, Rothmann C, Heller A, Malik Z, Salzberg S (2001) Structural characterization of erythroid and megakaryocytic differentiation in Friend erythroleukemia cells. *Exp Hematol* 29: 563-571.
18. Fibach E, Reuben RC, Rifkind RA, Marks PA (1977) Effect of hexamethylene bisacetamide on the commitment to differentiation of murine erythroleukemia cells. *Cancer Res* 37: 440-444.
19. Schroder B, Nickodemus R, Jurgens T, Bodemer W (2002) Upstream AUGs modulate prion protein translation in vitro. *Acta Virol* 46: 159-167.
20. Ford MJ, Burton LJ, Li H, Graham CH, Frobert Y, et al. (2002) A marked disparity between the expression of prion protein and its message by neurones of the CNS. *Neuroscience* 111: 533-551.
21. Otsuka Y, Ito D, Katsuoka K, Arashiki N, Komatsu T, et al. (2008) Expression of alpha-hemoglobin stabilizing protein and cellular prion protein in a subclone of murine erythroleukemia cell line MEL. *Jpn J Vet Res* 56: 75-84.
22. Chute JP, Ross JR, McDonnell DP (2010) Minireview: Nuclear receptors, hematopoiesis, and stem cells. *Mol Endocrinol* 24: 1-10.
23. Kaneda T, Murate T, Sheffery M, Brown K, Rifkind RA, et al. (1985) Gene expression during terminal differentiation: dexamethasone suppression of inducer-mediated alpha 1- and beta major globin gene expression. *Proc Natl Acad Sci U S A* 82: 5020-5024.
24. Mattern J, Buchler MW, Herr I (2007) Cell cycle arrest by glucocorticoids may protect normal tissue and solid tumors from cancer therapy. *Cancer Biol Ther* 6: 1345-1354.
25. Osborne HB, Bakke AC, Yu J (1982) Effect of dexamethasone on hexamethylene bisacetamide-induced Friend cell erythrodifferentiation. *Cancer Res* 42: 513-518.
26. Tilly G, Chapuis J, Vilette D, Laude H, Vilotte JL (2003) Efficient and specific down-regulation of prion protein expression by RNAi. *Biochem Biophys Res Commun* 305: 548-551.
27. Pfeifer A, Eigenbrod S, Al-Khadra S, Hofmann A, Mitteregger G, et al. (2006) Lentivector-mediated RNAi efficiently suppresses prion protein and prolongs survival of scrapie-infected mice. *J Clin Invest* 116: 3204-3210.
28. Singh A, Mohan ML, Isaac AO, Luo X, Petrak J, et al. (2009) Prion protein modulates cellular iron uptake: a novel function with implications for prion disease pathogenesis. *PLoS One* 4: e4468.
29. Singh A, Beveridge AJ, Singh N (2011) Decreased CSF Transferrin in sCJD: A Potential Pre-Mortem Diagnostic Test for Prion Disorders. *PLoS One* 6: e16804.
30. Clarke MF, Kukowska-Latallo JF, Westin E, Smith M, Prochownik EV (1988) Constitutive expression of a c-myc cDNA blocks Friend murine erythroleukemia cell differentiation. *Mol Cell Biol* 8: 884-892.
31. Chen J, Kremer CS, Bender TP (2002) A Myb dependent pathway maintains Friend murine erythroleukemia cells in an immature and proliferating state. *Oncogene* 21: 1859-1869.
32. Roucou X, LeBlanc AC (2005) Cellular prion protein neuroprotective function: implications in prion diseases. *J Mol Med* 83: 3-11.

33. Gougoumas DD, Vizirianakis IS, Triviai IN, Tsiftoglou AS (2007) Activation of Prn-p gene and stable transfection of Prn-p cDNA in leukemia MEL and neuroblastoma N2a cells increased production of PrP(C) but not prevented DNA fragmentation initiated by serum deprivation. *J Cell Physiol* 211: 551-559.
34. Christensen HM, Harris DA (2008) Prion protein lacks robust cytoprotective activity in cultured cells. *Mol Neurodegener* 3: 11.
35. Gauczynski S, Peyrin JM, Haik S, Leucht C, Hundt C, et al. (2001) The 37-kDa/67-kDa laminin receptor acts as the cell-surface receptor for the cellular prion protein. *EMBO J* 20: 5863-5875.
36. Graner E, Mercadante AF, Zanata SM, Forlenza OV, Cabral AL, et al. (2000) Cellular prion protein binds laminin and mediates neuritogenesis. *Brain Res Mol Brain Res* 76: 85-92.
37. Liu Y, Pop R, Sadegh C, Brugnara C, Haase VH, et al. (2006) Suppression of Fas-FasL coexpression by erythropoietin mediates erythroblast expansion during the erythropoietic stress response in vivo. *Blood* 108: 123-133.
38. Chang K, Elledge SJ, Hannon GJ (2006) Lessons from Nature: microRNA-based shRNA libraries. *Nat Methods* 3: 707-714.
39. Livak KJ, Schmittgen TD (2001) Analysis of relative gene expression data using real-time quantitative PCR and the 2^{(-Delta Delta C(T))} Method. *Methods* 25: 402-408.
40. Petrak J, Myslivcova D, Man P, Cmejlova J, Cmejla R, et al. (2007) Proteomic analysis of erythroid differentiation induced by hexamethylene bisacetamide in murine erythroleukemia cells. *Exp Hematol* 35: 193-202.

Figure legends

Figure 1.

The expression of PrP^C on mouse bone marrow (BM) and spleen erythroid precursors is upregulated in early erythroblasts and, then, decreases with the cells' maturation.

(A) Gating strategy for erythroid precursors: upper left - scattergram of BM cells; upper right – gating of viable 7-AAD negative cells (BM live); lower left – live BM cells labeled with CD71-FITC (FL1) and Ter119-eFluor450 (FL5): ProE - CD71⁺Ter119^{+/-} proerythroblasts; Ter119⁺ cells were further gated on CD71-FITC (FL1) and FSC plot (lower right): EryA - large CD71⁺ early basophilic erythroblasts, EryB - small CD71⁺ late basophilic and polychromatic erythroblasts, EryC - small CD71⁻ orthochromatic erythroblasts and reticulocytes.

(B) Quantitative FACS analysis of PrP^C expression on erythroid precursors in mouse bone marrow and spleen. Expression of PrP^C on early basophilic erythroblasts (EryA) is significantly higher ($p > 0.005$, $n=5$) in comparison with proerythroblasts (ProE), both in BM (upper) and spleen (lower). The initial increase of expression is followed by its decrease on late basophilic and polychromatic erythroblasts (EryB), and most mature small precursors (EryC) express a low number of PrP^C. Quantification is based on assumption that one molecule of MAb AH6 binds to one molecule of PrP^C.

Figure 2.

Initial increase of PrP^C protein expression in differentiating MEL cells is followed by its downregulation.

(A) Transcriptional activation of the Prnp gene in uninduced MEL cells (- HMBA) correlates with growth arrest in confluent culture at 72 h, as demonstrated by qRT-PCR. A similar, but lower, increase of PrP mRNA is seen in cells induced to erythroid differentiation (+ HMBA)

(B). Progress of cell differentiation is monitored by overall hemoglobin level (full line, $n=2$, mean \pm SD). The amount of PrP^C protein on western blots (WB) in uninduced cells (C) correlates with the level of mRNA (A). In contrast, the amount of PrP^C protein in differentiating cells (D) is highest 24-48 h after induction and, then, is downregulated, as shown by densitometry (F), despite the level of PrP mRNA continues to rise (B). Blots were developed with a mix of PrP^C mAbs (AH6, AG4, 6H4) and actin antibody was used as a loading control. Surface expression of PrP^C on HMBA induced differentiating MEL cells

measured by quantitative flow cytometry (E) correlates with the levels detected by WB (F) (n=2, means \pm range).

Figure 3.

The initial upregulation of PrP^C expression after the induction of MEL cells' differentiation by HMBA is not affected by dexamethasone (DEX).

(A) Overall hemoglobin level 120 h post induction. Cells were induced by incubation with HMBA for 12 h and then the medium was changed to contain HMBA, DEX, HMBA/DEX or medium only as shown on x- axis labels. Expression of PrP^C was monitored by western blot (WB) at 24 h and 120 h. The presence of HMBA during first 24 h of culture leads to increased levels of PrP^C irrespective of the presence of DEX. In contrast, DEX decreases the level of PrP^C in uninduced cells after 120 h to the level seen in differentiated cells.

(B) Overall hemoglobin level 120 h post induction in cells treated with HMBA for 24 h with a following medium change, as indicated x- axis labels. Again, the upregulation of PrP^C detected by WB after 24 h was not prevented by DEX. However, DEX prevented the upregulation of PrP^C in cells cultured without HMBA after 120 h, despite the level of hemoglobin in the cultures was similar. PrP^C was detected by mix of mAbs AH6, AG4 and 6H4. An actin antibody was used as a loading control. Hemoglobin was measured by TMB assay.

Figure 4.

Downregulation of PrP^C expression by RNAi in MEL cells after selection with puromycin.

(A) Both methods of retroviral vector delivery led to ~ 90% silencing of Prnp mRNA in both lines expressing anti-Prnp shRNAmir (LP1 and LP2) when compared with the MEL line expressing nonsilencing shRNAmir (LN), as depicted by qRT-PCR. (B) Confirmation of PrP^C downregulation in LP1- and LP2-transduced cells at the protein level by western blot. PrP^C was detected by mAb AH6. No silencing was observed in LP5 cell line. Actin was used as a loading control.

Figure 5.

Expression of PrP^C is stably repressed during the differentiation of MEL cells.

(A) Level of PrP mRNA measured with qRT-PCR in cell lines stably expressing anti-Prnp shRNAmir (LP1 and LP2) is downregulated in comparison with control (LN) during the course

of cell differentiation (2 experiments, mean \pm SD). **(B)** The effect of silencing on the level of PrP^C on cell membrane estimated by quantitative flow cytometry (four experiments, mean \pm SD). **(C)** Confirmation of stable PrP^C silencing on the protein level by western blot. PrP^C was detected by mAb mix AH6, AG4 and 6H4. Actin was used as a loading control.

Figure 6.

Differentiating MEL cells display similar characteristics irrespective to the level of PrP^C expression.

(A) Growth curves of LP1, LP2 and control LN lines during erythroid differentiation induced by HMBA. **(B)** Cell viability based on a Trypan Blue exclusion assay. **(C)** Concentration of total hemoglobin in the cells per 100 μ g/ mL of total cell proteins. **(D)** Number of CD71 (transferrin receptor) molecules per cell, analyzed by quantitative flow cytometry, based on assumption that one anti- CD71-PE mAb binds one molecule of transferrin receptor.

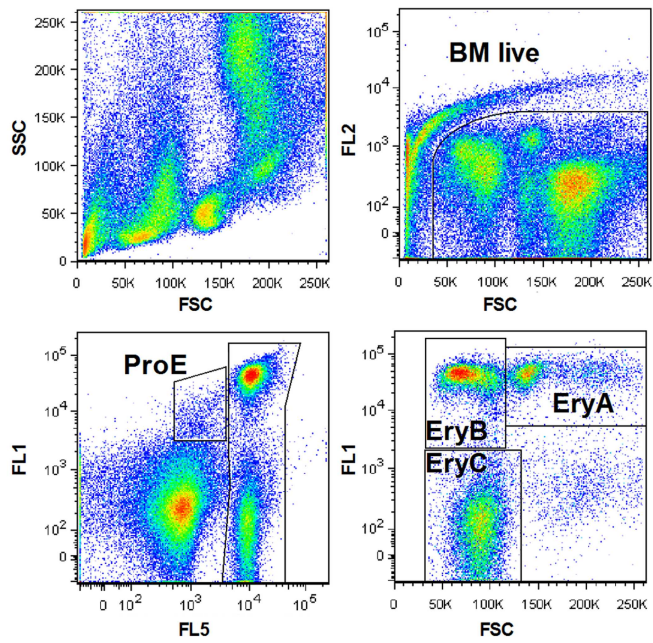
Figure 7.

Transcriptional levels of selected erythroid markers in differentiating MEL cells indicate a similar pattern, irrespective to PrP silencing.

(A) Expression of Eraf (α -hemoglobin stabilizing protein) and Hba (Hemoglobin α) in LP1- and LP2-transduced cells was compared with the level in the control LN-transduced cell line on individual days, as measured by qRT-PCR (n= 4, mean \pm SD). **(B)** Representative pattern of Eraf and Hba expression during differentiation. The level of expression in individual days was normalized to the level in the LN-transduced cell line in day 0.

Figure 1.

A



B

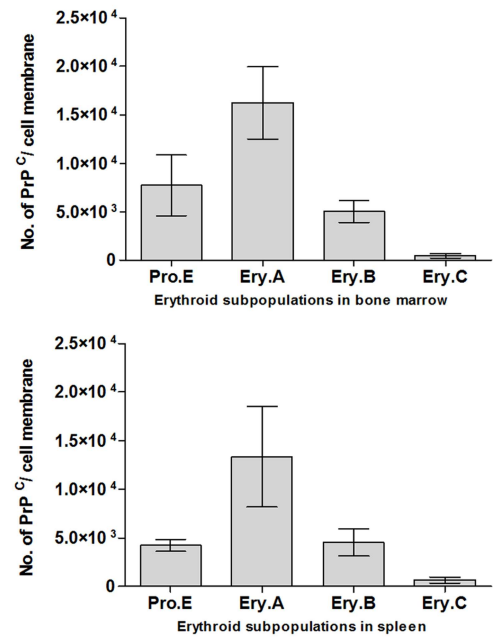


Figure 2.

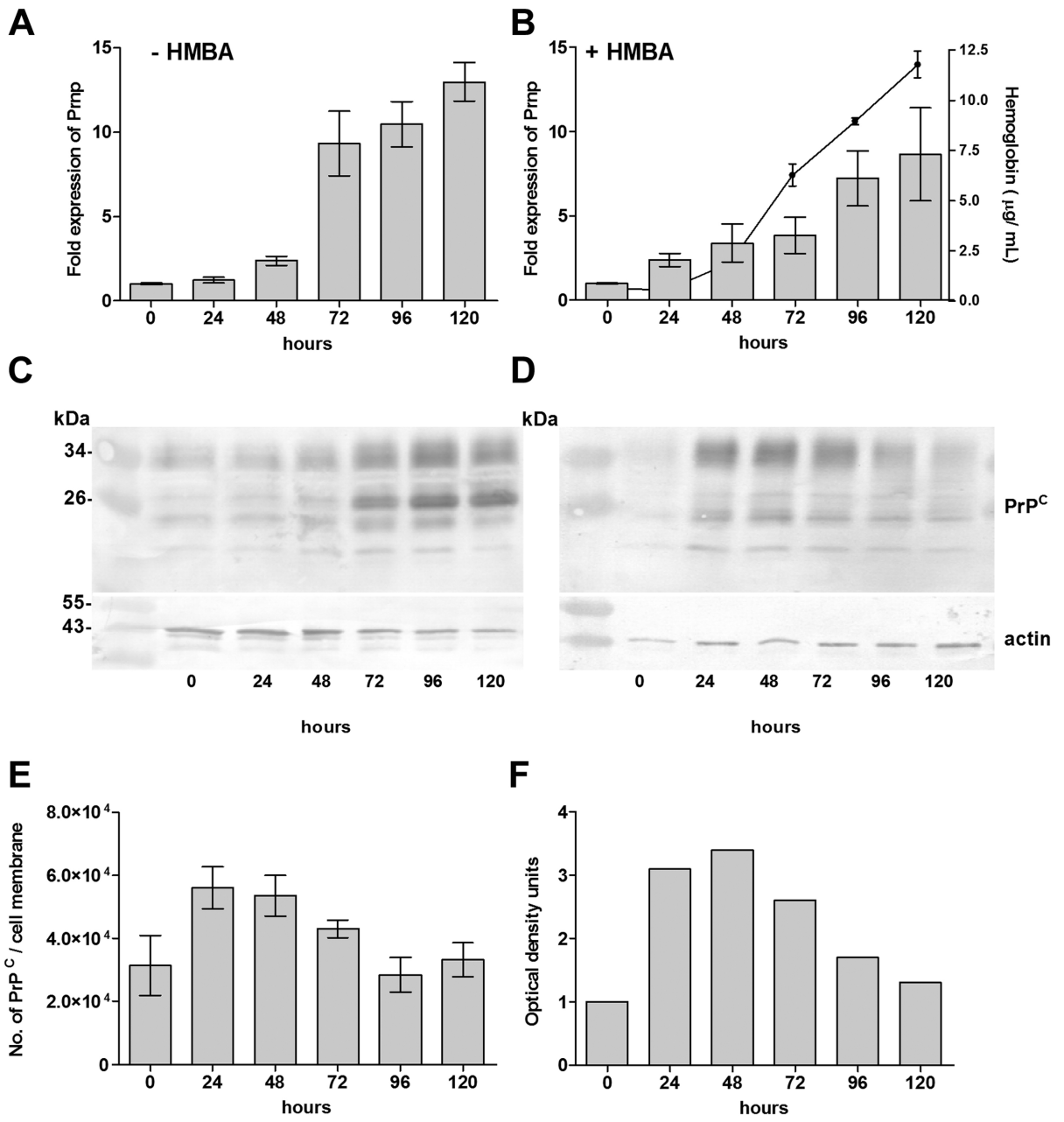


Figure 3.

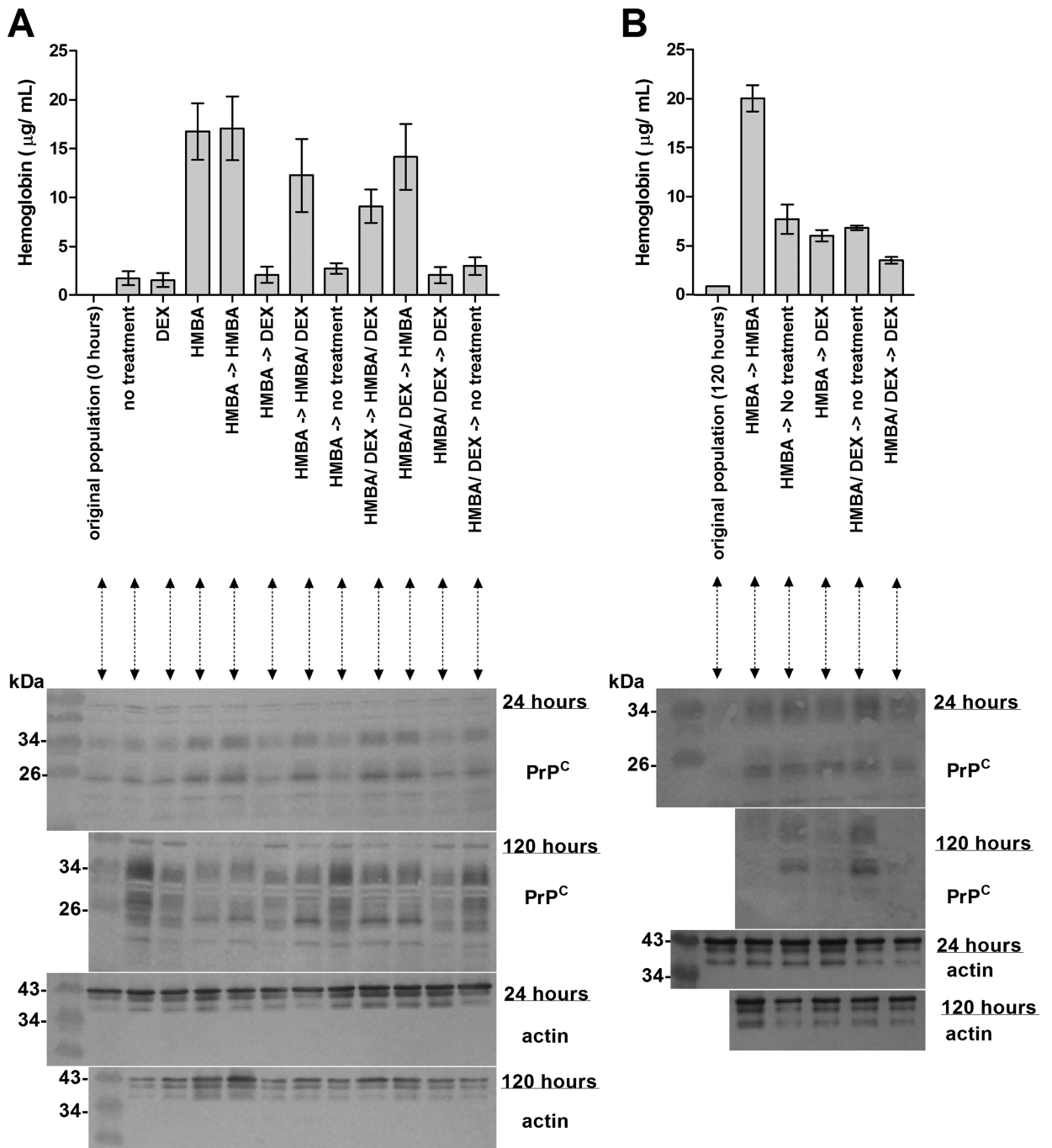


Figure 4.

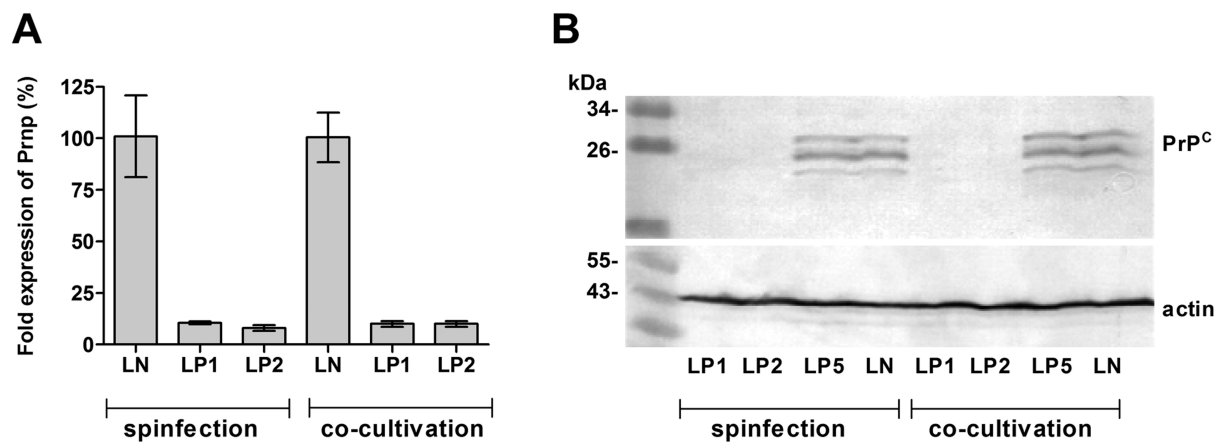


Figure 5.

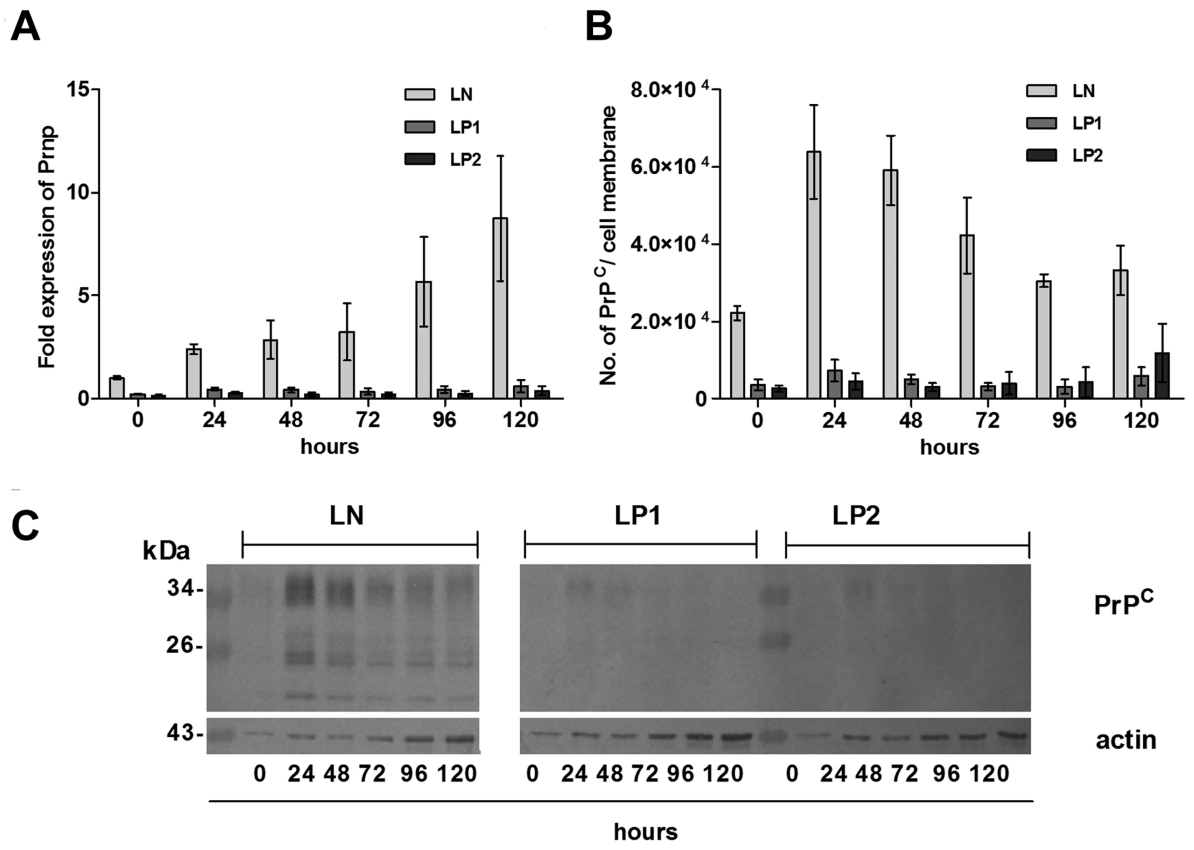
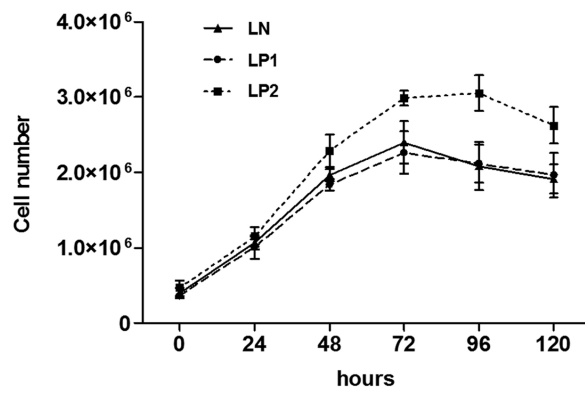
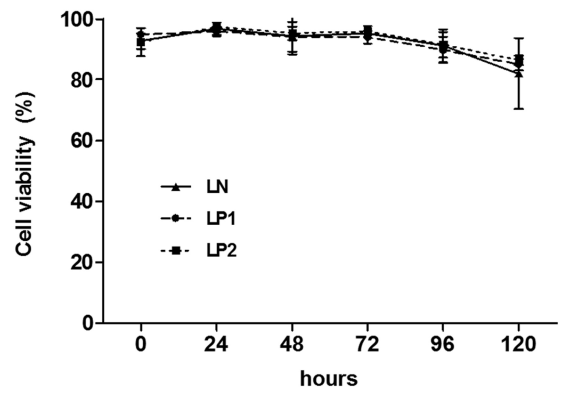


Figure 6.

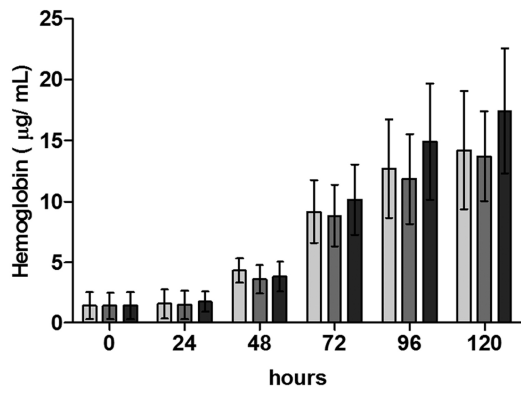
A



B



C



D

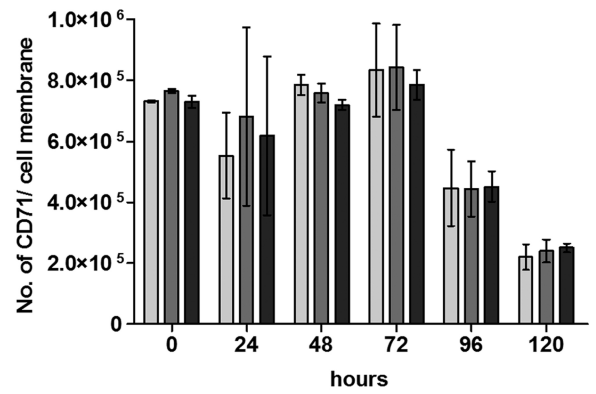
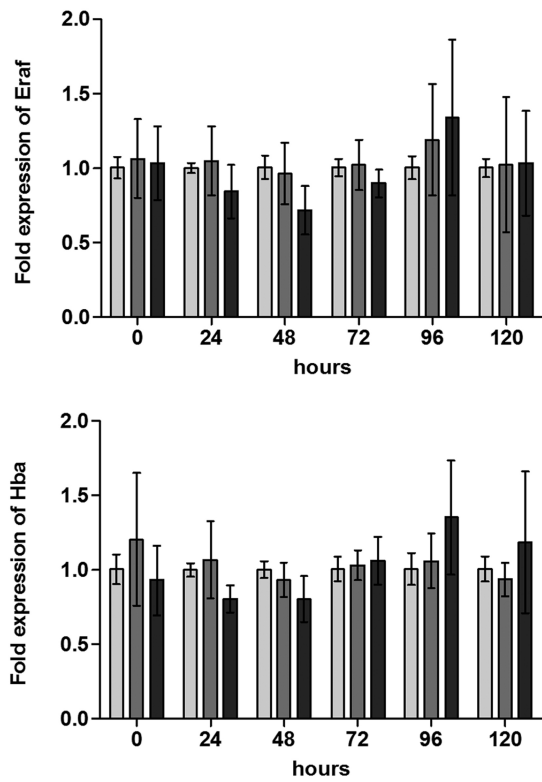


Figure 7.

A



B

